

ADVERTIMENT. La consulta d'aquesta tesi queda condicionada a l'acceptació de les següents condicions d'ús: La difusió d'aquesta tesi per mitjà del servei TDX (www.tesisenxarxa.net) ha estat autoritzada pels titulars dels drets de propietat intel·lectual únicament per a usos privats emmarcats en activitats d'investigació i docència. No s'autoritza la seva reproducció amb finalitats de lucre ni la seva difusió i posada a disposició des d'un lloc aliè al servei TDX. No s'autoritza la presentació del seu contingut en una finestra o marc aliè a TDX (framing). Aquesta reserva de drets afecta tant al resum de presentació de la tesi com als seus continguts. En la utilització o cita de parts de la tesi és obligat indicar el nom de la persona autora.

ADVERTENCIA. La consulta de esta tesis queda condicionada a la aceptación de las siguientes condiciones de uso: La difusión de esta tesis por medio del servicio TDR (www.tesisenred.net) ha sido autorizada por los titulares de los derechos de propiedad intelectual únicamente para usos privados enmarcados en actividades de investigación y docencia. No se autoriza su reproducción con finalidades de lucro ni su difusión y puesta a disposición desde un sitio ajeno al servicio TDR. No se autoriza la presentación de su contenido en una ventana o marco ajeno a TDR (framing). Esta reserva de derechos afecta tanto al resumen de presentación de la tesis como a sus contenidos. En la utilización o cita de partes de la tesis es obligado indicar el nombre de la persona autora.

WARNING. On having consulted this thesis you're accepting the following use conditions: Spreading this thesis by the TDX (www.tesisenxarxa.net) service has been authorized by the titular of the intellectual property rights only for private uses placed in investigation and teaching activities. Reproduction with lucrative aims is not authorized neither its spreading and availability from a site foreign to the TDX service. Introducing its content in a window or frame foreign to the TDX service is not authorized (framing). This rights affect to the presentation summary of the thesis as well as to its contents. In the using or citation of parts of the thesis it's obliged to indicate the name of the author



Departament de Teoria
del Senyal i Comunicacions



UNIVERSITAT POLITÈCNICA DE CATALUNYA

WDM/TDM PON Bidirectional Networks Single-Fiber/Wavelength RSOA-based ONUs Layer 1/2 Optimization

Author

Eduardo Tommy López Pastor

Advisors:

Josep Joan Prat Gomà
José Antonio Lázaro Villa

A thesis submitted in fulfillment for the degree of
Doctor of Philosophy

At the
Optical Communications Group (GCO)
Signal Theory and Communications Department (TSC)

Barcelona, July 2013

Abstract

This Thesis proposes the design and the optimization of a hybrid WDM/TDM PON at the L1 (PHY) and L2 (MAC) layers, in terms of minimum deployment cost and enhanced performance for Greenfield NG-PON. The particular case of RSOA-based ONUs and ODN using a single-fibre/single-wavelength is deeply analysed.

In this WDM/TDM PON relevant parameters are optimized. Special attention has been given at the main noise impairment in this type of networks: the Rayleigh Backscattering effect, which cannot be prevented. To understand its behaviour and mitigate its effects, a novel mathematical model for the Rayleigh Backscattering in burst mode transmission is presented for the first time, and it has been used to optimize the WDM/TDM RSOA based PON.

Also, a cost-effective, simple design SCM WDM/TDM PON with rSOA-based ONU, was optimized and implemented. This prototype was successfully tested showing high performance, robustness, versatility and reliability. So, the system is able to give coverage up to 1280 users at 2.5 Gb/s / 1.25 Gb/s downstream/upstream, over 20 Km, and being compatible with the GPON ITU-T recommendation.

This precedent has enabled the SARDANA network to extend the design, architecture and capabilities of a WDM/TDM PON for a long reach metro-access network (100 km). A proposal for an agile Transmission Convergence sub-layer is presented as another relevant contribution of this work. It is based on the optimization of the standards GPON and XG-PON (for compatibility), but applied to a long reach metro-access TDM/WDM PON rSOA-based network with higher client count.

Finally, a proposal of physical implementation for the SARDANA layer 2 and possible configurations for SARDANA internetworking, with the metro network and core transport network, are presented.

Table of Contents:

- List of Figures..... 10
- List of Tables..... 17
- Abbreviations and Acronyms 19
- Chapter 1 26
- 1. Introduction 26**
 - 1.1. State-of-Art 28**
 - 1.1.1. Active vs. Passive Optical Networks 28**
 - 1.1.2. Bidirectional Transmissions in PONs..... 29**
 - 1.1.3. Access Networks Architecture and topologies 30**
 - 1.1.3.1. Point-to-Point Architecture 30**
 - 1.1.3.2. TDM-PON architecture 31**
 - 1.1.3.3. WDM-PON architecture..... 32**
 - 1.1.3.4. Hybrid WDM/TDM-PON architecture 33**
 - 1.1.3.5. UDWDM-PON architecture 34**
 - 1.1.4. Reflective ONUs..... 36**
 - 1.1.4.1. ONU based on a RSOA 36**
 - RSOA basic characteristics 37**
 - 1.1.5. Rayleigh Backscattering (RB) 39**
 - 1.1.5.1. Backscatter Signal Analysis..... 39**
 - 1.1.6. PON and Next Generation PON (NG-PON) Standards..... 42**
 - 1.1.6.1. FSAN XG-PON ITU-T G.987 Recommendation..... 43**
 - 1.1.6.2. IEEE 10G-EPON (802.3av) Recommendation 46**
 - 1.1.6.3. ITU-T XGPON – IEEE 10GE-PON alignment 48**
 - 1.2. Thesis Outline 49**
 - 1.2.1. Objectives 49**
 - 1.2.2. Organization of this Thesis 49**
- Chapter 2 51
- 2. WDM and WDM/TDM–PON Network Optimization 51**
 - 2.1. Optimization of a rONU-based WDM-PONs in Rayleigh-limited by optimal ONU Gain and WDM position..... 53**
 - 2.1.1. Rayleigh Backscattering Analysis in Upstream path 53**

2.1.2.	Rayleigh Backscattering Analysis for Downstream	55
2.1.3.	Simulations performed	56
2.1.4.	Experimental Measures and Results	57
2.1.5.	Conclusion	59
2.2.	WDM/TDM PON architecture optimization	60
2.2.1.	Modulation Format definition	61
2.2.1.1.	SCM Modulation Format	62
2.2.2.	Computer Simulations	64
2.2.2.1.	OLT Schematic	64
2.2.2.2.	ONU Schematic	66
2.2.2.3.	Simulation results	67
2.2.2.4.	Pre-amplification at the OLT	69
2.2.2.5.	Feeder fibre optimal length	70
2.2.3.	RSOA: characterization and measurement	70
2.2.3.1.	RSOA characterization	71
2.2.3.2.	RSOA electrical bandwidth optimization	71
2.2.3.3.	RSOA Measurements	72
2.2.4.	SCM-DPSK Optimization	73
2.2.4.1.	B2B Full duplex measures	73
2.2.5.	System Optimization	74
2.2.5.1.	Simulations of Performance	75
2.2.5.2.	RSOA: Continuous stream/ Burst Mode transmission	77
2.2.5.3.	RSOA parameters as a function of Temperature	78
2.2.6.	Final Designs, Implementation and Results	81
2.2.6.1.	Back-to-back Reference	82
2.2.6.2.	SCM WDM/TDM PON Testbed Prototype	83
2.2.6.3.	Setup (1)	84
2.2.6.4.	Setup (2)	86
2.2.6.5.	Setup (3)	88
2.2.7.	Conclusions	92
2.3.	Final Conclusions	93
	Chapter 3	94
3.	TDM-PON RSOA-based ONU	94
3.1.	RB analysis in burst mode (BM) transmission	95
	RB analysis in BM transmission in a TDMA environment	96

3.1.1.	Rayleigh backscattering from the ONU burst output power (RBu).....	96
3.1.2.	Rayleigh backscattering effect between ONUs	97
3.1.2.1.	Rayleigh backscattering at the combiner output from “n” ONUs (RBoC).....	97
3.1.2.2.	Rayleigh backscattering RBoC at the ONU input (RBoCO).....	101
3.1.2.3.	Total Rayleigh backscattering at the ONU input (RBt).....	101
3.1.2.4.	Numerical Analysis and Simulations	101
3.1.3.	Analysis of the critical cases due to RB impairments.....	102
3.1.4.	Rayleigh reflected (RBr)	105
3.1.4.1.	Rayleigh reflected from the ONU at the OLT input (RBrO)	108
3.1.5.	Total Rayleigh at the OLT input.....	109
3.1.6.	Upstream optical Signal-to-Rayleigh Ratio (US-oSRR).....	109
3.1.7.	Conclusions	111
3.2.	TDM-PON rSOA-based ONU Network design and Optimization	112
3.2.1.	Analysis of the relevant parameters	112
3.2.1.1.	Extinction Ratio	112
3.2.1.2.	RSOA electro-optical modulation	113
3.2.1.3.	Carrier level Recovery	113
3.2.1.4.	Rayleigh Backscattering impairment	113
3.2.1.5.	ONU splitting factor	114
3.2.2.	Scenario and Network Topology	114
3.2.3.	TDM-PON rSOA-based ONU optimization	115
3.2.3.1.	DS direction flux	115
3.2.3.2.	US direction flux.....	115
3.2.4.	TDM-PON RSOA-based ONU Evaluation	116
3.2.4.1.	Experimental setup.....	116
3.2.4.2.	Experimental Evaluation.....	118
3.2.5.	Conclusions	122
Chapter 4	123
4	WDM/TDM-PON SARDANA Network.....	123
4.1	Network Architecture	124
4.1.1	SARDANA Wavelength Allocation.....	126
4.1.2	Key subsystems.....	126
4.2	Optical Network Unit (ONU) Subsystem	127
4.2.1	ONU subsystem RSOA based.....	128
4.2.2	Downstream cancellation requirement.....	129

4.2.2.1	A Basic Downstream Cancellation	129
4.2.2.2	Upstream BER with/without downstream cancellation	130
4.2.3	Optical network tests	132
4.2.3.1	Back-to-back Downstream Sensitivity tests	132
4.2.3.2	Back-to-back Upstream Sensitivity test	132
4.2.4	SARDANA ONU Layer 1 Prototype	133
4.2.4.1	ONU-RX section	133
4.2.4.2	ONU-TX section	133
4.2.4.3	Optical Coupler	135
4.2.4.4	SARDANA ONU Layer 1 Assembly	135
4.3	Central Office (CO)	137
4.4	OLT Subsystem	137
4.4.1	OLT optical Transmitter	138
4.4.1.1	Dithering for Rayleigh Backscattering Mitigation	138
4.4.1.2	Optical Source	139
4.4.1.3	Optical Modulator and Stabilization Circuit	140
4.4.1.4	RF Data Interface	141
4.4.2	OLT receiver	141
4.4.3	Optical Amplification	142
4.4.3.1	Pump generation	144
4.4.4	OLT subsystem racks	145
4.5	ODN (Optical Distribution Network)	146
4.6	Remote Node (RN)	147
4.6.1	SARDANA RN operation	148
4.7	SARDANA Test-bed	149
4.7.1	SARDANA Network tests	152
4.7.2	SARDANA Field Trial	154
4.8	Energy efficiency	156
4.9	Conclusion	158
Chapter 5	159
5.1.	SARDANA NG-PON (SPON) Layer 2	160
5.1.1.	SARDANA NG-PON Layer Architecture	160
5.1.1.1.	SARDANA OLT layer Architecture	161
5.1.1.2.	SARDANA ONU layer Architecture	162
5.1.2.	SARDANA Transmission Convergence (STC) Design	164

5.1.3.	SARDANA TC Service Adaptation Sub-layer	165
5.1.3.1.	SARDANA GEM (SGEM) Frame basic functions	165
a)	SGEM Header.....	165
b)	SGEM payload.....	167
5.1.4.	SARDANA TC (STC)Framing Sub-layer	168
5.1.4.1.	SARDANA Downstream Frame	168
a)	STC frame header	168
	PLOAMd message in SARDANA.....	168
	Bandwidth map (BWmap) in SARDANA	169
b)	STC Payload	171
5.1.4.2.	SARDANA Upstream Frame	171
a)	STC burst header	171
b)	Upstream STC burst Payload	173
5.1.5.	SARDANA TC - PHY Adaptation Sub-layer	174
5.1.5.1.	DS PHY frame	174
	Physical Synchronization Block (PSBd).....	174
	Downstream PHY frame payload	175
5.1.5.2.	US PHY burst	176
	Upstream PHY burst payload	176
	Upstream Physical Synchronization Block (PSBu)	176
	Guard Time	177
	Preamble time	179
	Delimiter time	179
	Upstream Burst Size – Minimum and Maximum values	181
5.2.	SARDANA Media Access Control Processes	182
5.2.1.	Timing relationships OLT-ONU in SARDANA network	183
	Quiet window (QW).....	183
5.2.2.	RSOA-based ONU Starting, Initialization and Registration	184
5.2.3.	RSOA-based ONU upstream transmission timing	187
a)	ONU response time	187
b)	ONU’s Equalization Delay (EqD).....	188
5.1.1.	Timing during ONU Serial Number Acquisition and Ranging	188
a)	Serial Number Acquisition process.....	188
b)	SARDANA quiet window calculation	190
c)	Ranging Process.....	192

5.1.2.	Optimization of the ONU activation process	193
5.1.1.	Equalization Delay (EqD) Calculus	199
5.1.2.	Timing during the Operation State of the PON.....	200
5.2.	Conclusions	202
Chapter 6.....		203
6.1.	SARDANA Layer 2 Implementation	204
6.1.1.	FPGA clock frequency and data path definition	204
6.1.2.	SARDANA sub-system prototyping	205
6.1.2.1.	Ethernet Interface Module	206
a)	10GE SNI Interface	206
b)	10/100/1000Base-T UNI Interface.....	207
6.1.2.2.	Optical interface module (TST 9061)	207
6.1.3.	OLT Layer 2 Prototyping.....	209
6.1.3.1.	OLT STC TX	209
6.1.3.2.	OLT STC RX.....	210
6.1.4.	ONU Layer 2 Prototyping.....	211
6.1.4.1.	ONU STCTX.....	211
6.1.4.2.	ONU STC RX.....	212
6.1.5.	Control of the SARDANA STC processes.....	213
6.1.6.	SARDANA Layer 2 system operation	216
6.1.7.	Interlayer encapsulation process in SARDANA.....	219
6.2.	SARDANA Internetworking	222
6.2.1.	Ethernet frame over SGEM	222
6.2.2.	Multi-Protocol Management (MPM).....	223
6.2.2.1.	MPM processing.....	223
6.2.2.2.	MPM processing for IP over Ethernet services	225
6.2.3.	Network interoperability across SARDANA	228
6.2.3.1.	SARDANA interoperability at Layer 1 level	228
6.2.3.2.	SARDANA interoperability at higher Layer level	229
MPLS over SGEM.....		229
6.2.3.3.	SARDANA capabilities for Core Network Services.....	230
GMPLS transport over SARDANA.....		231
a)	Internetworking at the SARDANA PHY level	231
b)	Internetworking at the SARDANA L2/L3 Layer	232
6.3.	Conclusions	234

Chapter 7.....	235
7.1. General Conclusions.....	235
7.2. Future research.....	238
Annex A	239
A.1. XGTC layer structure.....	239
A.2. XGTC layer procedures.....	239
a) In the downstream direction	239
b) In the upstream direction	240
A.3. Sub-Layers of the XGTC Layer.....	241
A.4. XGPON Management System.....	242

List of Figures

Fig. 1. 1 - Bidirectional transmission schemas in PONs: a) two-fibre, b) one-fibre, two-wavelength, c) one-fibre, one-wavelength. 29

Fig. 1. 2 - 10 Gbps P2P Ethernet LAN-to-LAN connection based on XFP transceivers. 31

Fig. 1. 3 - A typical TDM GPON ITU-T 984.x network architecture..... 32

Fig. 1. 4 - A typical WDM PON network architecture..... 33

Fig. 1. 5 – A WDM/TDM PON architecture based on a WDM ring and a TDM tree..... 34

Fig. 1. 6 – Scattering produced by a pulse $P(t)$ in a single-mode fibre..... 39

Fig. 1. 7 - Rayleigh Backscattering power as a function of the fibre length (experimental measures)..... 41

Fig. 1. 8 - A timeline of the evolution of the PON networks standards. 42

Fig. 1. 9 - Next-generation PON (NG-PON), and stages of the evolution..... 43

Fig. 1. 10 - Schematic of signal multiplexing in IEEE 10G-EPON [100]. 47

Fig. 1. 11 - Wavelength allocations of IEEE GE-PON & 10G-EPON and ITU-T G-PON & XG-PON ([100])... 47

Fig. 1. 12 - Structure of optical access standardization in ITU-T and IEEE (modified from [100]) 48

Fig. 2. 1 - Schematic of a plain WDM-PON with MUX at the fibre plant..... 53

Fig. 2. 2 - Theoretical C/S as a function of the feeder length for ONU gain of 10, 15 and 20 dB and for the optimal gain (Eq.2 in 1), with $\alpha(\text{dB})=0.2\text{dB/Km}$, $L_1+L_2=50\text{Km}$, $A=5\text{dB}$, Optical Distribution Network (ODN) total loss=15dB..... 54

Fig. 2. 3 - Optimal gain as function of the distance to different values of A..... 55

Fig. 2. 4 - Scenario for the downstream analysis..... 55

Fig. 2. 5 – Crosstalk-to-Signal (C/S)simulation as a function of the MUX position for ONU gain of 10, 15 and 20 dB in downstream and upstream transmission. 56

Fig. 2. 6 - Setup for the experimental measurements 57

Fig. 2. 7 - BER measurements for 10, 15 and 20dB of ONU gain with the MUX a) at the OLT side. b) at the ONU side c) at half way between OLT and ONU (Experimental and simulated curves). 58

Fig. 2. 8 - BER as a function of the MUX position to different ONU gain values (Simulations and Experimental results). 59

Fig. 2. 9 - WDM/TDM PON Reference Architecture..... 60

Fig. 2. 10 - Functional Scheme of the WDM/TDM PON System proposed 61

Fig. 2. 11 - Theoretical sensitivity for the proposed modulation formats 63

Fig. 2. 12 -DPSK scheme for up-converting a differential pre-coded signal at the OLT side (left), and for detecting such a signal at the ONU side after photo-detection (right)..... 63

Fig. 2. 13 - WDM-PON preliminary schema - Link in three stages 64

Fig. 2. 14 - VPI scheme of the OLT SCM System 65

Fig. 2. 15 - VPI scheme of the ONU Reference System 66

Fig. 2. 16 - RSOA functional model (based on SOA Ideal Amplifier + EAM)	66
Fig. 2. 17 - VPI scheme of the SCM receiver.....	67
Fig. 2. 18 - Q (dB) vs. OLT Input Power for different RB coefficients in the upstream path	67
Fig. 2. 19 - Q (dB) vs. OLT Input Power for different RB coefficients in the downstream path	68
Fig. 2. 20 - Performance of the system without Pre-Amp and with Pre-Amp	69
Fig. 2. 21 - Q-factor as a function of the WDM length fibre and the user's number to upstream and downstream paths	70
Fig. 2. 22 - Original Kamelian RSOA RF response: 600MHz of bandwidth at 6dB.....	71
Fig. 2. 23 - PCB layout of the electrical equalization of the RSOA.....	71
Fig. 2. 24 - RSOA mounting.....	72
Fig. 2. 25 – Equalized Kamelian RSOA RF response for Bias current of 90mA. The equalized response has a 6dB bandwidth of about 1.7GHz and a 10dB-bandwidth of about 2GHz which allows for 2.5Gbps transmission.	72
Fig. 2. 26 - BER measures for different Bias current versus receiver power.....	73
Fig. 2. 27 - Experimental setup for single fibre B2B full-duplex measurements.....	74
Fig. 2. 28 – Sensitivity results for the B2B full duplex SCM system.....	74
Fig. 2. 29 - Functional diagram of the new proposed model	75
Fig. 2. 30 - VPI schematic of the new proposed model.....	75
Fig. 2. 31 - Q-factor versus users' number in the upstream path.	76
Fig. 2. 32 - ONU Extinction Ratio and RSOA Gain.....	76
Fig. 2. 33 - RSOA Eye in continuous stream at 1.25Gps, bias of 70mA, modulation of 2Vpp and input signal of -15dBm.....	77
Fig. 2. 34 - Overview of frame in Burst Mode of the RSOA and Eye generated at a bit rate of 1.25Gbps, bias of 70mA, modulation of 2Vpp and input signal of -15dBm.	77
Fig. 2. 35 - Kamelian RSOA Amplified Spontaneous Emission versus temperature @1550nm for Bias current of 70mA.	78
Fig. 2. 36 - Kamelian RSOA Gain and ER versus ambience temperature for optical Pin=-20dBm and Bias current =70mA with 20dBm sinusoidal RF modulation at 500MHz.....	78
Fig. 2. 37 - RSOA OSNR and Noise Figure versus ambience temperature for optical Pin=-20dBm and for Bias current =70mA with 20dBm sinusoidal RF modulation at 500MHz.	79
Fig. 2. 38 - a) ASE response of the Kamelian RSOA. b) Gain and output power versus the optical input power.	82
Fig. 2. 39 – Prototype implementation of the SCM WDM/TDM PON at the GCO-UPC Laboratory.....	83
Fig. 2. 40 - Scheme of the 25km+1x8splitter+2km bidirectional single fibre setup (1).....	84
Fig. 2. 41 - Scheme of the 16km+1x40 AWG+2km+1x4 splitter+2km bidirectional single fibre setup (2). 86	
Fig. 2. 42 - Scheme of two fibres (16km) +1x40 AWG+2km+1x4splitter+2km bidirectional single fibre .. 88	
Fig. 2. 43 - a) Downstream and b) Upstream sensitivity curves for the three PON scenarios.....	91

Fig. 3. 1 - TDM-PON scenario with different Rayleigh backscattering impairments.....	96
Fig. 3. 2 – Rayleigh accumulation process at the combiner output from “n” ONUs.....	98
Fig. 3. 3 - Rayleigh power accumulation at the coupler output due to the burst signal from different ONUs affecting other ONUs (e.g. case of 32 ONUs).....	99
Fig. 3. 4 - Rayleigh Backscattering and power level at the combiner output and ONU input calculated for 2 up to 64 ONUs considering symmetric bandwidth allocation.....	102
Fig. 3. 5 – Scenario of analysis of critical values to total RB at the ONU 2 input as a function of different ONU 2 nominal power output and asymmetric burst length	102
Fig. 3. 6 – Total RB at the ONU 2 input as a function of different ONU 2 nominal output power and asymmetric burst length	103
Fig. 3. 7 – DS optical Signal-to-Rayleigh Ratio (DS-oSRR) at different asymmetrical duty cycles (ONU1/ONU2) and different ONU2 nominal output power	104
Fig. 3. 8 - ONU burst length divided into “n” parts for the calculating of the Rayleigh reflected and the influences of the RBU and RBoCO	106
Fig. 3. 9 - RBr total at the ONU input and RBr as a function of the impact of the G•RBU and G•RBoCO	108
Fig. 3. 10 - Rayleigh reflected values at the OLT input (RBrO) and at the ONU output (RBr) from 2 up to 64 ONUs, considering the same ONU gain for all ONUs.	109
Fig. 3. 11 – US-oSRR and total Rayleigh at the OLT input and the contributions from RBC and RBrO.....	110
Fig. 3. 12 – Optical Signal-to-Rayleigh Ratio (oSRR) as a function of the Extinction Ratio for different BER values.....	112
Fig. 3. 13 - RSOA optical output power for different injection bias current and optical carrier input power.	113
Fig. 3. 14 – Rayleigh penalty at the reception in upstream and downstream transmission.....	114
Fig. 3. 15 – The WDM/TDM PON network and the TDM tree section with the OLT on the place of the RN.	114
Fig. 3. 16 - Optimization flux diagram for a TDM-PON rONUwith FEC to BER 5E-4.....	116
Fig. 3. 17 - Experimental Setup block diagram.....	117
Fig. 3. 18 - The SARDANA tesbed and practical implementation for experimental evaluation.....	118
Fig. 3. 19 - DS power budget and US-oSRR tolerances for RSOA gain=21dB and ONU coupling factor 90/10 and 80/20, with BER 5E-4.	119
Fig. 3. 20 - Maximum data users in rONU-based PON: B2B transmission and US burst using DS remodulation with/without DS cancellation.....	120
Fig. 3. 21 - DS-oSRR and US-oSRR values for 16 and 32 users with ONU splitting loss 90/10 and 80/20, and feeder fibre of 15 km and 10 km.....	121
Fig. 4. 1 – Architecture model and main characteristics of the SARDANA network.	125
Fig. 4. 2 - SARDANA wavelength allocation plan	126
Fig. 4. 3 - SARDANA ONU basically architecture showing Layer 1 and Layer 2.....	128
Fig. 4. 4 - ONU-TX blocks diagram detail.....	128

Fig. 4. 5 - Block scheme of the ONU with downstream cancellation circuit	130
Fig. 4. 6 - Scheme of the upstream sensitivity measures versus Downstream ER.....	130
Fig. 4. 7 – a) Upstream Sensitivity curves for remodulated upstream transmission, with and without cancellation. b) Upstream eye diagram @2.5Gbps for ER (DS) =3dB without DS cancellation. c) with DS cancellation.	131
Fig. 4. 8 - Scheme for the downstream sensitivity measure and BER-Sensitivity for DS-ER of 10, 4 and 3dB.....	132
Fig. 4. 9 - Scheme and sensitivity measure of the Upstream Back-to-back.	132
Fig. 4. 10 – ONU-RX implementation: APD Fujitsu-RX with the Limiting Amplifier.	133
Fig. 4. 11 – ONU-TX system board.....	134
Fig. 4. 12 - ONU module front-end.....	135
Fig. 4. 13 - Blocks of the ONU Layer 1 prototype module.....	136
Fig. 4. 14 - SARDANA rack with two ONU prototypes: ONU layer 2 (above) and opto-electrical ONUs layer 1 (middle) subsystem	137
Fig. 4. 15 – General Scheme of the layer 1/2 SARDANA OLT	137
Fig. 4. 16 – Block diagram of the SARDANA OLT transmission.....	138
Fig. 4. 17 - Integration of: a) Dithering circuitry for delivering a dithering signal to the DFB laser diode; (b) DFB laser diode board;(c) and Current driver and temperature controller for the laser diode.	139
Fig. 4. 18 -Dependence of the emission wavelength on the temperature.	140
Fig. 4. 19 – a) Long-term measurements of the transmitted optical power over 12 hours for a stabilized modulator. b) Electro-optical response of the optical modulator. The 3dB bandwidth is 10.2 GHz.....	141
Fig. 4. 20 - OLT AC RX schematic diagram blocks.	142
Fig. 4. 21 - Hybrid amplifier design and prototype.....	144
Fig. 4. 22 - Internal scheme of the fibre based pump source for remotely pumped amplification and SARDANA prototype fibre laser pump source.....	144
Fig. 4. 23 - Remote Amplification System at the SARDANA Central Office	145
Fig. 4. 24 - OLT racks: The 2100mm rack is equipped with the Service switch, two OLT Layer 2 sub-racks, four OLT transmitter assemblies, two DWDM multiplexer/demultiplexer pairs for East and West ring segments, protection and monitoring assembly, and fibre connect.	145
Fig. 4. 25 – SARDANA metro-access Optical Distribution Network.....	146
Fig. 4. 26 - Remote Node a) basic structure and b) physical implementation	148
Fig. 4. 27 – Basic operation of aSARDANA Remote Node	149
Fig. 4. 28 - SARDANA testbed scheme (left), demo setup, downstream east spectrum, burst mode upstream frame, DS and US eyes (right).....	150
Fig. 4. 29 - SARDANA testbed implementation for the demo.	151
Fig. 4. 30 - Network setup for SARDANA demonstrator tests in Helsinki-Finland.	153
Fig. 4. 31 – a) Field trial network scheme, b) Detail of the Imaging Lab and Orange Lab connection, and c) Lannion ring map (in yellow).....	154
Fig. 4. 32 - Performances of the systems transported in the SARDANA test-bed.....	156

Fig. 4. 33 - Results on the consumption per user and Gbit as a function of the number of ONUs per Central Office, for the uplink limitation of 100 and 320 Gbit/s.	157
Fig. 5. 1 - SARDANA MAC architecture layer 2 overview	160
Fig. 5. 2 - SARDANA NG-PON system architecture.....	161
Fig. 5. 3 - SARDANA OLT system architecture on the OSI network reference model	162
Fig. 5. 4 - SARDANA ONU system architecture on the OSI network reference model.....	163
Fig. 5. 5 - Service Adaptation Sub-layer and SGEM framing.....	165
Fig. 5. 6 - GPON GEM frame and the new formats for the 10 Gbit/s GEM frames from FSAN and SARDANA.....	166
Fig. 5. 7 - Encapsulation process in the SARDANA framing sub-layer	168
Fig. 5. 8 - Downstream frame header and changes respect to GPON and XGPON.....	169
Fig. 5. 9 - BWmap structure in STC.....	170
Fig. 5. 10 - Upstream burst structures in XGTC, and changes for SARDANA TC.....	173
Fig. 5. 11 - Encapsulation process in the SARDANA PHY adaptation sub-layer	174
Fig. 5. 12 - Downstream PHY frame structure at the SARDANA TC layer.....	175
Fig. 5. 13 – Downstream PHY frame with payload and physical synchronization block (PSBd)	176
Fig. 5. 14 – Upstream PHY frame and PHY bursts	177
Fig. 5. 15 – Guard Time, Preamble and Delimiter structure in SARDANA networks.....	177
Fig. 5. 16 – Phase shifting between DS Signal and US signal reflected	178
Fig. 5. 17 - RSOA response time: initialization and additional delays due to associated circuitry ($t_{RSOAon} \approx 10$ ns, in 2ns/div).	179
Fig. 5. 18 – SARDANA Upstream Physical Synchronization Block (PSBu) definition values and OLT Receiver Timing setup (adapted from [150])	181
Fig. 5. 19 – US Burst with a PSBu of 128 ns.....	181
Fig. 5. 20 - Media access control based on bandwidth map allocation for two ONUs	183
Fig. 5. 21 – ONU synchronization state machine (modified from G.987.3_F10.3).	185
Fig. 5. 22 – ONU Activation processes flow.....	186
Fig. 5. 23 - ONU transmission timing diagram.....	187
Fig. 5. 24 - SARDANA ODN maximal distance: $L_{min}+D_{max} \approx 100$ km	189
Fig. 5. 25 - Timing during ONU Serial Number Acquisition	190
Fig. 5. 26 - ONU initialization values in SARDANA network	192
Fig. 5. 27 – Message exchange optimization on the ONU activation process in SARDANA network.	194
Fig. 5. 28 - Optimization sequence of the ONU activation process in SARDANA network	195
Fig. 5. 29 – Practical values from the optimization on the ONU activation process in SARDANA network	196
Fig. 5. 30 - ONU activation process: XG-PON and SARDANA without/with optimization.....	197

Fig. 5. 31 - A comparative between SARDANA and XG-PON for the ONU initialization process.	198
Fig. 5. 32 - Equalization delay calculation during SN process.....	199
Fig. 5. 33 - Maximum EqD value for the Dmax=20 km on the SARDANA network.	200
Fig. 5. 34 - Timing during the Operation State	201
Fig. 6. 1 - Two-stages SerDes implementation for the 32-bit SARDANA data path (modified from [174])	205
Fig. 6. 2 - OLT/ONU prototype base board based on FPGA Altera Stratix IV GX.....	206
Fig. 6. 3 - Ethernet interface modules for SNI a) HSMC CX4 Adapter Board b) HSMC board based on XAUI interface connects with Altera Stratix IV FPGA Development Kit.....	207
Fig. 6. 4 - Ethernet interface modules for UNI: HSMC 4-Ports 10/100/1000Base-T RJ-45 port Adapter Board	207
Fig. 6. 5 - Optical HSMC module board (TST9061) for the OLT and ONU assemblies.....	208
Fig. 6. 6 - Optical interface module (TST9061), connected on the MAC base board Altera Stratix IV GX	208
Fig. 6. 7 – Block diagram of the SARDANA OLT Layer1/Layer 2 implementation	210
Fig. 6. 8 – OLT Layer 1/Layer 2 implementation based on Altera Stratix IV FPGA GX card module pictorial diagram. The Interfaces through Ethernet CX4 adapter and Optics Interface TST9061, as well as the CPC control unit and the OLT Optics Assembly are shown.	211
Fig. 6. 9 - SARDANA ONU Layer1/Layer 2 and FPGA implementation	212
Fig. 6. 10 –The ONU Layer 1/Layer 2 implementation pictorial diagram, based on Altera Stratix IV FPGA GX card module. Interfaces through Ethernet 10/100/1000 Base-T adapter and Optics Interface TST9061, as well as the CPC control unit and the ONU optics assembly a	213
Fig. 6. 11 - SARDANA demonstrator network for Management & Control test.....	214
Fig. 6. 12 - SARDANA network system: MAC and PHY implementation	217
Fig. 6. 13 – SARDANA Layer 2 B2B setup used at the Tellabs OY (Espoo-Finland) for OMC/Ethernet and CLI/Telnet tests.....	218
Fig. 6. 14 - Interlayer encapsulation in the SARDANA Network Downstream process.....	220
Fig. 6. 15 - Ethernet frame mapping into SGEM payload (modified from G.987.3_F9-5).....	223
Fig. 6. 16 - Encapsulation between layers based on the OSI model and MPM processes.....	224
Fig. 6. 17 - IP header format.....	225
Fig. 6. 18 – IP header mapping from Ethernet frame for multi-protocol management in SARDANA metro/access network	226
Fig. 6. 19 – MPM mapped of the IP/Ethernet headers (from Ethernet frame), on the SGEM frame.....	227
Fig. 6. 20 – SARDANA – XGPON (or GPON/GE-PON) interoperability PHY layer processes, for interconnection through a SARDANA remote node (RN).	228
Fig. 6. 21 – MPLS packet mapping into XGEM frame	230
Fig. 6. 22 - SARDANA metro MPLS point-to-point transmission and overlay capacities for the GMPLS Transport Network	231

Fig. 6. 23 – Internetworking between a GMPLS network and an IP network by SARDANA tunnelling capabilities..... 233

Fig. A. 1 - Downstream SDU mapping at the XGTC layer (Modified from G.987.3_F6-1)..... 240

Fig. A. 2 -Upstream SDU mapping at the XGTC layer (Modified from G.987.3_F6-2)..... 241

Fig. A. 3 - The XGTC information flow (Modified from G.987.3_F6-3)..... 243

List of Tables

Table 1. 1 - RSOA parameter performances as a function of the optical input power and bias current values (modified from [35]).....	38
Table 1. 2 - Contents of the XG-PON G.987.x Recommendations	44
Table 1. 3 - Layered structure of XG-PON	44
Table 2. 1 - Bandwidth limits for different sub-carrier modulations	62
Table 2. 2 - Sensitivity values for $P_e = 10^{-10}$ and $P_e = 10^{-4}$	63
Table 2. 3 - Power Loss at ODN	64
Table 2. 4 –Simulation results for SCM WDM/TDM PON in the upstream path.....	68
Table 2. 5 – Simulation results for SCM WDM/TDM PON in the downstream path.....	69
Table 2. 6 - Operation points for several ambience temperature environments at worst polarization case and most critical carrier wavelength (1560nm).	80
Table 2. 7 - Complete detail of the measurements for several scenarios and features of the SCM WDM/TDM PON prototype @1550nm &25°C	81
Table 2. 8 - B2B Sensitivity	82
Table 2. 9 - Range of suitable OLT output powers and corresponding power budgets for a 25km+1x8 splitter+2km single fibre with a 70/30 splitter at ONU.....	85
Table 2. 10 - Range of suitable OLT output powers and corresponding power budgets for a 16km+1x40 AWG+2km +1x4splitter+2km single fibre with a 70/30 coupler at ONU.	87
Table 2. 11 - Range of OLT output powers and corresponding power budgets for a double-fibre (16km) +1x40AWG+2km +1x32 splitter+2km single fibre with its more appropriate coupler at ONU.....	89
Table 2. 12 - Range of OLT output powers and corresponding power budgets for a double- fibre (16km) +1x40AWG+2km +1x32 splitter+2km single fibre with a 70/30 coupler at ONU.	89
Table 2. 13 - Range of OLT output powers and corresponding power budgets for a double-fibre (16km) +1x40 AWG+2km +1x32 splitter+2km single fibre with 80/20 coupler at ONU.	90
Table 3. 1 - RSOA-based ONU and GPON/XGPON ONU comparative.....	121
Table 4. 1 - Requirements for the SARDANA ONU RSOA based.	129
Table 4. 2 - Upstream Sensitivity vs. Downstream ER.....	131
Table 4. 3 – ONU RX section input/output values.....	133
Table 4. 4 – ONU TX section input/output values.....	134
Table 4. 5 - ONU Layer 1 optical input/output characteristics.....	136
Table 4. 6 - ONU Layer 1 electrical input/output characteristics.....	136
Table 4. 7 - Zenko LT-05B95B-XFPGXreceiver optical and electrical specification	141

Table 4. 8 - Technical Specification of the high power amplifier	143
Table 4. 9 - Comparison of the performances.....	143
Table 4. 10 - Service Scenarios for SARDANA.....	147
Table 4. 11 – SARDANA’s performance in terms of ring length, maximum number of ONUs and down/up bit rates.	155
Table 5. 1 - PLOAM message structure	169
Table 5. 2 – PLOAM-L field code.....	170
Table 5. 3 – PLOAM status and DBRu status information code	172
Table 5. 4 - Probability of a severely errored burst as a function of delimiter length [125].....	180
Table 5. 5 - Burst mode overhead time recommended allocation for OLT functions.....	180
Table 5. 6 - Minimum and Maximum Size values for the burst of an US transmission	182
Table 5. 7 - Serial_Number_ONU PLOAMu message	189
Table 5. 8 - SN PLOAM burst response time from an ONU	189
Table 5. 9 – Quiet Window and QW offset comparative values between XG-PON and SARDANA.....	198
Table 6. 1 – Partial list of IP protocol numbers used in the Protocol field.....	225

Abbreviations and Acronyms

10G-EPON	10 Gigabit-EPON
A&D	Add and Drop Filter
AES	Advanced Encryption Standard
Alloc-ID	Allocation ID
AN	Access Network
APC	Angled Physical Contact (Connector)
APD	Avalanche Photo-Diode
APON	Asynchronous Passive Optical Network
AO	Allocation Overhead
ASE	Amplified Spontaneous Emission
ASK	Amplitude Shift Keying
ATM	Asynchronous Transfer Mode
AWG	Arrayed Waveguide Grating
B	Rayleigh Backscattering Coefficient
BE	Burst Enable
BER	Bit-error ratio
BERT	BER Tester
BIP	Bit-Interleaved Parity
BM	Burst Mode
BPF	Band Pass Filter
B-PON	Broadband Passive Optical Network
BPSK	Binary Phase Shift Keying
BW	Bandwidth
BWmap	Bandwidth map
CAPEX	capital expenditures
CID	Consecutive identical digits
CLI	Command Line Interface
CLR	Clock Recovery
CM	Continuous Mode
C/M	Control and Management
CML	Current Mode Logic
CO	Central Office
CPC	Control PC
CPE	Customer Premises Equipment
CRC	Cyclic Redundancy Check
C/S	Crosstalk-to-Signal ratio

CSMA/CD Carrier Sense Multiple Access with Collision Detection

CW Continuous Wavelength

dB Decibelio

DBA Dynamic Bandwidth Assignment

DBRu Dynamic Bandwidth Report upstream

DD Direct Detection

DCF Dispersion Compensating Fibre

DFB Distributed Feedback

DFE Decision Feedback Equalizer

DG Dying Gasp

DHCP Dynamic Host Configuration Protocol

DPSK Differential Phase Shift Keying

DS Downstream

DSC Downstream Cancellation

DSL Digital Subscriber Line

DWDM Dense Wavelength Division Multiplexing

EAM Electro-Absorption Modulator

EDF Erbium-Doped Fibre

EDFA Erbium-Doped Fibre Amplifier

EFM Ethernet in the First Mile

EMS Element Management System

E/O Electro/Optical

EPON Ethernet Passive Optical Network

EQ Equalizer

EqD Equalization Delay

ER Extinction Ratio

FEC Forward Error Correction

FEC Forwarding Equivalence Class (MPLS)

FFE Feed Forward Equalizer

FP Fabry-Perot

FPGA Field-Programmable Gate Array

FSAN Full Service Access Network

FSK Frequency Shift Keying

FTTx Fibre to the x (B – building, business; H – home; C – cabinet, curb)

FWI Forced Wake-Up Indication

FWM Four-Wave Mixing

Gb/s Gigabit per second

Gbps Gigabit per second

GEM G-PON encapsulation method

GHz Giga Hertz

GCO Optical Communications Group

GMPLS Generalized Multi Protocol Label Switching
GPON Gigabit-capable passive optical network
GTC G-PON transmission convergence
H Header
HDTV High Definition TV
HEC Header Error Control
HSMC High Speed Mezzanine Connector
IANA Internet Assigned Numbers Authority
ICMP Internet Control Message Protocol
ID Identifier
IEEE Institute of Electrical and Electronics Engineers
IL Insertion Losses
IM Intensity Modulation
IM/DD Intensity Modulation / Direct Detection
IP Internet Protocol
IPTV Internet Protocol TV
ISI Inter-Symbolic Interference
ISC Interface Switching Capability
ITU International Telecommunications Union
LAN Local Area Network
LD Laser Diode
LED Light Emitting Diode
LER Label Edge Router
LF Last Fragment
LO Local Oscillator
LOS Loss of signal
LPF Low Pass Filter
LSC Lambda Switch Capable
LT Line Termination
LVDS Low-Voltage Differential Signalling
LVPECL Low-voltage positive emitter-coupled logic
MAC Medium Access Control
MAN Metropolitan Access Network
MIB Management Information Base
MLSE Maximum Likelihood Sequence Estimation
MPLS Multi Protocol Label Switching
MPM Multi-Protocol Management
MUX Multiplexer
MZM Mach-Zehnder Modulator
NA Numerical Aperture
NF Noise Figure

NGN Next Generation Network
 NGA Next Generation Access
 NG-PON Next-Generation PON
 NMS Network Management System
 NRZ Non-Return-to-Zero (line code)
 NT Network Termination
 OAM Operation, Administration and Maintenance
 OAN Optical Access Network
 ODN Optical Distribution Network
 OEO Optical-Electronic-Optical (conversion)
 OFDM Orthogonal Frequency Division Multiplexing
 OLT Optical Line Terminal
 OMCC ONU Management and Control Channel
 OMCI ONU Management and Control Interface
 ONT Optical Network Terminal
 ONU Optical Network Unit
 OOK On-Off Keying
 OPEX Operational Expenditure
 ORL Optical Return Loss
 OSA Optical Spectrum Analyzer
 OSI Open System Interconnection
 OSNR Optical Signal-to-Noise Ratio
 OSRR Optical Signal-to-Rayleigh Ratio
 OTDR Optical Time-Domain Reflectometer
 OXC Optical Cross Connect
 P Parity
 P2MP Point-to-MultiPoint
 P2P Point-to-Point
 PC Polarization Controller
 PC Physical Contact (connector fibre)
 PCB Printed Circuit Board
 PDH Plesiochronous Digital Hierarchy
 PDL Polarization Dependent Loss
 PDU Protocol Data Unit
 PHY Physical Interface
 PLI Payload Length Indicator
 PLOAM Physical layer operations, administration and maintenance
 PMD Physical Medium Dependent
 PMD Polarisation Mode Dispersion
 PON Passive optical network
 POTS Plain old telephone service

PPG Pulse pattern generator
PPPoE Point-to-Point Protocol over Ethernet
PRBS Pseudo-Random Bit Sequence
PSB Physical Synchronization Block
PSK Phase Shift Keying
PSN Packet switched network
PT Payload Type
PTI Payload Type Indicator
QAM Quadrature Amplitude Modulation
QoS Quality of service
QPSK Quadrature phase shift keying
QW Quiet Window
R Responsivity of the photodiode
RB Rayleigh backscattering
RBc Rayleigh backscattering from carrier signal
RBoC Rayleigh backscattering at the Combiner output
RBoC Rayleigh backscattering from the Combiner output at the ONU input
RBr Rayleigh backscattering reflected
RBrO Rayleigh backscattering reflected at the OLT input
RBU Rayleigh backscattering from upstream signal
RBt Total Rayleigh backscattering
RE Reach extender
REAM Reflective electro absorption modulator
RL return loss
RN Remote node
RF Radio Frequency
RFC Request-for-Comments
RSOA Reflective semiconductor optical amplifier
RGC RSOA Gain Control
RS Reed-Solomon
RTCP RTP Control Protocol
RTD Round-Trip Delay
RTP Real-time Transport Protocol
RX Receiver
RZ Return to zero
S Scattering coefficient
SC Subscriber Connector
SCM Sub-Carrier Modulation
SDH Synchronous Digital Hierarchy
SDU Service Data Unit
SERDES SERialization/DESerealization

SFC Super Frame Counter
SFP Small Form-factor Pluggable (transceptor)
SGEM SARDANA GEM
SIP Session Initiation Protocol
SLA Service Level Agreement
SMA Sub-Miniature version A (connector)
SN Service node
SN Sequence Number
SNI Service node interface
SNMP Simple Network Management Protocol
SNR Signal to noise ratio
SOA Semiconductor optical amplifier
SONET Synchronous Optical Network
SR Status Reporting
SSB Single side band
STB Set-Top Box
STC SARDANA Transmission Convergence
SXGPON SARDANA XG-PON
TBD To be defined
TC Transmission Convergence
T-CONT Transmission container
TCP Transmission Control Protocol
TDM Time division multiplexing
TDMA Time-Division Multiple Access
TEC Temperature Controller
TIA Trans-Impedance Amplifier
TM Traffic monitoring
ToS Type-of-Service
TX Transmitter
U User plane
UDP User Datagram Protocol
UDWDM Ultra-Dense WDM
UNI User network interface
US Upstream
VLAN Virtual Local Area Network
VOA Variable Optical Attenuator
VoD Video-on-Demand
VoIP Voice over IP
VPI Virtual Photonics Inc.
VPN Virtual Private Network
WBS Wavelength Broadcast and Select

WDM Wavelength division multiplexing
WR Wavelength Routed
WS Wavelength Splitting
XAUI 10 Gigabit Attachment Unit Interface
XFP 10-Gigabit Small Form Factor Pluggable
XGEM XG-PON Encapsulation Method
XG-PON 10-Gigabit passive optical network, G.987 series
XTC XGPON Transmission Convergence (or XGTC)

Chapter 1

1. Introduction

A passive optical network (PON) access features a point-to-multi-point (P2MP) architecture to provide broadband traffic to final users. The P2MP architecture has become the most popular solution for FTTH network deployment among service providers and telecom operators. GPON and EPON standards have guided the development of the PON in the last decade.

However, with the growing popularity of bandwidth demanding services such as HDTV, Video-on-Demand (VoD), and video-conferencing applications, there is an increasing demand on broadband access, and operators expect more from PON networks.

Solutions have been presented for FSAN and IEEE standardization groups through XG-PON [1] and 10G-EPON [2] respectively to improve bandwidth. Nevertheless, other requirement that includes long reach and service support capabilities, as well as cost-effective architectures, enhanced performance of access nodes and improved bandwidth assignments need to be satisfied. Also, PON deployments have been aiming to combine the capacity of metro and access networks in the last mile of the Internet service provisioning.

Although great efforts have been made by research groups on dense technologies (OFDM [3-9], UDWDM [10-12], coherent transmission [13-16], etc.), these are not yet mature, and are not

standardized. This is a key issue to decision making for the telecom industry. A powerful alternative is the optimization over existing PON networks.

An optimization process is a measurable improvement of a process or system. In that direction, a redesign and optimization of the access network technologies, its architecture, access control, bandwidth management and latency requirements, and devices and infrastructures, in terms of minimum deployment cost for greenfield PON, is a good alternative.

In this sense, WDM-PON architecture, often seen as the next generation trend, when combined with time division multiplexing (TDM) techniques, in a hybrid WDM/TDM, is a beneficial solution due to their high capacity. To maintain the cost-effectiveness of PONs, reflective network units such as reflective semiconductor optical amplifiers (RSOA) at the customer premises are a suitable approach. However, due to the bidirectional nature, degradations from physical effects like Rayleigh backscattering between the optical line terminal (OLT) and the optical network unit (ONU) arise and lead to decreased performance. To mitigate these penalties and offer higher performance, over a cheaper and faster broadband access solution, different optimization processes, at Layer 1 (PHY) and Layer 2 (MAC) are presented in this work.

1.1. State-of-Art

1.1.1. Active vs. Passive Optical Networks

In general, there are two important types of architectures that make fibre-to-the-home (FTTH) broadband implementation: active optical networks (AONs) and passive optical networks (PONs). Each has advantages and disadvantages as compared to the other.

Active optical access networks uses electrically powered switching equipment, such as a router or a switch aggregator and take advantage of repeaters based on O/E/O regenerators for reach extension to have additional intelligence located closer to the subscriber that can reduce latency, flexibly add bandwidth, isolate faults, switch, schedule and queue traffic— and maximize bandwidth utilization between the switch aggregator and central office [17-20].

On the other hand, a passive optical network does not include electrically powered switching equipment and no active components are deployed in the optical distribution network, this is between the operator and the final user [21-23]. Instead, it uses optical splitters to separate and collect optical signals as they move through the network. In this way, economic advantages deriving from maintenance of active devices can be obtained as they are situated either at the CO of the provider, principally, or at the customer premises. So, PON networks are gaining interest from network providers and researchers.

Here, the trade-off is one additional active or powered expensive element versus a passive power splitter with an inherently lower failure rate and economically feasible but no ability to isolate faults, switch local traffic or provision narrow transmissions [20]. However, these functionalities can be implemented in the PON on the layer 2 in the OLT at the Central Office.

So, due to a major advantage and great interest, this Thesis is focused only in PON networks.

A hybrid access network between AONs and PONs, where the fibre plant is in principle subject to passive components but contains service nodes referred to as local exchanges, where electrically powered equipment such as amplifiers are also implemented [24-29]. For this thesis they are, strictly speaking, not passive, although the absence of higher layer functionality in these network nodes.

1.1.2. Bidirectional Transmissions in PONs

In FTTH PON technologies Optical Distribution Network (ODN) infrastructure is a critical constraint when deploying the access network. The target for novel designs is a function of scalability (number of users, bit rate and coverage) and implementation cost per subscriber. In this scenario, bidirectional single-fibre/single wavelength transmission is the most cost-effective proposal in terms of CAPEX.

In general, for bidirectional transmission, different criteria for its implementation must be taken into account. Fig. 1.1 shows the basic implementation options.

An ODN based on two-fibre implementation, consisting in one fibre for each direction is shown in Fig. 1a. This ODN structure is adopted for most of the actual commercial technologies for PONs, due to that optical components employed at the OLT and ONU are less restrictive and inexpensive laser or even LED sources can be employed achieving correct transmission results, despite this is not a cost-effective ODN architecture.

Other advantage of this type of implementation is that signal impairments caused by back-reflected light can be eliminated with the appropriate use of optical isolators.

A more efficient solution for ODN implementation is single fibre transmission because only half of the amount of fibre is necessary; as well, the cost for connectors, splices and other network components decrease.

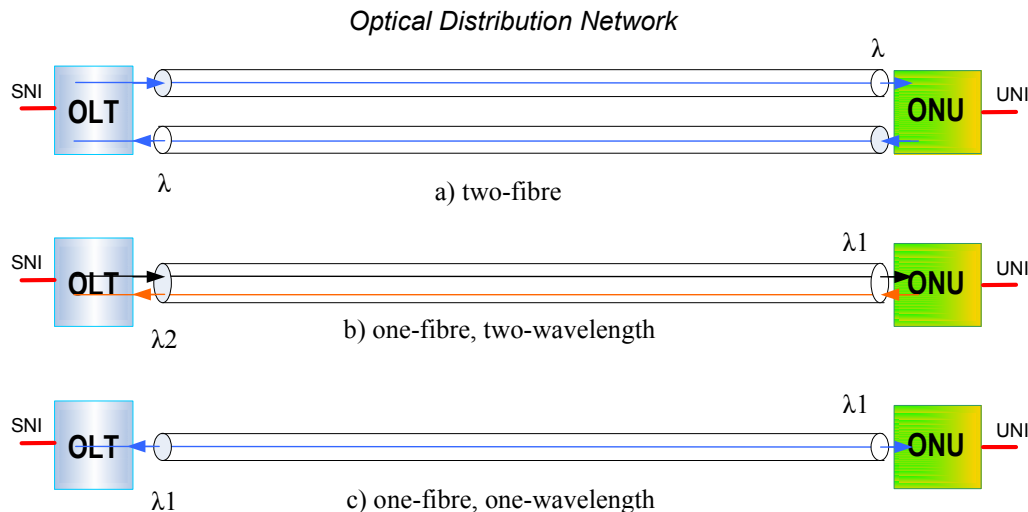


Fig. 1. 1 - Bidirectional transmission schemas in PONs: a) two-fibre, b) one-fibre, two-wavelength, c) one-fibre, one-wavelength.

Transmission over a single fibre can be implemented using two implementations. The simplest is to bidirectional data transmit using different wavelength, as shown in Fig. 1.1b. This implementation requires optical sources of different wavelength as well as optical filters to divide uplink and downlink channels. Thus, the signals do not interfere with each other, as they are carried in separated frequencies [30].

The second implementation consists in using the same wavelength in both directions, as shown in Fig. 1.1c. It allows spatial economy in WDM systems where the number of wavelength is limited. With bidirectional signalling, the total aggregate data throughput can be doubled because downstream and upstream traffic can occur at the same wavelength. This implementation is preferred from the perspective of hardware efficiency, latency, network integrity, network management and reduction of costs for fibres and components [31].

However, coherent crosstalk due to Rayleigh backscattering and reflections, present in this type of implementation, needs to be mitigated, as well as new ONU TX/RX designs are required.

1.1.3. Access Networks Architecture and topologies

1.1.3.1. Point-to-Point Architecture

Point-to-point (P2P) access networks do not distribute the signal via a splitter and there is a dedicated fibre span between each OLT and ONU as a basis to implement its ODN. In this network, no infrastructure is shared (as in the fibre plant as at the central office). It typically utilizes one or two wavelengths for half or full-duplex bidirectional data transmission for the end-user, allows thereby high transmission capacities operating in continuous mode with simple transmitters and receivers, as it is the case in optical intensity modulation/direct detection (IM/DD) transmission systems. However, such solutions are not considered to be cost-efficient for access.

A commercial development is based on Ethernet Point-to-Point fibre optic networks. This systems use standard Ethernet technology for transmitting services to the end subscriber. Commonly available components (switches and routers with optical interfaces), can therefore be used for the subscriber as CPE (Customer Premises Equipment).

To use dedicated fibre optics to the subscriber, bandwidth can be customised. Physical interface bandwidths of 1000 Mbps and SFP transceivers (1 Gbps) and XFP (10 Gbps) symmetrically are standard. In particular, 10 Giga-Ethernet P2P use IEEE802.3ae standard transmission interfaces. However, software can of course adjust the bandwidth actually supplied to below the physical bandwidth to suit each customer. In this aspect, P2P architecture is superior to the PON's P2MP architecture. Just by adding boards, subscribers can obtain an upgrade, without the network architecture or the service of other subscribers having to be changed. Fig. 1.2 shows a 10 Gbps P2P Ethernet connection, based on 802.3ae for using XFP transceivers.

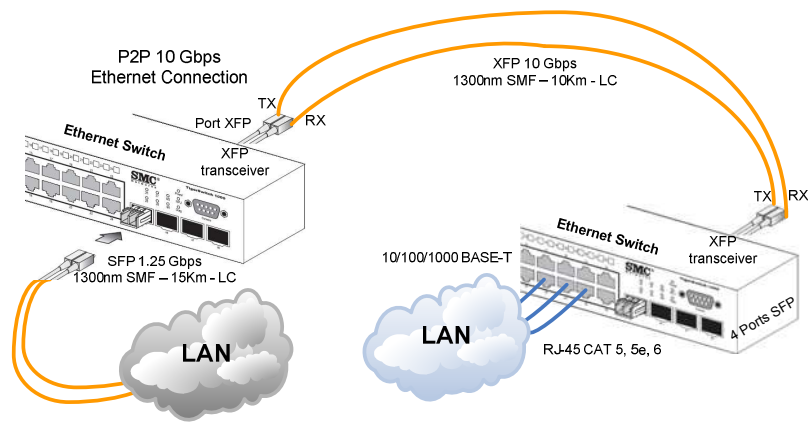


Fig. 1. 2 - 10 Gbps P2P Ethernet LAN-to-LAN connection based on XFP transceivers.

1.1.3.2. TDM-PON architecture

This architecture implements a topology to share the fibre plant among a higher number of customers by using a power signal splitting [32-33]. So, several ONUs are connected to a single OLT. For such, a TDM scheme, to avoid collisions between the data uplink from the users sharing the same wavelength, needs to be implemented. So, medium access control (MAC) allows each user to obtain a time slot to its own upstream data transmission.

This sharing scheme leads to a reduction in the data rate per user. However, considering the statistical nature of the internet traffic, a mechanism based on dynamic bandwidth allocation (DBA), can compensate for this disadvantage.

The TDM scheme requires burst-mode (BM) transmission at the uplink. Although this does not introduce a significant cost increase at the ONU transmitter and the OLT receiver, since it has in principle no effect on the optical and electro-optical components [34], the required timing demands short preambles in the order of a few nanoseconds for synchronization and threshold detection [35].

Maximum possible ONUs number for TDM is a function of the ONU and ODN implementation (one/two-fibre, one/two-wavelength, and amplification), transmission rate, network reach and impairments (Rayleigh backscattering and reflections) due to particular topology. Typical splits in the order of 1:32 [36-38] and much higher split values up to 1:4000 have been reported in scientific literature [39-41]. Reach extensions have been reported mainly by using Raman amplification [42].

In TDM, the maximization of the common fibre link leads to a higher share of infrastructure. The implementation based on one-fibre/one-wavelength for a PON completely passive allows higher cost-efficiency and is desirable also for a green-field deployment.

Standards (ITU-T -G.984 for GPON or Ethernet 802.3 EPON) have been established for key parameters of TDM PON systems. Fig. 1.3 shows a typical TDM PON network architecture based on ITU-T 984.x GPON.

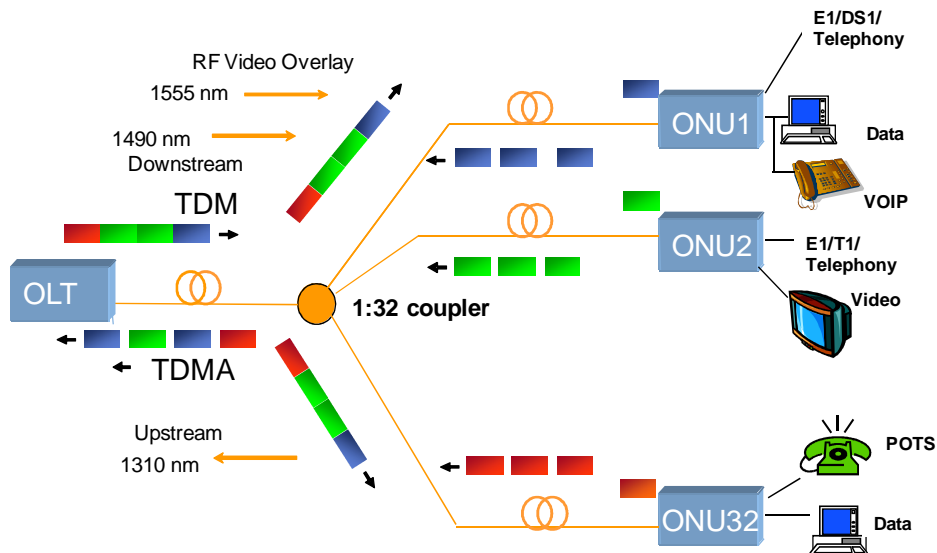


Fig. 1. 3 - A typical TDM GPON ITU-T 984.x network architecture (modified from [46])

1.1.3.3. WDM-PON architecture

Wavelength Division Multiplexing (WDM) PON provides an independent wavelength channel to each user in each communication direction while the fibre architecture is shared. It therefore combines the fibre efficiency of a TDM-PON with the powerful features of P2P connectivity. Fig. 1.4 shows a typical WDM PON network architecture.

WDM PON is currently an emerging FTTH technology and vendor-specific in its implementation at the optical layer. A major advantage is the long reach that WDM PON offers, and so it is mostly used today in backhaul scenarios to serve base stations, OLTs, or other aggregation devices. WDM architecture, as TDM, allows to share common infrastructure between multiple users, but multiplexing in the optical frequency domain based on a WDM multiplexer [43,31]. The WDM-PON increases the spectral efficiency of the access network by taking advantage of the high optical bandwidth of optical fibres.

The continuous mode (CM) data transmission can accommodate high guaranteed data rates up to 10 Gbps, without the introduction of additional intelligence in the MAC layer, due to the exclusive wavelength channel of each user.

Typical customer densities are 40 per employed waveband, while up to 3 wavebands in S-band, C-band and L-band could be effectively used to maintain low optical losses in the ODN.

Nowadays, the granularity of commercial components for WDM multiplexers is limited, so that a fine channel grid that provides a larger number of wavelengths per waveband cannot be achieved. Typical channel spacing is 100 GHz, but is still expected to decrease which is also confirmed by research, where a spacing of down to few GHz for using UDWDM has been demonstrated [44-45].

In turn, a larger number of data channels would also require powerful and electrically powered optical amplifiers that are placed inside the ODN, since Raman amplification or remotely pumped EDFs at the common trunk span are not able to provide significant gain for a dense comb of data signals [35].

WDM PON architectures are being developed by many companies but no standards exist for them yet. However, FSAN launched the NGPON2 recommendations mid-2012 that has WDM PON, i.e. a lambda pair-per-user, considered as an option. It is important to note that FSAN advanced XPON to NGPON2 by adding more wavelength channels into the network. In that sense, the migration path to more capacity in access is surely based on WDM. Most systems have 100 or 200 GHz channel spacing and have several tens of nm between upstream and downstream channel clusters.

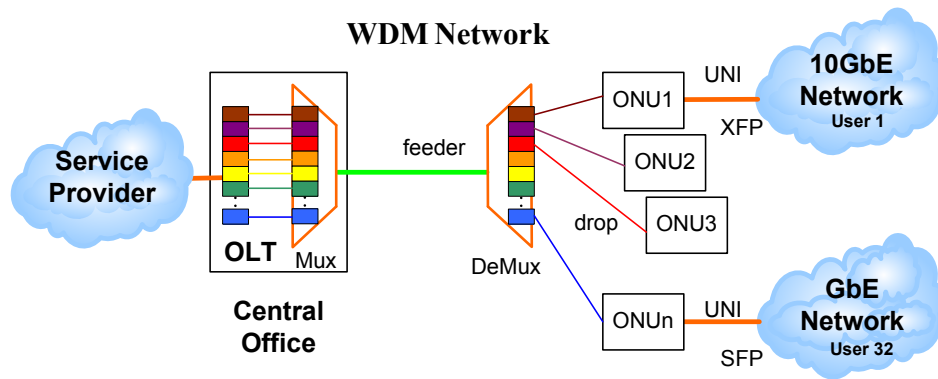


Fig. 1. 4 - A typical WDM PON network architecture.

1.1.3.4. Hybrid WDM/TDM-PON architecture

Hybrid PON architecture maximizes the customer density by incorporating WDM and TDM techniques. Different hybrid WDM/TDM PON architectures are proposed in the literature [46-56,33]. A set of wavelengths is thereby fed together via a common and in general long trunk or ring segment, and a WDM demultiplexer then spreads the single data channels towards a bunch of TDM trees – sometimes referred to as “spurs”, each of them containing a feeder fibre, a power splitter and a short drop fibre. In this way, the multiplexing factors of WDM and TDM segment are multiplied and a high number of customers can be served by the operator. A hybrid PON can be seen as an overlay of TDM-PONs, whose trunk segment is partially shared over a single fibre span.

The wavelength broadcast and select (WBS-PON), uses passive power splitters to broadcast all the wavelengths to all the users, and leave it to the MAC layer to schedule time slots as well as wavelengths for different users. It requires tunability at the ONU.

Other architecture, named wavelength splitting (WS-PON), uses a combination of a wavelength splitter (arrayed waveguide grating, AWG) and a power splitter to share each wavelength among multiple ONUs using TDM. It requires low-cost fixed wavelength transceivers at the ONU. However, the ONU becomes coloured. Though this architecture significantly improves the power budget, it reduces the overall flexibility available in the WBS PON. The other architecture, the wavelength routed (WR-PON) uses a combination of power splitters and optical switches to switch any wavelength to any TDM PON [52-53]. The WR PON significantly improves upon the data security compared to the WBS PON while keeping the flexibility of dynamically switching wavelengths from one TDM PON to another (contrary to the fixed wavelength allocation scheme of the WS PON). However, the WR PON introduces active

equipment in the remote node and the combination of flexibility and security comes at the expense of power budget and cost [54]. Other hybrid WDM/TDM PON architectures that use wavelength selective switches at the remote node to improve flexibility, data security and power budget, is shown in [55].

In the SARDANA network [56], the most interesting state-of-the-art hybrid WDM/TDM NG-PON demonstration, a number of 1024 users can be served at 2.5 or 10 Gb/s, guarantying a bandwidth between 100M and 1G per user, at distances over 60-100 km with proper power budget balance, splitting ratio and number of wavelengths.

This offers a Ring+Tree topology. The access trees length is up to 20 km, inherited from current PON standards, while the ring length may span longer distances towards a metropolitan coverage. This architecture is compatible with a colourless design of the ONU, and also with pure WDM-PON, operating as a resilient TDM over WDM overlay. It will be presented in chapter 4. Fig. 1.5 shows a hybrid WDM/TDM PON architecture based on a WDM ring and a TDM tree, as used in SARDANA project [51].

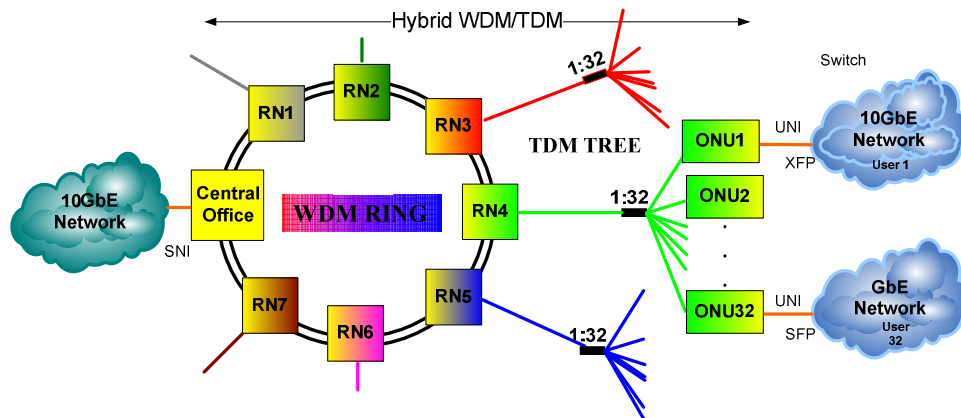


Fig. 1. 5 – A WDM/TDM PON architecture based on a WDM ring and a TDM tree.

The junction between the WDM and the TDM segment is often used to incorporate some network intelligence or means of amplification. While in networks that contain electrically powered equipment these so-called remote nodes include routers [57] or protocol terminators [58], the SARDANA network, the SUCCESS network and other approaches provide optical amplification by remotely pumping rare-earth doped fibres [46-47].

1.1.3.5. UDWDM-PON architecture

WDM-PONs with ultra-dense wavelength allocation is an emerging type of access network that allows increasing the customer density of the PON and avoids narrow-band classical WDM multiplexers, by placing passive splitters as signal distribution elements, as it is the case in TDM-PONs, and in turn coherent detection to overcome the introduced high loss budget of the network [59]. Thus, UDWDM increments the spectral efficiency with respect to current optical access systems (TDM and WDM) that make poor use of the transmission capacity of optical fibre.

Ultra dense WDM (UDWDM) technology requires an array of discrete lasers or multi-frequency sources with extreme wavelength stability. So, the large number of individual transmitters and receivers that are required at the OLT demands progress in photonic large-scale integration. Also, a broad homogenous gain of the erbium doped fibre (EDF) is the main problem to overcome in EDF based optical comb sources [60-63].

Coherent detection of a specific data channel requires a tuneable laser source [64] at the ONU and is in principle contradictory to cost-effective mass deployment. However, progress has been made on the development of lower cost tuneable lasers that can be also used for data modulation at bit rates up to 2.5 Gbps [65].

A typical data rate would be 1 Gbps that is compatible with a channel spacing of 3 GHz [36]. This would assure a customer density of 1000 users or more, however, with the restriction of having a limited maximum data rate for which no simple upgrade path is given. Also, to send ~1000 wavelengths to all users is questionable from the viewpoint of energy efficiency [35]. In addition, the reception sensitivity has to be very low to avoid nonlinear effects at the feeder fibre close to the OLT where many wavelengths are present with too high overall optical power.

1.1.4. Reflective ONUs

Cost-effective solutions must be developed to be able to offer future-proof NG-PON service broadband connections to end users at a reasonable cost. A key element for such purpose is the Optical Network Unit (ONU) at the Customer Premises, having a direct impact on the cost of service by user. Thus, simple ONUs needs to be designed. Reflective ONUs is the principal candidate for this target.

The integration of the reflective modulators with optical amplifiers is a promising solution for the ONU [66-68]. Centralized light control and wavelength management (at the OLT) and colourless operation (WDM-capable) can be obtained by means of reflective ONUs. It avoids laser source at the ONU and associated circuitry (stabilization and provisioning circuitry), for re-using downstream wavelength, implementing a cost-effective system.

Also, this system allows bidirectional transmission by using single-fibre/single-wavelength transmission, in order to reduce network size and connection complexity of the outside plant [69], reducing cost and simplifying the ODN design.

In a reflective ONU, the electrical upstream data re-modulates the optical downstream signal on this wavelength at the same time, performing wavelength reuse. This process can be achieved either by using orthogonal modulation formats for DS/US with frequency or phase shift keying (FSK, PSK) or by suppression of the amplitude shift keyed (ASK) downstream pattern before the optical carrier is again modulated with ASK upstream data [35].

Extensive research work has been focusing on reflective ONUs [70-77]. So, the reflective semiconductor optical amplifier (RSOA), the reflective electro-absorption modulator (REAM) or integrated versions of SOA and REAM, are promising candidates for this purpose.

1.1.4.1. ONU based on a RSOA

The earliest use of a laser amplifier for modulation in local access is reported in [78-79]. A reflector amplifier is introduced for modulation, and its amplifying and reflecting characteristics were analysed. Upstream modulation systems are reported in [80-81]. In [82], the capability of a SOA operating as a photo-detector was verified.

An electro-optic transceiver based on a single Reflective Semiconductor Optical Amplifier (RSOA), used as Optical Network Unit, appears as a potential cost effective solution for a FTTH passive optical platform with bidirectional operation along single fibre outside plant. It performs modulation and detection operations at the bit rate 2.5 Gb/s (upstream modulation) and 10 Gb/s (downstream detection) [51], performing the loss budget that are proposed in GPON [83].

Upstream transmitters at 10 Gb/s were finally found with the help of SOA/REAMs [84-85] or spectrally compressed modulation formats such as duobinary [86] or quaternary amplitude modulation [87].

However, the RSOA-based transmitters suffered from strong performance degradation. So, it is just suitable for a low loss Budget [35].

Incoming light is modulated by the RSOA injection current carrying the upstream user data and amplified before being transmitted. RSOA also acts as a photo-detector by sensing the voltage variation of the electrode. This ONU design is wavelength independent, allowing an easier design of the rest of the system.

RSOA is implemented within the Indium-Phosphide semiconductor material system. These III-V semiconductor components provide a by far smaller form-factor and are therefore in course of the miniaturization of future customer premises equipment (CPE) [35]. However, parasitic side effects during modulation, such as chirp and the limited electro-optical bandwidth, penalize the data transmission. It is therefore often required to compensate these unwanted effects by additional electronic means like passive or adaptive electronic equalization.

RSOA basic characteristics

Gain and Noise Figure (NF)

In a RSOA, with a redesign of its back-facet towards a retro-reflector, the gain and noise emission is different with respect to a normal SOA. A moderate gain is expected to be obtained with a lower bias current due to the fact that the signal passes the active region twice. On the other hand, the effect of gain saturation will therefore approach at lower values of input power. The RSOA has a higher noise figure due to its retro-reflective design. For a low input power of -30 dBm and a bias current of 100 mA, the NF would be about 3 dB higher than the optimum working point of the SOA, where a NF of 7.5 dB can be obtained for the same bias current but an input power of -5 dBm [35].

Electro-Optical Modulation Bandwidth

Limitations are given by the electro-optical (E/O) response of the RSOA semiconductor [106], which will prevent to reach high modulation data rates.

The electro-optical response of the SOA depends on the chosen point of operation [88], for which stringent limitations for the applied modulation can be imposed. Next to the physical processes inside the semiconductor material that are related with the applied bias current and optical signal input of the SOA, also the packaging of the device has to be taken into account. In addition, the electrical interface of the bias electrode will introduce a natural low-pass transfer function for the electrical signal [89]. Typically, commercial SOA devices are not intended to be primarily used as intensity modulator so that the bonding interface inside the package is not optimized for high modulation bandwidths.

Chirp

The intensity modulation process carried for the RSOA, for modulation of the injected bias current, leads also to modulation of the optical frequency due to band filling effects. The introduced phase modulation for the signals that are originally intended to be purely intensity modulated, can lead to problems.

Thus, chirping during modulation introduces, together with a dispersive transmission link penalties for the reception, especially for modulation with large extinction ratios [90]. A possibility to reduce this unwanted effect is to apply a holding beam that maintains the separation of the quasi-Fermi levels and prevents therefore chirping [35].

Dependence on Bias Current and Optical Input Power

The performance of operation of RSOA depends on the bias current and the optical input power, which define the bias point. Different applications such as modulation or amplification will exploit different performance in terms of gain, NF, or modulation bandwidth in different operation values. Table 1.1, from [35] summarizes RSOA parameter performances as a function of the optical input power and bias current values.

Table 1. 1 - RSOA parameter performances as a function of the optical input power and bias current values (modified from [35]).

RSOA		Optical Input Power		
		Low Pin < -15 dBm	Medium -15 dBm < Pin < -5 dBm	High Pin > -5 dBm
bias current	High	High gain and NF for very low input powers, Good modulation ER For long devices, capable to modulate the optical phase	Gain decreases due to saturation but low NF, Good modulation Bandwidth for short devices	Low gain, NF increases with input power level, large modulation bandwidth for short devices
	Medium	Moderate gain, moderate-high NF, modulation bandwidth reduced	Moderate gain and NF	Low gain, higher NF, Good modulation Bandwidth for short devices
	Low	quite low gain, higher NF, low modulation bandwidth	Low gain, high NF, Low modulation bandwidth	No gain, high NF

1.1.5. Rayleigh Backscattering (RB)

To maintain the cost-effectiveness of PONs, reflective network units such as RSOA at the customer premises with single-fibre/single-wavelength ODN are a suitable approach. However, due to the bidirectional nature, its network configuration suffer from additional penalties associated with discrete back-reflections from connectors and Rayleigh backscattering(especially with ONUs RSOA-based which amplify these effects).Although connector reflections can be sufficiently reduced using appropriately designed connectors(by employing elements with low return loss and APC connectors or fibre splices) [70,91], RB remains principal noise impairment in this type of networks.

RB is an inherent effect of the fibre and cannot be prevented. Due to the irregular amorphous structure of the glass and microscopic defects (much smaller than the wavelength of the light), light is diffusely scattered into the fibre. A fraction of the light is back scattered towards the transmitter. It overlaps with data signal sent from the opposite direction and induces crosstalk between these two counter-propagating waves [92]. RB cannot be eliminated due to its random nature, but can be mitigated by reducing overlap between upstream and downstream optical spectra.

1.1.5.1. Backscatter Signal Analysis

The light travelling along a fibre with the distance exhibits an exponentially decreasing power level. The power transmission relation between fibre incident light (P_o) and transmitted power ($P(r)$) at a distance r is (α is the attenuation coefficient):

$$P(r) = P_o \cdot e^{-\alpha \cdot r}$$

The scattered power dP_{RB} , at the position r within an infinitesimal small interval dr is proportional to the pulse power $P(r)$. This is shown in Fig. 1.6.

$$dP_{RB} = k \cdot P(r)dr$$

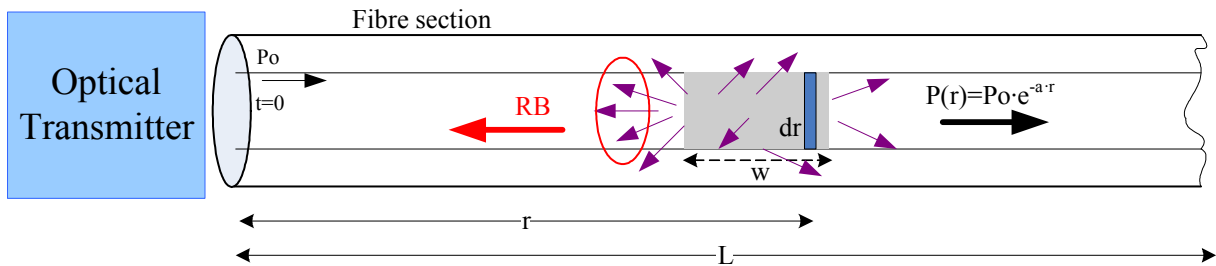


Fig. 1. 6 – Scattering produced by a pulse $P(r)$ in a single-mode fibre.

With $k = S \cdot \alpha_s$, α_s is the scattering coefficient ($\sim \lambda^{-4}$) and S (backscattering capture coefficient) is the fraction of the light scattered in all directions that is captured and guided back to emitter.

$$S = \left(\frac{NA}{n_0} \right)^2 \cdot \frac{1}{m}$$

With NA: fibre's numerical aperture; n_0 : refractive index of the fibre core; and "m" depends on the refractive index profile (4.55 for single mode fibre [93]).

Summing up the light power backscattered from infinitesimal short intervals dr from the whole pulse w , and by considering that part of the signal power returns, it yields:

$$P_{RB}(w) = \int_0^w S \cdot \alpha_s \cdot P_0 e^{-2 \cdot \alpha r} dr$$

The total RB of a fibre with length L , if excited by a continuous wave signal, can be obtained integrating P_{RB} for small pulse widths over the total length of the fibre.

$$\begin{aligned} P_{RB}(L) &= \int_0^L P_{RB}(r) dr \\ &= S \cdot \alpha_s \cdot P_0 \int_0^L e^{-2 \cdot \alpha \cdot r} dr \\ &= \frac{S \cdot \alpha_s \cdot P_0}{2 \cdot \alpha} \cdot (1 - e^{-2 \cdot \alpha \cdot L}) \end{aligned}$$

If we define B =Rayleigh Backscattering Coefficient,

$$B = \frac{S \cdot \alpha_s}{2 \cdot \alpha}$$

then:

$$P_{RB}(L) = P_0 \cdot B \cdot (1 - e^{-2 \cdot \alpha \cdot L}) \quad \dots(1.1)$$

Fig. 1.7 shows experimental measures of Rayleigh Backscattering power as a function of the fibre length (incident light power = 0 dBm). With increase of the fibre length, the interference level of RB also increases and converges after about 20 km asymptotically to a maximum value. This value depends on the transmission wavelength. For 1550 nm single-mode fibre it is about 34.5 dB below the fibre input power, as demonstrated experimentally in [70].

The critical distinction of RB noise is that it is coloured while ASE and electrical noise (i.e. thermal and shot noise) are white. RB analyses vary significantly depending on whether the RB overlaps in frequency with the signal or if the RB is separated in frequency from the signal. Worst case overlapping RB noise will be called coherent RB crosstalk while partially overlapping RB noise will be called incoherent RB crosstalk. Coherent crosstalk does not imply that the signal and noise fields are mutually coherent but rather that they share a common carrier frequency. The phase of the RB field and signal field are always statistically independent in practical situations and thus interference cross-terms average to zero [31].

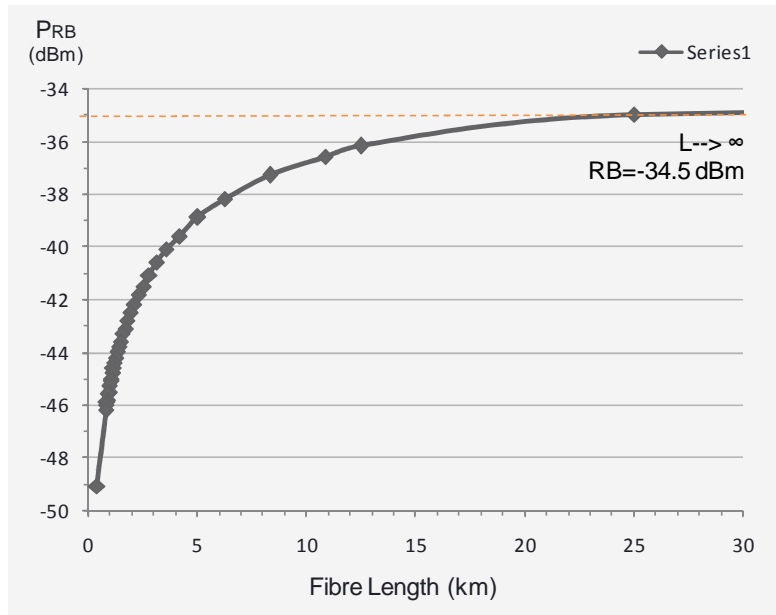


Fig. 1. 7 - Rayleigh Backscattering power as a function of the fibre length (experimental measures).

Thus, the degradation is stronger if signals coming from different directions fall into the same wavelength range, so that the differential frequency of two optical frequencies (Δf_{opt}) can temporarily fall within the electrical receiver bandwidth, leading to additional coherent crosstalk. An expression for the photocurrent, according to the square-law characteristic of the photodiode, when signal power $P_s(t)$ and crosstalk $P_c(t)$ overlap, is shown in equation 1.2 (polarisation is not considered).

$$I_{ph} = R \cdot [\underbrace{P_s(t)}_{\text{Detected Signal}} + \underbrace{P_c(t)}_{\text{Incoherent Crosstalk}} + 2 \cdot \underbrace{\sqrt{P_s(t) \cdot P_c(t)} \cdot \cos(2\pi\Delta f_{opt}(t) + \Delta\varphi_{opt}(t))}_{\text{Coherent Crosstalk}}] \quad \dots(1.2)$$

With:

R: responsivity of the photodiode.

$\Delta f_{opt}(t)$: time-dependent differential frequency of signal and crosstalk.

$\Delta\varphi_{opt}(t)$: time-dependent optical phase difference.

Coherent crosstalk can have much stronger effect than incoherent crosstalk due to the $P_s(t) \cdot P_c(t)$ product (with $P_s(t) \gg P_c(t)$). Coherent crosstalk is only relevant if the difference frequency of the optical carriers is within the detection bandwidth.

In chapter 2 and chapter 3 expressions for the Rayleigh backscattering effects in WDM and TDM networks will be deduced.

1.1.6. PON and Next Generation PON (NG-PON) Standards

Current PON technology is a powerful option for deep-fibre broadband access. Serious efforts to standardize and develop this technology have steadily extended the feature set of PON to make the technology more flexible in terms of deployment and services.

The five major PON standards are BPON (ITU-T G.983 - broadband PON, currently only of historical interest), GPON (ITU-T G.984) [83], EPON (802.3ah) [94], 10GE-PON (802.3av) [2] and XGPON (G.987) [1]. Fig. 1.8 shows a timeline of the evolution of standards for PON networks [95]. Also, demonstration field trial from SARDANA, a European NG-PON project (presented in chapter 4), are indicated.

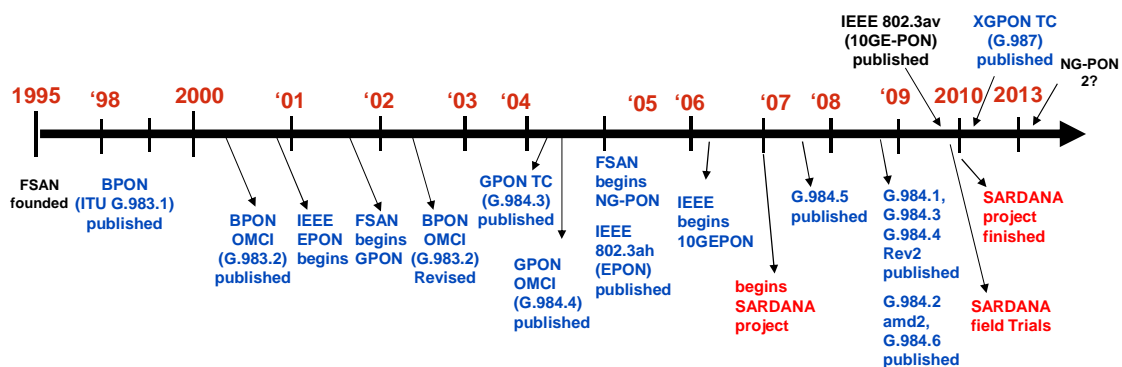


Fig. 1. 8 - A timeline of the evolution of the PON networks standards (modified from [46]).

BPON, its successor GPON and XGPON are ITU-T recommendations sponsored by FSAN, a vendor and operator committee. EPON is an IEEE option developed by the IEEE Ethernet in the First Mile (EFM) initiative. The IEEE 10G EPON Study Group was established in March 2006 and it has produced the standard named “802.3av-2009 IEEE Standard for Information Technology - Part 3: (CSMA/CD) Access Method and Physical Layer Specifications Amendment 1: Physical Layer Specifications and Management Parameters for 10 Gb/s Passive Optical Networks”. It was approved in September 2009 and publicised in October 30, 2009.

The FSAN NGA work group has been formed to study the evolution of optical access systems beyond GPON. A first product is 10 Gigabit-capable Passive Optical Network (XG-PON) 987.x standard (2010). As much as possible, this Recommendation maintains characteristics from BPON and GPON. This is to promote backward compatibility with existing Optical Distribution Networks (ODN) that complies with those Recommendations. Furthermore, this recommendation provides a mechanism that enables seamless subscriber migration from GPON and E-PON to XG-PON using WDM defined in the G.984 series.

There are two flavours of XG-PONs based on the upstream line rate: XG-PON1 featuring a 2.5Gbit/s upstream path and XG-PON2 featuring a 10Gbit/s one. The initial phase of this specification only addresses XG-PON1. XG-PON2 will be addressed at later phase when the technology becomes more mature.

In parallel the research community are reporting various future developments of optical access technology (e.g. WDM, increased reach/split, number of users, backward-compatible with old PON or even IEEE 10GE-PON) to a next generation access system. The next-generation PON (NG-PON) defines two stages of evolution: NG-PON1 and NG-PON2, as shown in Fig. 1.9.

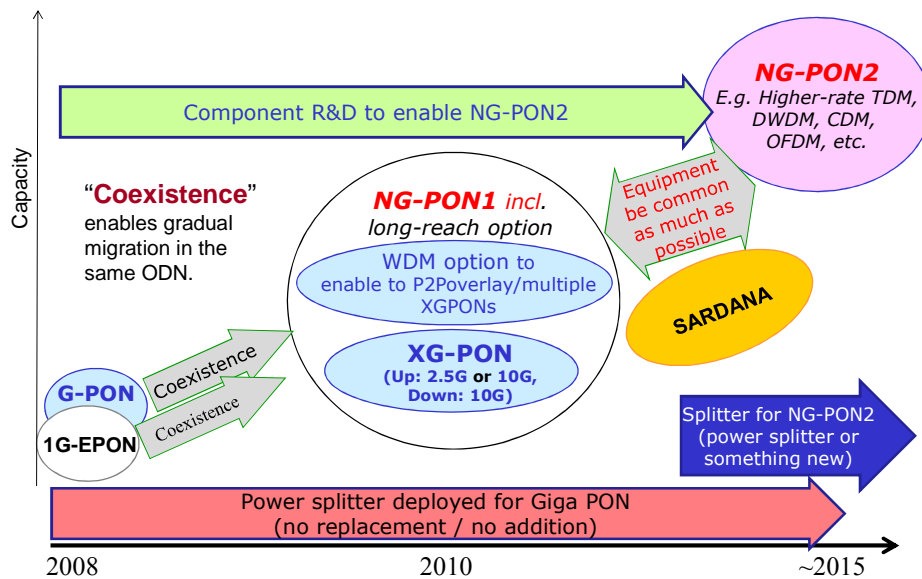


Fig. 1. 9 - Next-generation PON (NG-PON), and stages of the evolution.

NG-PON1 is compatible with GPON deployments in accordance with G.984.5. Compatibility with a GPON reach extender is also expected. XG-PON1 is the principal exponent of this stage, which supports data rates of 10Gbps downstream and 2.5Gbps upstream. A symmetric system, which supports 10Gbps in downstream and upstream (XG-PON2) and WDM option to overlay PONs and P2P connections on the same fibre infrastructure in G.984.5 enhancement bands are hoped.

ITU-T has not constrained NGA2 by the GPON ODN, recognizing that G.984 definitions will not be suitable forever and new developments will obviate the need for backward compatibility. It is anticipated that NG-PON 2 products will be available around 2015. NG-PON 2 may use a new fibre network, introducing in particular the ability to use ultra-dense wavelength-division multiplexing (UDWDM) splitters instead of power splitters to separate users via different wavelengths on the same ODN. A bridge NG-PON architecture between NG-PON 1 and NG-PON 2 is SARDANA network.

SARDANA is a novel FTTH hybrid architecture for Next Generation WDM/TDM-PON, with new functionality and extended performances: Resilience (against fibre cut), extended reach (100Km) and number of homes (>1000), full compatibility with 10G XG-PON, truly passive, better fibre utilization and smooth scalability. It is a transparent solution to metro-access convergence. It will be analysed in chapter 4.

1.1.6.1. FSAN XG-PON ITU-T G.987 Recommendation

10-Gigabit Passive Optical Network (XG-PON) is a PON system supporting nominal transmission rates on the order of 10 Gb/s in at least one direction, and implementing the suite of protocols specified in the ITU-T G.987 series of Recommendations. XG-PON is a sub-class of NG-PON1 [1].

The ITU-T G.987 Recommendation for XG-PON is formed by four technical documents. Titles and contents of these recommendations are summarized in Table 1.2.

Table 1. 2 - Contents of the XG-PON G.987.x Recommendations

Rec.	Title	Content
G.987.1 [1]	XG-PON: General requirements	Requirements for services, interfaces to other systems, scalability (distance, split ratio, etc.). Smooth migration from the Gigabit-class PON is one of the important requirements as well and the maximum loss budget, as a function of the existing fibre infrastructure that many network operators have already deployed.
G.987.2 [96]	XG-PON: Physical Media Dependent (PMD) layer specification	Optical parameter specifications of transmitted and received signals between OLT and ONU as well as optical-path characteristics between OLT and ONU. The same allocation as IEEE 10G-EPON has been selected (i.e., 1260–1280 nm upstream and 1575–1580 nm downstream), so that the optical components can be common with IEEE 10G-EPON ones and smooth migration from the Gigabit-class PON is ensured.
G.987.3 [97]	XGPON Transmission Convergence layer specification	It will define the frame structure for accommodating various client protocols, the TDMA function for controlling upstream signal timeslots, the function for activating ONUs, the function for encrypting downstream signals, and so on. How to extend the GTC frame structure to XG-PON is one of the key issues.
G.987.4 [98]	XG-PON: ONU management and control interface specification (OMCI)	Specifications of protocol and message formats of management information base (MIB) for managing/controlling XG-PON ONUs. Because many G-PON OMCI definitions can be applied to XG-PON, generalizing OMCI to various PON systems is introduced.

Layered structure of XG-PON optical network

The two layers considered in XG-PON are the physical medium dependent layer and the XTC layer. It is shown in Table 1.3 [1].

Table 1. 3 - Layered structure of XG-PON

Path Layer			
Transmission Medium Layer (with OAM functions)	XTC layer	Adaptation	XGEM encapsulation
		PON Transmission	DBA XGEM port BW allocation QoS handling & T-CONT management Privacy and security Frame alignment Ranging Burst synchronization Bit/Byte synchronization
	Physical medium layer		E/O adaptation Wavelength Division Multiplexing Fibre connection

The XTC layer is divided into PON transmission and adaptation sub-layers, which correspond to the Transmission Convergence sub-layer of the X-GEM conveying various data types. The PON transmission sub-layer terminates the required transmission function on the ODN. The PON-specific functions are terminated by the PON transmission sub-layer, and it is not seen from the adaptation sub-layer. The XTC layer will be analysed in chapter 5.

Physical layer Requirements

XG-PON architecture is based on a single fibre transmission using fibre types described in ITU-T G.652. To achieve a low cost implementation of such a compatibility feature, the retained wavelengths are:

- for the upstream "O- Band" ranging from 1260 to 1280nm,
- for the downstream "1577nm" ranging from 1575 to 1580nm.

In the optical power budget, co-existence of GPON and XG-PON on an ODN featuring class B+ [99] optical budget is the nominal requirement. With the additional loss introduced by the new architecture, two "Nominal" power budget classes have been selected: Nominal1 (29dB) and Nominal2 (31dB) at BER of 1E-12. In addition, co-existence of Gigabit PON and XG-PON on an ODN featuring C+ optical budget drives the extended power budget requirement, allowing for an additional split in the ODN with appropriate margins, or alternatively an increase in the supported system reach.

By considering split ratios, as many network operators have constructed their ODN infrastructure with 1:32 to 1:64 split for GPONs; 1:64 split (subject to the overall loss budget) shall be the minimum requirement for XG-PON to allow coexistence.

Also, ITU-T G.987 introduces the concept of fibre distance and maximum differential fibre distance. XG-PON1 must support the maximum fibre distance of at least 20 km.

In addition, XG-PON1 TC layer needs to support the maximum fibre distance of 60 km. XG-PON1 TC layer also needs to support the maximum differential fibre distance of up to 40 km.

System level requirements are also considered. Power saving in telecommunication network systems has become an increasingly important concern in the interest of reducing operators' OPEX and reducing the network contribution to greenhouse emission gasses. The primary objective of the power saving function in access networks is to keep providing the lifeline service(s). Full service mode, dozing mode, and sleep mode are the options that can offer various levels of power saving during the normal mode of operation. In addition, when the mains outage happens, power shedding should be activated for the power saving capability [1].

Also, the XG-PON OLT shall support DBA for the efficient sharing of upstream bandwidth among the connected ONUs and the traffic-bearing entities within the individual ONUs based on the dynamic indication of their activity. The dynamic activity indication can be based on the following two methods:

- Status reporting (SR) DBA employs the explicit buffer occupancy reports that are solicited by the OLT and submitted by the ONUs in response;
- Traffic monitoring (TM) DBA employs OLT's observation of the actual traffic amount in comparison with the allocated upstream transmission opportunities.

It is outside the scope of the requirement specification to define which specific methods have to be supported.

In this work, a special interest is for ITU-T 987.3 FSAN recommendation. It is present in Annex A and is discussed in Chapters 5 and 6.

1.1.6.2. IEEE 10G-EPON (802.3av) Recommendation

The IEEE 10G EPON Study Group has produced the standard 802.3av-2009 IEEE Standard that defines the access method and Physical Layer Specifications and Management Parameters for 10Gb/s Passive Optical Networks [2].

Some necessary amendments to the MAC layer and above layers to accommodate the new physical layer specifications as well as to achieve a smooth system upgrade are accepted. For this, the following three types of ONUs can coexist in the same PON.

- 1) Symmetric Downstream 10G/Upstream 10G,
- 2) Asymmetric Downstream 10G/Upstream 1G,
- 3) GE-PON Downstream 1G/Upstream 1G.

Fig. 1.10 shows the scheme for achieving this. 10G/1G signals are transmitted in different wavelength bands (i.e., 1575–1580 nm downstream and 1480–1500 nm upstream) at the OLT, and the ONU selects one signal or the other by using wavelength-division multiplexing (WDM). 1G/10G signals are transmitted within the same/overlapped wavelength band (1260–1360 upstream and 1260–1280 nm downstream) at ONUs, but the upstream signal from each ONU is transmitted so as to arrive at the OLT at a different timing from those of the others under the OLT's control using TDMA. To receive consecutive upstream signals having different speeds (i.e., 1G or 10G) and different powers from each other, a dual-rate burst receiver is necessary in OLT. The 10G-EPON standard includes the dual-rate receiver implementation [100].

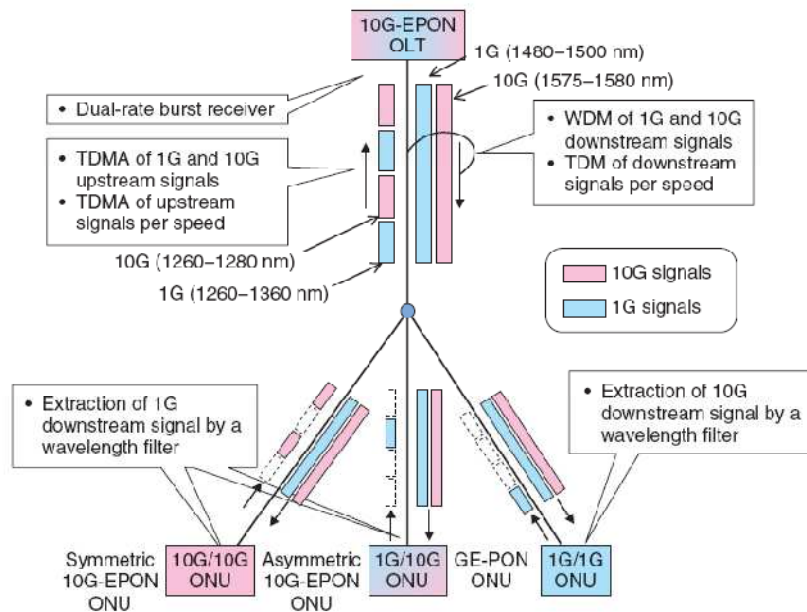


Fig. 1. 10 - Schematic of signal multiplexing in IEEE 10G-EPON [100].

The wavelength allocations of GE-PON [94], asymmetric 10G-EPON, and symmetric 10G-EPON are summarized in Fig. 1.11. Also, wavelength allocations of GPON and XG-PON, for compatibility considerations are shown.

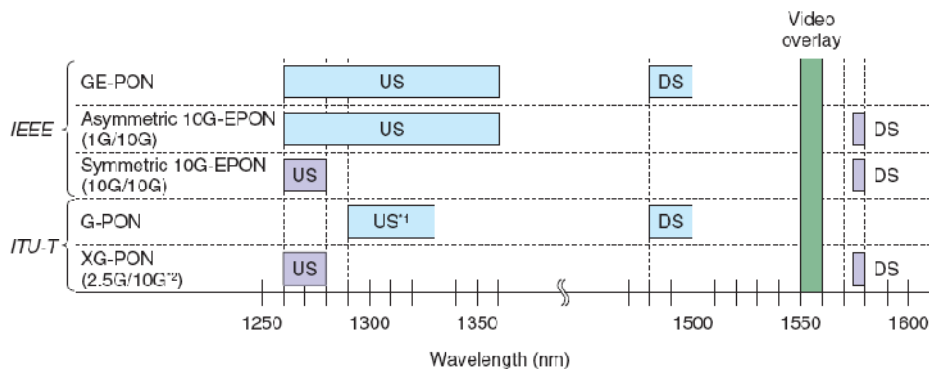


Fig. 1. 11 - Wavelength allocations of IEEE GE-PON & 10G-EPON and ITU-T G-PON & XG-PON ([100]).

10G-EPON uses a high-gain forward error correction (FEC) code, Reed-Solomon (255, 223), to make possible low-cost optical transceiver modules. Aside from the physical layer specifications, specifications for achieving the following features are included in the standard.

So, different of GE-PON, which was a fixed value, adjustable laser on/off time is considered in multipoint MAC control (MPMC), to allow flexible system operation matched to the performances of the lasers transmitting the upstream burst signals

Also, extended MAC control frames to allow various MAC-control implementations that are not defined in IEEE standard 802.3 to accommodate various system requirements flexibly; and activation of a ranging window for each upstream speed in MPMC to allow the coexistence of the three types of ONUs and discrimination between GE-PON and asymmetric 10G-EPON from the same 1G upstream frame. Dynamic bandwidth allocation (DBA) algorithm is out of the scope of the standard.

1.1.6.3. ITU-T XGPON – IEEE 10GE-PON alignment

Also, likely directions for the development of the NG-PON should consider the IEEE 802.3av alignment. The standardization of IEEE 10G-EPON and ITU-T XG-PON is being conducted through active exchanges of liaison documents as shown in Fig. 1.12.

This cooperation is expected to lead to greater value in both standards. This liaison would allow ITU NG-PON systems to leverage volumes of 10G-EPON optics (cost/benefits). However, other proposed alternative PMDs for NG-PON (DWDM-based channelization) exists, and the NG-PON 2 proposed exists, incompatible with GPON and GE-PON legacies.

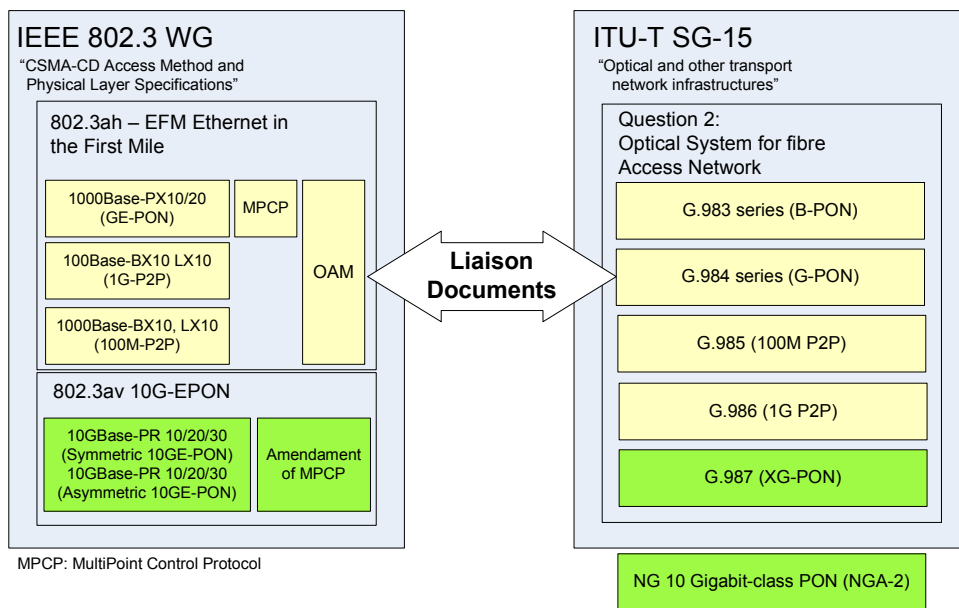


Fig. 1. 12 - Structure of optical access standardization in ITU-T and IEEE (modified from [100])

1.2. Thesis Outline

1.2.1. Objectives

The general objective of this thesis is to design and to optimize a WDM/TDM PON bidirectional single-fibre/single-wavelength RSOA-based ONU network, at PHY and MAC layers, as an alternative of reliable, cost-effective deployment and faster broadband access solution for greenfield PON.

The specific objectives of this thesis are the following:

- 1) To do, for the first time, a deep analysis of the Rayleigh backscattering in burst mode transmission to obtain mathematical expressions to understand its behavior and to apply techniques to mitigate their effects.
- 2) To optimize a WDM-PON RSOA-based ONU network by analyzing the RB behavior and by demonstrating that the Rayleigh substantially varies depending on the position of the distribution element. This optimization process can be used efficiently to minimize the RB effect in the next generation WDM access networks.
- 3) To design and optimize a TDM-PON RSOA-based ONU Single-fibre/wavelength network, to obtain the maximum number of user over the standard length (20 km), focusing on the best tradeoff between the most critical parameters.
- 4) To design and optimize a WDM/TDM PON with ONU rSOA and SCM modulation based. The target is to obtain a cost-effective, simple and with full service coverage network (up to 1280 users) at 2.5 Gb/s / 1.25 Gb/s downstream/upstream, over 20 Km, and being compatible with the GPON ITU-T recommendation.
- 5) To extend the design, architecture and capabilities of a WDM/TDM PON RSOA-based for a long reach metro-access network at the layer 2 level. A proposal of Transmission Convergence sub-layer (OSI model layer 2), is a relevant objective of this work. It is based on the optimization of the standards GPON and XG-PON (for compatibility), but applied to SARDANA network.
- 6) To establish the connectivity requirements and possible configurations for SARDANA internetworking in the context of broadband access, metro and transport network level, by empowering Transmission Convergence (TC) layer functionalities.

1.2.2. Organization of this Thesis

This work is organized as follows.

Chapter 2 introduces some practical optimization aspects for a WDM-PON network, related with the WDM multiplexer position, the Rayleigh backscattering and RSOA gain, to go to deeper analysis of a WDM/TDM PON SCM-based and its optimization.

Chapter 3 presents a Rayleigh backscattering analysis in burst mode transmission for a TDM-PON network. Based on this analysis a TDM-PON rSOA-based ONU network is designed and optimized.

Chapter 4 focuses in SARDANA network, a Metro-Access WDM-TDM NG-PON network. Physical layer characteristics and field trial are shown.

Chapter 5 presents a new proposal for Transmission Convergence (TC) layer of SARDANA network, compatible with TC of XG-PON. This novel TC allows SARDANA to deploy internetworking functions. An agile ONU activation process by simplification of the ranging state is also shown. Although SARDANA is long reach (up to 100 km), this optimization improves a 44% the performance with respect to XG-PON (20 km).

Chapter 6 shows a physical implementation for the STC SARDANA architecture over the SXGPON original draft. OLT/ONU prototypes and suitable interfaces for interconnection with higher layer clients and OLT/ONU optical assemblies at the PHY layer are deployable. Also, connectivity requirements and possible configurations for SARDANA internetworking with other communications systems, in the context of broadband access, are proposed. Different internetworking services can be implemented at the PHY level, at the metro network level or at core transport network level.

Finally, in Chapter 7, conclusions of this work and future research are presented.

Chapter 2

2. WDM and WDM/TDM-PON Network Optimization

The existing recommendations and standards for PONs, as the IEEE 803.2ah Ethernet Passive Optical Network (EPON), the IEEE 803.2av 10-Gigabit Ethernet Passive Optical Network (10G-EPON), the ITU-T G.984 Gigabit-capable Passive Optical Network (GPON) and the ITU-T G.987 10 Gigabit-capable Passive Optical Network (XGPON), are based in TDM technology, offering different degrees of service and network performance.

A particular PON architecture still in research, where different wavelengths are used in order to increase the number of channels by means of wavelength division multiplexing (WDM) technology is called WDM-PON.

The upgrade of PONs with WDM technology requires the controlled generation of different wavelength for transmission. This can be readily done at the OLT, but can be a major problem at the ONUs, because of the wavelength stability required and the inventory complexity to supply a different DFB laser at each customer. A possible solution is the use of a tunable laser at the ONU, but its control is complex and its cost is still too high. In consequence, the best realistic option is the reflective ONU with centralized seeding light at the Optical Light Termination (OLT) [82], as the best cost-effective potential solution. This avoids the use of any wavelength generation at ONU and is suited for bidirectional single-fibre access, simplifying the fibre plant. Also, it implements a cost effective NG-PON network by the use of a

single-fibre for both, upstream and downstream transmission, and uniform and wavelength independent components at the ONU (colourless) for a transparent WDM-PON scenario. Reflective SOAs (RSOAs) are promising devices to implement such reflective ONUs, because their simultaneous amplification, detection and modulation capabilities. However, Rayleigh backscattering arises as the dominant impairment in this type of implementation respect to others interferences [74].

In this first section the penalties in the upstream and downstream paths in WDM-PON networks due to RB signals are analysed with respect to the relevant design parameters and to optimize the system by establishing the most adequate location of the distribution element, considering the optimum ONU gain on each case.

Furthermore, advances in WDM photonics and in electronics may provide scalability from commercial FTTH TDM PON infrastructures. A combination of TDM and WDM technologies in the Optical Distribution Network (ODN) would allow increasing the number of ONUs served. These latter's technologies are part of the next generation of PON networks (NG-PON). Thus, in the second section of this chapter, a WDM/TDM PON system with reflective ONU was designed, simulated, optimized, implemented and tested.

Characterization of the device parameters and impairment effects, in order to establish the elements most suitable were analytically modeled. Definition of the best modulation formats for the prototype was established. Several advanced techniques have been proposed and tested by means of simulations. Functional and electrical/optical schemes and mathematical analysis, in bidirectional transmission, were obtained. Results are shown in terms of power budget, splitting ratio, up/down tradeoff, and power values in key points of the system.

This prototype was successfully tested showing high performance, robustness, versatility and reliability. So, the system is able to give coverage up to 1280 users at 20 Km of fibre length, at 2.5 Gb/s in downstream and 1.25 Gb/s in upstream.

2.1. Optimization of a rONU-based WDM-PONs in Rayleigh-limited by optimal ONU Gain and WDM position

A cost-effective and efficient development in PONs proposes to employ a reflective structure at the Optical Network Unit (ONU), with centralized seeding light at the Optical Light Termination (OLT) [70,74,82]. The carrier signal (CW) is modulated with the user data at the ONU and back reflected in the upstream direction on the same wavelength. In this full-duplex single-fibre bidirectional transmission context, Rayleigh backscattering is the dominant impairment with respect to others interferences [74].

In this section the penalties in the upstream and downstream paths due to RB signals are analysed with respect to the relevant design parameters and to optimize the system by establishing the most adequate location of the distribution element (WDM-MUX) in WDM-PON networks, considering the optimum reflective ONU gain on each case.

After the theoretical and experimental analysis, it is determined that best Crosstalk-to-Signal ratio (C/S) is achieved if the multiplexer is placed either in the ONU or OLT vicinity, and the ONU gain has a new optimum value depending on the position. Also, it is demonstrated that Rayleigh Backscattering (RB) is generally irrelevant in downstream transmission. Other effects, like the RB gain saturation [101] and the variation of the bandwidth of the receiver and the optical filter [102], are not considered in this analysis.

2.1.1. Rayleigh Backscattering Analysis in Upstream path

In WDM-PON, the MUX in the fibre path separates the wavelength channels, introducing a fixed attenuation. This splits the RB analysis into two zones: the feeder section ($RB_{OLT-MUX}$) and the drop section ($RB_{ONU-MUX}$), as shown in Fig. 2.1.

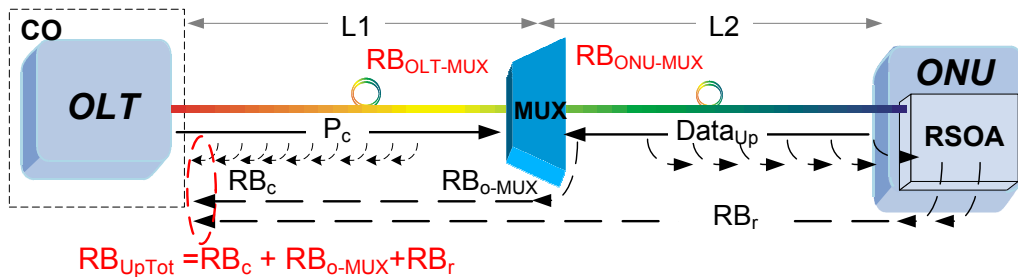


Fig. 2. 1 - Schematic of a plain WDM-PON with MUX at the fibre plant.

The crosstalk (C) at the upstream path, defined as the RB power at the OLT input, is the incoherent sum of the several RB contributions. The RB generated by the downstream carrier signal at the OLT-MUX section ($RB_c = P_c \cdot B(1-l_1^2)$); the Rayleigh produced at the MUX output in upstream direction ($RB_{o-MUX} = P_c \cdot B(1-l_2^2) \cdot A^2 \cdot l_1^2$); and the RB generated by the upstream signal, reflected and reamplified by the ONU and transmitted to the OLT (RB_r), which dominates in the drop side, although it is reduced in one order of magnitude lower (twice the insertion losses of the MUX), being: $RB_r = P_{o-ONU} \cdot B(1-l_2^2) \cdot (g \cdot l_1 \cdot l_2 \cdot A)$, where l_1 and l_2 are the fibre losses in the feeder and the drop sections, respectively ($l_n = e^{-\alpha \cdot L_n}$), L_n is the corresponding fibre length (with $L=50\text{km}$), g is the ONU gain, P_{o-ONU} is the ONU output

power ($P_{o-ONU} = P_c \cdot (g \cdot l_1 l_2 A)$), P_c as the OLT output power, A is the MUX insertion loss, α is the fibre attenuation and B is the Rayleigh coefficient (here $3.2 \times 10^{-5} \text{ Km}^{-1}$) [93].

The resulting Crosstalk-to-Signal ratio C/S or $OSRR^{-1}$ (inverse Optical Signal-to-Rayleigh Ratio), is then:

$$\left[\frac{C}{S} \right] = B \frac{(1-l_1^2) + (1-l_2^2) \cdot A^2 \cdot l_1^2 + (l_1 l_2 A)^2 (1-l_2^2) g^2}{(l_1 l_2 A)^2 g} \quad \dots\dots(2.1)$$

The second term is generally negligible, as attenuated by A^2 . Fig. 2.2 shows theoretical C/S as a function of the feeder length for ONU gain of 10, 15 and 20 dB. It is observed that there is a strong dependency on the gain, especially at the edges. Thus, it is found relevant to minimize the C/S ratio; an optimal gain g_{opt} as a function of the MUX position can be obtained by

$$\partial(C/S)/\partial g = 0, \text{ resulting in: } g_{opt} = \frac{1}{l_{total}} \sqrt{\frac{(1-l_1^2)}{(1-l_2^2)}} \quad \dots\dots(2.2)$$

With the MUX in an intermediate position, the optimum gain is equal to the total link loss $l_{total} = l_1 l_2 A$ (here, 15 dB). If the MUX is in the ONU vicinity, the optimum ONU gain values increases to about 20 dB and higher. In contrast, if the MUX is near the OLT, a low ONU gain between $10\text{--}15 \text{ dB}$ improves the C/S performance.

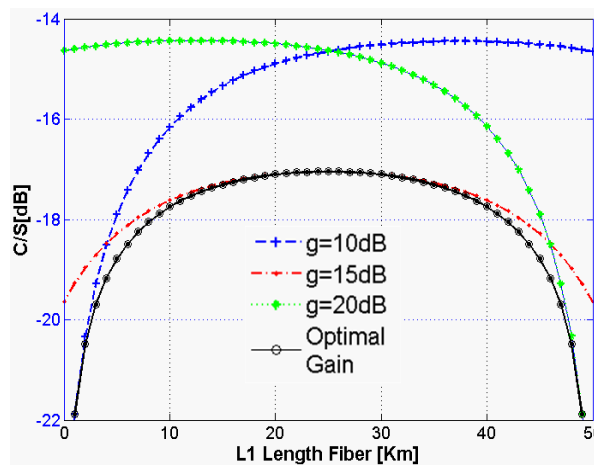


Fig. 2. 2 - Theoretical C/S as a function of the feeder length for ONU gain of 10, 15 and 20 dB and for the optimal gain (Eq.2 in 1), with $\alpha(\text{dB})=0.2\text{dB/Km}$, $L1+L2=50\text{Km}$, $A=5\text{dB}$, Optical Distribution Network (ODN) total loss= 15dB .

In Fig. 2.2, the C/S with optimum gain is also plotted; minimum C/S corresponds to MUX close to the OLT or close to the ONU. It is preferred the MUX close to the ONU as for this case, the optimal gain is higher than the link losses, providing a valuable power margin. Also, the use of a unique fibre carrying all wavelengths near to the ONU premises is more cost-effective.

Fig. 2.3 plots the optimal gain vs. MUX position for different MUX loss (A) values. We observe a wide range around the intermediate position where the optimum value is about the link loss. At the edges, the performances improved, although the behaviour gets rather critical with the gain selection. The worst

positions for the MUX as a function of the gain are obtained differentiating equation 2.1 and equalizing it to 0:

$$\frac{\partial(C/S)}{\partial l_1} = 0 \Rightarrow L_1 = \frac{1}{4\alpha} \cdot \ln\left(\frac{1}{A^2 \cdot g^2}\right) + L \quad \dots\dots\dots(2.3)$$

For $g=10, 15,$ and $20dB$, maximal C/S are found in $L_1=37.5$ km, 25 km and 12.5 km respectively. It is somehow remarkable that again equal to the total link loss ($15dB$) is optimum at the intermediate position but, at the same time, the intermediate position is slightly the worst for this gain.

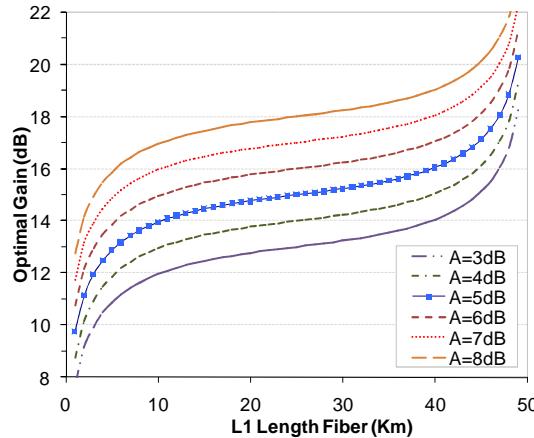


Fig. 2. 3 - Optimal gain as function of the distance to different values of A.

2.1.2. Rayleigh Backscattering Analysis for Downstream

For this analysis, the OLT generates a wavelength carrier intensity modulated with NRZ data signal. This downstream signal is detected at the ONU with the photo-detector, together with the RB at the ONU input. This is shown in Fig. 2.4.

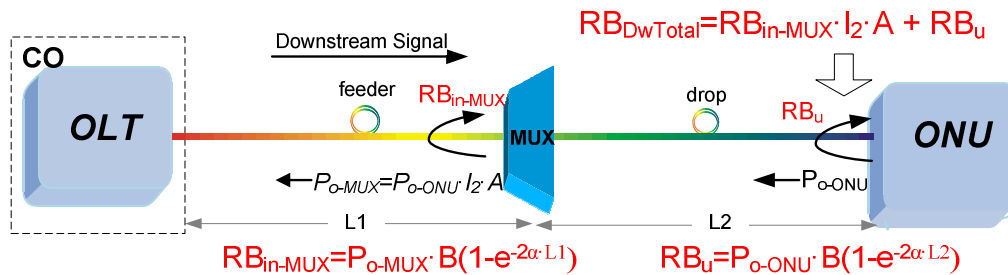


Fig. 2. 4 - Scenario for the downstream analysis.

From Fig. 2.4, the RB at the ONU input is given by:

$$RB_{DwTotal} = P_{o-ONU} \cdot B \cdot [l_2^2 \cdot A^2 (1 - l_1^2) + (1 - l_2^2)] \quad \dots\dots\dots(2.4)$$

From Eq. 2.4, it is observed that the $RB_{DwTotal}$ depends more on the RB due to ONU output power, where a considerable reduction of the RB_{in-MUX} is received at the ONU, about one order of magnitude lower (twice the insertion losses of the MUX) than the RB_u at the drop section. So, when l_2 is maximum (MUX at the OLT), then: $RB_{DwTotal} \approx RB_u$. In this location RB_u is maximal too and $RB_{DwTotal}$ becomes the relevant expression, especially when the ONU gain is above the link loss. The optimum case is when the MUX is

near ONU, $L_2 \rightarrow 0$, and $RB_{DwTotal}$ is minimal.

2.1.3. Simulations performed

Simulations were performed using the VPI Transmission Maker software of Virtual Photonics Inc. A data rate of 1.25 Gb/s with PRBS of $2^{15}-1$ was used. The OLT consists of a CW-laser, a Mach-Zehnder Modulator, a circulator, and an APD in the receiver side. OLT output power is fixed to 0dBm. ODN is composed of 50 Km of *Universal Fibre* with 0.2 dB/Km of attenuation; a WDM MUX with 5dB of losses is the distribution element. ODN power loss is, thus, 15 dB nominally. The ONU is formed by an Electro-Absorption Modulator (EAM) + Semiconductor Optical Amplifier (SOA) like Reflective-SOA (RSOA), with extinction ratio of 13dB.

Simulations were performed on both, un-modulated carrier and down data transmission. Results in terms of RB power level and BER are the same; although the spectral distributions are different, they overlap. Experimental test will consider the worst case: the distribution of a CW carrier, corresponding to a narrower RB spectrum and then affecting more to the BER [103].

Fig. 2.5 shows obtained C/S as a function of the feeder length for ONU gains of 10, 15 and 20 dB for up-down transmission. In upstream the C/S ratio agrees with theoretical Fig. 2. In downstream, C/S ratios are better than the ones obtained in upstream (especially for $g < 20dB$), and depend on the ONU gain. This dependence does not affect the BER performance that remains well below by several orders of magnitude. Also, it is observed that the best position for the MUX is near ONU. These results demonstrate that the RB power in downstream is negligible, and only becomes relevant when the ONU gain is above the ODN losses with the MUX positioned furthest from the ONU, as also will be shown in Fig. 2.8.

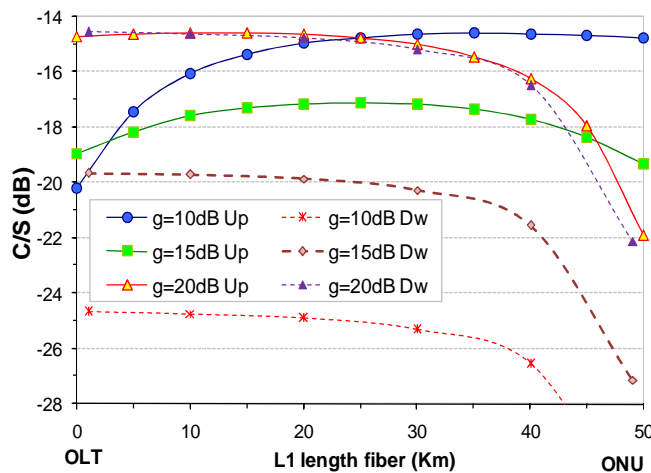


Fig. 2. 5 – Crosstalk-to-Signal (C/S) simulation as a function of the MUX position for ONU gain of 10, 15 and 20 dB in downstream and upstream transmission.

2.1.4. Experimental Measures and Results

Fig. 2.6 shows the experimental setup. At the OLT, a tunable laser was used to feed the ONU at 1550.14 nm , matching the MUX channel. The power applied to the feeder fibre was 0 dBm . The upstream reception was carried out by an APD (sensitivity of -22.5 dBm for $BER=10^{-10}$). An optical filter ($BW\ 34.5\text{ GHz}$) was introduced before the photo-detection. A variable attenuator was used to obtain the sensitivity curve (Fig. 2.6). The link was formed by two fibre sections of 25 km ($att.\ total=-10\text{ dB}$). A MUX with 5 dB insertion loss was employed.

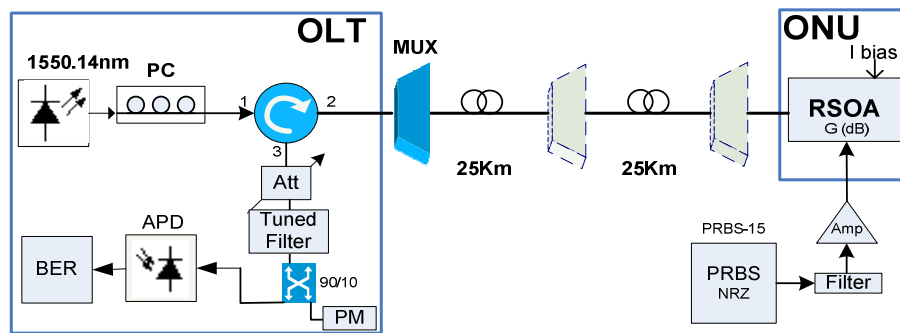


Fig. 2. 6 - Setup for the experimental measurements

The ONU was formed by a *Kamelian RSOA 18-TO-37-08*, directly modulated with the upstream data at 1.25 Gbit/s , ($PRBS\ 2^{15}-1$, $ER=11\text{ dB}$). The RSOA gain values (10 , 15 and 20 dB) were characterized as a function of the bias current (34 , 45 and 80 mA).

Several measurements were carried out for different MUX positions: at the OLT side ($L1=0\text{ km}$, $L2=50\text{ km}$); at the ONU premises ($L1=50\text{ km}$, $L2=0\text{ km}$); and at half-way of the link ($L1=25\text{ km}$, $L2=25\text{ km}$). Back-to-back was performed too (Fig. 2.7). These experimental measurements are compared to the simulation results in Fig. 2.7, performed in the same power and conditions, based in GPON standard, providing similar results.

With the MUX near the OLT, the ONU gain of 10 dB performs the best (2.2 dB penalty), while the worst case is for a gain of 20 dB , with a $BER=10^{-8}$ error floor. This result is due to the high influence of the RB_{UpRef} at the ONU.

At the ONU side, higher amplification improves the system. The penalty for $G=20\text{ dB}$ is 1.5 dB . In this case, there is an error floor in the order of $BER=10^{-7}$ for the lowest gain (10 dB), since RB_c is the limiting factor and the upstream signal is weak. The reflected RB is not relevant due to the double attenuation by the MUX and the feeder fibre.

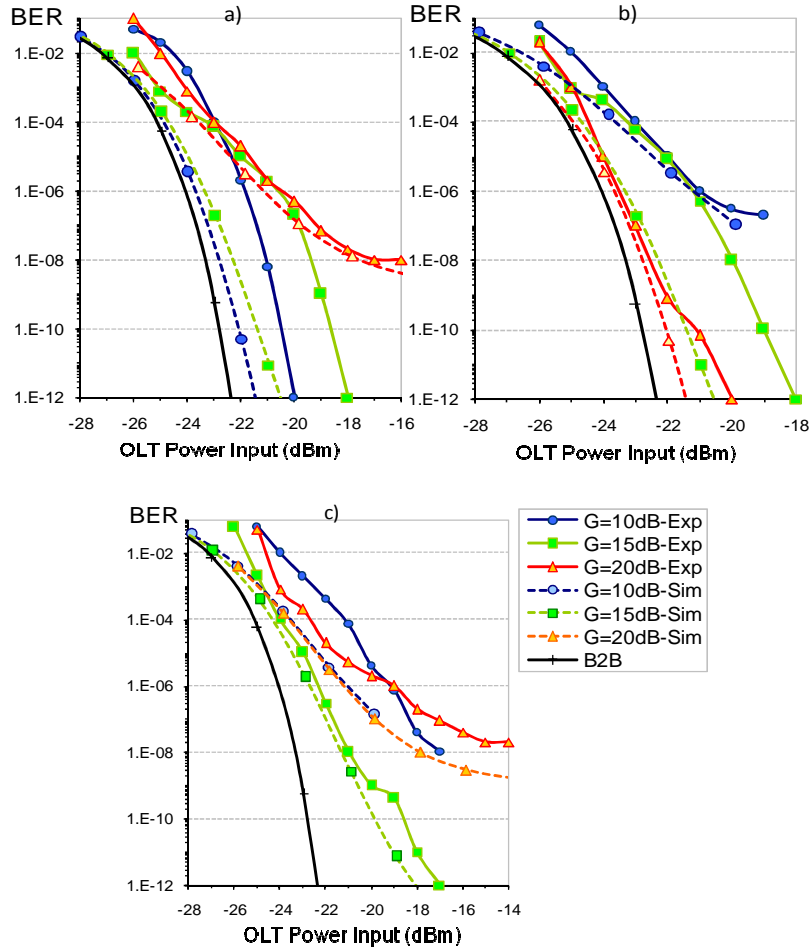


Fig. 2. 7 - BER measurements for 10, 15 and 20dB of ONU gain with the MUX a) at the OLT side. b) at the ONU side c) at half way between OLT and ONU (Experimental and simulated curves).

For the MUX located in the middle of the link, performances are, in general, worse; because the $25km$ of fibre on each side are long enough for the RB generation in both sections. RB_c is the most relevant for low ONU gain while RB_{UpRef} is for high gain. In this case, the ONU gain equal to the link loss is the best (penalty of $3.9dB$).

The BER in upstream and downstream for different values of ONU gain is also shown in Fig. 8 (simulation/experimental). We observe that at any position of the MUX, with an ONU gain recovering the ODN loss ($15dB$), the BER performance is always better than 10^{-10} , at the RX sensitivity specified. However, for low or high gain values (e.g. $10dB$ and $20dB$, respectively), it is possible to be below the required BER only if selecting the MUX location properly. For a $ONU_{gain}=20 dB$, it is better to place the MUX within $10 km$ from the ONU, since longer drop fibre will highly increase C/S . Gain values smaller than $10dB$ are not recommendable because of the receiver noise. For the input powers received at the RSOA ($\approx -15dBm$), no significant gain saturation of the RSOA is observed, that could potentially reduce the crosstalk [101,103].

The upstream BER curves follow the same tendency as the simulation; some differences are due to the limited RX sensitivity, to the difficulty measuring BER values better than 10^{-12} during real tests, and also to the simulation model where only RB noise was taken into account. Fig. 2.8 also includes the results

from BER simulations in downstream.

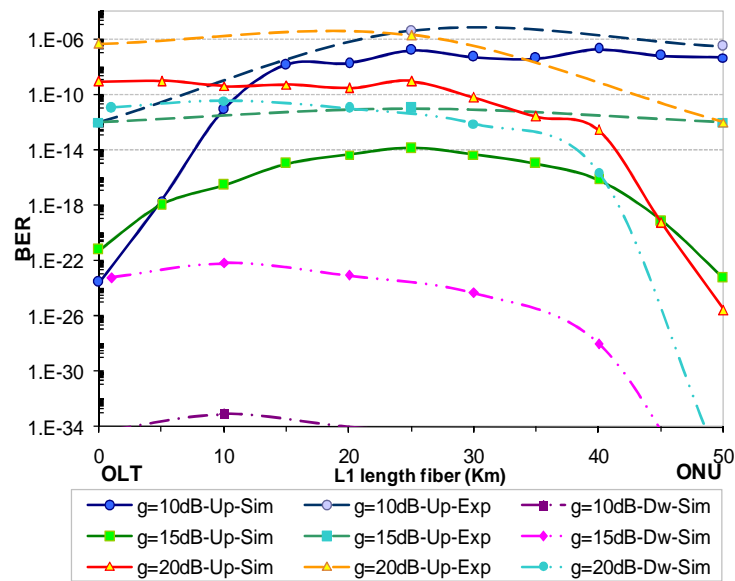


Fig. 2. 8 - BER as a function of the MUX position to different ONU gain values (Simulations and Experimental results).

2.1.5. Conclusion

We demonstrated that the Rayleigh crosstalk signals substantially vary depending on the position of the distribution element, since they are determined by the length of the fibre and by the ONU gain applied. Although, in a real-world deployment, the position of the distribution element is usually determined by more practical considerations, like the cost, the physical distribution of the customers, etc, this study provides relevant information in terms of transmission optimization in WDM-PON. The results revealed that the best performance can be achieved if the distribution element is placed either in the ONU or OLT vicinity, at the expense, in such cases, that the ONU gain takes a new optimum depending on that exact position. Also, it was demonstrated that the downstream RB power is generally irrelevant for the data transmission. These results can be used efficiently to minimize the RB effect in the next generation WDM access networks.

2.2. WDM/TDM PON architecture optimization

A combination of TDM and WDM technologies in the Optical Distribution Network (ODN) would allow increasing the system capacity. In this context, a new WDM/TDM PON architecture with bidirectional operation along single-fibre/single wavelength is proposed, aiming to reach a greater number of users or a higher range in a way cost effective by using reflective ONUs.

This section describes this architecture as a part of the project “Scaling PON systems beyond current standards” developed by UPC-Optical Communications Group and Tellabs Inc. It had as main goal the design and implementation of the best WDM/TDM-PON ONUs based on RSOA. Optimization processes were done. For such effect, a series of tasks were developed and are presented.

Fig. 2.9 shows the proposed architecture over the PON reference system, considering the fundamental impairments present in a WDM-PON.

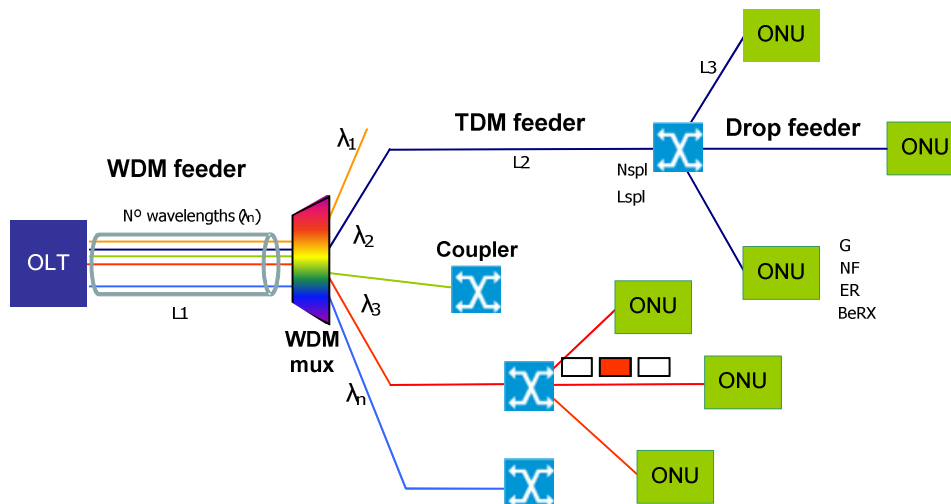


Fig. 2. 9 - WDM/TDM PON Reference Architecture

This approach was tested and optimized over the reference architecture [83,104] at bit rates of 2.5/1.25 Gbit/s, and considering the fundamental impairments present in the WDM-PON, like reflections, Rayleigh backscattering, ASE noise, APD noise, ONU noise accumulation, WDM multiplexer optical response, burst transient response, non-linearity, etc.

The characterization of the device parameters and impairment effects in order to establish the elements most suitable to next implementation were done: APD detectors, extinction ratios, BER/Q factors, and Rayleigh backscattering were analytically modelled. The modulation formats most suitable for this architecture were defined.

Our first WDM/TDM PON model proposed, according to the ITU-T nomenclature, is shown in the Fig. 2.10.

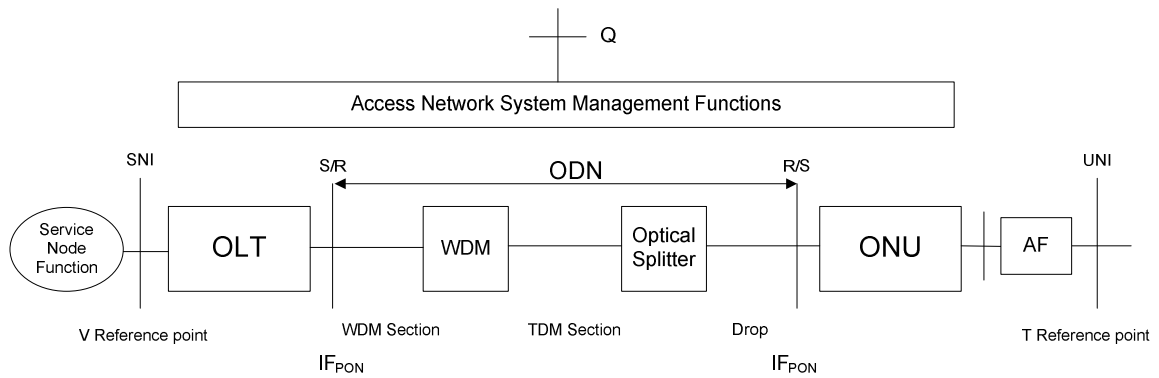


Fig. 2. 10 - Functional Scheme of the WDM/TDM PON System proposed

- ONU: Optical Network Unit
- ODN: Optical Distribution Network
- OLT: Optical Line Termination
- WDM: Wavelength Division Multiplex Module
- AF: Adaptation Function (Sometimes, it may be included in the ONU.)
- SNI: Service Node Interface
- UNI: User Network Interface
- S: Point on the optical fibre just after the OLT (Downstream)/ONU (Upstream) optical connection point
- R: Point on the optical fibre just before the ONU (Downstream)/OLT (Upstream) optical connection point

2.2.1. Modulation Format definition

One great challenge in WDM-PONs is the transmitter at the ONU, which must have a wavelength that is precisely aligned with specifically allocated WDM grid wavelength. A cost-effective solution would ideally employ the same components in each ONU, which should thus be independent of the wavelength (“colourless”) assigned by the network. Optical carriers are distributed from head-end office to different ONUs to produce the upstream signals. Re-modulation of downstream signal to generate upstream signal further reduces the cost by wavelength reuse [105-106].

However, as both downstream (DS) and upstream (US) share the same wavelength, they may easily suffer from crosstalk, which has to be minimized. So, it is very important that modulation formats of the DS and US signals should be carefully defined.

Several re-modulation schemes have been proposed, using both DS and US on-off keying (OOK) [107]. For such, the extinction ratio of the downstream signal had to be small enough to minimize the residual modulation present at the upstream signal, but large enough for correct detection at the ONU. Substantial efforts have been done to develop wavelength re-modulated WDM-PON technology including non-return-to-zero (NRZ) coding with RSOA [108]. The NRZ coding requires amplitude compression of downstream signal with gain saturated RSOA. NRZ pulse shape-defined formats have generally narrower spectrum than RZ pulse shape-defined formats. The modulation format for the downstream, without substantial increase in the hardware complexity, was Intensity Modulation with reduced extinction ratio [82].

As an alternative, the downstream data can be modulated with a modulation format constant in amplitude, such as frequency shift keying (FSK) or phase shift keying (PSK), whereas ASK is used for the upstream data. The advanced modulation formats: differential phase-shift keying (DPSK) [106] or quaternary DPSK (QDPSK) [109] could be exploited for the downstream signal to tackle the problem of reduced extinction ratio of the downstream signal. Moreover, in optically amplified systems, DPSK requires nearly 3 dB lower SNR than OOK formats, enabling extended reach. DPSK erasure and orthogonal DPSK/intensity modulation (IM) scheme for virtual private network has also been proposed [110]. In [111], the re-modulation scheme using DPSK modulation format in both downstream and upstream signals for “colourless” dense (DWDM) PONs are proposed and demonstrated.

Another solution is to use sub-carrier multiplexing (SCM) in the electrical domain carrying uplink and downlink in different RF sub-carrier. Thus, signals are spectrally separated and do not interfere with each other. Here, we analyze this SCM-IM modulation format [111-113], because it does not require extra optical devices.

2.2.1.1. SCM Modulation Format

In PON networks different modulation schemes for down/up transmission have been demonstrated [82,114-117]. However, these methods may not be cost-effective due to the components needed for the modulation and detection of these signals. A more cost-effective solution is the use of a sub-carrier multiplex (SCM) technique with direct modulation [118-119].

Optical sub-carrier multiplexing (SCM) is a scheme where multiple signals are multiplexed in the radiofrequency (RF) domain and transmitted by a single wavelength. A significant advantage of SCM is that microwave devices are more mature than optical devices in terms of stability, frequency selectivity and coherent detection, and more advanced modulation formats can be applied easily.

A summary of the total required bandwidth needed at the ONU receiver for each proposed modulation for 2.5 Gb/s, can be found on Table 2.1. According to that table, the more efficient are multi-level PSK. However, they are the more complex to be implemented.

Table 2. 1 - Bandwidth limits for different sub-carrier modulations

Modulation Format	Double-sided modulation bandwidth	Sub-carrier frequency	Minimum photo-detector bandwidth
SCM-DPSK	3.75 GHz	5 GHz	7.5 GHz
SCM-BPSK	3.75 GHz	5 GHz	7.5 GHz
SCM-QPSK	1.875 GHz	2.5 GHz	4.375 GHz
SCM-DQPSK	1.875 GHz	2.5 GHz	4.375 GHz

The theoretical sensitivity, in order to define the modulation format most adequate for our system is shown in Fig. 2.11. Error probability (P_e) for several modulation formats are obtained from [120]. For DSPK SCM modulation the Error probability is given for:

$$P_e = 0.5 \cdot e^{-OSNR}$$

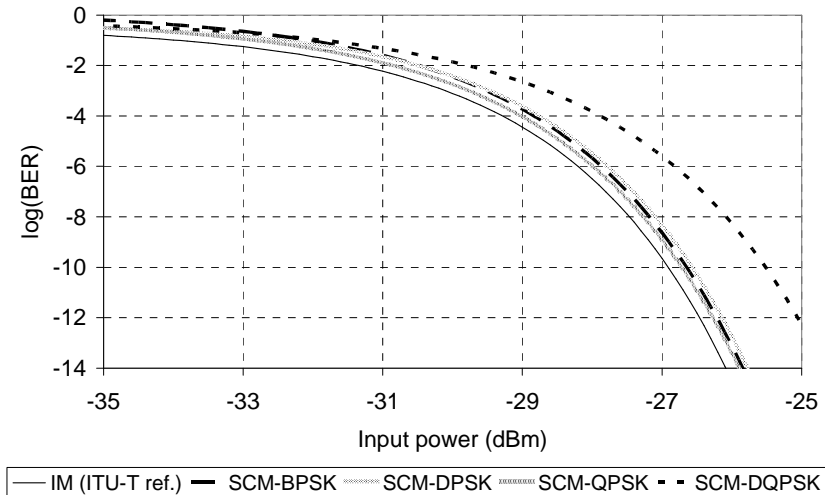


Fig. 2. 11 - Theoretical sensitivity for the proposed modulation formats

The main sensitivity values found are shown in Table 2.

Table 2. 2 - Sensitivity values for $P_e = 10^{-10}$ and $P_e = 10^{-4}$.

	Sensitivity ($P_e 10^{-10}$)	Sensitivity ($P_e 10^{-4}$)
IM 2.5 Gbps (ITU-T)	-27 dBm	-29.3 dBm
SCM-BPSK	-26.7 dBm	-28.9 dBm
SCM-DPSK	-26.6 dBm	-28.8 dBm
SCM-QPSK	-26.8 dBm	-29.1 dBm
SCM-DQPSK	-25.5 dBm	-27.8 dBm

SCM DPSK is the most simple and low-cost for implementing, since there is no need for electrical phase-locking. It will be the modulation format used for the implementation of our SCM-WDM/TDM PON system. Simplified electrical scheme for the DPSK is shown in Fig. 2.12.

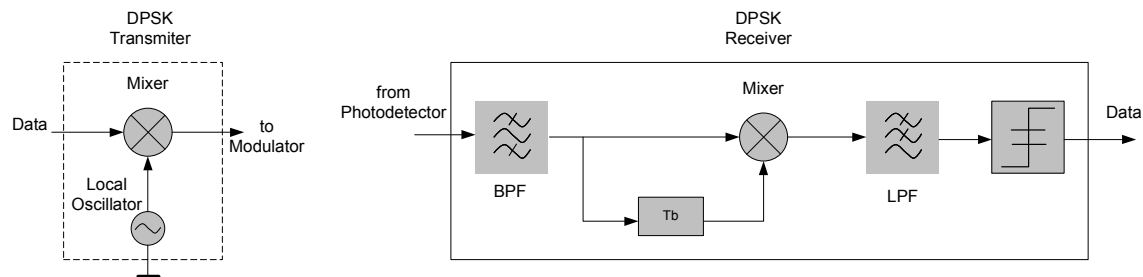


Fig. 2. 12 -DPSK scheme for up-converting a differential pre-coded signal at the OLT side (left), and for detecting such a signal at the ONU side after photo-detection (right).

SCM has been limited to 1.25 Gbps downstream up to now, with the electrical schemes not optimized [111-113].

2.2.2. Computer Simulations

Computer simulation of the full system for using Virtual Photonics Inc. (VPI) Transmission Maker was done. A definition of the WDM/TDM-PON network reference scenario in terms of schematic, components and main requirements have been established.

A preliminary approach is shown in Fig. 2.13 at 2.5/1.25 Gbit/s bit rates. Here, the ONU and OLT are represented as VPI's galaxies. In these simulations are considered the fundamental impairments present in the WDM/TDM PON (reflections, Rayleigh backscattering, ASE noise, APD noise, WDM multiplexer optical response, non-linearity's). In this first stage, the bidirectional transmission link is divided in three stages: WDM feeder, TDM feeder and Drop fibre.

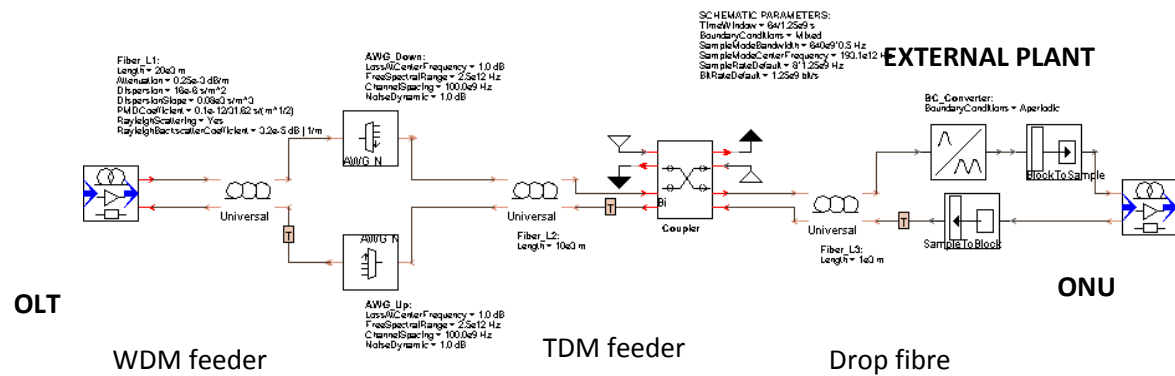


Fig. 2.13 - WDM-PON preliminary schema - Link in three stages

In this design, the Power budget at the ODN is detailed in the Table 2.3.

Table 2.3 - Power Loss at ODN

Power Budget at ODN		
Element	Insertion Loss	Comment
Fiber Length	5.0 dB	20 Km x 0.25dB/Km
AWG	4.0 dB	
Coupler	3.2 dB	(-3.2 dB by 2^n ONUs)
Total	12.2 dB	

2.2.2.1. OLT Schematic

The downstream data signal is modulated on an RF sub-carrier by using SCM-DPSK modulation. An electrical oscillator, running at 5 GHz, is used. Two band-pass 4th-order Bessel filters, centred at 5 GHz and 3.75 GHz bandwidth, are placed at both, the transmitter and receiver sides.

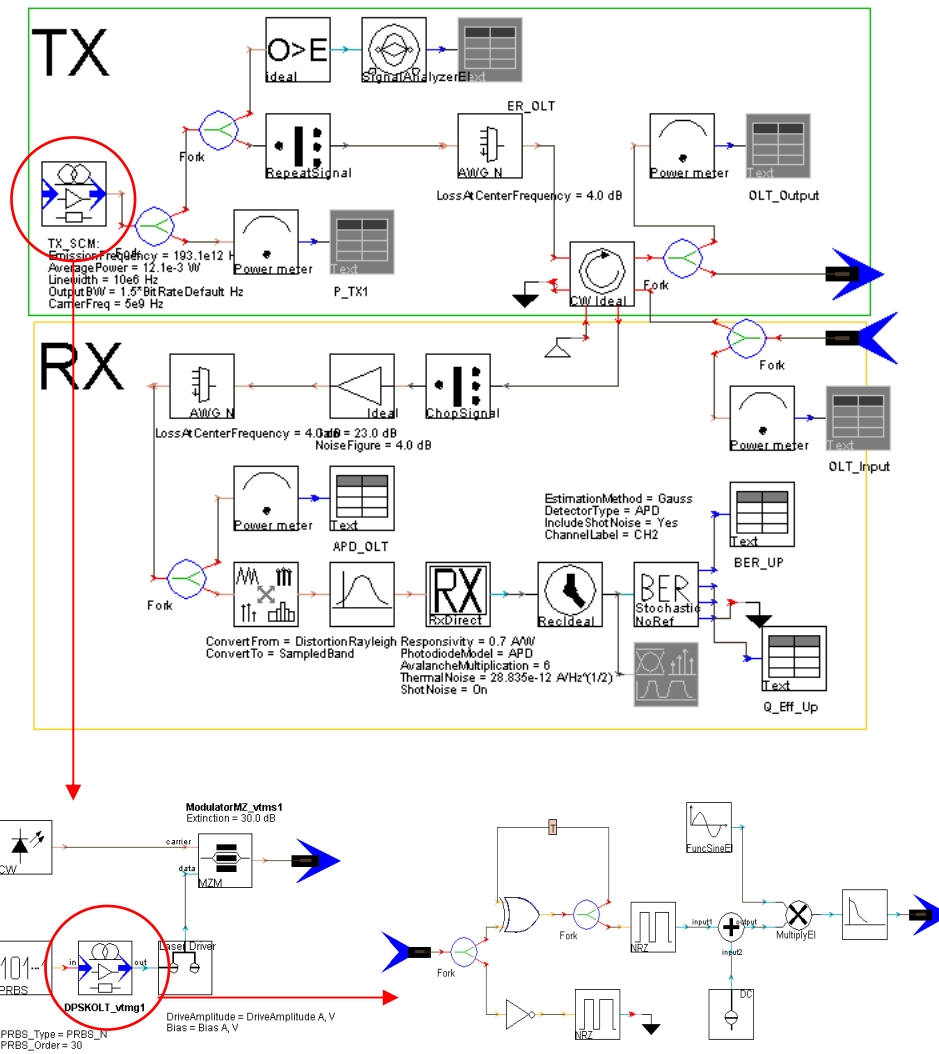


Fig. 2. 14 - VPI scheme of the OLT SCM System

The resultant signal modulates an optical carrier via a MZM. The Extinction Ratio at the OLT is set through a Laser Driver module. Fig. 2.14 shows the OLT VPI scheme. The SCM transmitter is inside in the TX galaxy.

OLT Characteristics values:

TX:

- ER-OLT=8.4dB
- Power Output= 0dBm
- SCM-TX: Output BW= 1.5*Bit Rate Default, Carrier Frequency = 5GHz.
- Loss at the OLT-TX = Loss Modulation + IL (AWG) + IL (Circulator)

RX:

- APD Receiver (OLT) with Thermal Noise= $28.835E-12 \text{ A/Hz}^{1/2}$, responsivity=0.7 A/W and Avalanche Multiplication = 6.0.
- Loss at the OLT-RX = IL (AWG) + IL (Circulator) = 4dB + 1.5dB = 5.5dB.

2.2.2.2. ONU Schematic

ONU VPI scheme, shown in Fig. 2.15, include the SCM-RX and a RSOA galaxies.

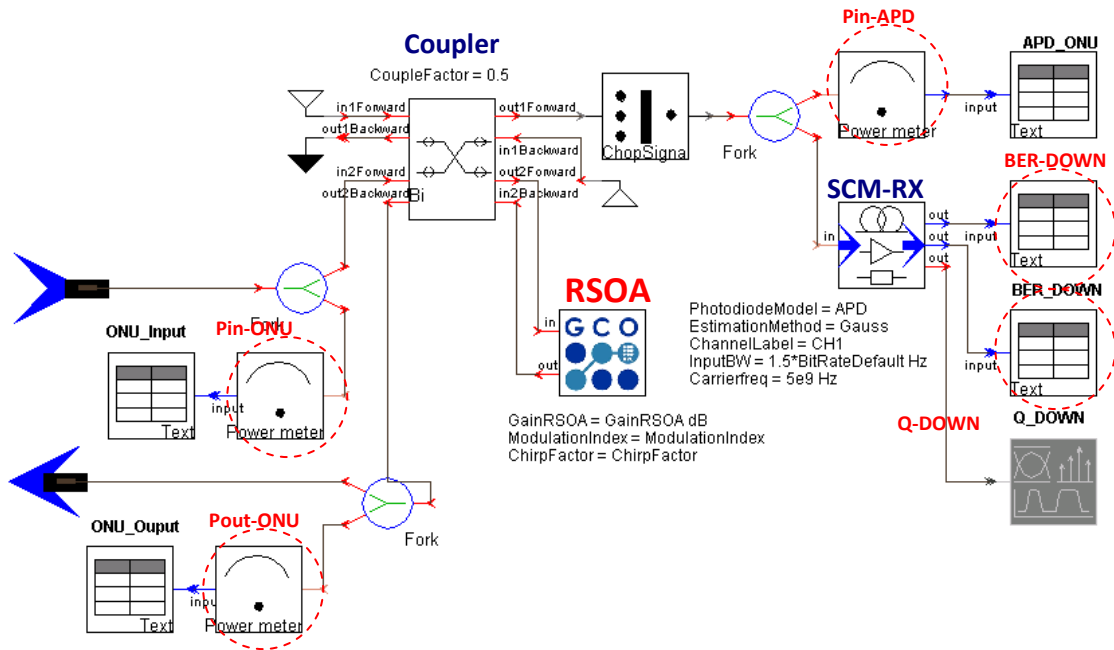


Fig. 2. 15 - VPI scheme of the ONU Reference System

RSOA VPI Model

The RSOA was modeled in VPI software as a functional Block instead of a Sample module (described by a physical model of the device). The difficulties to manipulate some parameters directly (Noise Figure, Extinction Ratio and Chirp) and the computation time, was determining for not using the full physical model.

Thus, RSOA was emulated with an Ideal Amplifier (Gain and Noise Figure parameters) and an Electro-Absorption Modulator (EAM) (characterized by the bias, chirp and ER (through the modulation index)). This RSOA functional model is shown in Fig. 2.16. The ONU extinction ratio is setting in 13 dB (modulation index = 0.95).

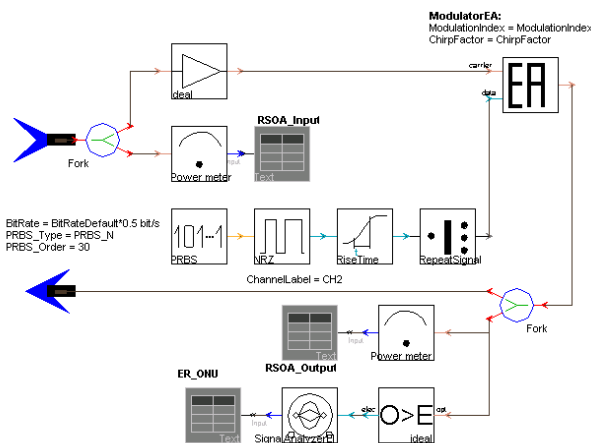


Fig. 2. 16 - RSOA functional model (based on SOA Ideal Amplifier + EAM)

SCM Receiver

The SCM scheme (at the ONU receiver) is shown in Fig. 2.17. It includes the photo-detector, the RF filter, the differential demodulator, the LP filter and the BER estimator. The simulations show the performances depending on shot and thermal noise and as a function of the photo-detector bandwidth. In particular, a Q factor of 6 can be achieved for a detection bandwidth of only 5 GHz.

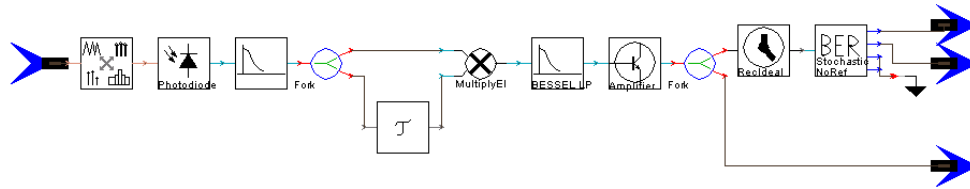


Fig. 2. 17 - VPI scheme of the SCM receiver

2.2.2.3. Simulation results

Simulations in upstream and downstream paths were realized to determine the Rayleigh penalty in SCM modulation format.

Path Upstream

First, Back-to-Back SCM System was implemented. The sensitivity to BER=1.0E-10 (without Rayleigh effect) was found to be -21.77dBm. Later, simulations including RB were done. This is shown in Fig. 2.18. The OLT sensitivity value for RB 1dB-penalty was Pin-OLT=-20.77 dBm and the oSRR = 19.74 dB.

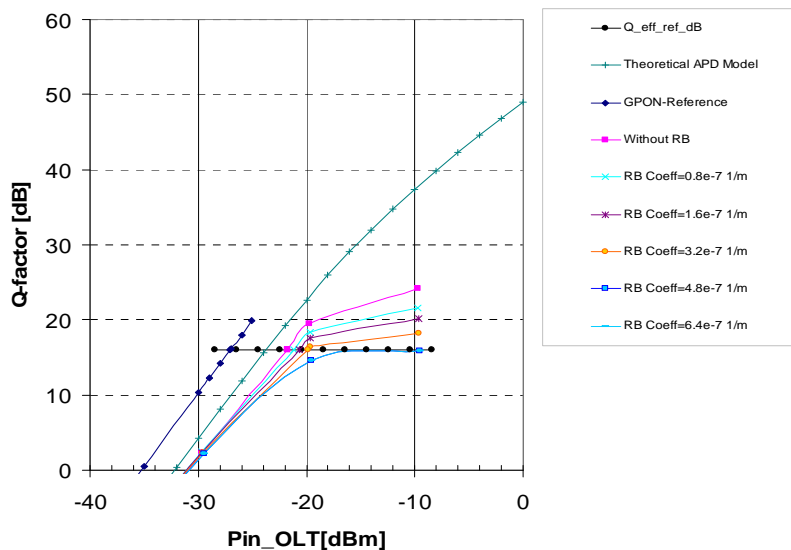


Fig. 2. 18 - Q (dB) vs. OLT Input Power for different RB coefficients in the upstream path

Table 2.4 shows results obtained with the SCM WDM/TDM PON in the upstream path respect to ideal GPON system.

Table 2. 4 –Simulation results for SCM WDM/TDM PON in the upstream path

Modulation Format	SCM/IM		GPON Reference System	
Bit Rate	2.5/1.25Gbps		2.5/1.25 Gbps	
ER (dB)	OLT	8.4dB	OLT	100
	ONU	13dB	ONU	100
Sensitivity without RB (dBm)	-27.3dBm		-28dBm	
Sensitivity with RB (dBm)	-26.32dBm		--	
oSRR (dB) (1dB Penalty) Robustness	19.74 dB		--	
Penalty over Reference	0.68 dB		0	

Downstream Path

Back-to-Back was implemented. The sensitivity to BER=1.0E-10 (without RB effect) was -21.26dBm. Later, simulations including RB were done. The sensitivity value for RB 1dB-penalty was -20.26 dBm and the oSRR was 21.11 dB as shown in Fig. 2.19.

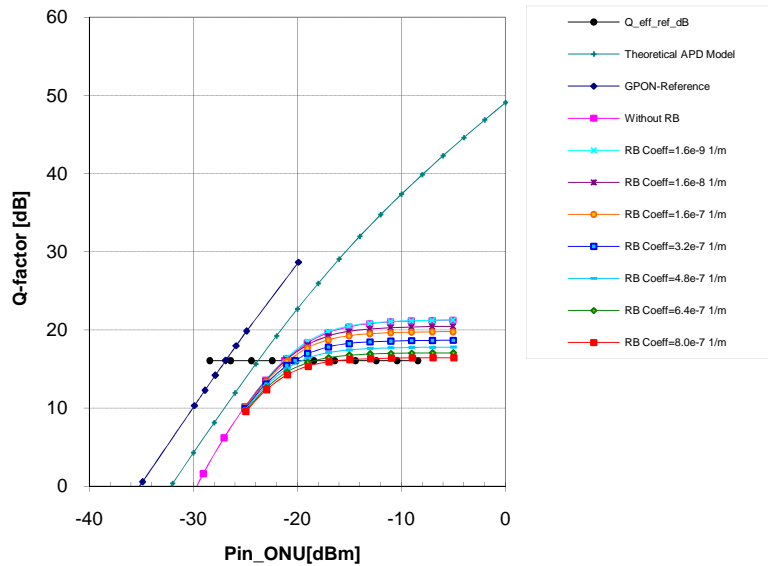


Fig. 2. 19 - Q (dB) vs. OLT Input Power for different RB coefficients in the downstream path

Table 2.5 shows results obtained respect to ideal GPON system.

Table 2. 5 – Simulation results for SCM WDM/TDM PON in the downstream path

Modulation Format	SCM/IM		GPON Reference System	
Bit Rate	2.5/1.25Gbps		2.5/1.25 Gbps	
ER (dB)	OLT	8.4dB	OLT	100
	ONU	13dB	ONU	100
Sensitivity without RB (dBm)	-24.27dBm		-27dBm	
Sensitivity with RB (dBm)	-23.27dBm		--	
oSRBR (dB) (1dB Penalty) Robustness	21.11 dB		--	
Penalty over Reference	2.73 dB		0	

2.2.2.4. Pre-amplification at the OLT

An EDFA Pre-Amplifier at the OLT was incorporated to improve the performance in the upstream path. This provides an important extra power budget and allows sharing this extra power budget between the upstream and downstream signals by means of an adequate ONU splitter configuration.

Fig. 2.20 shows performance of the system without / with Pre-Amp EDFA at the OLT with a nominal gain=23dB and NF=4dB. The impact can be seen in the increment of the Q-factor in upstream (6dB).

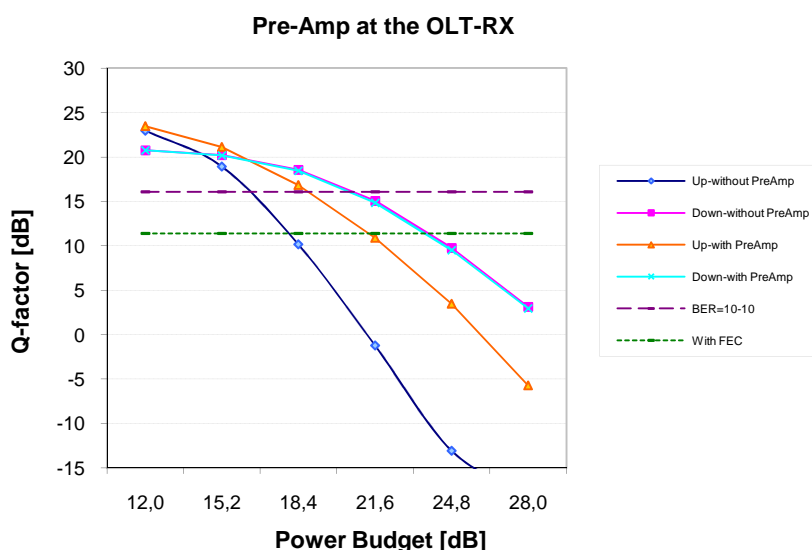


Fig. 2. 20 - Performance of the system without Pre-Amp and with Pre-Amp

In this configuration, a power budget of 18.4 dB is obtained for the sensitivity value ($BER=1 \times 10^{-10}$). However, only 8 users per wavelength could be served (up to 16 users by using FEC).

2.2.2.5. Feeder fibre optimal length

The most adequate feeder fibre length configuration, for an ODN of 20 Km, was evaluated as a function of the system performance (Q-factor, BER).

By establishing a drop fibre length of 1 Km and varying the lengths of the WDM (L1) and TDM (L2) fibre sections simultaneously, we obtained the values shown in Fig. 2.21, for upstream and downstream path, as a function of the number of ONUs to be served. Simulations were done by considering chromatic dispersion ($1.6 \times 10^{-6} \text{ s/m}^2$) and Rayleigh (with RB Coefficient= $1.6 \times 10^{-8} \text{ dB} \cdot \text{m}^{-1}$) impairments.

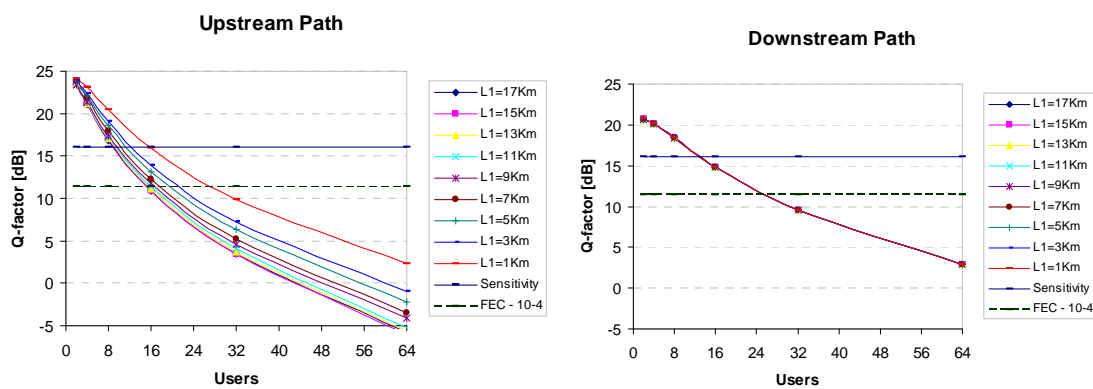


Fig. 2. 21 - Q-factor as a function of the WDM length fibre and the user's number to upstream and downstream paths

The results show that for shorter lengths of the WDM fibre section, the performance in the path upstream will be better. Thus, with $L1 = 1 \text{ Km}$ and $L2 = 18 \text{ Km}$ up to 16 users could be served. These results are expected from crosstalk effect produced by Rayleigh. So, if $L1$ is longer, the crosstalk effect will be more degrading.

In the Downstream path the variation of the lengths for the $L1$ y $L2$ is irrelevant. Here, in the best one of the cases, a maximum of 8 users could be served (16 with FEC).

2.2.3.RSOA: characterization and measurement

Characterization and measurements were done for a RSOA low cost from Kamelian, with nominal 18dB gain, implemented by a long SOA cavity (600um).

RSOA	Provider: Kamelian
Part	RSOA-18-TO-C-FA

Serial Number	29-06-0301146132
Description	18 dB Gain, TOCAN package, C-band

2.2.3.1. RSOA characterization

Original RSOA RF response is shown in Fig. 2.22. This has a 6dB bandwidth of about 600MHz, and it shows a quasi-linear decreasing slope RF response dropping from the low frequencies, which limits for 1.25 Gbps bit rate transmission.

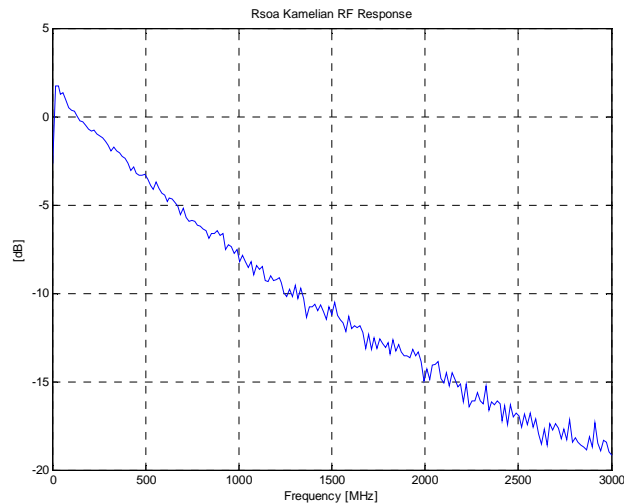


Fig. 2. 22 - Original Kamelian RSOA RF response: 600MHz of bandwidth at 6dB

2.2.3.2. RSOA electrical bandwidth optimization

To increase the device bandwidth and to optimize the RF response, the RSOA has been electrically equalized with a simple RC filter (43 ohm in parallel fashion with a 5.1pF capacitor), in order to improve its electrical bandwidth.

The scheme of the equalizer mounted in the first electrical prototype is shown in Fig. 2.23.

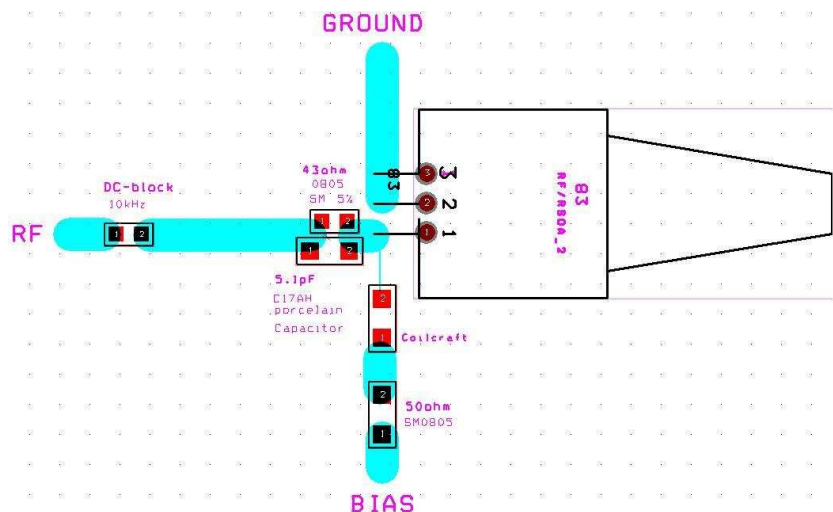


Fig. 2. 23 - PCB layout of the electrical equalization of the RSOA

The board is standard 1.6mm fibre glass board and the width of the micro-strip path is 2.87mm in order to adapt de transmission line from the RF input to the RSOA Anode (Pin 1) to 50 ohm. Anode pin has been taken to 2mm length for RF efficiency. Cathode and case pins from the RSOA are ground connected. This new circuit allows giving directly bias current to the RSOA. Fig. 2.24 shows a picture of this first prototype.

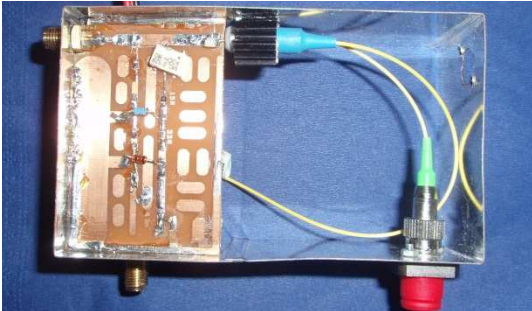


Fig. 2. 24 - RSOA mounting

In Fig. 2.25, the electrical bandwidth of the equalized RSOA is shown. The electrical equalizer produces a signal pre-distortion compensating the low bandwidth limitations of the device. For using the equalization circuit, the 6dB electrical bandwidth has been increased from 0.6 GHz to 1.75 GHz, and will allow using the RSOA device for bit rate transmission even higher than the 1.25 Gbps standard. The bandwidth enhancement is obtained paying the cost of electrical losses at the RF electrical input what will force to the use of a powerful electrical driver.

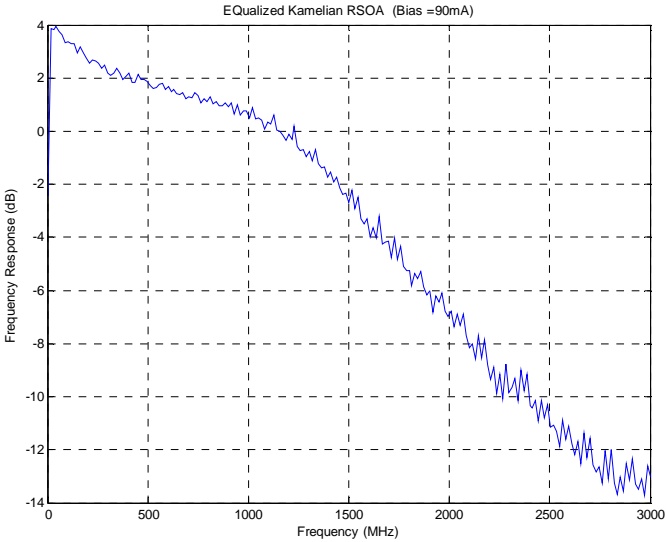


Fig. 2. 25 – Equalized Kamelian RSOA RF response for Bias current of 90mA. The equalized response has a 6dB bandwidth of about 1.7GHz and a 10dB-bandwidth of about 2GHz which allows for 2.5Gbps transmission.

2.2.3.3. RSOA Measurements

Fig. 2.26 shows BER measurements at 1.25 Gbps as a function of the RSOA optical input power (-20 dBm), with a 200GHz Optical Filter. It can be concluded that the bias current increase demands to

increase the Modulation deep to keep almost the same BER. On the other hand, the transmission can even be improved by working with higher Gain (Bias) together with the maximum available modulation index.

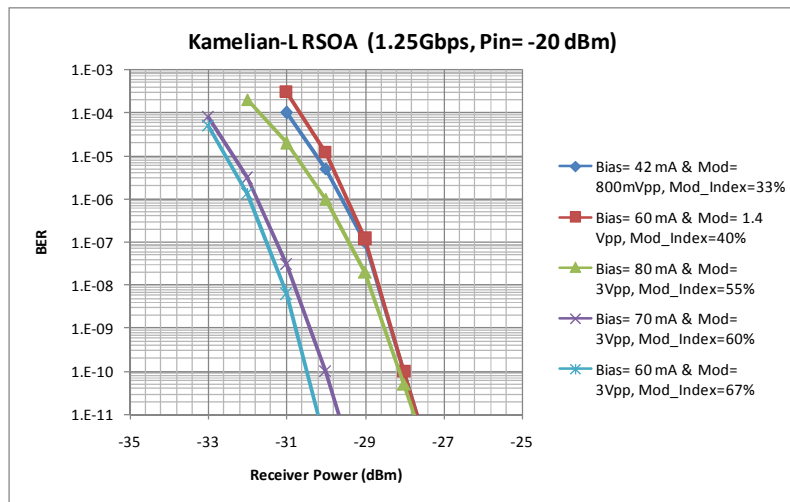


Fig. 2. 26 - BER measures for different Bias current versus receiver power.

The best performance (BER = 1.0E-10) with bias current consumption at the power supplier = 60 mA & Modulation = $\pm 3V_{pp}$ has been obtained at -30.2dBm of input signal power at OLT receiver.

2.2.4.SCM-DPSK Optimization

The objective is to achieve an operating rate at 2.5 Gbps downstream using the SCM technique. Data upstream, at rate 1.25 Gbps, will modulate the downstream carrier (for re-use) at RSOA using IM modulation.

For a downstream rate of 2.5 Gb/s, the sub-carrier frequency is fixed at 5 GHz, allowing a good band margin between DS and US. As the 3dB bandwidth of the data stream is approximately 4 GHz (double-sided), the photo-detection bandwidth needed is of almost 7 GHz [111-113].

2.2.4.1. B2B Full duplex measures

The experimental setup @ 1550nm is shown in Fig. 2.27. For the downstream signal, a PRBS $2^{31}-1$ is pre-coded inside the Pulse Pattern Generator (PPG1) and mixed with a 5 GHz electrical oscillator by using a standard double balanced mixer. With the mixer's frequency response, the band-pass filter, typically used at the transmitter side, is not required [111]. The mixer's bandwidth has been measured by using the three-mixer method [119], showing a bandwidth of ± 1.9 GHz, centred at 5 GHz, enough for 2.5 Gb/s; and a rejection better than 20 dB for frequencies beyond ± 2.9 GHz.

At the electrical side of the ONU receiver a delay-and-multiply scheme [120] was implemented using a double balanced mixer. Since it does not require any electrical oscillator placed in the ONU, data detection becomes simpler and phase-locking between detected carrier and electrical oscillator is avoided.

An ER of 8.4dB provided by the OLT-TX generates a penalty (BER at 10^{-10}) of 1.5 dB, both experimentally or theoretically [111-112].

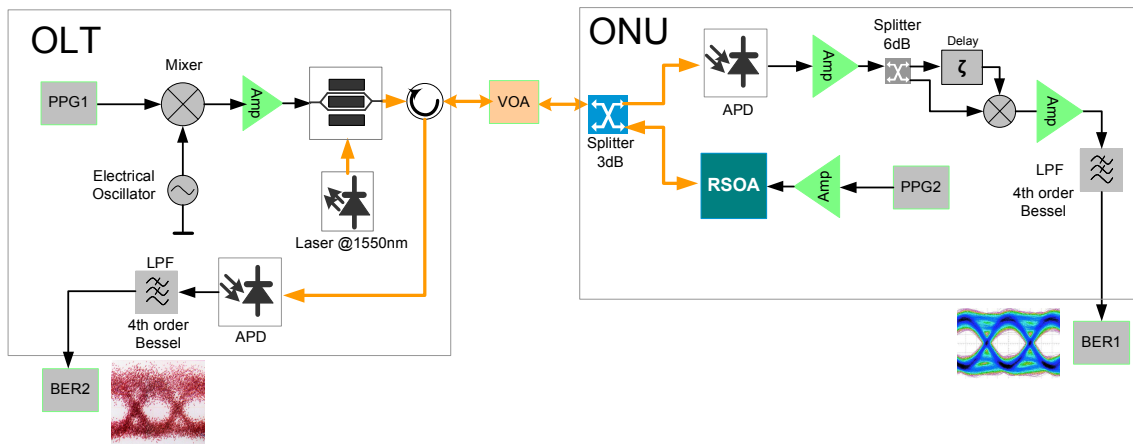


Fig. 2. 27 - Experimental setup for single fibre B2B full-duplex measurements.

Initially an ONU splitting ratio of 50:50 was used. For the upstream signal at 1.25 Gb/s, a PRBS length of $2^{31}-1$, by means of a pattern generator (PPG2), was used. The RSOA gain was of 17 dB. At the OLT side, a low pass filter was placed after photo-detection, in order to properly reject re-modulation noise from downstream signal. The sensitivity is shown in Fig. 2.28. For the downstream (BER 10^{-10}) -23,4dBm was achieved. For the upstream, -22,6dBm.

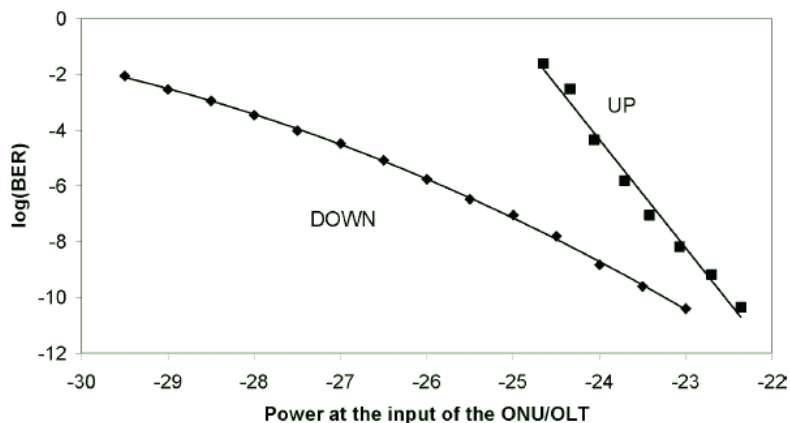


Fig. 2. 28 – Sensitivity results for the B2B full duplex SCM system.

Because VOA is placed in between OLT and ONU (attenuating both ONU output power and RSOA input power), OSNR is more degraded at the ONU output and the upstream curve shows this shape.

2.2.5. System Optimization

Initial design proposed has a strong limitation in the amount of users to be served. An optimization of the system is necessary. Thus, a new model based on a reconfiguration of the WDM feeder, now two-fibers based, is proposed. In this way, we expect counterattacking the RB effect, our principal impairment. Fig. 2.29 shows the functional diagram for this new model, according to ITU-T nomenclature.

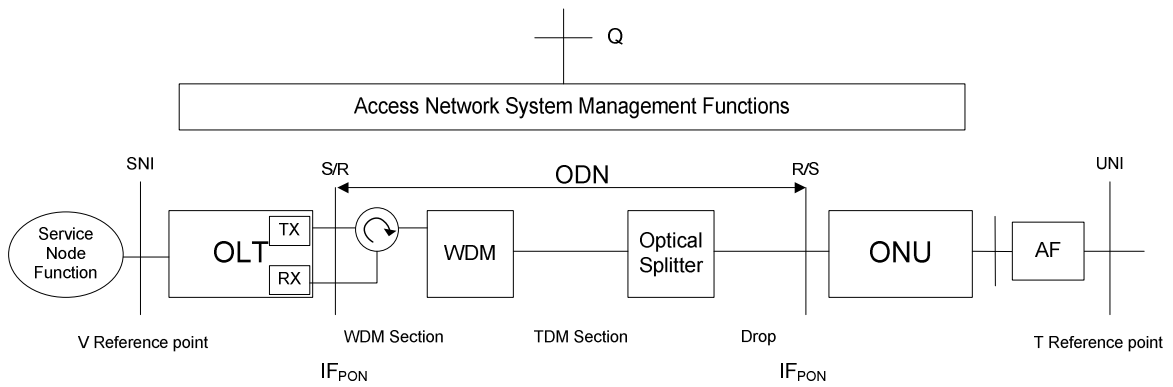


Fig. 2. 29 - Functional diagram of the new proposed model

By considering that the two-fibre model is the most suitable solution to the implementation of the project prototype, optimization of the parameters to its model was done via VPI simulations.

With two-fibres at the feeder section, RB is not critical and OLT output power could be incremented to improve the power budget. Here, non-linearity would be considered.

VPI Schematic

Fig. 2.30 shows the VPI schematic of the new proposed model. Now, two fibres are used between the OLT and AWG.

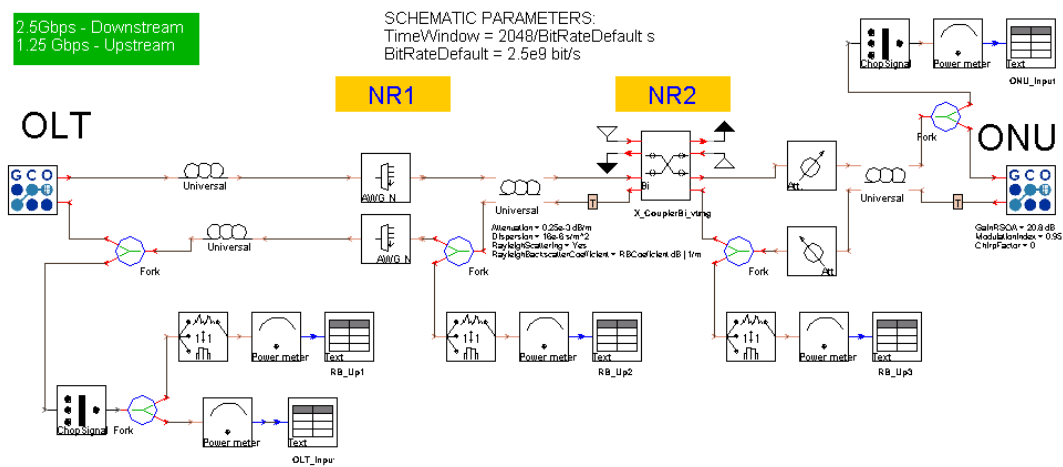


Fig. 2. 30 - VPI schematic of the new proposed model

2.2.5.1. Simulations of Performance

Fig. 2.31 shows Q-factor vs. number of users in the upstream path. A sensitivity increment of the OLT receiver due at the reduction of the RB effect is shown. Thus, up to 32 users is possible with configurations WDM feeder (L1)/TDM feeder (L2) from 17/2 to 9/10 km. By FEC application it is possible to achieve up to 64 users, with configurations L1/L2 from 17/2 to 13/6 Km.

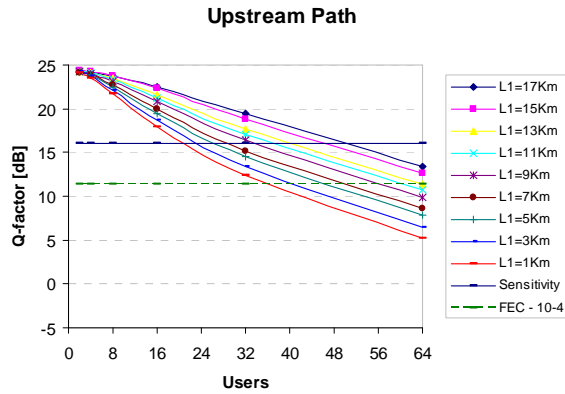


Fig. 2. 31 - Q-factor versus users' number in the upstream path.

In the downstream path new configuration to improve the quality of signal has not effect. In the other hand, because a power budget increment in the US path and the use of the pre-amplifier at the OLT, a de-balanced between US and DS is produced. A trade-off adjustment will be done in the splitter/combiner at the ONU.

Extinction Ratio and RSOA gain

Simulation tests with Non-linear effects and Rayleigh was done. The typical dispersion coefficient of 16us/m² for SSMF has been used. SPM, XPM and FWM were included. Fig. 2.32 shows the measured BERs (20 log Q) versus the OLT power input for different ER (8.5, 10 and 13 dB) and RSOA Gain (14, 17 and 20 dB) to 16, 32 and 64 users/wavelength. A bigger ER and an adapted Gain at the ONU offers best performance. Thus, with an ER=13dB and a Gain=20dB is possible to obtain the optimal value of 32 users/wavelength (up to 64 users/wavelength with FEC).

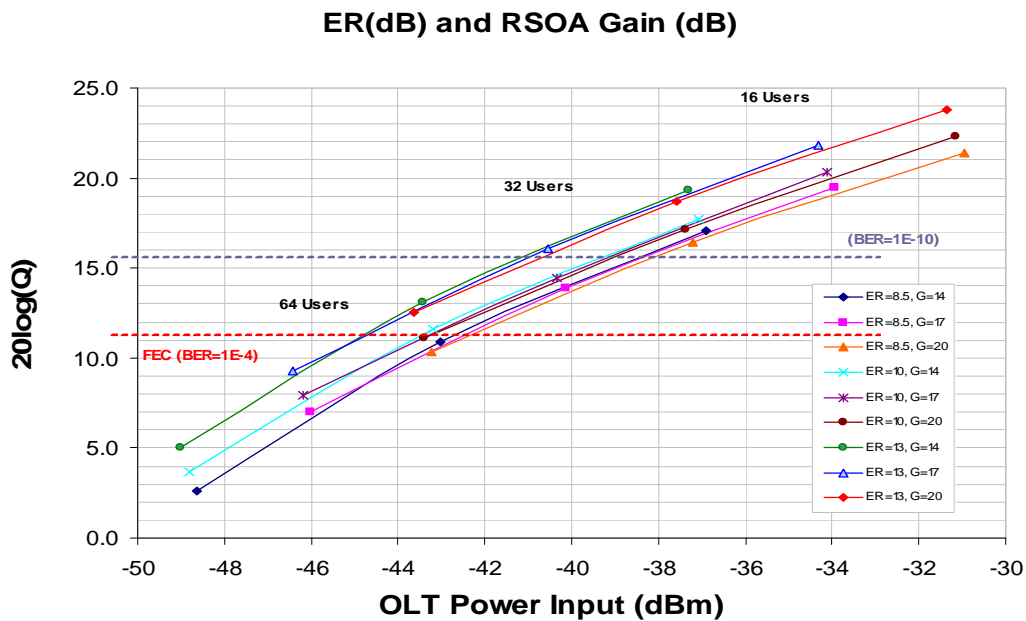


Fig. 2. 32 - ONU Extinction Ratio and RSOA Gain

Also, RSOA chirp factor was analysed. This has a little influence in the upstream signal quality (for fibre length 20 Km and 2.5/1.25 Gbps). A RSOA chirp commercial value of 6 (the worst case) was adopted.

2.2.5.2. RSOA: Continuous stream/ Burst Mode transmission

Continuous stream transmission

The E/O BW has been improved for 1.25Gbps by applying optimal bias current of 70mA. A PRBS of 2³¹-1 was used. Error free was measured by a Parallel Bert (Agilent) at 1.25Gbps. This is shown in Fig. 2.33.

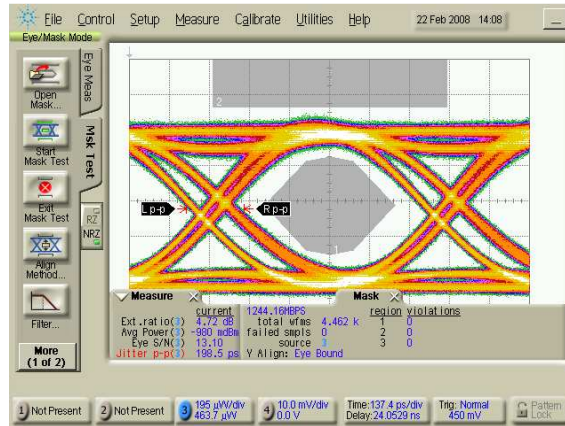


Fig. 2. 33 - RSOA Eye in continuous stream at 1.25Gps, bias of 70mA, modulation of 2Vpp and input signal of -15dBm.

A modulation deep of $\pm 1V$ was used (lower than the recommended of $\pm 3.15V$ by limitation of the instrument), with an Optical input power of $P_{in} = -15dBm$.

Burst Mode transmission

Burst mode transmission had been tested for several packet lengths up to 1440 bits packet (720 bits of data / 720 bits of no-data). Fig. 2.34 shows an overview of this burst and the eye generated. Small swing can be seen due to the DC block situated at the RF input of the RSOA.

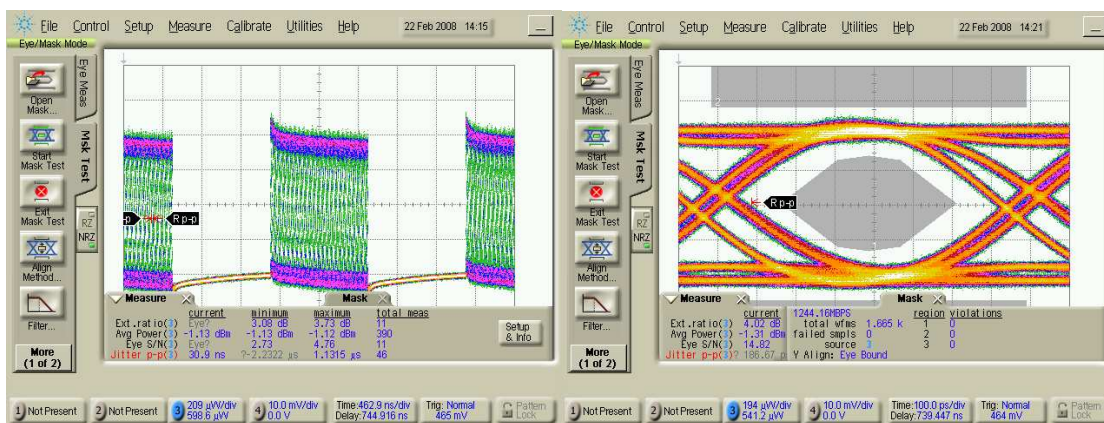


Fig. 2. 34 - Overview of frame in Burst Mode of the RSOA and Eye generated at a bit rate of 1.25Gbps, bias of 70mA, modulation of 2Vpp and input signal of -15dBm.

2.2.5.3. RSOA parameters as a function of Temperature

Optical gain, extinction ratio (ER), optical signal to noise ratio (OSNR) and Noise Figure (NF) has been analysed as function of temperature. As can be seen in Fig. 2.35 (ASE curves), the optical efficiency drops with temperature. Reducing the temperature to less than 25°C the efficiency can be increased.

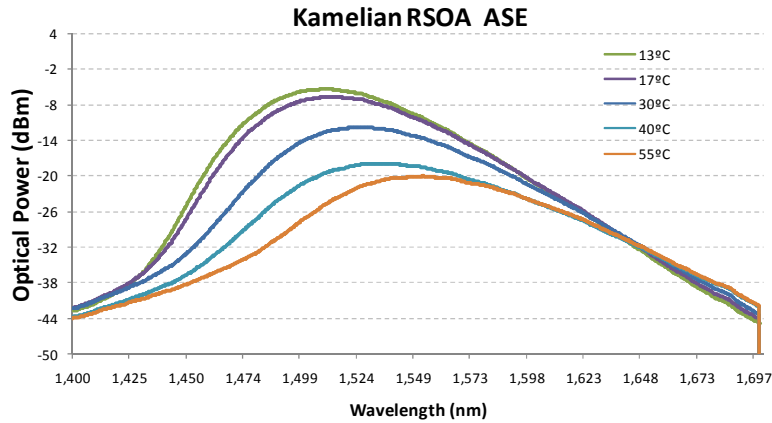


Fig. 2. 35 - Kamelian RSOA Amplified Spontaneous Emission versus temperature @1550nm for Bias current of 70mA.

The optical gain drops similarly with temperature in the whole C-Band. Reducing the temperature to less than 25°C, the gain can be increased as can be seen in Fig. 2.36(a). The ER exhibits its maximum around 25°C and drops when temperature moves away to the edges, increasing or decreasing. That behaviour is quite similar in the whole C-Band. The available temperature range, keeping ER>9, goes from 25°C to 40°C as can be seen in Fig. 2.36(b).

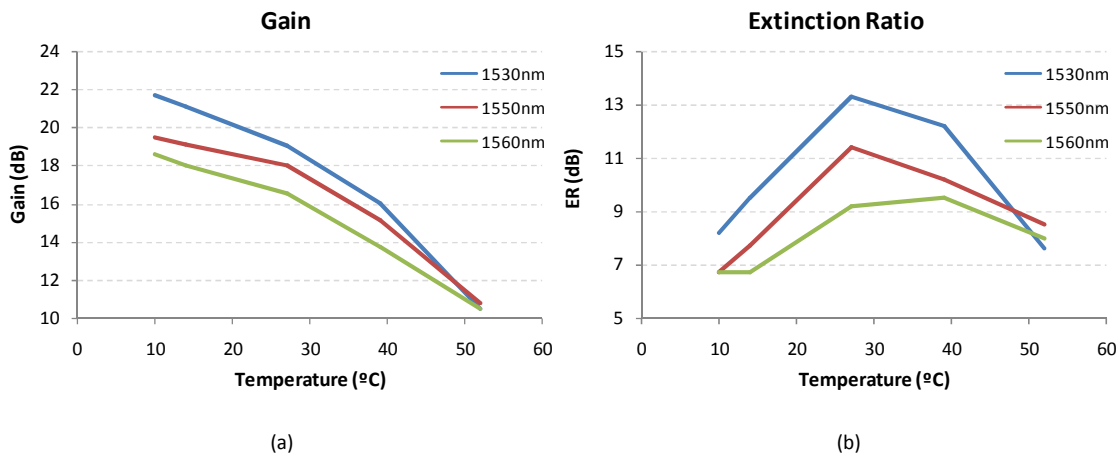


Fig. 2. 36 - Kamelian RSOA Gain and ER versus ambience temperature for optical Pin=-20dBm and Bias current =70mA with 20dBm sinusoidal RF modulation at 500MHz.

The best OSNR trade-off into the whole C-Band is 25° to 40°C temperature range. Out of that range, the OSNR drops when wavelength and temperature decrease. But it becomes even worse when temperature increases as can be seen in Fig. 2.37(a). Similarly to the OSNR, the optimum NF is 25° to 40°C temperature range, as shown in Fig. 2.37(b).

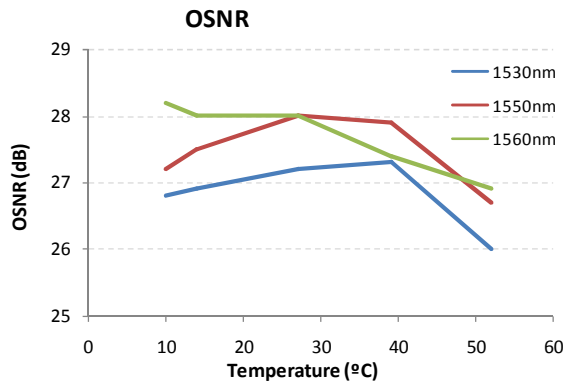


Fig. (a)

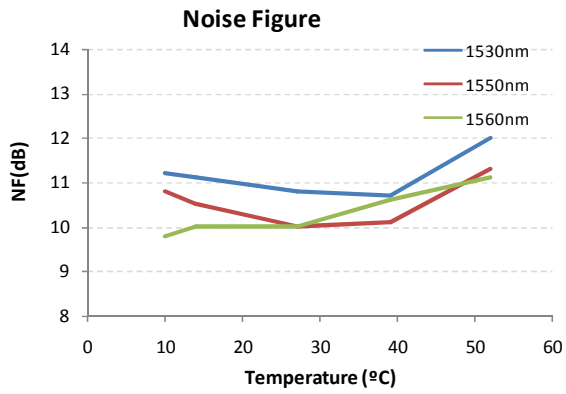


Fig. (b)

Fig. 2. 37 - RSOA OSNR and Noise Figure versus ambience temperature for optical Pin=-20dBm and for Bias current =70mA with 20dBm sinusoidal RF modulation at 500MHz.

As a conclusion, the Kamelian RSOA has found suitable to optical data transmission at 1.25Gb/s at 25°C at the established working point (Bias current = 70mA with 20 dBm of RF modulation = ±63mA). But satisfying the Gain, ER, OSNR, and NF requirements (Gain>18, ER>9) into the whole C-Band demands to keep the un-cooled RSOA device in an environment with temperature stabilized around 25°C, because the Gain & ER parameters and the electro-optical efficiency performance highly drops with temperature (gain reduces about 10 dB).

Several scenarios can be considered: to place the RSOA device at the user ‘home’, or RSOA into a temperature stabilized cabinet, with heat-sink and air renewing systems.

At 50°C ambience temperature, to achieve optical output power in the range of -3 to 0 dBm, it is necessary to reduce the optical input requirements to ≥ -15 dBm. The best operation point (for the worst polarization case and the most critical carrier wavelength of 1560nm) is for Bias current of 90mA, that allows achieving optical gain around 12 dB at that extreme temperatures. For bias currents higher than 90mA, the temperature of the device also increases leading to gain reduction and optical output power dropping.

The ER drop at extreme temperatures of 50°C and also 0°C can be easily improved increasing the data modulation deep to values around 22dBm (±80mA).

In Table 2.6, the electrical and optical conditions summary, regarding the operation point versus temperature, is presented. All data are considered for the worst polarization case at the wavelength of 1560nm which presents the worst RSOA optical performance. It is expected that the RSOA will work better for lower wavelengths in the range from 1530 to 1550 nm.

Table 2. 6 - Operation points for several ambience temperature environments at worst polarization case and most critical carrier wavelength (1560nm).

Temperature	10°C	25°C	50°C
Bias current	70mA	70mA	70-90 mA
RF deep modulation	22 dBm (± 80 mA)	20 dBm (± 60 mA)	22 dBm (± 80 mA)
Optical Input Power	≥ -20 dBm	≥ -20 dBm	≥ -15 dBm
Optical Gain	≥ 18 dB	≥ 16 dB	≥ 11 dB
Optical Output Power	≥ -3 dBm	≥ -3 dBm	≥ -3 dBm
Extinction Ratio	≥ 9 dB	≥ 9 dB	≥ 9 dB
OSNR	> 27 dB	> 27 dB	> 32 dB
Noise Figure	< 11 dB	< 11 dB	< 11 dB

2.2.6. Final Designs, Implementation and Results

Three different bidirectional PON scenarios based on SCM/IM modulation format and reflective ONUs were implemented and tested, for a minimum system margin of 3 dB.

- 1) A TDM PON network, emulating an standard GPON, used as a network reference;
- 2) A hybrid WDM/TDM PON network, based on one-fibre / one-wavelength in whole ODN;
- 3) An optimized WDM/TDM PON network based on two-fibre / one-wavelength in the WDM feeder section (one fibre in the drop).

Table 2.7 shows a summary of the results for these bidirectional transmission scenarios.

Table 2. 7 - Complete detail of the measurements for several scenarios and features of the SCM WDM/TDM PON prototype @1550nm &25°C

	Scenario		
@ 1550nm&25°C	(1)	(2)	(3)
WDM Feeder	1 fibre	1 fibre	2 fibre
Distance	25+2 km	16+2+2 km	16+2+2 km
AWG	-	1x40	1x40
Splitter	1x8	1x4	1x32
DS Sensitive	-26 dBm	-26 dBm	-26 dBm
US Sensitive	-18.5 dBm	-20,3 dBm	-28 dBm
OLT-Out	-1 to +5 dBm	0 to +5dBm	≥ 10 dBm
Power Budget	17 dB	17.4 dB	27.6 dB
Total Users	8	4x40	32x40
Extra-Loss	1 dB	1 dB	1 dB
DS-Margin	> 2 dB	> 2 dB	> 2 dB
US-Margin	> 2 dB	> 2 dB	> 2 dB
ONU Splitting Ratio	70/30	70/30	70/30
ONU-Out	> 0.5 dBm	> 0.5 dBm	> 0.5 dBm

To determine the system power budget, insertion Losses (IL) of the network elements have been considered from its nominal values plus 1-dB extra-losses to compensate the deviation to the real IL fibre values and connector losses.

In the (1) and (2) scenarios, bidirectional transmission over one single fibre is deployed, so the upstream sensitivities are limited from the Rayleigh backscattering interference which forces to have the OLT output power controlled.

Scenario (3) deploys double fibre in the WDM feeder network avoiding Rayleigh backscattering which saves the OLT from the output power limits and allows achieving higher power budgets.

Into the OLT will be necessary to use an AWG to distribute each wavelength to its appropriate TDM tree. This will produce extra losses which can be compensated by using an EDFA pre-amplifier at the input of the AWG multiplexer.

2.2.6.1. Back-to-back Reference

The TX & RX Back-to-back sensitivity has been measured for downstream and upstream @1550nm to have the limits of the operation. This is summarized in Table 2.8.

- 2.5Gbps-B2B downstream sensitivity (PRBS-31 & BER= 10^{-10}) of -26.5dBm at the APD input (Fujitsu FRM5N143DS) which is almost the limit of the APD.
- 1.25Gbps-B2B upstream sensitivity (PRBS-31 & BER= 10^{-10}) of -27dBm at the APD input (ZENKO LT-XXB7/46B).

Table 2. 8 - B2B Sensitivity

Sensitivity @ 1×10^{-10}	Downstream (APD input)	Upstream (APD input)	Upstream (1.25G standard APD input)
B2B	-26.5	-27	-28

The gain performance of the RSOA @1550nm&25°C is shown in Fig. 2.38.

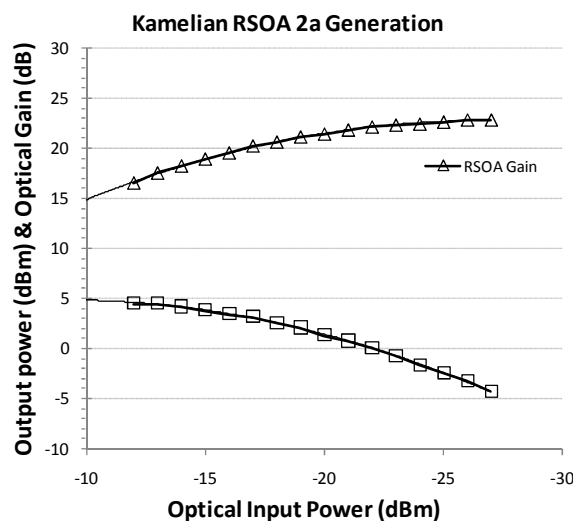


Fig. 2. 38 - a) ASE response of the Kamelian RSOA. b) Gain and output power versus the optical input power.

The scenarios to be considered require 3 principal restrictions to be fulfilled:

- 1) To have an OSRR > 15dB, which is the measured value for SCM modulation for bidirectional transmission over one single fibre.
- 2) In agreement with the RSOA penalties table versus wavelength, every scenario will be forced to have a power margin of at least 2dB to allow the optical transmission in the whole C-Band for a device temperature range going from 30°C to 10°C.
- 3) ONU output has to be higher than 0.5dBm.

Theoretically, because of the unbalanced sensitivities values for the RSOA and the ONU-APD, when looking for the best power budget it leads to the use of a 70/30 coupler ratio, with 70% output connected to the RSOA.

2.2.6.2. SCM WDM/TDM PON Testbed Prototype

Fig. 2.39 shows the testbed prototype of the SCM WDM/TDM PON implemented at the UPC-GCO laboratory.

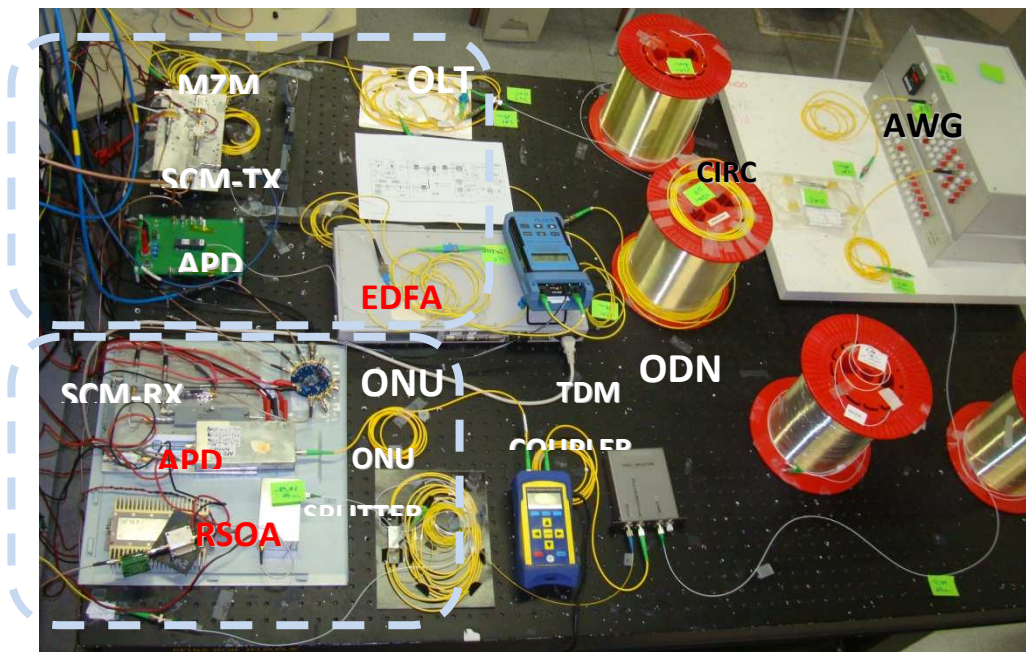


Fig. 2. 39 – Prototype implementation of the SCM WDM/TDM PON at the GCO-UPC Laboratory

2.2.6.3. Setup (1)

A bidirectional transmission over one single feeder fibre (25km), splitting 1x8 and drop fibre (2kms). This setup is shown in Fig. 2.40.

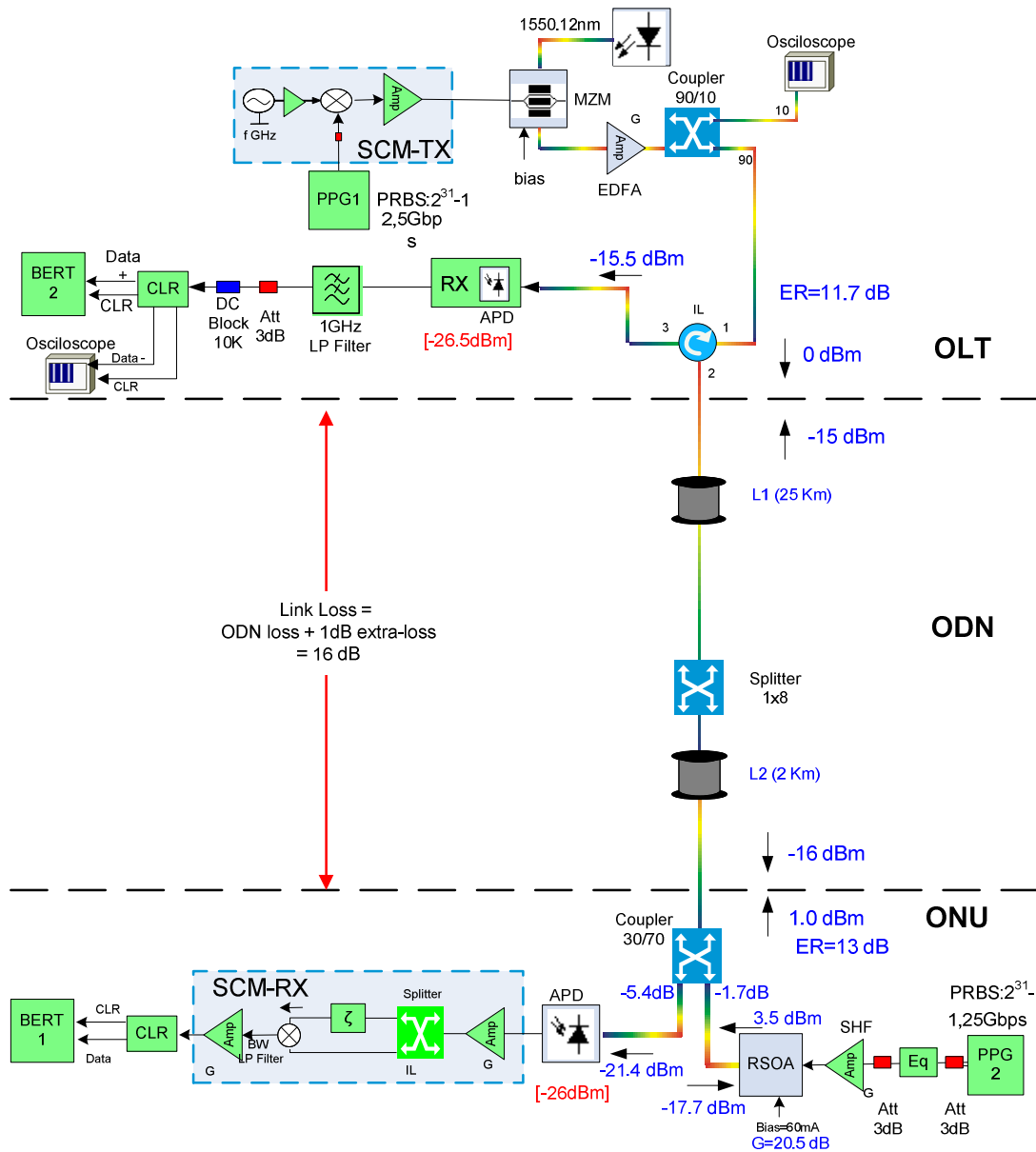


Fig. 2. 40 - Scheme of the 25km+1x8splitter+2km bidirectional single fibre setup (1).

Because of the bidirectional transmission over one single fibre/wavelength, the limits in the power budget come from the Rayleigh backscattering (RB). The 0dBm optical power from the OLT output is injected to the 25km feeder fibre and generates a RB power of -33.5dBm. The 1 dB penalty upstream Optical-Signal-to-RB-Ratio (OSRR) has been measured to be 17.5dB.

Table 2.9 shows a range of suitable OLT output power and corresponding power budgets for this scenario. An output power ≤ -4 dBm does not satisfy the 2-dB minimum system margin condition. An output power ≤ -1 dBm forces the ONU output to be lower than 0.5dBm, while a power higher than 6dBm does not satisfy the upstream $OSRR \geq 15$ dB requirement for this SCM modulation.

Table 2. 9 - Range of suitable OLT output powers and corresponding power budgets for a 25km+1x8 splitter+2km single fibre with a 70/30 splitter at ONU

OLT out (dBm)	OSRR (dB)	Link Loss (dB)	Power Budget (dB)	DS-Margin (dB)	US-Margin (dB)	ONU-out (dBm)
6	14.4	OSRR<15dB				
5	15.3	16	21.3	9.6	5.3	3.5
0	18.5	16	19.5	4.6	3.5	1.8
-1	19	16	19	3.6	3	0.5
-2	20.1	16	18.4	2.6	2.4	-0.1
-4	20.1	16		0.6	1.1	
-5	20.3	< DS-Sensitiv				

Upstream and downstream curves were measured. For a BER 1.0E-10, upstream sensitivity was -18.4 dBm, while for downstream the sensitivity was -20.1. These results are shown in Fig. 2.43.

With these results, downstream power budget was 19.4 dB (system margin = 3.4 dB), whereas the downstream power budget was 20.1 dB (system margin = 4.1 dB).

2.2.6.4. Setup (2)

This bidirectional transmission WDM/TDM PON setup is composed of one single WDM feeder fibre pool (16km), a 1x40 AWG demultiplexer, a power splitter 1x4 and a drop fibre pool (2kms). This setup is shown in Fig. 2.41.

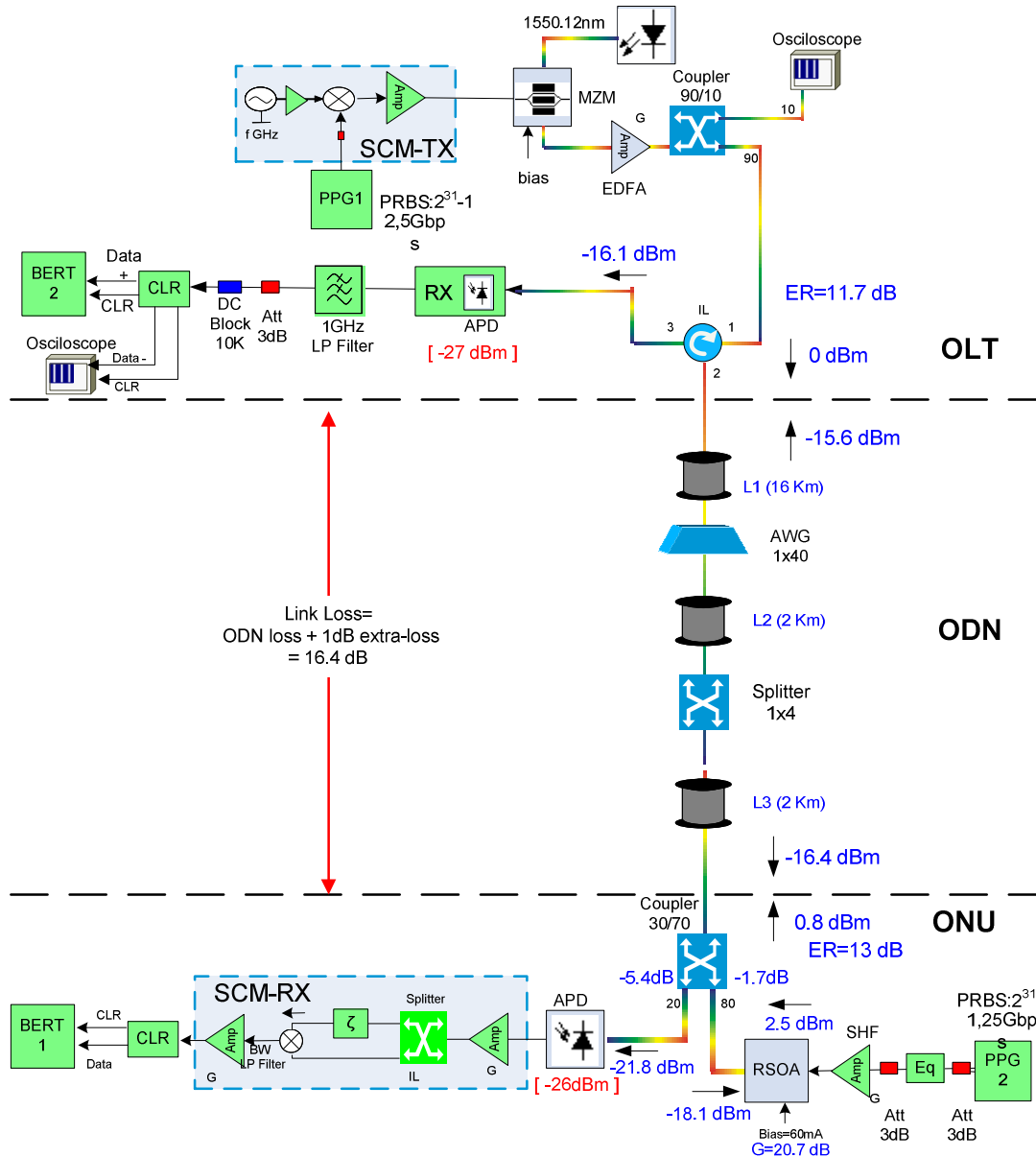


Fig. 2. 41 - Scheme of the 16km+1x40 AWG+2km+1x4 splitter+2km bidirectional single fibre setup (2).

Similar to scenario (1), RB of -33.5dBm from the 0dBm OLT optical output power limits the power budget at the upstream path. The 1 dB penalty due to the RB has been measured for OSRR to be 16.9 dB.

The upstream sensitivity ($BER=10^{-10}$) has been measured to be $OLT_{SENS} = -19dBm$, while the downstream sensitivity was -20.6dBm. This is shown in Fig. 2.43.

The downstream power budget for this scenario with OLT output power of 0dBm was 20.6dB (system margin of 4.2dB), whereas the upstream power budget was 19.8dB (system margin of 3.4dB). This

scenario offers the specific WDM functionality with the AWG 1x40 by reducing the splitter ratio to 1x4. This deployment allows up to $4 \times 40 = 160$ users.

The suitable OLT output range goes from 0 to 5dBm. An OLT output power lower than 0dBm does not satisfy the ONU output power (higher than 0.5dBm) condition, while an output power higher than 5dBm does not satisfy the upstream OSRR > 15dB requirement for this SCM modulation. This is shown in Table 2.10.

Table 2. 10 - Range of suitable OLT output powers and corresponding power budgets for a 16km+1x40 AWG+2km +1x4splitter+2km single fibre with a 70/30 coupler at ONU.

OLT out (dBm)	OSRR (dB)	Link Loss (dB)	Power Budget (dB)	DS-Margin (dB)	US-Margin (dB)	ONU-out (dBm)
6	14.7	OSRR<15dB				
5	15.5	16.4	23	9.2	6.6	2.7
0	18.6	16.4	20.6	4.2	4.7	0.8
-1	19.1	16.4	19.6	3.2	4.2	0.3
-2	19.5	16.4	18.6	2.2	3.6	-0.3
-3	19.8	16.4	17.6	1.2	2.9	-1
-5	20.3	< DS-Sensitiv				

2.2.6.5. Setup (3)

An optimized bidirectional transmission WDM/TDM PON over two fibres in the WDM feeder fibre spool (16km), with 1x40 AWG demultiplexer, TDM feeder fibre spool (2Km), power splitting 1x32 and one single drop fibre spool (2kms) is shown in Fig. 2.42.

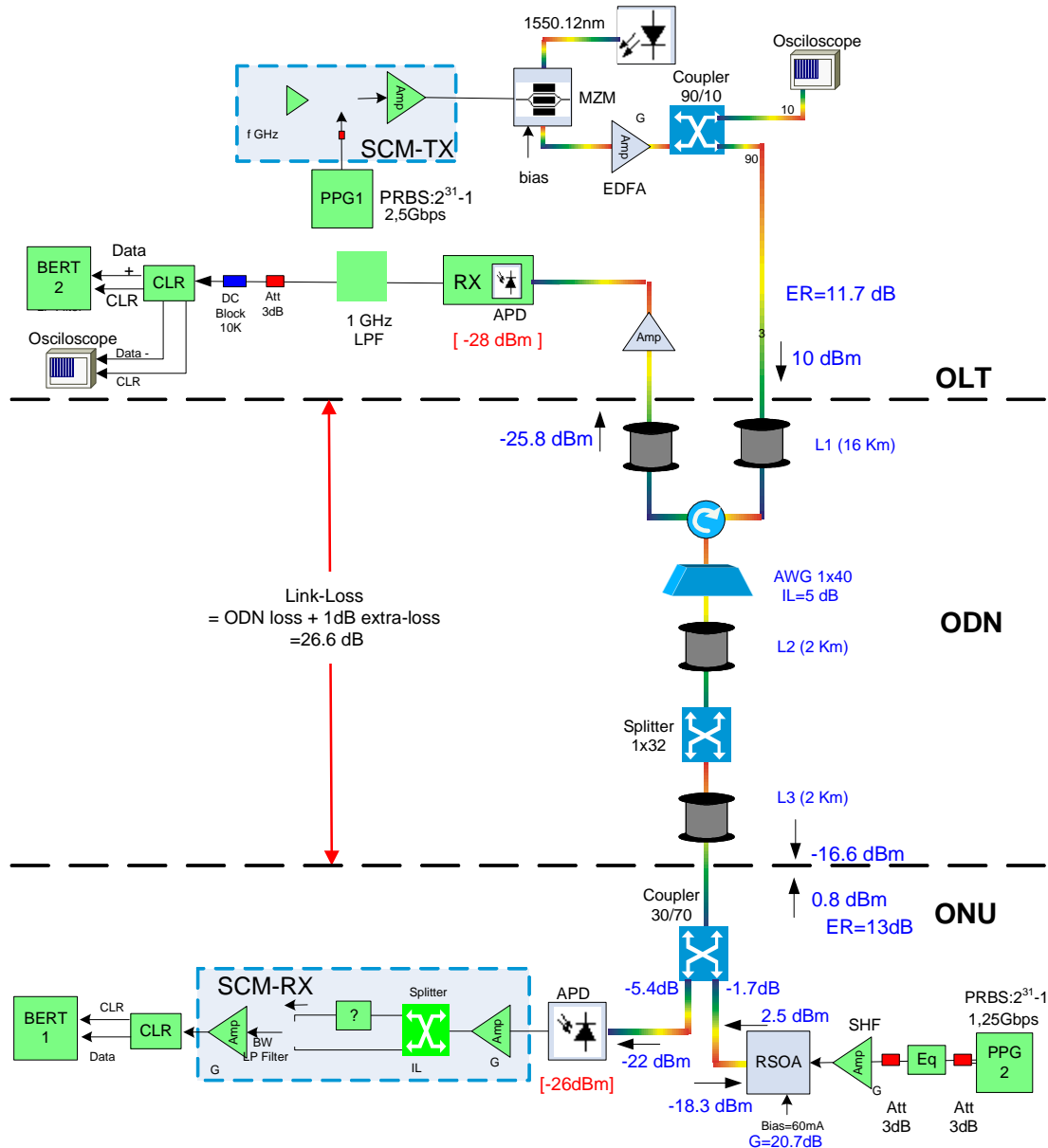


Fig. 2. 42 - Scheme of two fibres (16km) +1x40 AWG+2km+1x4splitter+2km bidirectional single fibre Two-fibres in the WDM feeder section reduce dramatically the RB effect over the upstream path and it is negligible. This allows increasing the OLT output power. So it is possible to exit from the OLT even with more than 10dBm. These conditions improve the power budget of the system. Thus, up to 40x32 users (1280 users) can be covered.

In this scenario, the total link loss was 26.6 dB. An optical pre-amplifier was incorporated at the upstream detection, since there was no RB limitation and OLT costs are shared among all users of the network.

Table 2.11 details the network performance for several OLT output powers. An OLT output power of 10dBm allows a splitting ratio of 1x32, while accomplishing the imposed initial conditions regarding OSRR, power margin and ONU output.

When the OLT output power is reduced, both the power budget and the splitting ratio must be reduced and the required ONU output condition is not satisfied.

Table 2. 11 - Range of OLT output powers and corresponding power budgets for a double-fibre (16km) +1x40 AWG+2km +1x32 splitter+2km single fibre with its more appropriate coupler at ONU.

OLT out (dBm)	Link Loss (dB)	Power Budget (dB)	Splitting Ratio	Coupler Ratio	DS-Margin (dB)	US-Margin (dB)	ONUout (dBm)
0 dBm	20.1 dB	22.8	8	50/50	2.7	3.7	-4.1
5 dBm	23.3 dB	26.8	16	60/40	3.5	3.6	-1.1
5 dBm	23.3 dB	25.6	16	70/30	2.3	4.4	-0.3
10 dBm	26.6 dB	28.8	32	70/30	4	2.2	0.8
10 dBm	26.6 dB	28.8	32	80/20	2.2	3	1.5

For this 10dBm OLT output operation point, we have chosen the 70/30 coupling even that the required conditions are accomplished also with the 80/20 coupler ratio configuration, as it can be seen in Tables 2.12 and 2.13.

Table 2. 12 - Range of OLT output powers and corresponding power budgets for a double- fibre (16km) +1x40AWG+2km +1x32 splitter+2km single fibre with a 70/30 coupler at ONU.

OLT out (dBm)	Link Loss (dB)	Power Budget (dB)	Coupler Ratio	DS-Margin (dB)	US-Margin (dB)	ONU-out (dBm)
9	26.6 dB	28.2	70/30	3	1.7	0.2
10	26.6 dB	28.8	70/30	4	2.2	0.8
12	26.6 dB	29.7	70/30	6	3.1	1.7
15	26.6 dB	30.7	70/30	9	4.1	2.7

Table 2. 13 - Range of OLT output powers and corresponding power budgets for a double-fibre (16km) +1x40 AWG+2km +1x32 splitter+2km single fibre with 80/20 coupler at ONU.

OLT out (dBm)	Link Loss (dB)	Power Budget (dB)	Coupler Ratio	DS-Margin (dB)	US-Margin (dB)	ONU-out (dBm)
9	26.6	27.8	80/20	1.2	2.4	1
10	26.6	28.8	80/20	2.2	3	1.5
12	26.6	30.4	80/20	4.2	3.8	2.4
15	26.6	31.3	80/20	7.2	4.7	3.3

Suitable OLT output powers keeping this performance are for values higher than 10dBm. The power budgets with OLT output power ≥ 10 dBm are better than 28dB, but these output powers could cause interferences by nonlinear effects.

The upstream sensitivity curves ($BER=10^{-10}$) has been measured to be $OLT_{SENS} = -28.8\text{dBm}$. The downstream sensitivity was -19.6dBm . This is shown in Fig. 2.43. Thus, a symmetrical power budget of 29.6 dB (system margin of 4 dB) was achieved.

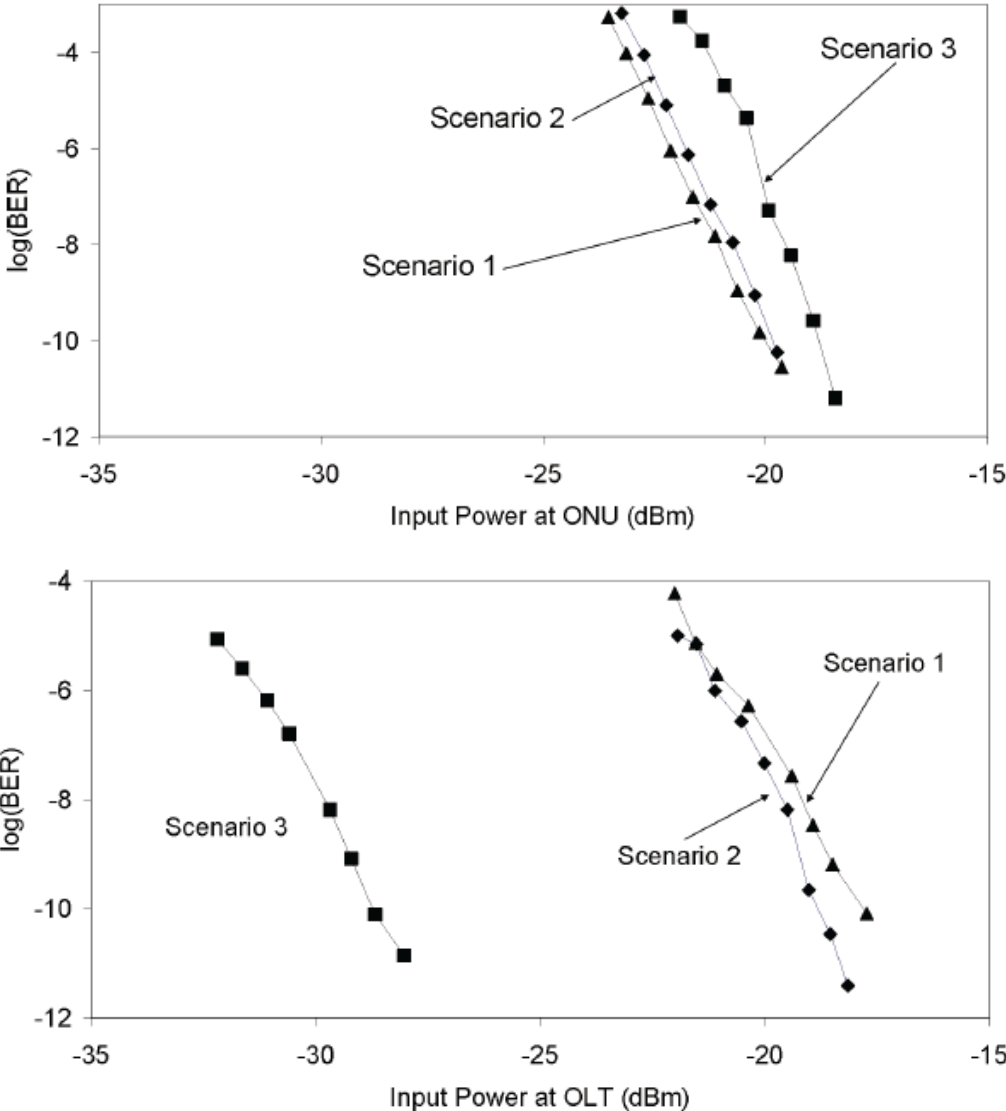


Fig. 2. 43 - a) Downstream and b) Upstream sensitivity curves for the three PON scenarios

2.2.7. Conclusions

A SCM WDM/TDM PON system with a reflective-SOA ONU was simulated, optimized, implemented and tested.

A SCM (sub-carrier multiplexing) modulation format was used. Data downstream was modulated in DPSK over an electrical sub-carrier at 5 GHz, to leave spectral space to the IM (intensity modulation) baseband upstream, over the same wavelength, for full duplex operation over the same fibre and same wavelength.

The measurement, modelling and characterization of commercial RSOAs and the list of design parameters, impairment effects and design relations was experimentally performed in order to define the elements and characteristics of the reflective ONU. The evaluation of the RSOA to be used for the colourless ONU was undertaken. Low cost RSOA exhibits a limited RF response which could highly limit the transmission bit rate. A best RF response, by optimum impedance adaptation and electronic equalization, to increase the device bandwidth was done. The best transmission operation point in the low range of the C-band is for Bias Current 70mA and Amplitude Modulation ± 60 mA.

Evolution schemes, as a function of new requirements, were a characteristic in this process. The possibility to include a Pre-amplification at the OLT and the determination of the lengths of the feeder fibre sections were evaluated. It was assessed that the bidirectional crosstalk (Rayleigh backscattering) limits single-fibre transmission at 20 Km and restricts the OLT output power as a function of the upstream oSRR.

Thus, initial designs proposed had a strong limitation in the power budget and in consequence in the amount of users to be served (8 users). Considering power budget differences between upstream and downstream paths, two parameters, OLT output power and ONU coupler splitting ratio, become important optimization elements in order to find the best upstream/downstream trade-off.

To overcome these limitations, a design based in two fibers in the WDM feeder section was adopted and implemented. This prototype was successfully tested showing high performance, robustness, versatility and reliability. So, the system is able to give coverage up to 32 users per wavelength at 20 Km of fibre length, power budget of 28dB compatible with the ITU-T G.984.2B+ G-PON system recommendation deployments, but for a total of 1280 users, at 2.5 Gb/s in downstream and 1.25 Gb/s in upstream.

This system is intended to take place in the access network as a solution within the frame of the next generation optical access network scaling from current GPON systems.

2.3. Final Conclusions

In WDM-PON and hybrid WDM/TDM PON different parameters are susceptible to be optimized to obtain a better performance of the system.

Thus, although in practical deployments, the position of the distribution element (in this case, a DEMUX) is usually determined by different considerations (cost, distribution of the customers, business opportunity, etc.), this study provides relevant information in terms of transmission optimization in WDM-PON. The results show the best performance can be achieved if the distribution element is placed either in the ONU or OLT vicinity, by demonstrating that the Rayleigh substantially varies depending on the position of the distribution element since they are determined by the fibre length and by the ONU gain applied. In such cases, the ONU gain takes a new optimum depending on that exact position. These results can be used efficiently to minimize the RB effect in the next generation WDM access networks.

In the second part of this chapter, a SCM WDM/TDM PON system with a colourless ONU rSOA based, cost-effective, simple design and full service coverage, was designed, simulated, optimized and implemented.

Considering upstream/downstream power budget differences, several parameters (OLT output power, ONU splitting ratio, ERs, feeder fibre length, RSOA gain, modulation formats, etc.), become important optimization elements in order to find the best upstream/downstream trade-off.

The initial designs proposed had a strong limitation in the power budget (only 8 users to be served). To overcome these limitations, a design based in two fibres in the WDM feeder section was adopted and implemented. This prototype was successfully tested showing high performance, robustness, versatility and reliability. So, the system is able to give coverage up to 1280 users at 20 Km, at 2.5 Gb/s in downstream and 1.25 Gb/s in upstream, and being compatible with the GPON ITU-T recommendation.

Chapter 3

3. TDM-PON RSOA-based ONU

In the implementation of practical next-generation PON (NG-PON) the most critical issue is how to realize low cost transmitters at subscriber ends [82]. The use of a reflective structure at the ONU (rONU) is a suitable approach cost/effective compared with the DFB laser-based typical ITU-standard ONU [83,104]. A rONU may consist of a reflective semiconductor optical amplifier (RSOA), a loop comprising an optical amplifier and an external modulator, or a self-injected FP laser [74]. In particular, the use of a RSOA-based ONU allows simultaneous re-modulation capabilities and broadband amplification, colourless operation, integration, CAPEX/OPEX reduction and wavelength reuse [7,51,121-123], freeing-up wavelength spectrum for future extension. However, due to single fibre/wavelength scenario, Rayleigh backscattering (RB) is the dominant impairment with downstream/upstream optical signal-to-rayleigh ratio (oSRR) critical relation.

In this chapter, the design of a Single-Wavelength/Fibre TDM-PON rSOA-based ONU, in burst operation, is theoretical and experimentally discussed. Impairments from Rayleigh Backscattering are analysed and modelled, and optimal TDM-PON design values are presented in order to reach the maximum number of users for efficient exploitation.

3.1. RB analysis in burst mode (BM) transmission

Rayleigh analysis in Burst Mode shows especial characteristics due principally to the short time of the data signal that it originates and the burst power. In this chapter, special attention is for the burst signal from a reflective ONU.

By considering a burst signal generated at the ONU travelling along a fibre, this signal exhibits an exponentially decreasing power level with the distance (and the propagation time). The power relation between the nominal ONU output power and transmitted power over the fibre after a time “t” is:

$$P(t)=P_0 \cdot e^{-\alpha \cdot V_g \cdot t} \quad (3.1)$$

With: $\alpha=0.046 \text{ km}^{-1}$, the single-mode fibre attenuation (0.2 dB/km), $V_g \approx 2.0 \times 10^5 \text{ km/s}$, the group velocity in the fibre.

For this burst signal, the scattered power $dP_{rb}(t)$ at the time t within an infinitesimal time interval dt is proportional to the burst power $P(t)$.

$$dP_{rb}(t)=k \cdot P(t) dt \quad (3.2)$$

where $k=S \cdot \alpha_s \cdot V_g$, with $S=1 \times 10^{-3}$, the fraction of the light scattered in back direction [93,25]; $\alpha_s = 3.2 \times 10^{-2} \text{ [km}^{-1}]$, the Rayleigh scattering loss.

Thus, from (1) and (2), summing up the light power backscattered from infinitesimal short time intervals dt from the whole burst, yields:

$$P_{rb}(t) = \int_0^{t_{burst}} k \cdot P(t) dt$$

$$P_{rb}(t) = k \cdot P_0 \int_0^{t_{burst}} e^{-2\alpha \cdot V_g \cdot t} dt \rightarrow P_{rb}(t) = \frac{S \cdot \alpha_s}{2 \cdot \alpha} \cdot P_0 (1 - e^{-2\alpha \cdot V_g \cdot t_{burst}})$$

By considering B =Rayleigh Backscattering Coefficient (from Chapter 1), $B = \frac{S \cdot \alpha_s}{2 \cdot \alpha}$, then,

$$P_{rb}(t) = P_0 \cdot B \cdot (1 - e^{-2 \cdot \alpha \cdot V_g \cdot t_{burst}}) \quad (3.3)$$

For example, for a rONU output power of 0 dBm, with $B=34.6 \text{ dB}$, the RB power generated for a burst time $t_{burst} = 10 \text{ us}$ is -42.3 dBm, and for a $t_{burst} = 1 \text{ us}$ is -52 dBm. Then, the backscattered power is proportional to the duration of the burst.

RB analysis in BM transmission in a TDMA environment

A particular relevant scenario, a TDM-PON section (it forms part of a WDM/TDM PON overlay, as seen in chapter 2), full-duplex single-fibre/single-wavelength bidirectional transmission with burst mode upstream signal and reflective ONU with wavelength-reuse, is shown in Fig. 3.1.

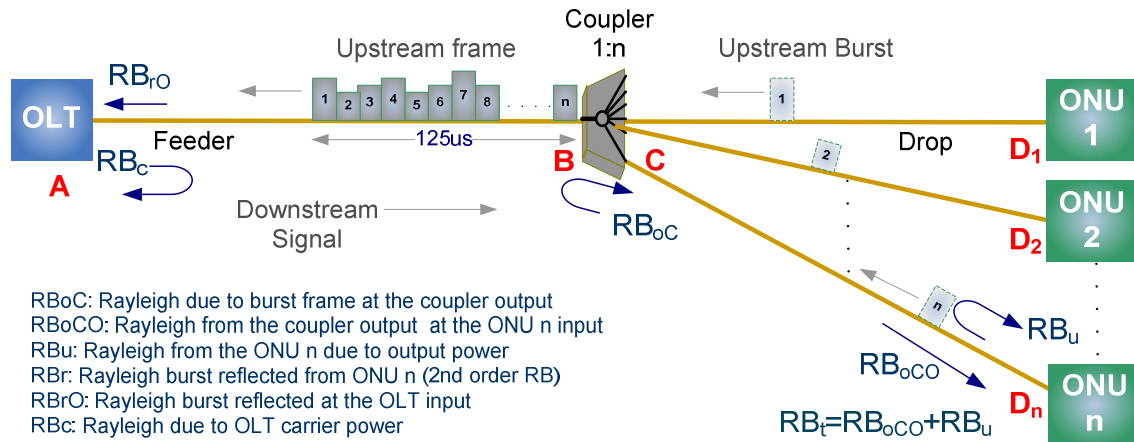


Fig. 3. 1 - TDM-PON scenario with different Rayleigh backscattering impairments

Here, all ONUs are served by the same OLT and are using the same wavelength. Also, the ONU burst time is associated with an upstream frame (in ITU-T FSAN it is 125us [124-125]) that bunches all contributions from different ONUs.

Different RB power values can be found as a function of the analysis point into ODN. These will be described below.

3.1.1. Rayleigh backscattering from the ONU burst output power (RB_u)

By considering this Rayleigh is generated by the upstream burst signal from the ONU, it will be named RB_u (Rayleigh Backscattering from upstream burst signal).

In the environment of a TDMA (it characteristic of an upstream transmission), a good practical approximation to obtain the RB_u is considering the ONU output power (P_o) value as a function of its burst time into the upstream total frame shared by all ONUs. So, and considering a static bandwidth assignment access for all ONUs [71]:

$$P_{o \text{ burst}}(\text{dBm}) = P_o(\text{dBm}) - (10 \cdot \text{Log}(N^\circ \text{ ONUs}))(\text{dB}) \quad \dots\dots\dots(3.4)$$

For a TDMA based on a dynamic bandwidth assignment (DBA), the ONU burst output power (P_o) depends of the burst time into the upstream total frame. In such condition, an approximation to obtain the RB_u is considering [126]:

$$P_{o \text{ burst}}(\text{dBm}) = P_o(\text{dBm}) + 10 \cdot \text{Log}(\% \text{ burst time})(\text{dB}) \quad \dots\dots\dots(3.5)$$

Where “% burst time” is the percentage of time of burst assigned by the MAC of the OLT (through the bandwidth map) to this ONU into the upstream frame (125us).

For example, by considering $P_o=0$ dBm and 32 ONUs, from (4) $P_{o \text{ burst}} = -15$ dBm. Now, if we consider that the burst time percentage is 3.125% (equivalent a one ONU in a PON with 32 ONUs), from (3.5) $P_{o \text{ burst}} = -15$ dBm.

Thus, a good approximation to obtain the RB_u is:

$$RB_u = P_{o \text{ burst}} \cdot B \cdot (1 - e^{-2 \cdot \alpha \cdot L_{\text{burst}}}) \quad \dots\dots\dots(3.6)$$

Nevertheless, the L_{burst} is usually as long as L_{drop} (a small burst of 10 us has a length of 2 km), then a most practical expression for the RB_u is:

$$RB_u = P_{o \text{ burst}} \cdot B \cdot (1 - e^{-2 \cdot \alpha \cdot L_{\text{drop}}}) \quad \dots\dots\dots(3.7)$$

In eq. (3.7) is considered only the drop length fibre instead the total length fibre, because in the TDM-PON ODN (feeder fibre + splitter/combiner + drop fibre, as shown in Fig. 1), the Rayleigh contributions at the ONU input beyond of the splitter/combiner are negligible due to the high splitter losses [123].

Unlike from eq. (3.3), that describes the Rayleigh effect for a burst signal of a general way, eqs. (3.6) and (3.7) are defined for a practical environment shared, such as a TDMA. Also, these expressions are described as a function of the length fibre (the burst time is implicit into the $P_{o \text{ burst}}$ expression). However, by considering that:

$$P_o = \sum_{ONU \ 1}^{ONU \ n} P_{o \text{ burst}}$$

and the $L_{\text{drop}} = V_g \cdot t_{\text{burst}}$, eqs (3.3) and (3.7) come to be equivalent.

3.1.2. Rayleigh backscattering effect between ONUs

Although the drop section isolates each ONU (this fibre section is not shared), an undesirable effect due to the Rayleigh backscattering accumulated at the combiner output from the burst power from other ONU’s can affects the downstream data signal arriving at an ONU. This phenomenon, that causes crosstalk among ONUs, will be discussed below. Here, the combiner device is the part of the coupler view in upstream direction, and combines all the burst from the ONUs to form the upstream frame (Fig. 3.1).

3.1.2.1. Rayleigh backscattering at the combiner output from “n” ONUs (RBoC)

In this section, the Rayleigh backscattering at the combiner output (“B” point in Fig. 3.1), from “n” ONUs is analysed. Fig. 3.2 shows a scenario of “n” ONUs transmitting bursts (in sequential way) on a GPON frame of 125us. When an ONU is in on-state during a determined time, others ONUs are in off-state.

However, their bursts (transmitted when they were in on-state) have produced Rayleigh that is accumulated at the combiner output. This Rayleigh (RB_{oC}) is added with the RB_u at the ONU input and affects the downstream signal.

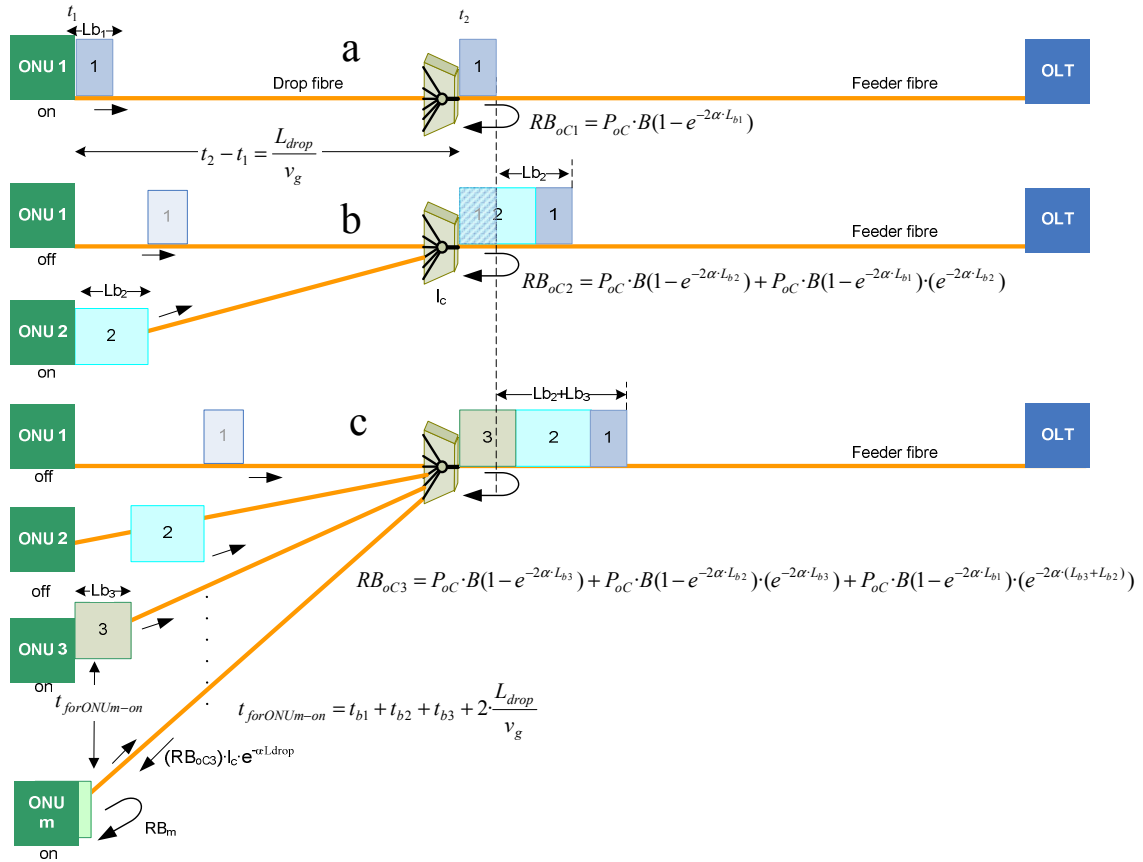


Fig. 3. 2 – Rayleigh accumulation process at the combiner output from “n” ONUs

Considering an initial state ($t_1=0$), and from the ONU₁, the Rayleigh produced by the burst of this ONU₁ at the combiner output in the instant t_2 will be [126]:

$$RB_{oC1} = P_{oC1} \cdot B(1 - e^{-2\alpha \cdot L_{b1}}) \dots \dots \dots (3.8)$$

with:

RB_{oCn} : Rayleigh power at the combiner output from the ONU “n” (here, $n=1$)

P_{oC} : Combiner output power, where $P_{oC} = P_{o-ONU} - (l_{coupler} + l_{drop})$

L_{bn} : Burst length from the ONU n (fibre length occupied in the burst duration)

l_c : Coupler loss, l_{drop} : Drop fibre loss.

t_{bn} : burst time of the ONU_n.

Now, considering the Rayleigh accumulation for two ONUs (at “b” step), and assuming that L_{drop} is the same for all ONUs:

$$RB_{oC2} = P_{oC2} \cdot B \cdot (1 - e^{-2\alpha \cdot L_{b2}}) + P_{oC1} \cdot B \cdot (1 - e^{-2\alpha \cdot L_{b1}}) \cdot (e^{-2\alpha \cdot L_{b2}})$$

and for three ONUs, as shown in “c” and in Fig. 3.3:

$$RB_{OC3} = P_{OC3} \cdot B \cdot (1 - e^{-2\alpha \cdot L_{b3}}) + P_{OC2} \cdot B \cdot (1 - e^{-2\alpha \cdot L_{b2}}) \cdot (e^{-2\alpha \cdot L_{b3}}) + P_{OC1} \cdot B(1 - e^{-2\alpha \cdot L_{b1}}) \cdot (e^{-2\alpha \cdot (L_{b2} + L_{b3})})$$

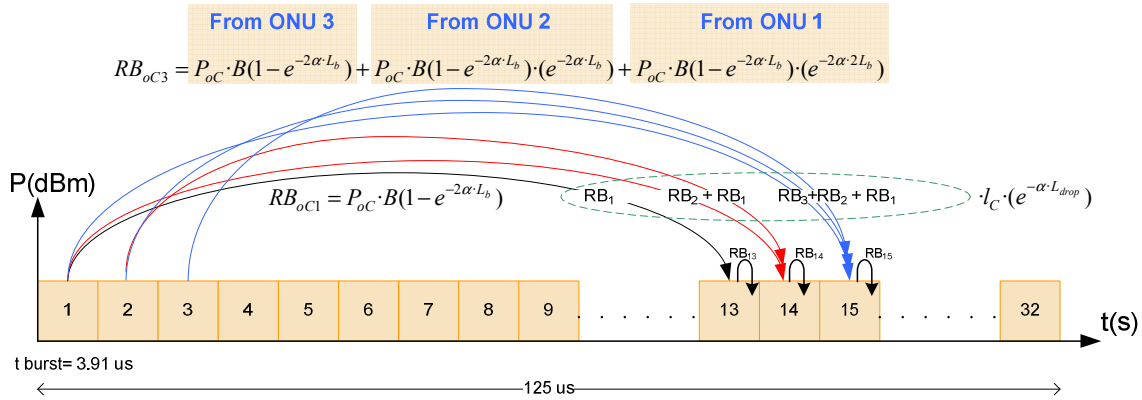


Fig. 3. 3 - Rayleigh power accumulation at the coupler output due to the burst signal from different ONUs affecting other ONUs (e.g. case of 32 ONUs)

By considering that ONU “m” is in on-state transmission in this moment, this Rayleigh arrives to it after a time given by:

$$t_{forONU_m} = t_{b1} + t_{b2} + t_{b3} + 2 \cdot \frac{L_{drop}}{v_g}$$

In general, for n ONUs transmitting in their burst time (as shown in Fig. 3.2):

$$RB_{OCn} = B \cdot [P_{OCn}(1 - e^{-2\alpha \cdot L_{bn}}) + P_{OCn-1}(1 - e^{-2\alpha \cdot L_{b(n-1)}}) \cdot (e^{-2\alpha \cdot L_{bn}}) + P_{OCn-2}(1 - e^{-2\alpha \cdot L_{b(n-2)}}) \cdot (e^{-2\alpha \cdot (L_{bn} + L_{b(n-1)})}) + P_{OCn-3}(1 - e^{-2\alpha \cdot L_{b(n-3)}}) \cdot (e^{-2\alpha \cdot (L_{bn} + L_{b(n-1)} + L_{b(n-2)})}) + \dots + P_{OC1}(1 - e^{-2\alpha \cdot L_{b1}}) \cdot (e^{-2\alpha \cdot (L_{bn} + L_{b(n-1)} + L_{b(n-2)} + \dots + L_{b2})})]$$

.....(3.9)

Let’s now consider a static bandwidth allocation from the OLT MAC for analysing the impact of eq. (3.9). Then L_{bn} is of the same length for all n ONUs, and then $L_{bn} = L_b$. Also, considering n ONUs transmitting at the same power:

$$RB_{OCn} = P_{OC} \cdot B[(1 - e^{-2\alpha \cdot L_{bn}}) + (1 - e^{-2\alpha \cdot L_{b(n-1)}}) \cdot (e^{-2\alpha \cdot L_{bn}}) + (1 - e^{-2\alpha \cdot L_{b(n-2)}}) \cdot (e^{-2\alpha \cdot (L_{bn} + L_{b(n-1)})}) + (1 - e^{-2\alpha \cdot L_{b(n-3)}}) \cdot (e^{-2\alpha \cdot (L_{bn} + L_{b(n-1)} + L_{b(n-2)})}) + \dots + (1 - e^{-2\alpha \cdot L_{b1}}) \cdot (e^{-2\alpha \cdot (L_{bn} + L_{b(n-1)} + L_{b(n-2)} + \dots + L_{b2})})]$$

Thus, the Rayleigh at the output of the combiner from n ONUs from the 125us upstream frame is:

$$RB_{OCn} = P_{OC} \cdot B(1 - e^{-2\alpha \cdot L_b}) \cdot (1 + (e^{-2\alpha \cdot L_b}) + (e^{-2\alpha \cdot 2 \cdot L_b}) + \dots + (e^{-2\alpha \cdot (n-1) \cdot L_b}))$$

This process is cyclic. Thus, for others GPON time slots, other contributions from these ONUs also should be considered. Therefore, for “N” burst contributions from these n ONUs transmitting at the same power, burst time and drop length, the Rayleigh at the coupler output is:

$$RB_{OCN} = P_{OC} \cdot B(1 - e^{-2\alpha \cdot L_b}) \cdot \left[\sum_{k=1}^N (e^{-2\alpha \cdot (k-1) \cdot L_b}) \right]$$

.....(3.10)

The “real” limit for “N” is given by L_{feeder} , with $L_{feeder} = N \cdot t_{burst} \cdot Vg$

Adapting eq. (3.10) to the geometric series, when $N \rightarrow \infty$, this expression converge to

$$\frac{1}{1 - e^{-2\alpha \cdot L_b}}, \text{ due to } e^{-2\alpha \cdot L_b} < 1$$

so,

$$RB_{oCN} = P_{oC} \cdot B(1 - e^{-2\alpha \cdot L_b}) \cdot \left[\frac{1}{1 - e^{-2\alpha \cdot L_b}} \right]$$

Then, for this special case, the Rayleigh accumulated by N bursts (with $N \rightarrow \infty$) from “n” ONUs, when the feeder fibre is infinitely long, approximates to:

$$RB_{oCN} \approx P_{oC} \cdot B \tag{3.11}$$

i.e., for the conditions assumed, the Rayleigh RB_{oC} has a dependency with the combiner output power (as a function of the combiner losses), as B (backscattering coefficient) is constant ($B = 34.8E-5 \approx -34.6$ dB).

Where,

$$P_{oC}(dBm) = P_{iC}(dBm) - l_c(dB) \tag{3.12}$$

By considering n = number of ONUs (n is a power of 2 for practical reasons).

$$l_c: \text{ coupler loss, } l_c = 3 \cdot \frac{\log(n)}{\log 2} \text{ dB} + \text{ excess loss,} \tag{3.13}$$

and excess loss ≈ 1 dB.

$$P_{iC}: \text{ coupler input power, } P_{iC} = P_{oONU} \cdot e^{-\alpha \cdot L_{drop}} \tag{3.14}$$

A good practical approach to accumulated Rayleigh (RB_{oCn}) from (10), by considering that multiples burst had been transmitted and the burst length from each ONUs had occupied the feeder fibre would be:

$$RB_{oCn} = P_{oC} \cdot B(1 - e^{-2\alpha \cdot L_b}) \cdot \left[\sum_{n=1}^{\infty} (e^{-2\alpha \cdot (n-1) \cdot L_b}) \right]$$

$$RB_{oCn} = P_{oC} \cdot B \underbrace{(1 - e^{-2\alpha \cdot L_b}) \cdot (1 + (e^{-2\alpha \cdot L_b}) + (e^{-2\alpha \cdot 2 \cdot L_b}) + \dots \dots (e^{-2\alpha \cdot (n-1) \cdot L_b}))}_{\approx (1 - e^{-2\alpha \cdot L_{feeder}})}$$

Then:

$$RB_{oCn} \approx P_{oC} \cdot B(1 - e^{-2\alpha \cdot L_{feeder}}) \tag{3.15}$$

Regardless the power considerations assumed and bandwidth distribution.

3.1.2.2. Rayleigh backscattering RBoC at the ONU input (RBoCO)

The Rayleigh contribution from the combiner output at the ONU input, from eq. (3.15) is [126]:

$$RB_{oCO} = RB_{oCn} \cdot e^{-\alpha \cdot L_{drop}} \cdot e^{-lc} \dots\dots\dots(3.16)$$

3.1.2.3. Total Rayleigh backscattering at the ONU input (RBt)

Then, two Rayleigh contributions are present at the ONU input: the RB accumulated at the output combiner, due to the signal power from different ONUs affected by the losses in the drop fibre and the combiner (RB_{oCO}), and the RB due to the output power of the same ONU (RB_u) [126].

$$RB_t = RB_u + RB_{oCO} \dots\dots\dots(3.17)$$

3.1.2.4. Numerical Analysis and Simulations

Figure 3.4 shows Rayleigh Backscattering and power level at the combiner output and the ONU input, calculated for 2, 4, 8, 16, 32 and 64 ONUs, considering symmetric bandwidth allocation. For each case, the burst time varies as a function of the number of ONUs, in order to complete the 125us GPON time slot capacity. Here, it was considered a drop fibre length of 5 km and the feeder fibre length of 15 km, with the ONUs equidistant at the same distance with respect to the coupler. The nominal ONU output power for this simulation is 0dBm.

It is noted in Fig. 3.4 that RB_{oC} follow the combiner output power curve (P_{oC}), displaced by the Rayleigh constant value (B), and that RB_u is the predominant Rayleigh. So, the resultant Rayleigh (RB_t) at the ONU input approximates at the RB_u . However, for low number of ONUs, RB_{oCO} value becomes more important effect because the losses at the coupler output are minor, and the power at the ONU input is higher. It does the crosstalk effect between ONUs more relevant. Then, the most critical case, only two ONUs in the PON, was analysed

Also, the RB_t is higher because RB_u is proportional to burst output power and, as minor is the number of ONUs, as higher is the power distribution in the frame from each ONU. So, the most critical case is when only two ONUs in the PON will be analysed below.

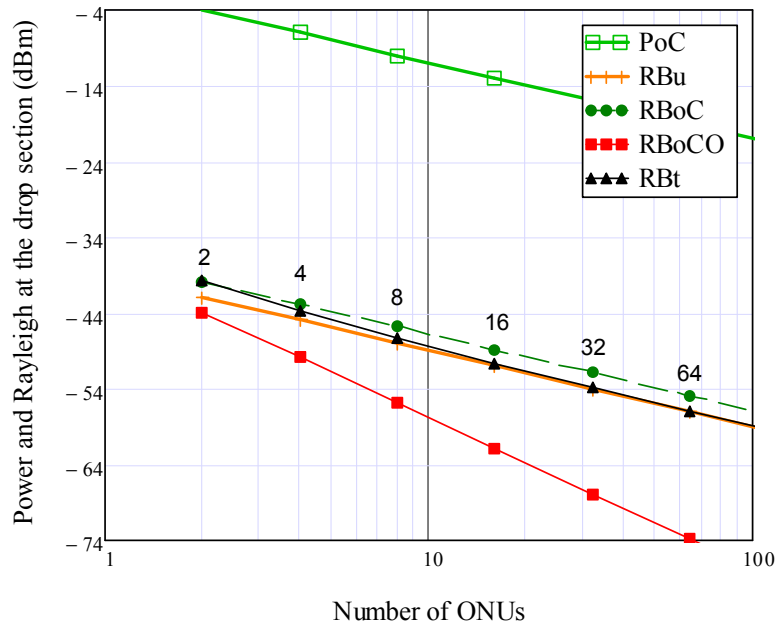


Fig. 3. 4 - Rayleigh Backscattering and power level at the combiner output and ONU input calculated for 2 up to 64 ONUs considering symmetric bandwidth allocation.

3.1.3. Analysis of the critical cases due to RB impairments

Here, two ONUs in a TDM-PON are considered, as shown in Fig. 3.5. Different extreme conditions are possible in this particular scenario, with conditions similar to those that can be found in a PON rural. A higher range of powers from the combiner output, due to lower splitting losses and by having asymmetric bandwidth allocation will be analysed. This last condition allows analysing the effects due to different burst length between ONUs and critical scenarios in DBA.

With $P_{o-ONU1}=5\text{dBm}$, nominal ITU GPON standard maximum output power [104], and P_{o-ONU2} varied between -5 to 5 dBm, and different GPON burst time allocations, the target is to find the reliability threshold values for the PON design in this critical scenario.

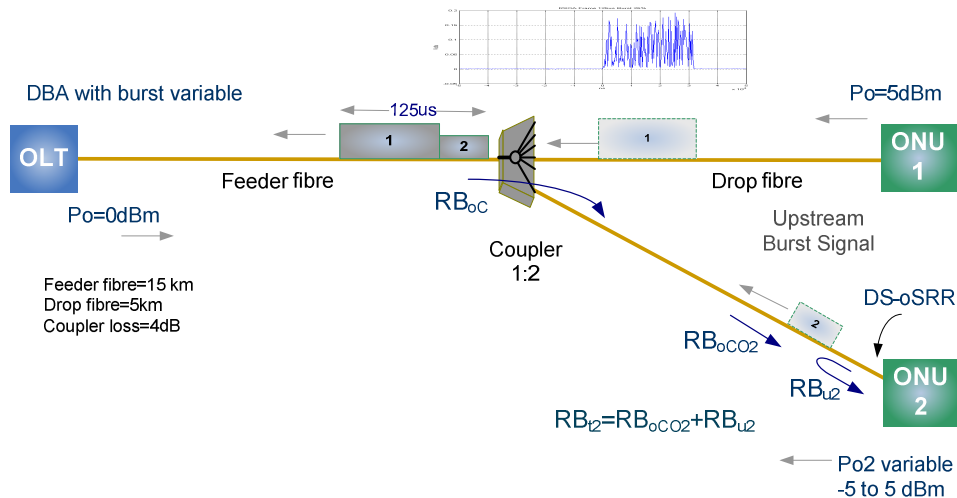


Fig. 3. 5 – Scenario of analysis of critical values to total RB at the ONU 2 input as a function of different ONU 2 nominal power output and asymmetric burst length

A symmetrical allocation ONU1/ONU2 50%/50% is used as a reference to observe the RB effect due to different powers between ONUs, as shown in Fig. 3.6. So, the RB_{oC} at the ONU 2 (RB_{oCO2}) is predominant over the RB_t at the ONU 2 (RB_{t2}) when P_{o-ONU1} is at least twice time the P_{o-ONU2} . This is also facilitated by the lower combiner losses, by using eq. (13), 4 dB. Otherwise, RB_{u2} would increase strongly the RB_t .

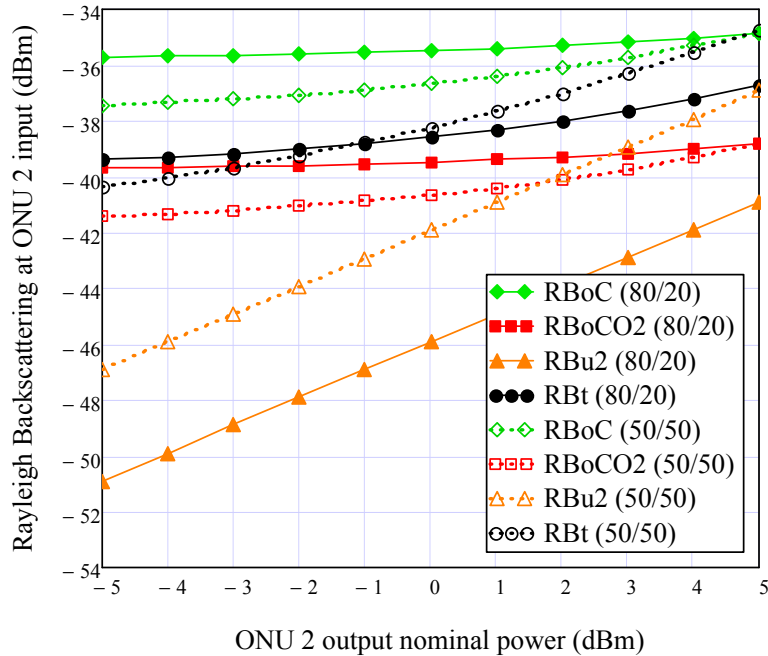


Fig. 3. 6 – Total RB at the ONU 2 input as a function of different ONU 2 nominal output power and asymmetric burst length

However, an asymmetrical allocation, by using ONU1/ONU2 80%/20%, combined with the different powers between these ONUs originates that $RB_{oCO2} > RB_u$ for all the output power values of the ONU 2 considered in the simulation (from -5 to 5 dBm). Despite this fact, the total Rayleigh affecting the ONU 2 is not greater than the symmetrical allocation, due to lower impact of RB_{u2} , because the lower duty cycle (20%).

From these results we can infer (by extrapolation) that asymmetrical bandwidth values with $ONU1 < ONU2$ will affect more the total Rayleigh at the ONU 2 due to the greater impact of the RB_u .

Fig. 3.7 continues with this analysis and justifies at the last asseveration. The downstream optical Signal-to-Rayleigh ratio (oSRR) is shown to different asymmetrical duty cycles between the ONU1 and the ONU2, and different ONU 2 nominal output power. Here, OLT output power is fixed at 0 dBm and ODN loss=8dB.

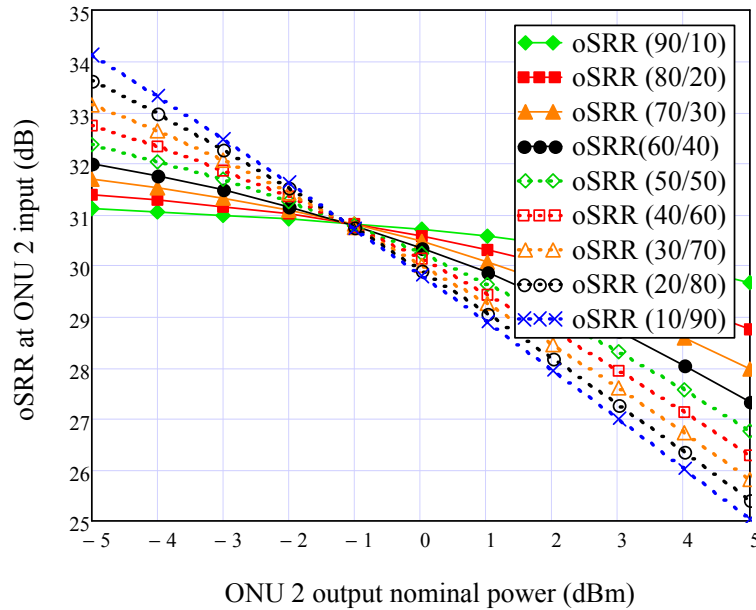


Fig. 3. 7 – DS optical Signal-to-Rayleigh Ratio (DS-oSRR) at different asymmetrical duty cycles (ONU1/ONU2) and different ONU2 nominal output power

To obtain a BER of $1E-10$ with a DS-ER=10dB (GPON 984.2) [83,104], an oSRR>20dB is required. For a rONU-based PON, with restrictions of DS-ER due to wavelength reuse, a DS-ER=4dB with downstream cancellation (DSC) is required. For this value, an oSRR>25.5 dB is mandatory [127].

So, the critical DS-oSRR values are reached for duty cycles ONU1/ONU2 10/90 and 20/80, for ONU₂ power output values ≥ 5 dBm. In these cases the ONU₂ burst signal power has higher energy and, then, the RB_u effect on RB_t is greater.

Therefore, in this critical two-ONUs scenario, a DBA algorithm should avoid these quite asymmetrical allocations and must be capable of assigning adequately the burst time for each ONU. Other option is has a balanced power output adjust for a ONU as a function of the duty cycle. In this case, the OLT must provide a power levelling mechanism, already defined at the G.984.3 specification [124-125]. It requires that the ONU is capable of increasing/decreasing the transmitted power upon reception of downstream *Change_Power_Level* message sent from the MAC-OLT.

In practical PON implementations, this critical scenario, with few ONUs could be possible in rural PON access. In such cases, a static bandwidth allocation, with fixed bandwidth, could results more appropriated.

Other alternative, now more suitable, is the use of FEC. For using FEC and DSC technique, oSRR limits can be re-established for suitable data decodification. For a FEC of BER $5E-4$, up to 5 dB of gain is possible [127]. This will be seen latter.

3.1.4. Rayleigh reflected (RBr)

In a PON rONU-based, Rayleigh contributions at the ONU input are remodulated, reamplified, reflected and transmitted in upstream direction, added coherently at the signal data burst. Rayleigh reflected is possible only when $t=t_{\text{RSOA on}}$. In other case, RB_r is negligible (ideally $RB_r=0$, with $ER=\infty$). To RSOA_{off}-state, the upstream signal and Rayleigh reflected are upstream propagated with loss given by $e^{-\alpha \cdot L_{\text{drop}}}$.

Two important parameters in RB_r are the ONU gain and the burst length from this ONU. Here, ONU gain (G) is expressed by:

$$G = \text{ONU}_{\text{input power}} + \text{RSOA}_{\text{gain}} + \text{ONU}_{\text{losses}}$$

With: $\text{RSOA}_{\text{gain}}$, the gain of the Reflective SOA inside the ONU, and the losses inside the ONU, where $\text{ONU}_{\text{losses}} = 2 \cdot \text{ONU}_{\text{splitting}} + \text{Other}_{\text{losses}}$.

To obtain an expression for the impact of the ONU burst length, it is divided into “n” parts of length ΔL , as shown in Fig. 3.8. The Rayleigh reflected is calculated by steps, in order to examine, also, the Rayleigh effects from other ONUs.

Upstream burst length (L_b) from the ONU_k is partitioned in “n” parts. So, $L_b = n \cdot \Delta L_b$.

The Rayleigh from this ΔL_{burst} from eq. (3.6) is given by:

$$RB_u = P_{o\text{burst}} \cdot B(1 - e^{-2\alpha \cdot \Delta L_{\text{burst}}})$$

The accumulated Rayleigh is given in eq. (3.10), and the accumulated Rayleigh at the coupler output reaching the ONU_k (RB_{oCOk}) is given in eq. (3.16).

In the time $t=t_1$, the Rayleigh reflected by the RSOA of the ONU_k is:

$$RB_{r(t1)} = P_{o\text{-burst}} \cdot B(1 - e^{-2\alpha \cdot \Delta L_b}) \cdot G + G \cdot RB_{oCOk}$$

In $t=t_2$:

$$RB_{r(t2)} = (RB_{r(t1)} + P_{o\text{-burst}}) \cdot G \cdot B(1 - e^{-2\alpha \cdot 2\Delta L_b}) + G \cdot RB_{oCOk}$$

In $t=t_3$:

$$RB_{r(t3)} = (RB_{r(t2)} + P_{o\text{-burst}}) \cdot G \cdot B(1 - e^{-2\alpha \cdot 3\Delta L_b}) + G \cdot RB_{oCOk}$$

In $t=t_4$:

$$RB_{r(t4)} = (RB_{r(t3)} + P_{o\text{-burst}}) \cdot G \cdot B(1 - e^{-2\alpha \cdot 4\Delta L_b}) + G \cdot RB_{oCOk}$$

In general, for $t=t_n=t_{\text{RSOA-off}}$, with $L_b = V_g \cdot t_n = n \cdot \Delta L_b$

$$RB_{r(tn)} = (RB_{r(t(n-1))} + P_{o\text{-burst}}) \cdot G \cdot B(1 - e^{-2\alpha \cdot n\Delta L_b}) + G \cdot RB_{oCOk}$$

Now, developing each of these expressions by searching a compact expression for this Rayleigh:

In $t=t_1$:

$$RB_{r(t1)} = P_{o\text{-burst}} \cdot B(1 - e^{-2\alpha \cdot \Delta L_b}) \cdot G + RB_{oCOk} \cdot G$$

In $t=t_2$:

$$RB_{r(t2)} = P_{o\text{-burst}} \cdot G^2 \cdot B^2(1 - e^{-2\alpha \cdot \Delta L_b}) \cdot (1 - e^{-2\alpha \cdot 2\Delta L_b}) + RB_{oCOk} \cdot G^2 \cdot B(1 - e^{-2\alpha \cdot 2\Delta L_b}) + (P_{o\text{-burst}} \cdot G \cdot B(1 - e^{-2\alpha \cdot 2\Delta L_b}) + G \cdot RB_{oCOk})$$

In $t=t_3$:

$$RB_{r(t_3)} = (P_{o\text{-burst}} \cdot G^3 \cdot B^3 (1 - e^{-2\alpha \cdot \Delta L_b}) \cdot (1 - e^{-2\alpha \cdot 2\Delta L_b}) \cdot (1 - e^{-2\alpha \cdot 3\Delta L_b}) + RB_{oCOK} \cdot G^3 \cdot B^2 (1 - e^{-2\alpha \cdot 2\Delta L_b}) \cdot (1 - e^{-2\alpha \cdot 3\Delta L_b}) + (P_{o\text{-burst}} \cdot G^2 \cdot B^2 (1 - e^{-2\alpha \cdot 2\Delta L_b}) \cdot (1 - e^{-2\alpha \cdot 3\Delta L_b}) + G^2 \cdot B \cdot RB_{oCOK} \cdot (1 - e^{-2\alpha \cdot 3\Delta L_b}) + (P_{o\text{-burst}} \cdot G \cdot B (1 - e^{-2\alpha \cdot 3\Delta L_b}) + G \cdot RB_{oCOK})$$

In $t=t_4$:

$$RB_{r(t_4)} = P_{o\text{-burst}} \cdot G^4 \cdot B^4 (1 - e^{-2\alpha \cdot \Delta L_b}) \cdot (1 - e^{-2\alpha \cdot 2\Delta L_b}) \cdot (1 - e^{-2\alpha \cdot 3\Delta L_b}) \cdot (1 - e^{-2\alpha \cdot 4\Delta L_b}) + P_{o\text{-burst}} \cdot G^3 \cdot B^3 (1 - e^{-2\alpha \cdot 2\Delta L_b}) \cdot (1 - e^{-2\alpha \cdot 3\Delta L_b}) \cdot (1 - e^{-2\alpha \cdot 4\Delta L_b}) + P_{o\text{-burst}} \cdot G^2 \cdot B^2 (1 - e^{-2\alpha \cdot 3\Delta L_b}) \cdot (1 - e^{-2\alpha \cdot 4\Delta L_b}) + P_{o\text{-burst}} \cdot G \cdot B (1 - e^{-2\alpha \cdot 4\Delta L_b}) + RB_{oCOK} \cdot G^4 \cdot B^3 (1 - e^{-2\alpha \cdot 2\Delta L_b}) \cdot (1 - e^{-2\alpha \cdot 3\Delta L_b}) \cdot (1 - e^{-2\alpha \cdot 4\Delta L_b}) + RB_{oCOK} \cdot G^3 \cdot B^2 (1 - e^{-2\alpha \cdot 3\Delta L_b}) \cdot (1 - e^{-2\alpha \cdot 4\Delta L_b}) + RB_{oCOK} \cdot G^2 \cdot B (1 - e^{-2\alpha \cdot 4\Delta L_b}) + RB_{oCOK} \cdot G$$

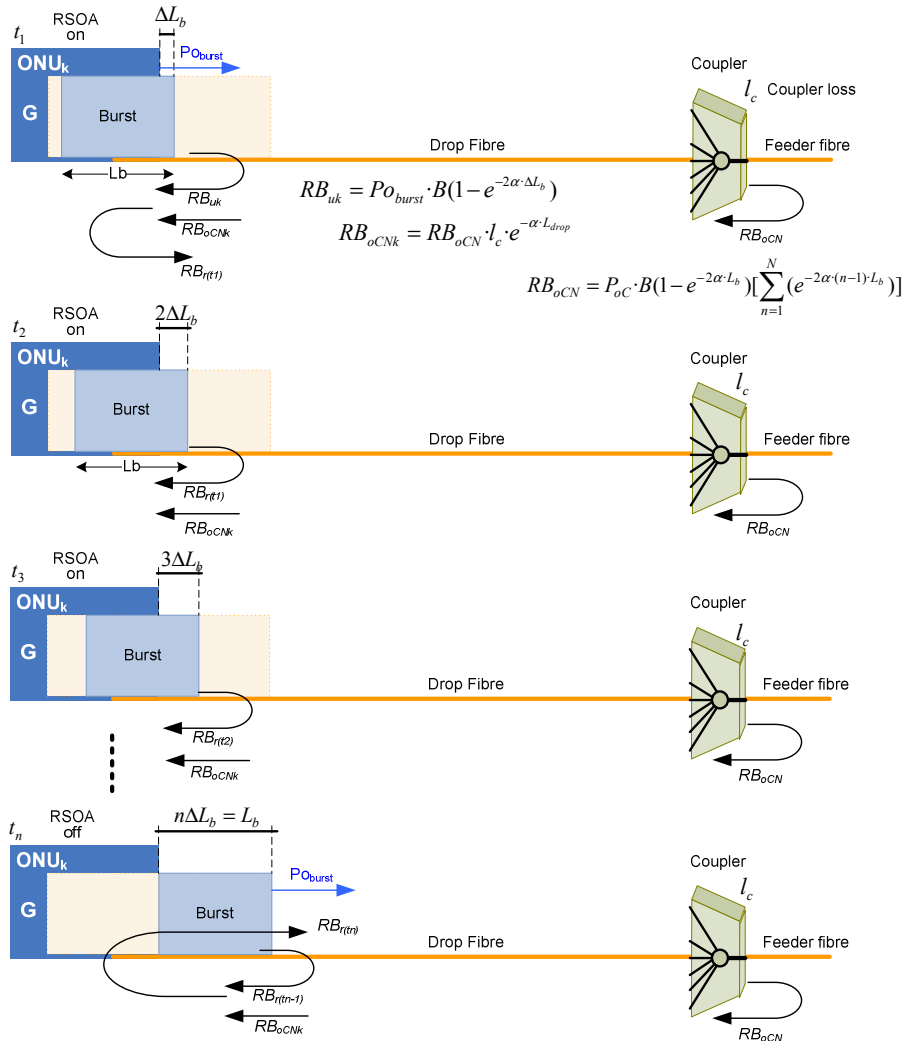


Fig. 3. 8 - ONU burst length divided into "n" parts for the calculating of the Rayleigh reflected and the influences of the RBU and RBoCO

Now, considering the m -th divisions of the burst (in $t=t_m$):

$$\begin{aligned}
RB_r(t(m)) = P_{o-burst} & \left((G \cdot B)^m [1 - \prod_{n=1}^m (e^{-2\alpha \cdot n \cdot \Delta L_b})] + (G \cdot B)^{m-1} [1 - \prod_{n=2}^m (e^{-2\alpha \cdot n \cdot \Delta L_b})] \right. \\
& + (G \cdot B)^{m-2} [1 - \prod_{n=3}^m (e^{-2\alpha \cdot n \cdot \Delta L_b})] + (G \cdot B)^{m-3} [1 - \prod_{n=4}^m (e^{-2\alpha \cdot n \cdot \Delta L_b})] \dots \left. \right) \\
& + G \cdot RB_{oCOk} \left((G \cdot B)^{m-1} [1 - \prod_{n=2}^m (e^{-2\alpha \cdot n \cdot \Delta L_b})] + (G \cdot B)^{m-2} [1 - \prod_{n=3}^m (e^{-2\alpha \cdot n \cdot \Delta L_b})] \right. \\
& \left. + (G \cdot B)^{m-3} [1 - \prod_{n=4}^m (e^{-2\alpha \cdot n \cdot \Delta L_b})] \dots \right)
\end{aligned}$$

Finally, the compact expression for the Rayleigh reflected, resulting for the “m” time divisions of the burst length (L_b) is:

$$\begin{aligned}
RB_r(t_m) = P_{o-burst} \cdot & \left(\sum_{n=1}^m (G \cdot B)^{m-(n-1)} [1 - \prod_{k=n}^m (e^{-2\alpha \cdot k \cdot \Delta L_b})] \right) + G \cdot RB_{oCOk} \\
& \cdot \left(\sum_{n=1}^m (G \cdot B)^{m-n} [1 - \prod_{k=n+1}^m (e^{-2\alpha \cdot k \cdot \Delta L_b})] \right)
\end{aligned} \dots\dots\dots(3.18)$$

Eq. (3.18) allows calculating the RB_r in a determined instant of the burst time, as a function of the contribution from “m” elements of the burst length. As a consequence, this expression evidences that the RB_r value depends strongly on the burst length as of the ONU gain.

Fig. 3.9 shows RB_r total at the ONU input from eq. (3.15) and RB_r as a function of the impact of the $G \cdot RB_u$ (1st term of the eq. 18) and $G \cdot RB_{oCO}$ (2nd term of the eq. 18), for a PON system with 2 up to 64 ONUs. It is observed that RB_u has more influence at the total RB_r due to its higher power. So, a good practical approximation to RB_r calculation from an ONU can be straightforward obtained from the Rayleigh contributions at the ONU input ($RB_u + RB_{oCO}$), reamplified by the ONU gain (G). So:

$$RB_r = (RB_u + RB_{oCO}) \cdot G$$

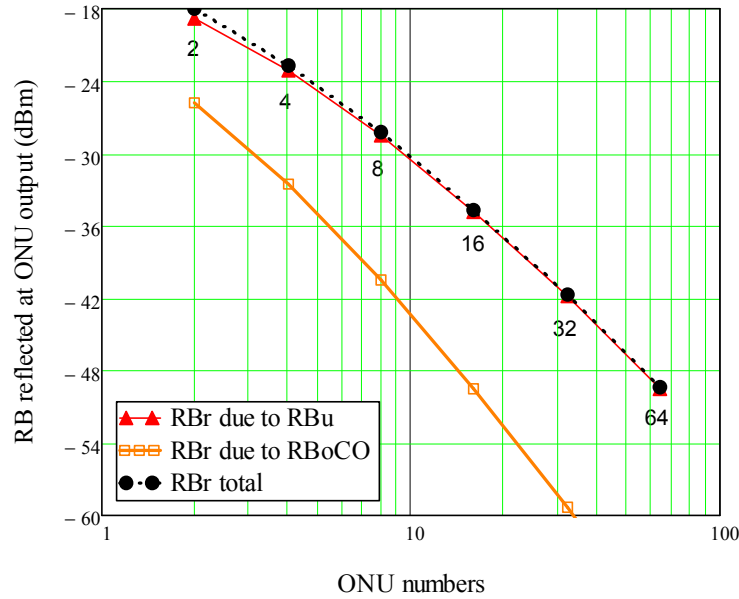


Fig. 3. 9 - RBr total at the ONU input and RBr as a function of the impact of the G•RBu and G•RBoCO

Also, from this Fig. 3.9, RB_r is critical when ONU numbers <4 , due to the fact that the burst power that originates the RB_u has more energy as it has more bandwidth into the upstream frame.

3.1.4.1. Rayleigh reflected from the ONU at the OLT input (RBrO)

Considering the Rayleigh reflected from the ONU_k

$$RB_{rk} = RB_{tk} \cdot G_k$$

With $RB_{tk} = RB_{uk} + RB_{oCOk}$, the total Rayleigh at the ONU_k , and G_k is the ONU_k gain

This Rayleigh, after being attenuated at the drop section, is combined at the coupler with the RB_{rN-1} from all “ $N-1$ ” ONUs in the PON. The resultant Rayleigh is affected by the ODN losses together with the upstream data frame, before arriving at the OLT. An expression for the RB_r at the OLT input (RB_{rO}) is shown in eq. (3.19).

$$RB_{rO} = \left(\sum_{k=1}^N RB_{rk} \cdot e^{-\alpha \cdot L_{drop}} \right) \cdot e^{-\alpha \cdot L_{feeder}} \cdot L_c \quad \dots(3.19)$$

Fig. 3.10 shows the Rayleigh reflected values at the OLT input (RB_{rO}) and the Rayleigh reflected values at the ONU output (RB_r) from 2 up to 64 ONUs, by assuming that ONU gain is the same for all ONUs.

As the number of ONUs in the PON increases, as the sum of the RB_r powers from all ONUs at the coupler, it overpass the ODN losses.

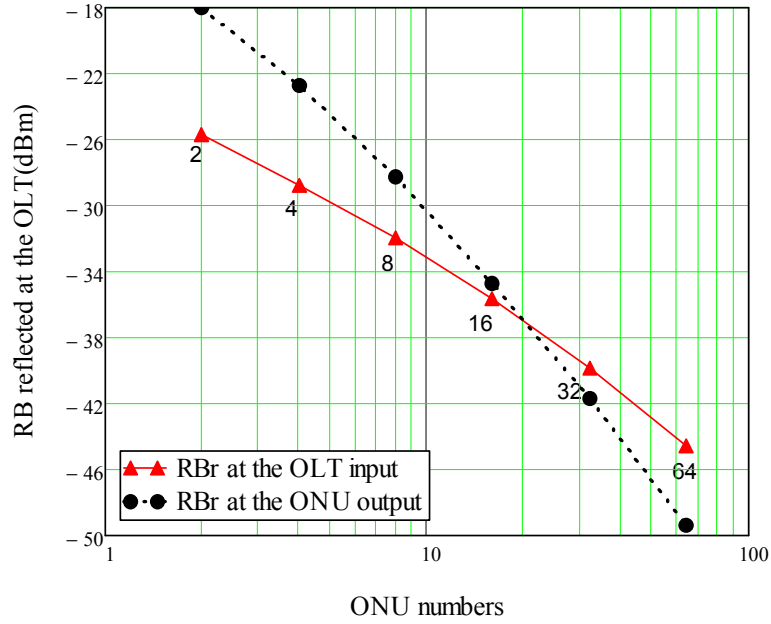


Fig. 3. 10 - Rayleigh reflected values at the OLT input (RBrO) and at the ONU output (RBr) from 2 up to 64 ONUs, considering the same ONU gain for all ONUs.

3.1.5. Total Rayleigh at the OLT input

At the OLT input two Rayleigh impairments are present: RB due to OLT output power (RB_c) and Rayleigh reflected from the ONUs (RB_{rO}). So:

$$RB_{OLT} = RB_c + RB_{rO} \quad \dots(3.20)$$

RB_c is obtained from eq. (1.1) (Chapter 1) [70,74]. It is determinant in the calculus of the OLT output power and the upstream power budget in the PON design and establishes the US-oSRR thresholds.

3.1.6. Upstream optical Signal-to-Rayleigh Ratio (US-oSRR)

An expression to calculate of the US-oSRR is given for the eq. (3.18) [70]:

$$US\text{-oSRR} = OLT_{input} / RB_{OLT} \quad \dots(3.21)$$

With RB_{OLT} defined in eq. (3.20). OLT input power can be given by:

$$OLT_{input} = ONU_{out} \cdot ODN_{losses} \quad \dots(3.22)$$

With ODN_{losses} , the losses in the optical distribution network:

$$ODN_{losses} = e^{-\alpha \cdot L_{drop}} \cdot e^{-lc} \cdot e^{-\alpha \cdot L_{feeder}} \quad \dots(3.23)$$

and with the combiner losses defined in eq. (3.13).

A polynomial approximation from experimental results obtained of a particular commercial RSOA (RSOA-18-TO-C-FA from Kamelian) is used to obtain the ONU output power. Thus,

$$\text{RSOA}_{\text{gain}} = -0.0159x^2 + 0.0945x + 8.5929 \quad \dots\dots\dots(3.24)$$

Then, the nominal ONU output power (ONU_{out}) can be obtained from eq. (3.24):

$$\text{ONU}_{\text{out}} = -0.0159 \cdot (\text{ONU}_{\text{in}} + \text{ONU}_{\text{loss}})^2 + 0.0945 \cdot (\text{ONU}_{\text{in}} + \text{ONU}_{\text{loss}}) + 8.5929$$

Fig. 3.11 shows the US-oSRR and total RB at the OLT input. For higher splitter losses, $\text{RB}_c \gg \text{RB}_{r0}$. So, $\text{RB}_{\text{total}} \approx \text{RB}_c$, and US-oSRR strongly depends of the OLT output power, as this originates the RB_c and of the ONU gain, to reach the sufficient power at the OLT input.

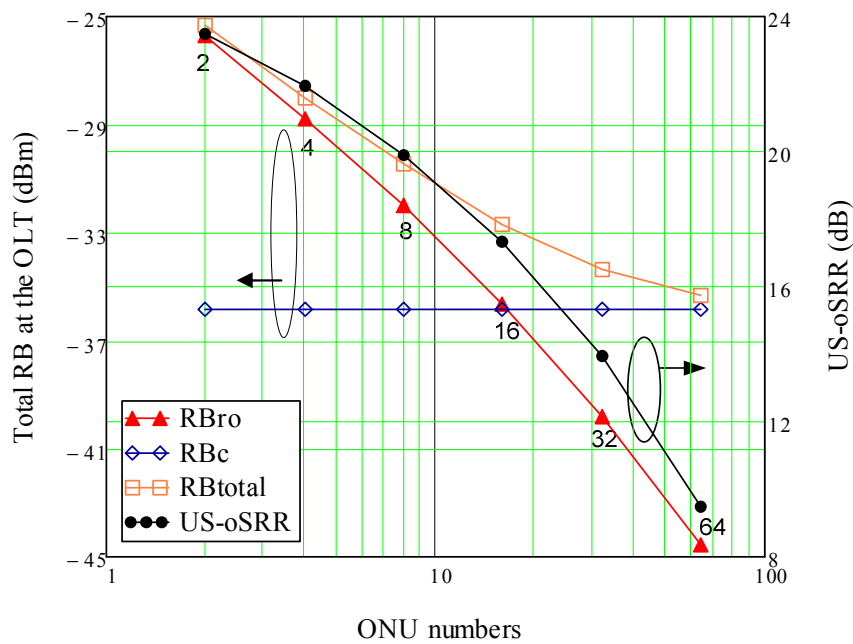


Fig. 3. 11 – US-oSRR and total Rayleigh at the OLT input and the contributions from RBc and RBrO

3.1.7. Conclusions

A deeper analysis for Rayleigh Backscattering effect in burst mode transmission was done. From this analysis, equations for Rayleigh backscattering from the ONU burst output power (R_{Bu}), Rayleigh backscattering at the combiner output (R_{BoC}), R_{BoC} at the ONU input (R_{BoCO}), Rayleigh backscattering reflected (R_{Br}) and R_{Br} at the OLT input (R_{BrO}) were deterministically formulated to determine their behavior, effects and dependences.

Critical cases are present in downstream transmission for configurations with lower ONU numbers due to a higher energy concentration in the upstream burst and lower tree losses and the resulting Rayleigh.

So, the resultant Rayleigh (R_B) at the ONU input approximates at the R_{B_u}. However, for low number of ONUs, R_{B_{oCO}} value becomes more important effect because the losses at the coupler output are minor, and the Rayleigh power at the ONU input is higher. It does the crosstalk effect between ONUs more relevant. Then, the most critical case, only two ONUs in the PON, was analysed.

Asymmetrical allocations for this scenario were studied. By using ONU1/ONU2 80%/20%, and different powers between these ONUs originates that R_{BoCO2} >R_{Bu}. Despite this fact, the total Rayleigh affecting the ONU 2 is not greater than the symmetrical allocation, due to lower impact of R_{Bu}. For asymmetrical bandwidth, now with ONU1 < ONU2, the total Rayleigh at the ONU 2 will be higher due to the greater impact of the R_{Bu}.

When compared with GPON (BER of 1E-10 with a DS-ER=10dB) where an oSRR>20dB is required, a rONU-based PON, with restrictions of DS-ER (4dB) due to wavelength reuse, an oSRR>25.5 dB is mandatory. So, critical DS-oSRR values are reached for duty cycles ONU1/ONU2 10/90 and 20/80, for ONU₂ power output values ≥ 5 dBm. Therefore, in this critical two-ONUs scenario, a DBA algorithm should avoid these quite asymmetrical allocations and must be capable of assigning adequately the burst time for each ONU.

In practical PON implementations, this critical scenario, with few ONUs could be possible in rural PON access. In such cases, a static bandwidth allocation, with fixed bandwidth, could results more appropriated than DBA techniques.

3.2. TDM-PON rSOA-based ONU Network design and Optimization

In this section, the design of a Single-Wavelength/Fiber TDM-PON rSOA-based ONU in burst operation is discussed and optimized to reach the best exploitation point, and up to 32 ONUs are demonstrated, by selecting adequately the power outputs and the tradeoff between DS power budget and US-oSRR.

3.2.1. Analysis of the relevant parameters

3.2.1.1. Extinction Ratio

DS signal with $ER > 5$ dB would be difficult to be data-cleaned before being directly IM data remodulated at RSOA-based ONUs. Reduction of DS Extinction Ratio (ER) is required to achieve good enough feed-forward cancellation. The optimum DS-ER to keep minimized DS-residual during its space bits for US remodulation is a tradeoff: too low DS-ERs result in an unacceptable high penalty for its detection, while a too high ER degrades the US performance [122].

BER dependency of ER and oSRR (@ 1dB penalty) has been experimentally measured on the TDM section of the SARDANA network (as will be seen in chapter 5), through a B2B connection [127], and the results are shown in Fig. 3.12. The lower ERs, the higher are the oSRR requirement. So, for BER of $1E-9$ with a DS-ER=10dB (GPON 984.2) [83,104], an oSRR>20dB is required, whilst for a DS-ER=4dB, an oSRR>25dB is mandatory. This fact will limit dramatically the maximum splitting ratio and the power budget of the system.

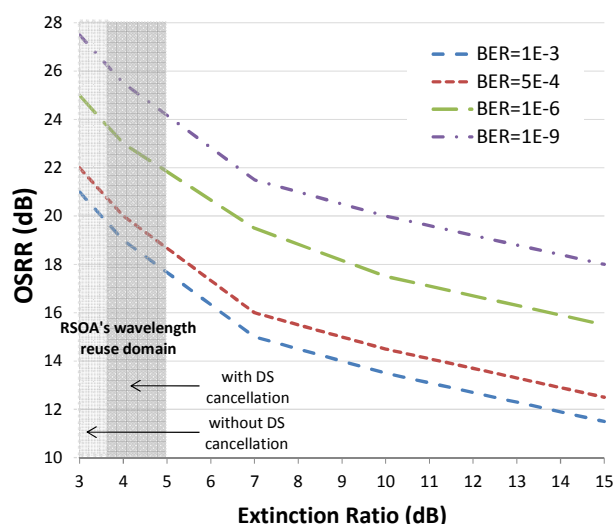


Fig. 3. 12 – Optical Signal-to-Rayleigh Ratio (oSRR) as a function of the Extinction Ratio for different BER values. However, Fig. 3.12 also shows that is possible to achieve an oSRR optimal value by using FEC to BER 5E-4 and DSC technique. So, oSRR limits are established for suitable data decoding: $DS-oSRR_{limit} \geq 20$ dB and $US-oSRR_{limit} \geq 14.5$ dB, with $US-ER=9$ dB to fulfill the required power budget.

3.2.1.2. RSOA electro-optical modulation

RSOA operation, presented in Fig. 3.13, shows the available electro-optical modulation range for different RSOA optical carrier input powers and injection bias currents. It is observed that for bias current < 80mA the output is quite linear, and it becomes saturated for higher bias current. The best BER performance has been obtained with bias current =60 mA and modulation = ± 3 Vpp. These best tradeoff values allow a modulation index $\approx 70\%$, with an US-ER > 9dB.

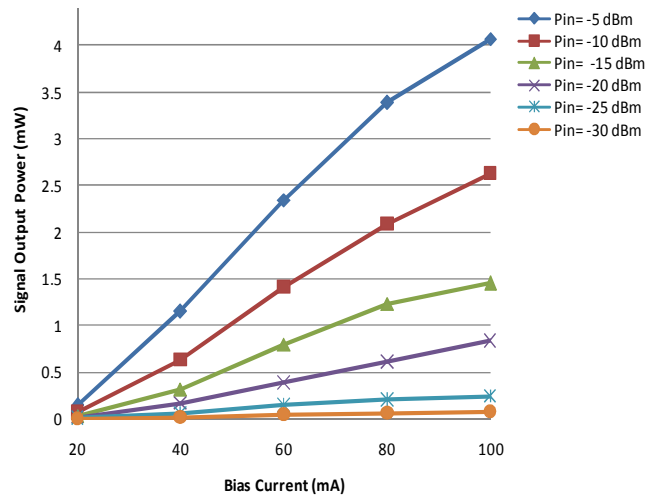


Fig. 3. 13 - RSOA optical output power for different injection bias current and optical carrier input power.

3.2.1.3. Carrier level Recovery

Also, because of the direct US remodulation on the same DS stream, carrier level recovery techniques had been required to erase the DS pattern [128-130]. As carrier recovery by gain saturation requires the high injection power, insufficient in PONs with high tree loss, an additional feed-forward cancellation circuit [121] has been used. This consists of an electrical delay ($\Delta\tau$) for fine tuning of the path lengths, a derivative filter (DF) and RF amplifier combinatory to subtract the inverted DS information.

3.2.1.4. Rayleigh Backscattering impairment

As was analysed in previous section, Rayleigh penalizes at oSRR. Fig. 3.14 presents details of the Rayleigh penalty and shows how the upstream signal is over penalized, while the downstream remains less sensitive to Rayleigh, basically because of burst signal generates less Rayleigh.

For example, when the OLT output is 0dB, the ODN fibre length is 20 km (Rbc = 34.6 dBm, ODN fibre losses -4 dB), and the ODN splitting ratio is 1:32 (-16 dB power losses), the oSRR is of only 14.6 dB, if considering an ONU gain of 20 dB (upstream signal power at the OLT input is -20 dBm). This value highly penalizes the reception.

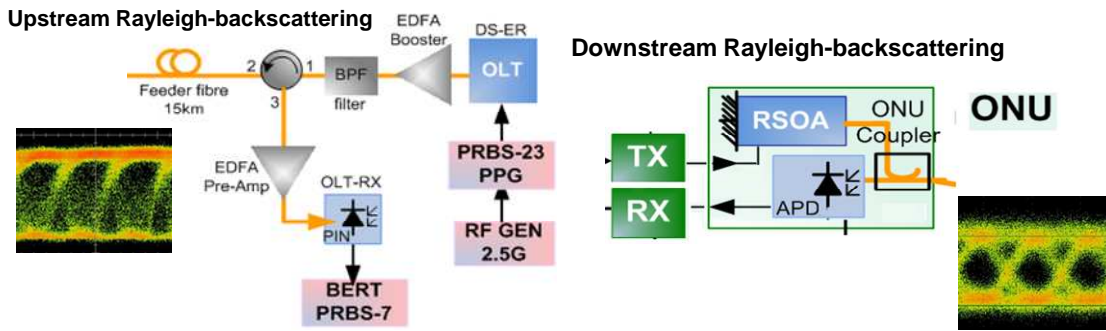


Fig. 3. 14 – Rayleigh penalty at the reception in upstream and downstream transmission.

3.2.1.5. ONU splitting factor

The splitting inside the ONU splits input optical power to the RSOA to be remodulated, and to the APD for downstream detection.

Due to downstream remains less sensitivity to Rayleigh, ONU output power must be a maximum to avoid upstream Rayleigh penalties, so as much power reaches the RSOA much better. The idea is to give more than 50% to RSOA whilst the remaining power is enough to the APD to detect.

ONU splitting factor is a key parameter to matching downstream power budget and upstream oSRR critical trade-off.

3.2.2. Scenario and Network Topology

The TDM setup with single-fibre/wavelength scenario is based on SARDANA PON tree section [51,123], and is shown in Fig. 3.15. This implements colourless reflective-ONUs based on RSOA and burst mode US operation. To emulate a common TDM-PON [104], an OLT from central office (CO) is placed in the site of the remote node (RN). This configuration is fully compatible with other TDM tree topologies. The ODN is fixed in 20 km (standard reach) @2.5/1.25Gbps and operates at 1552.52 nm. Each ONU transmits burst carried on 125us GPON US frames. Here, a static bandwidth assignment is considered for simplicity. So, duty cycles are in correspondence with the ODN splitting ratio.

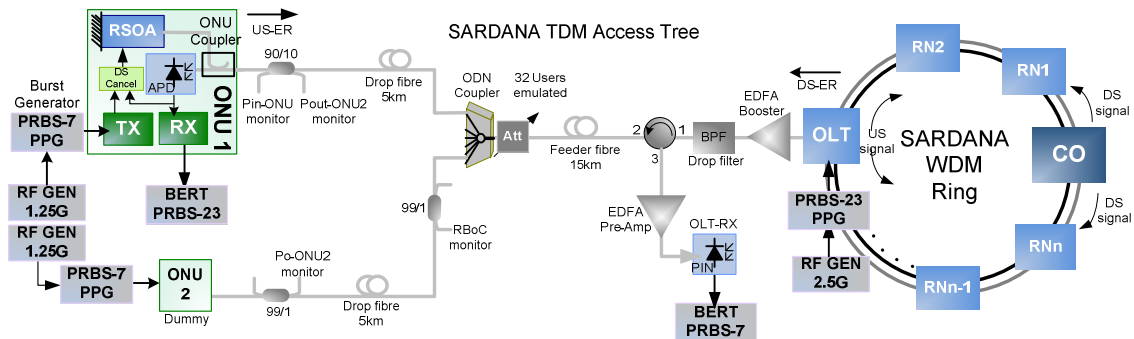


Fig. 3. 15 – The WDM/TDM PON network and the TDM tree section with the OLT on the place of the RN.

3.2.3. TDM-PON rSOA-based ONU optimization

The target is to analyze and optimize the TDM-PON rONU to obtain the best power budget and higher users' number.

Optimization Flux Diagram

Fig. 3.16 shows an optimization's flux diagram of this PON with decision blocks, dependence processes between blocks and expressions for DS continuous /US burst signal and RB impairments [70,123].

Because of the single-fiber/single-wavelength PON configuration, RB will be present as the most relevant optical impairment both in continuous mode as in burst mode. As a consequence, relevant decision blocks are the DS-oSRR and the US-oSRR.

3.2.3.1. DS direction flux

In DS direction, the CW OLT output power is evaluated as a function of the length feeder fibre and the RB_c power that it produces. So, a block decision does a test of the US-oSRR level for such power signal and power impairment. If this level is lower than an oSRR threshold ($US-oSRR < z$), OLT output power must be adjusted.

At the ONU input, other block decision compares for a suitable DS-oSRR level based on the DS signal reaching the ONU and the RB_u as a function of the ONU output power. In general, due to higher number of ONUs (and higher tree losses), the DS signal power at ONU tends to be low. However, smaller burst from the ONU originates low transmitted power. So, RB_u has low effect on this ONU, consequently DS-oSRR is not generally limiting. In the case that DS-oSRR is lower than a target level ($DS-oSRR < y$), the ODN coupler must be adjusted for a smaller ONU numbers in the PON.

In the RX device, if the RX sensitivity is sufficiently tolerant at the actual input level or the minimum BER is not reached yet, it is possible to adjust the ONU splitting ratio to favor the ONU TX section.

3.2.3.2. US direction flux

In US direction, a RSOA gain decision block establishes an operational limit for the system. So, $RSOA \text{ gain} \geq \text{budget loss} + \text{ONU loss}$ satisfies the system requirements; otherwise, US-oSRR will be critic due to a lower US reach level because high tree losses and, also, a high RB_c value, as a function of the CW OLT output power. In this last case, RSOA parameters would be adjusted, or considered to change the device to other with more gain. It still, if minimum US-oSRR is not reached, the ODN coupler must be adjusted for a smaller ONU numbers in the PON.

In general, combining ONU splitting factor and RSOA gain a suitable combinations can be obtained. RSOA gain and the more unbalanced coupling always improve the tolerance margin for the Power Budget and oSRR. 80/20% becomes the most useful (better than 90/10%) because the more unbalanced coupling the more coupling total losses which penalizes the receiver.

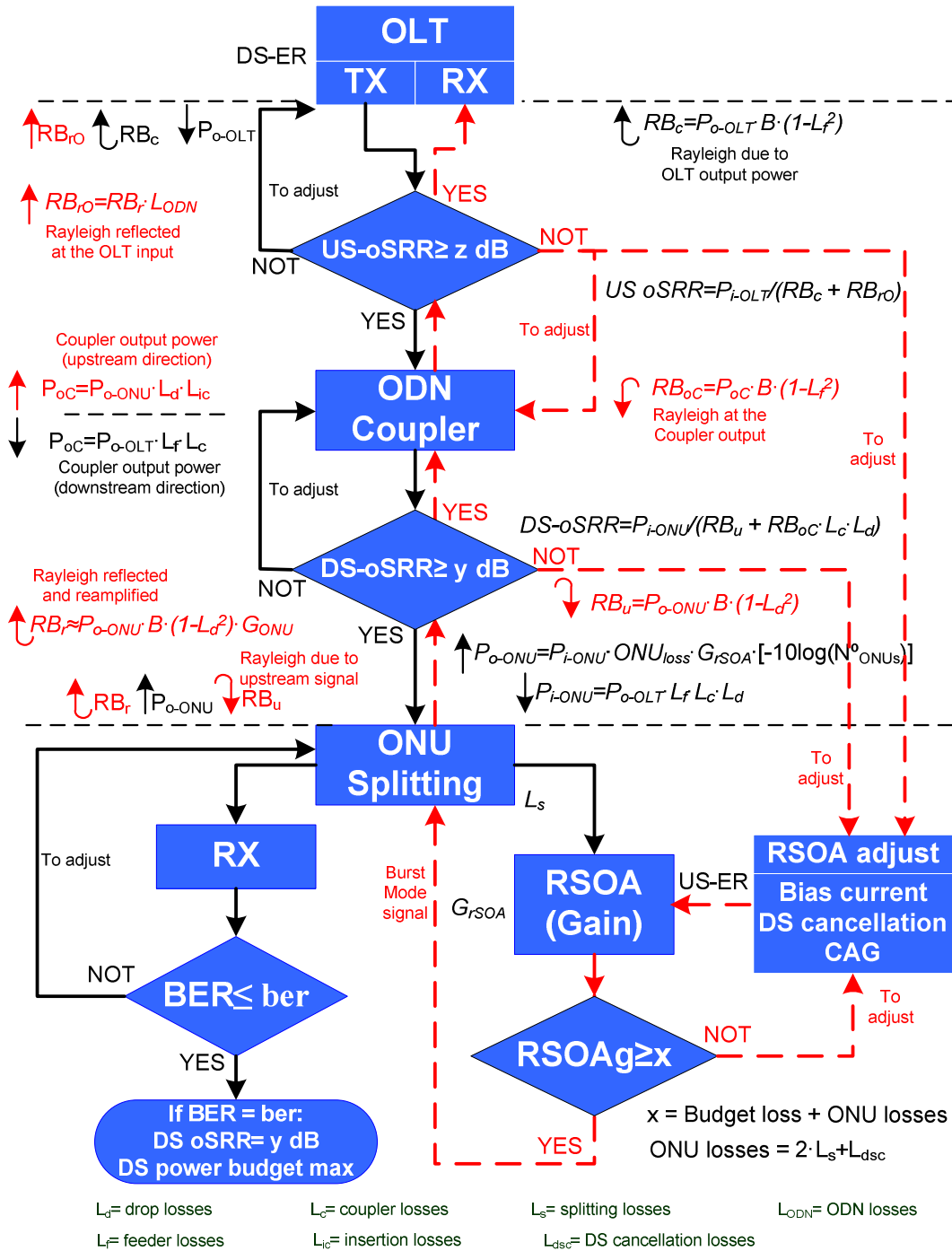


Fig. 3. 16 - Optimization flux diagram for a TDM-PON rONU with FEC to BER 5E-4.

3.2.4. TDM-PON RSOA-based ONU Evaluation

3.2.4.1. Experimental setup

Experimental setup is based on tree section of the SARDANA metro-access network @2.5/1.25 Gbps rates, as shown in Fig. 3.17. The simplest implementation case, and the most critical, is with two ONUs

(ONU2 is used as dummy). Also, it provides the contribution of the all remaining ONUs.

Each ONU transmits data burst into 125us GPON upstream frame, with duty cycles of 50%, 25% and so on, up to 3.125%, in correspondence with the emulated ODN splitting ratio (1x2 to 1x32 respectively). Fresnel back-reflections have been avoided by using angled connectors.

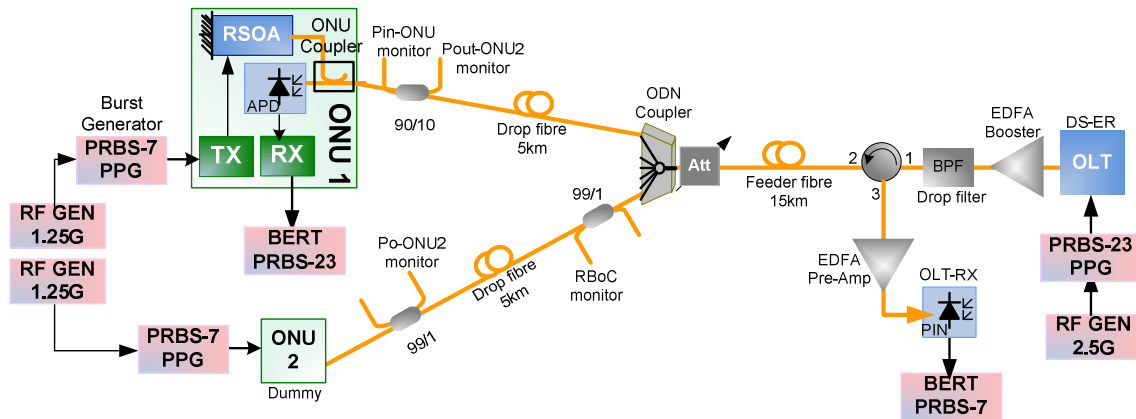


Fig. 3. 17 - Experimental Setup block diagram

At the OLT, TX transmits at 2.5Gbits suitable for give a higher power values excursion for the test proposes (up to 5dB optical power by an EDFA optical booster amplifier with a 100G ASE filter). The Receiver has an EDFA preamp allowing for receiver sensitivities around -30dBm. So, the OLT fulfils the requirements of the GPON 984.2 B+ [104].

Each ONU consists in a RSOA device with 15dB to 21dB gain, and APD receiver with sensitivity of -30dBm @10Gbps and an optical splitter to share input power towards RSOA and APD simultaneously. In TX, a system with DS cancellation allows the RSOA maximal reuse of the DS wavelength. ONU transmits a 1.25Gbp/s Burst mode as standard GPON.

At the ODN, drop fibre (from 5 to 10 each) and feeder fibre (from 15 to 10 km), in order to have a fibre link of 20km, as a GPON standard, are the data transmission paths. A two-port splitter/combiner (-4dB) plus a digital attenuator allow emulating different tree losses as a function of the ONU numbers in the PON. The SARDANA tesbed and practical implementation is shown in Fig. 3.18.



Fig. 3. 18 - The SARDANA testbed and practical implementation for experimental evaluation

3.2.4.2. Experimental Evaluation

Bidirectional transmission with RSOA-ONU in burst mode with US direct remodulation with/ without DS cancellation was measured. The appropriate balance between the DS signal output power and the ONU gain, and on the other hand, the power budget and the power loss, as a function of the DS/US oSRR boundaries are necessary to reach the best PON's operating point. Increasing the users' number - proportionally with the splitter losses- the DS signal power and the US-oSRR level decrease. When the OLT power increases DS power budget improves, but the RB_c limits the US-oSRR.

On the other hand, the ONU output value increases the US-oSRR but depends directly on the RSOA gain and the ONU losses. So, the best operating point is a tradeoff of good tolerance for the DS power budget and the US-oSRR together.

Fig. 3.19 shows results obtained experimentally for the tolerance margin (dB) matching Downstream power budget and Upstream oSRR as a key parameter to choose the coupling factor. Both are for a RSOA gain of 21dB. Splitting factor into ONU for 80%/20% and 90%/10% (90% of power goes to the RSOA to be remodulated whilst 10% power is for data detection) are tested.

OLT output power values are considered into the ITU GPON range [124-125]. Critical 16 and 32 ONUs scenarios are evaluated.

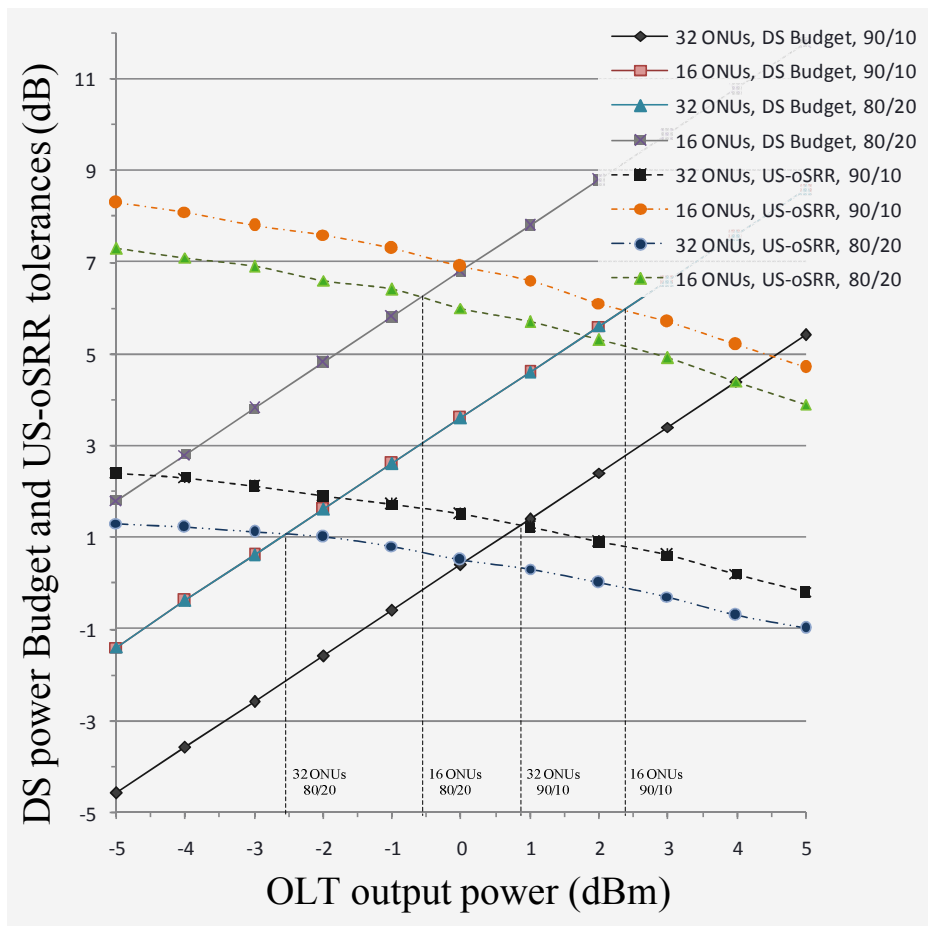


Fig. 3. 19 - DS power budget and US-oSRR tolerances for RSOA gain=21dB and ONU coupling factor 90/10 and 80/20, with BER 5E-4.

The coupling factor at the ONU input to feed the RSOA unit and the RX confirms to be an important parameter to take the best profit of the received power. For a splitting of 80/20, the results are in agreement with [126] and the best tradeoffs DS power budget / US-oSRR are to OLT output power values between 0 and -3 dBm.

For the coupling factor 90/10, where the maximum splitting ratio depends on the ONU photo-detector sensitivity, the best tradeoff is for values between 0 and 3 dBm. Here, it is possible to superimpose the undesirable RBC with a higher upstream power from the higher ONU gain.

Now, PON performances using RSOAs with nominal $G=16\text{dB}$ and 21dB are analyzed experimentally and optimized to obtain the maximum number of users (Fig. 3.20). An OLT output power 0 dBm allows the RSOA gain matching the ODN power budget.

The DS power budget -at the APD RX- has a higher dependency with the RX/TX splitting ratio 90/10 into the ONU. Fig. 3.20 shows that up to 32 users are possible with nominal 21 dB ONU gain. The DS cancellation is adjusted to 1dB maximum penalty.

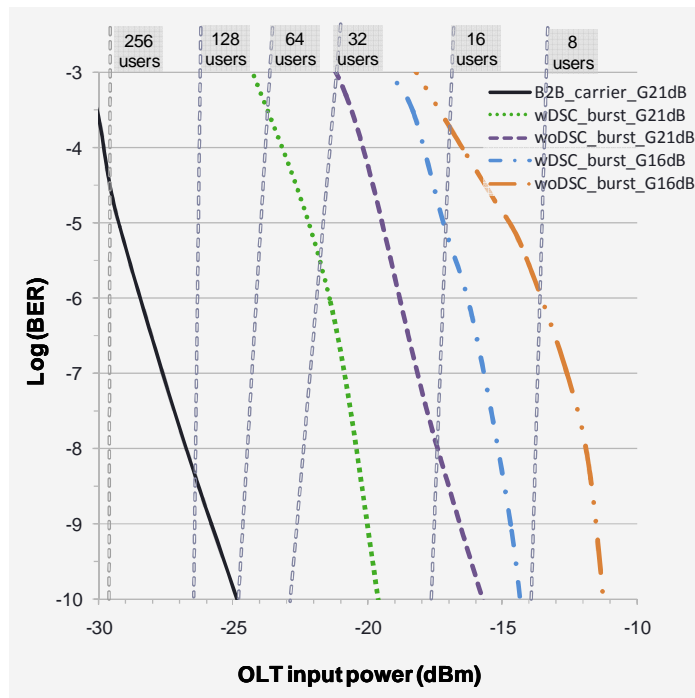


Fig. 3. 20 - Maximum data users in rONU-based PON: B2B transmission and US burst using DS remodulation with/without DS cancellation

The US-oSRR value is penalized for higher tree losses and as a function of the Po-OLT (because of the RB_c). The key parameter to save US-oSRR penalty depends on the ONU gain as RSOA gain > Budget Loss + ONU Loss. RSOA gain=16dB allows for 16 users PON with Power-Tolerance>5dB, while RSOA gain=21dB reaches up to 32 users with Power-Tolerance>0.5dB.

A sensitivity improvement > 2 dB is reached by using Downstream Cancellation.

An ODN (20km) redistribution (by feeder fiber reduction while the drop fiber increases), avoids for high RB_c values by improving the US-oSRR tolerance, as shown in Fig. 3.21. RSOA gain=21dB on 10km feeder with 10km drop increases Power-budget-tolerance to >1.5dB for up to 32 users, while DS-oSRR is always into the tolerable range, US-oSRR requires 90/10 coupling into ONU.

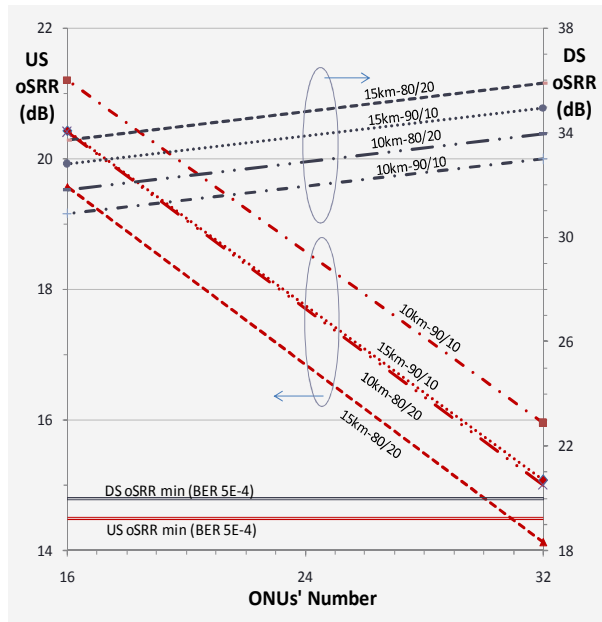


Fig. 3. 21 - DS-oSRR and US-oSRR values for 16 and 32 users with ONU splitting loss 90/10 and 80/20, and feeder fibre of 15 km and 10 km.

Some important design parameter values in TDM-PON RSOA-based ONU are compared with ONUs based on ITU standards GPON G.984.2 ONU [104] and XGPON G.987.2 [83]. Table 3.1 shows this comparative.

Table 3. 1 - RSOA-based ONU and GPON/XGPON ONU comparative

ONU type	DS-ER (dB)	Loss Budget (dB)	Phy Reach (km)	Optical Splitter	Optical Budget (dB)	BER DS Ref.	RX Sensitivity (at BER level)	Path Penalty (dB)	λ used	Bit Rate (DS/US) (Gbit/s)
GPON ONU (G.984.2 B+)	>10	28	20	1:32	13-28	1E-10	-27 dBm	0.5	2	2.5/1.25
RSOA-based ONU (SARDANA)	<5	28	20	1:32	13-28	5E-4 (FEC)	-30 dBm	0.5	1	2.5/1.25
XGPON ONU (G.987.2)	>8.2	N1: 29 N2: 31	20	1:64	N1: 14-29 N2: 16-31	1E-3 (FEC)	-28 dBm	1	2	10/2.5 10/10

From Table 3.1, RSOA-based ONU take advantage over the ITU-standards (GPON and XGPON) in the re-use of the wavelength and colourless capacity. It gives the potential for transparent Metro-access interoperability without Electro-optical conversion (with low cost ONUs) at the cost of fewer users (1x32). It would be possible to reach up to 64 splitting with powerful RSOAs with Gain>25dB and high sensitivity APDs (better than -30dBm). Also, free-up spectrum, for future expansion, and reduce CAPEX/OPEX is obtained.

Furthermore, the lower optical powers can be considered as a green factor because of the energy saving.

3.2.5. Conclusions

In this section, a TDM-PON rSOA-based ONU Network design and Optimization, looking for colorless, low cost, single-fibre with wavelength reuse and truly passive, was presented.

In this network, the number of users and the network coverage determine the power budget. Although it could be managed by injected more power from the TX, it introduces the Rayleigh backscattering which penalizes the oSRR. Then, RB limits the OLT output power and so, limits the power budget. As a consequence, and to compensate these limitations, high ONU gain is required. Other critical parameter is the DS-ER, reduced to allow wavelength reuse by carrier level recovery.

In the upstream direction, the difficult are for scenarios with 32/64 ONUs, due to higher tree losses. Single-fiber/wavelength reflective PON has been optimized focusing on the best tradeoff between ODN power budget and US-oSRR. RSOA gain and ONU splitting factor are the key parameter. By using FEC to BER $5E-4$, optimal DS cancellation, RSOA gain=21dB, the appropriate OLT output power between 0 to 3 dBm and 90/10 ONU splitting ratio, up to 32 users can be reached.

For using FEC and DSC technique, oSRR limits can be re-established for suitable data decodification. For a FEC of BER $5E-4$, up to 5 dB of gain is possible.

This TDM-PON rSOA-based ONU design takes advantage over the ITU-standards in the re-use of the wavelength and colourless capacity with low cost ONUs. The lower optical powers can be considered as a green factor because of the energy saving.

Chapter 4

4 WDM/TDM-PON SARDANA Network

Current development on new FTTH network architectures and technologies aim at enabling universal communications with a substantial increase in terms of bidirectional capacity, connected users and distance reach, as well as incorporating enhanced security, scalability, service integration and other key functionalities. With this aim, recent proposals for next generation FTTH, in the so-called NGA-NGPON2, intensify the use of the WDM dimension to extend the performances of PONs.

SARDANA constitutes a new network model into the NGPON2. It stands for “Scalable Advanced Ring-based passive Dense Access Network Architecture” [82,131]. SARDANA implements a hybrid WDM/TDM-PON consists of the organization of the optical distribution network as the TDM access trees passively connected, through a cascadeable passive add&drop Remote Nodes, with a WDM bidirectional ring. The proposed Ring + Trees topology can be considered as an evolution towards an integrated Metro-Access network, covering similar geographical area, users and services, but concentrating electronic equipment at a unique site (the Central Office), and implementing an all-optical passive alternative, operating as a resilient TDM-over-WDM overlay, by optimizing and extending the capabilities and performance of the WDM/TDM network presented in chapter 2. This can constitute a transparent passive approach of what is today known as metro-access convergence.

This FP7 European project was development between January 2008 and December 2010 and was composed by 7 pre-eminent institutions (industries and research centres): Universitat Politècnica de Catalunya (UPC-Spain), France Telecom (FT/Orange-France), Tellabs (Finland), Intracom (Greece),

Instituto de Telecomunicações (IT-Portugal), ISCOM (Italy) and AIT (Greece) [51]. SARDANA is an approach to demonstrate how the huge bandwidth available through the fibre access can be exploited in an extended, cost efficient and reliable manner. SARDANA, following the acronym, features:

- **Scalable:** SARDANA is able to serve up to 1024 users with symmetrical 100-1000 Mbit/s per user, spread along distances up to 100 km, at 10Gbit/s, in a flexible way. This one order of magnitude increase in every of these features provides a virtually unlimited broadband access for all. Since operators face a high degree of uncertainty at this level (take rates, user demands, etc) and the necessity of deferring the investments, incremental scalability has become a major objective. SARDANA is capable of continuous growth of the network, as new users get connected, providing continuous branching in physical, time and wavelength domains, at longer distances in new areas, and as higher bandwidth is demanded.

- **Advanced:** to reach the project goals, a series of innovations are proposed and implemented:

- Adoption, adaptation and optimization of new opto-electronic technologies, like reflective semiconductor optical amplifier, remotely pumped fibre amplification, wavelength shifting, etc.
- Signal processing and communication techniques, like orthogonal optical modulation formats to reuse the same wavelength in down- and up-stream, non-linear electronic equalization of the different optical impairments present, hybrid domain signal multiplexing (wavelength and time domain, routing the optical packets without collisions or extra delays).

- **Ring-based passive:** the network topology is hybrid with a central WDM ring and TDM single-fibre trees to the homes. Strict passiveness is preserved in the fibre plant, to simplify the deployment and maintenance of the network.

- **Dense Access Network Architecture:** related to the concept of the user density in an area; it can range from a rural scenario (long reach) to an urban scenario with several thousand homes, all optically interconnected from one wide ring through the trees.

4.1 Network Architecture

SARDANA implements an alternative NG-PON architecture consisting of the organization of the optical distribution network (ODN) as a WDM bidirectional ring and TDM access trees, interconnected by means of cascable optical passive add&drop remote nodes (RN), as shown in Fig. 4.1.

G.987) standard, has been developed and demonstrated, together with conventional LAN and MAN communications, supporting advanced new broadband multimedia services.

4.1.1 SARDANA Wavelength Allocation

SARDANA uses the wavelength band between 1530nm and 1565nm (C-band), with optional extension to 1565-1625 nm (L-band). This wavelength plan is well above the GPON up/down wavelengths, (1490nm DS, 1310nm US) [132], and compatible, in L-band, only in downstream, with XG-PON1 (1575-1580nm DS, 1260-1280nm US) [133]. A key difference is of course that in this band, SARDANA uses DWDM with strict wavelengths generation (centralized at OLT) aligned with the ITU Grid. This implies that SARDANA should allow DS XGPON1 wavelengths, but US signals should be converted at US XGPON1 wavelengths at the OLT. In the GPON case, wavelengths have to be converted to the SARDANA wavelengths.

Also, SARDANA opts for not supporting the Video Overlay Service (that was defined at 1550-1560 nm), due to it overlaps with the DWDM C-band, and would require too stringent optical filters to combine both. Besides, the video overlay downstream signal, intrinsically an analogue sub-carrier multiplex (SCM), requires a very high SNR to be provided to the user for an acceptable quality (about 20dB higher than the digital signal); this facts limits the overall power budged and produces inter-service crosstalk. Nowadays, the VoIP is a much advanced and cleaner solution to be integrated in the IP PON stream. Thus, the interoperability with a video service operator is via an IP connection, with a specified SLA.

Fig. 4.2 shows wavelength plan for SARDANA. Wavelengths for the pump generation for remote amplification, OTDR monitoring and control are shown too.

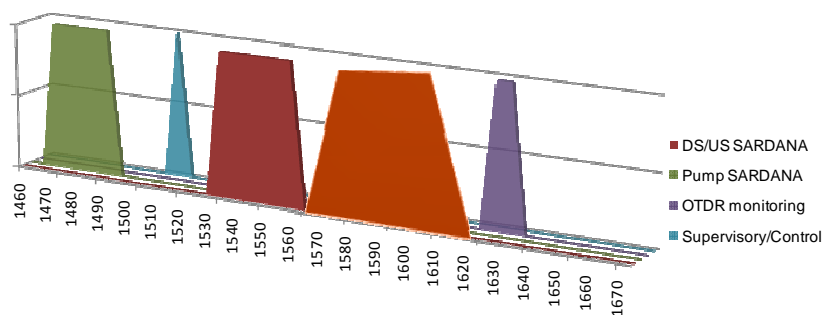


Fig. 4. 2 - SARDANA wavelength allocation plan

4.1.2 Key subsystems

The implementation of the network subsystems: colourless Optical Network Unit (ONU), Optical Line Terminal (OLT) at the Central Office (CO), the Optical Distribution Network (ODN) and the passive Remote Node (RN), encompasses a number of technical challenges. Along the project, although several solutions have been investigated, the decision on the selected one for network demonstration is made on the basis of cost and robustness, leaving more complex advanced solutions for parallel research.

4.2 Optical Network Unit (ONU) Subsystem

A key requirement of the ONU is to be colourless and to reuse the DS wavelength, in full-duplex operation compatible with xPON. A reflective-ONU based on RSOA has been taken as preferred option because its simplicity and colourlessness. However, it can rise up serious impairments operating in full-duplex with wavelength reuse, as seen in chapters 2 and 3. To overcome the bandwidth, noise and crosstalk limitations, a complete study of the possible optical modulation formats has been done and several compensating techniques have been developed:

- Reduced-ER downstream with feed-forward cancellation at ONU [134]
- Wavelength dithering to reduce Rayleigh backscattering and reflections [135]
- Upstream chirped-managed RSOA with offset-filtering, reaching 10G operation [136]
- Adaptive electronic equalization, using MLSE and DFE/FFE at 10G [136-137]
- Integrated colourless optical FSK demodulation with a SOA/REAM [138].
- Wavelength shifting at ONU for reduction of Rayleigh scattering [139]
- Other modulation formats tested like SCM [111-113], SSB and homodyne PSK [131] are kept as longer term research.

The ONU subsystem of the SARDANA includes the electro-optical ones for the ONU optical interfaces (ONU layer 1) and for the ONU MAC (ONU layer 2). This section presents the architecture and the specification of the components used in the ONU layer 1. SARDANA ONU layer 2 will be shown in chapters 5 and 6.

The ONU input/output PON interface is a single optical fibre with bidirectional transmission over the same wavelength of the PON. Its opto-electrical subsystems are based on an APD optical receiver that detects the 10Gbps downstream signal and an optical transmitter that emits upstream on the same wavelength, but at 2.5Gbps, for using a 600MHz bandwidth RSOA, with bandwidth enhancement to achieve 2.5Gbps transmission, as seen in chapter 2.

A commercial ONU alternative, based on low cost tuneable laser from PIRELLI and a Luminent APD receiver was also considered. However, by considering a cost-efficient bidirectional data transmission and focusing on strategies for the implementation of full-duplex data delivery by using foremost the simple ASK modulation format, reflective-ONU optical transceiver RSOA-based has been taken as the preferred option, although it raises extra significant impairments in full-duplex transmission with wavelength reuse, specially Rayleigh backscattering impairment [25,74,93,141-146]. To overcome some limitations of the RSOA when used as an ONU (bandwidth, noise and crosstalk limitations), several compensating techniques as downstream ER cancellation, upstream chirped-managed offset-filtering wavelength dithering and adaptive electronic equalization are implemented [35,70-71,126,135].

4.2.1 ONU subsystem RSOA based

The opto-electrical ONU based on a RSOA enables bidirectional transmission over a single fibre with the same wavelength. The upstream transmission rate has been established to be 2.5Gbps in burst mode in order to be TDM compatible as required in the tree part of the SARDANA PON network. A basically scheme of the ONU subsystem layer 1 is shown in Fig. 4.3. The ONU-TX is a RSOA device, which is upstream re-modulated while the arriving downstream signal is partially erased by means of a downstream cancellation circuit. The ONU-RX consists of a 10G APD photo-detector with TIA.

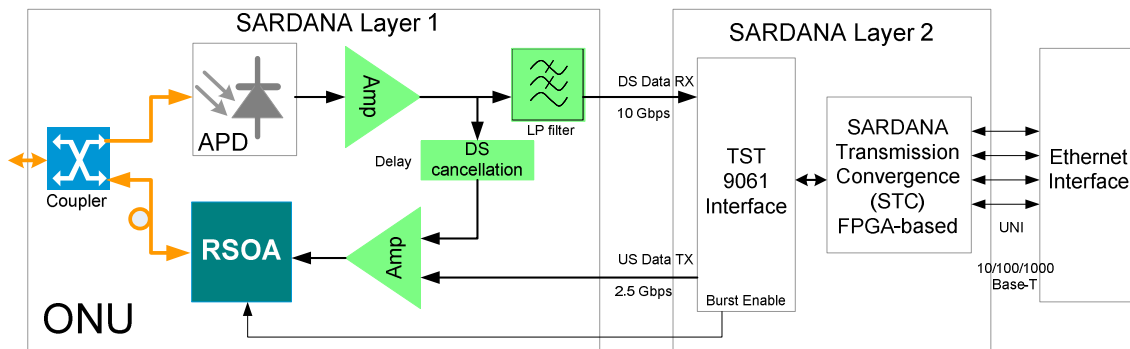


Fig. 4. 3 - SARDANA ONU basically architecture showing Layer 1 and Layer 2

Fig. 4.4 shows block diagram of the ONU-TX section. TX section requires 3 electrical inputs: the BE signal to activate the transmission at every burst and inject the bias current to the RSOA electro-optical device; the 2.5 Gbps differential upstream data; and the downstream cancellation signal coming from the ONU-RX.

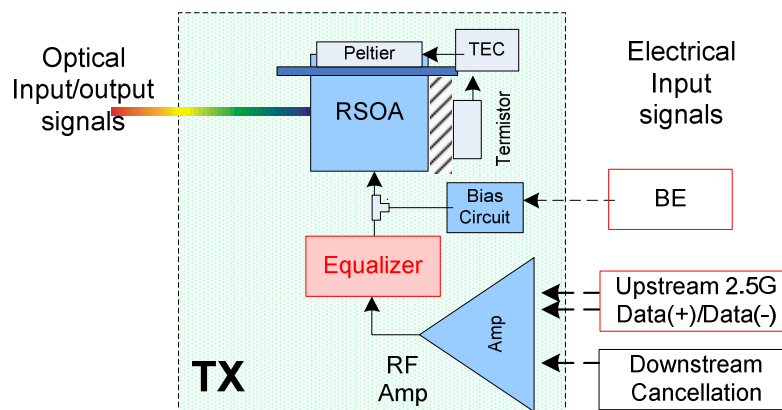


Fig. 4. 4 - ONU-TX blocks diagram detail

The main requirements of these subsystems are listed in Table 4.1.

Table 4. 1 - Requirements for the SARDANA ONU RSOA based.

Input Optical Power	> -15 dBm
Input DS ER	3 - 4 dB
Nominal RX Bit Rate	10 Gbit/s
RX Sensitivity	< -17 dBm
RX electrical Output	CML levels >350mVpp (AC-coupling)
Output Optical Power	< -2 dBm
Output ER	> 6 dB
Optical Gain	> 15 dB
TX electrical inputs	CML > 350 mVpp
Burst-Enable input	0.5 (OFF)/2.5 (ON)
Nominal TX Bit Rate	2.5 Gbit/s

4.2.2 Downstream cancellation requirement

The re-use of a single wavelength for full-duplex transmission guarantees low CapEx since no extra amplifiers for a second optical carrier have to be used and the fibre plant can be shared among a higher number of users due to a higher spectral efficiency. However, the signal to be re-used requires a process of reconditioning.

For the RSOA, the re-modulation of the downstream signal provides a 3 level upstream signal, which reduces the upstream eye and makes the transmission more sensitive to impairments like noise and distortion. The RSOA partially cancels that downstream data intrinsically thanks to the gain saturation of a SOA. In order to achieve a clearest upstream transmission, electrical and optical techniques for downstream cancellation from the most basically and cheapest, as counter injecting the same downstream signal in opposed phase, to advanced techniques can be implemented, differentiating in their performance and induced complexity [35].

4.2.2.1 A Basic Downstream Cancellation

The RSOA signal is optically delayed to synchronize the DS received data with the electrical data modulation at the RSOA. A longer optical path in the RSOA way allows to achieve the required delay to quasi suppress the downstream remaining signal. Fig. 4.5 shows the ONU block diagram with DS suppression.

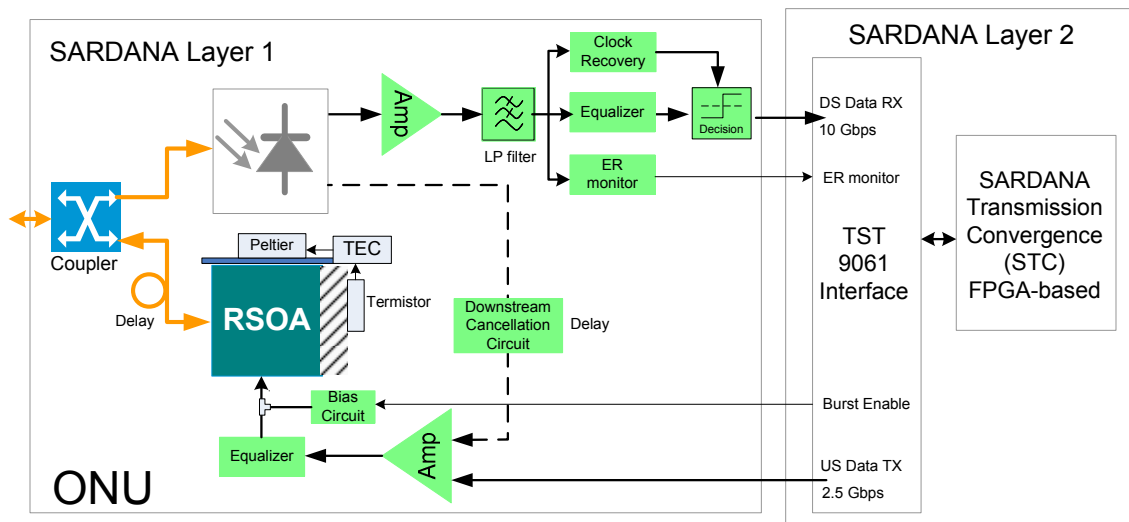


Fig. 4. 5 - Block scheme of the ONU with downstream cancellation circuit

4.2.2.2 Upstream BER with/without downstream cancellation

Testbed scheme to measure US sensitivity vs. DS ER, by using re-modulated upstream transmission, with and without downstream cancellation, is presented in Fig. 4.6. The PON data transmission is emulated with two PRBS generators, one for the DS at 10Gbps DFB-MZM-TX and other for the US at 2.5Gbps. ER-DS is fixed to 3dB, while ER-US is 6dB. RSOA optical gain is of 14dB. At the OLT sub-system, an ASE rejection filter has been used to adjust the optical input power to a 20GHz receiver. Sensitivity curves are shown in Fig. 4.7a.

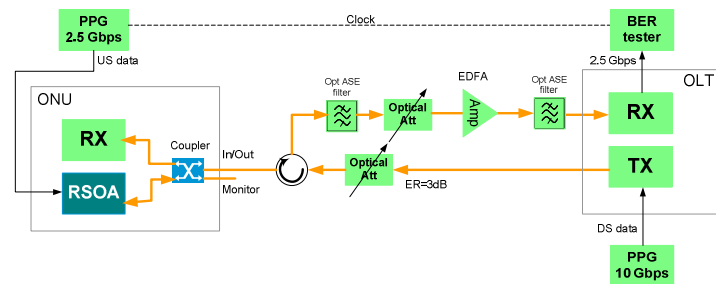


Fig. 4. 6 - Scheme of the upstream sensitivity measures versus Downstream ER

This shows that for appropriate error free upstream operation, the DS cancellation is required; otherwise there is not error-free upstream transmission.

Fig. 4.7b and 4.7c show the transmitter US eye without and with DS cancellation. Due to the remaining DS signal, the US data becomes nearly closed eye. By using DS cancellation, upstream signal eye becomes open allowing for error free data detection.

The RSOA re-modulation tries to erase the 10 Gbit/s downstream signals; it cannot be done perfectly because the RSOA-TX has a bandwidth of only 1.8 GHz and upstream sensitivity decreases with downstream ER. So there is a key trade-off on the downstream ER.

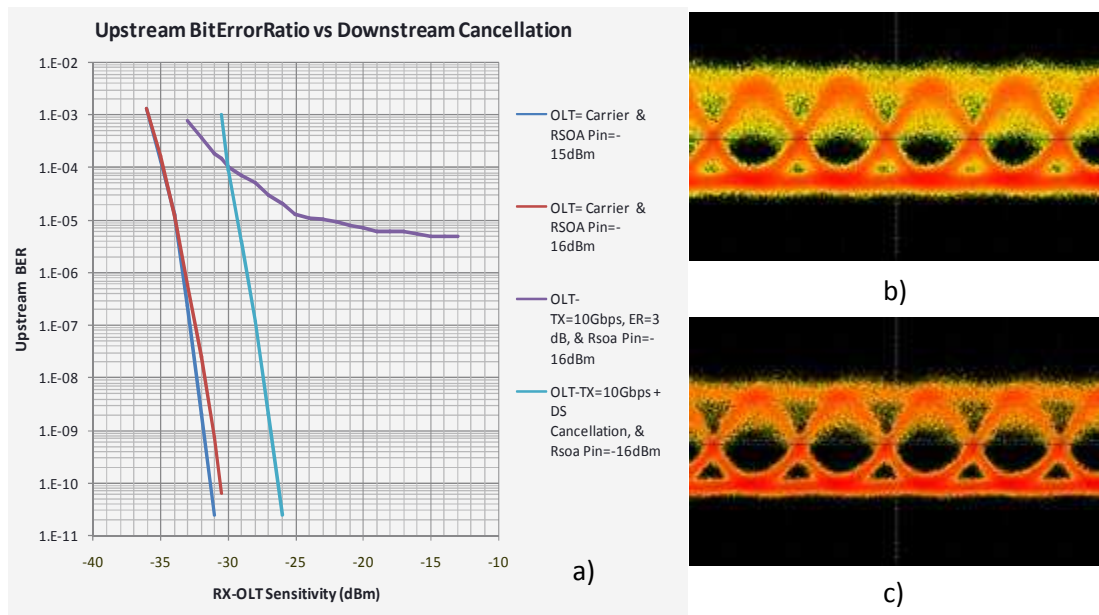


Fig. 4. 7 – a) Upstream Sensitivity curves for remodulated upstream transmission, with and without cancellation. b) Upstream eye diagram @2.5Gbps for ER (DS) =3dB without DS cancellation. c) with DS cancellation.

The sensitivity with ER=4dB is between -26 and -29 dBm, as shown in Table 4.2.

Table 4. 2 - Upstream Sensitivity vs. Downstream ER

Upstream BER	Upstream Sensitivity			
	ER=3dB	ER=4dB	ER=4.5dB	ER=5dB
1E-10	-26.9	-26.3	Floor (1E-08)	Floor (1E-06)
1E-06	-29.2	-29	-28.5	-28.2

The optimum DS cancellation signal at the ONU-TX input is found to be around 30mVpp. The ONU-TX Data input amplitude is Vpp CML standard 400mVpp single ended (800mVpp differential) & DS cancellation signal. Downstream ER higher than 4dB do not allows for error free transmission.

4.2.3 Optical network tests

Full characterization of ONU requires back-to-back downstream and upstream sensitivity test over SARDANA with the ER limitation imposed for the bidirectional transmission over the same wavelength.

4.2.3.1 Back-to-back Downstream Sensitivity tests

A downstream signal with ER = 3 to 4 dB is used. Fig. 4.8 shows the scheme and values for the downstream sensitivity measure.

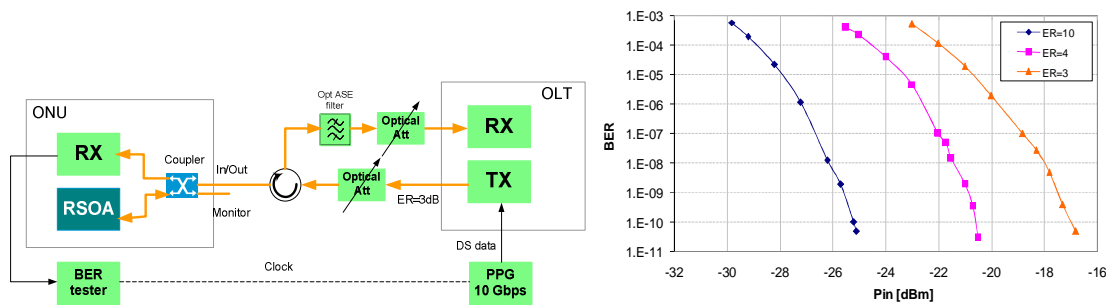


Fig. 4. 8 - Scheme for the downstream sensitivity measure and BER-Sensitivity for DS-ER of 10, 4 and 3dB.

The obtained sensitivities are -25.3, -20.6 and 17 dBm, for ER of 10, 4 and 3dB, respectively. As can be seen, the penalty due to the ER reduction from ER=10 to ER=3dB is around 8 dB, while it is around 5dB for ER=4dB. APD multiplication factor is adjusted to $M=8$, with a bias voltage of 21.1V, providing proper bandwidth, gain and sensitivity.

4.2.3.2 Back-to-back Upstream Sensitivity test

An external optical source has been used to generate the ER=3dB 10Gbps DS signal to be in the same conditions as the real US and DS bidirectional operation in SARDANA network. Fig. 4.9 shows the block diagram for the US B2B sensitivity measure and the upstream sensitivity curves (without EDFA preamplifier at the OLT-RX).

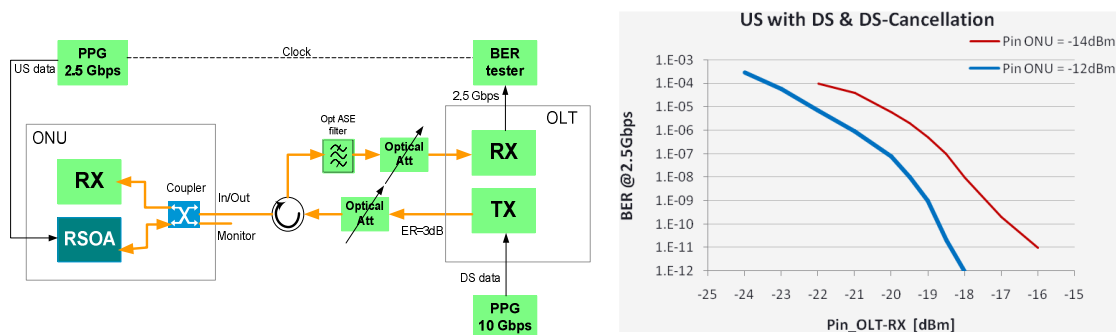


Fig. 4. 9 - Scheme and sensitivity measure of the Upstream Back-to-back.

Because the tested RSOA gain was of 14dB, in order to have 0dBm at the RSOA output, the recommended input power to the ONU would be of -12dBm to compensate 2dB input coupler loss. Can be observed that for an optical power at the ONU input of -14 dBm the upstream sensitivity is about -17dBm, while increasing the ONU input power in 2 dB the sensitivity improves also in 2dB.

4.2.4 SARDANA ONU Layer 1 Prototype

The ONU Layer 1 Prototype is mainly composed by an ONU-RX system, an ONU-TX system, an optical coupler and a DS cancellation circuit.

4.2.4.1 ONU-RX section

The ONU-RX section is based on a FRM5N Fujitsu APD receiver + 10Gbps limiting amplifier (based on a MAX3945). Fig. 4.10 shows a layout of the 10G opto-electrical receiver at the ONU.

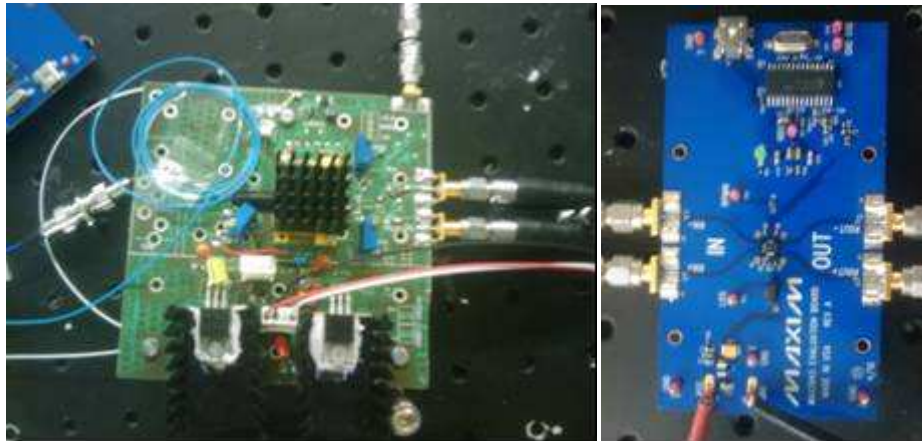


Fig. 4. 10 – ONU-RX implementation: APD Fujitsu-RX with the Limiting Amplifier.

Table 4.3 shows the min/max and typical values of the input/output at the RX section of the SARDANA ONU.

Table 4. 3 – ONU RX section input/output values

Label	Name	Connector	Minimum Values	Typical values	Maximum Values
APD IN	Optical Input	SC/PC	-21dBm	-17dBm	-5dBm
DS Out	DS cancellation	SMA	10mVpp	20mVpp	30mVpp
Data Out(+)	DS-RXsignal(+)	SMA		400mVpp	
Data Out(-)	DS-RX signal(-)	SMA		400mVpp	

4.2.4.2 ONU-TX section

The RSOA was acquired in TO-CAN package for lowest cost, and is here externally in temperature (to about 25 degrees), by means of a designed mechanical assembly. The transmission target is @ 2.5Gbps, allowing burst mode operation and being TDM compatible. The TX includes a DS input signal to cancel the DS signal arriving on the optical carrier. The erase procedure is made by re-modulating a delayed sample of that DS signal in opposed phase in order to counteract the DS incoming data.

Fig. 4.11 shows the layout of the electrical scheme of the 2.5G burst mode transmitter with RSOA device at the ONU TX section. It has a high-frequency part with pre-equalizer, another for low frequency, DC and Burst Enable.

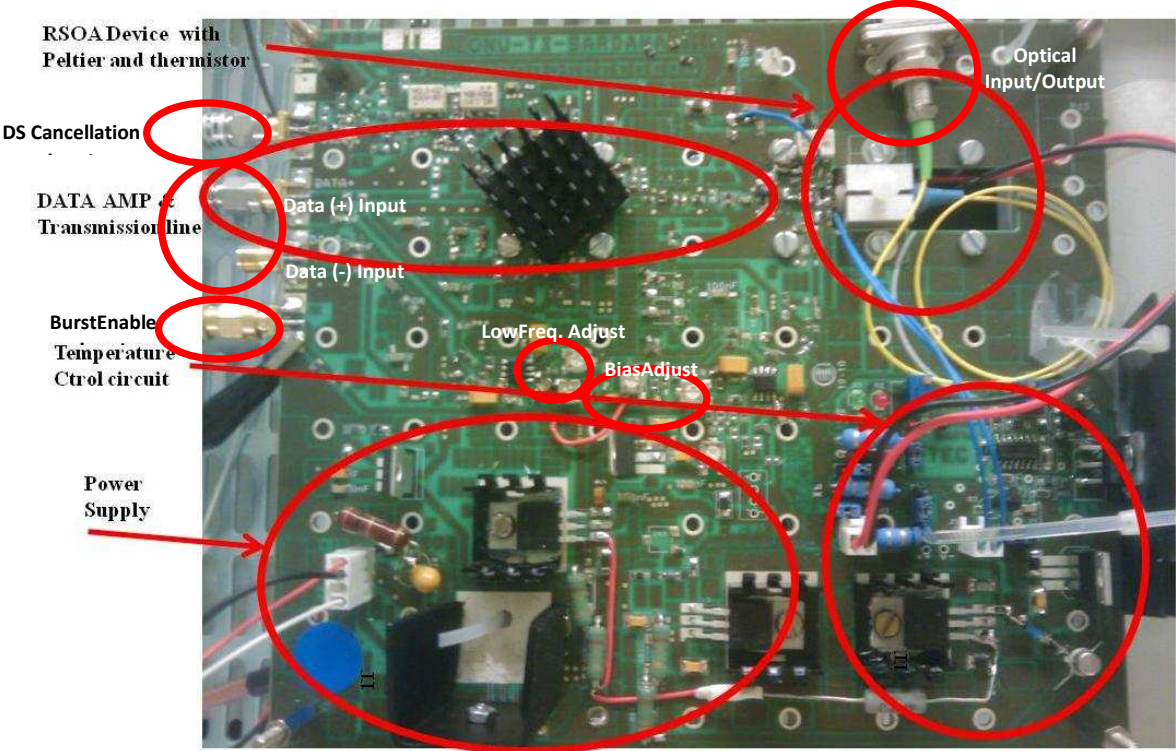


Fig. 4. 11 – ONU-TX system board.

The prototype allows bias current being adjusted by a potentiometer between 50 and 80 mA. Optimum bias current is around 55 to 60 mA. Also, low frequency gain can be adjusted.

Table 4.4 shows the minimum/maximum and typical values of the input/output at the TX section of the SARDANA ONU.

Table 4. 4 – ONU TX section input/output values

Label	Name	Connector	Minimum Values	Typical values	Maximum Values
RSOA Input/Output	Optical Input	PC/APC	-17dBm	-14dBm	-5dBm
Data IN(+)	Upstream (+)	SMA	250mVpp	350mVpp	400mVpp
Data IN(-)	Upstream (-)	SMA	200mVpp	350mVpp	500mVpp
BE	Burst Enable Input	SMA	1.75 Vp step	2.5 Vp step	3.3Vp
DS Input	Downstream cancellation	SMA	10mVpp	20mVpp	30mVpp

4.2.4.3 Optical Coupler

Due to the optical path in the tree section is bidirectional single fibre/single wavelength, a 2x2 optical coupler is used in order to share signal in the same port between the RX systems and to feed the reflective TX system, while the 2nd port is used as TX monitor.

For a RSOA gain of 14dB, to have around 0dBm optical power at the RSOA output is required an optical power at the RSOA input around -14dBm, while to have an error free downstream at RX, around -17dBm are required. This 3dB difference between the required optical powers for each device can be provided by the appropriate optical coupler 70%/30%. A 70% of the input power would be for feeding the RSOA (1.7dB of losses) and a 30% for feeding the APD receiver (5.4dB of losses).

4.2.4.4 SARDANA ONU Layer 1 Assembly

SARDANA ONU prototype front end module is shown in Fig. 4.12, with the detail of the electrical and optical input/outputs. The optical input is for the bidirectional connector which takes the DS signal to the ONU and which gives the optical US after DS erasing. The “Monitor” label points for the optical monitoring output of the ONU.

RX electrical connector is the digitalized output (through a 10Gbps limiting amplifier) to provide the digital CML electrical inputs suitable for electrical connection to the ONU Layer 2 board in differential mode. TX electrical connectors are the electrical input data to be modulated for US transmission. The BE electrical labelled is the electrical Burst Enabled input provided by the ONU Layer 2 circuit to activate the ONU transmission.



Fig. 4. 12 - ONU module front-end.

Fig. 4.13 shows the picture of the mounted ONU prototype. The RX, the TX, and the DS cancellation blocks are pointed out. The DS cancellation consists on a double delay line, on one hand, the optical path to the rONU-TX must be delayed for the RX to detect the DS and re-inject that detected data on the TX to counteract the optical arriving signal synchronously. A fine electrical delay tuning allows for the DS data matching.

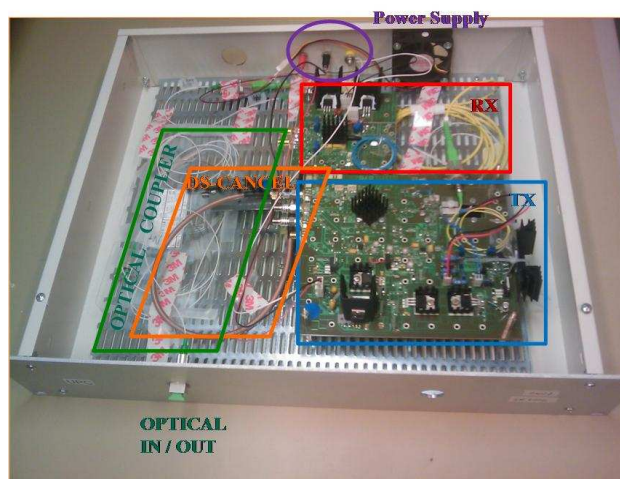


Fig. 4. 13 - Blocks of the ONU Layer 1 prototype module.

Optical and electrical I/O characteristics of the ONU L1 are show in Tables 4.5 and 4.6.

Table 4. 5 - ONU Layer 1 optical input/output characteristics

Label	Name	Fibre	Connector	Minimum Values**	Typical Values**	Maximum Values**
OPTICAL TX/RX*	Optical Input/out	Bidirectional input	SC/PC	-15 dBm	-12 dBm	-10dBm
OPTICAL TX/RX*	Optical Input/out	Bidirectional output	SC/PC	-5 dBm	-2 dBm	0 dBm
OPTICAL MON	Optical Monitor	output	SC/PC	-9 dBm	-6 dBm	-2 dBm

* OPTICAL TX/RX is only one connector for bidirectional operation (Input and output)

** Output and Input values are considered for a 70%/30% optical coupler.

Table 4. 6 - ONU Layer 1 electrical input/output characteristics

Label	Name	Connector	Minimum Value	Typical Value	Maximum Value
Data IN(+)	Upstream(+)	SMA	250mVpp	350mVpp	400mVpp
Data IN(-)	Upstream (-)	SMA	250mVpp	350mVpp	400mVpp
BE IN	Burst Enable	SMA	1.75 Vp step	2,5 Vp step	3.3Vp
Data OUT(+)	Downstream (+)	SMA		400mVpp	
Data OUT (-)	Downstream (-)	SMA		400mVpp	

Fig. 4.14 shows ONU Layer 1 and ONU Layer 2 prototypes in a rack of the SARDANA Network subsystems.



Fig. 4. 14 - SARDANA rack with two ONU prototypes: ONU layer 2 (above) and opto-electrical ONUs layer 1 (middle) subsystem

4.3 Central Office (CO)

The CO centralizes the light generation for the whole network and its control. The optics at the CO includes OLT boards, WDM multiplexers, optical pre/post-amplifiers, equalizers, protection switches and monitors. Protection is centrally actively controlled from the OLT.

4.4 OLT Subsystem

This subsystem includes the OLT optical transmitter and the OLT optical receiver. Fig. 4.15 shows the basically architecture of the OLT, including of the Layer 2 OLT, that will be presented in chapter 6.

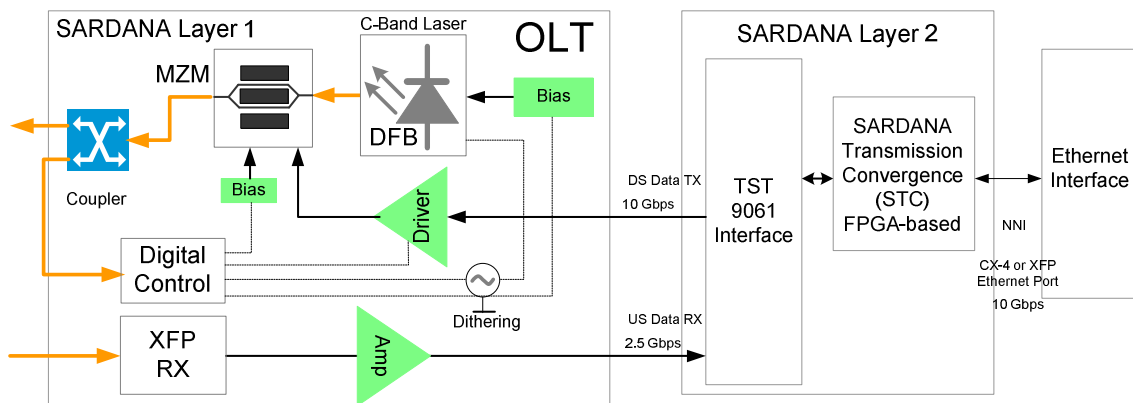


Fig. 4. 15 – General Scheme of the layer 1/2 SARDANA OLT

In the OLT optical transmitter, dithering for the downstream carrier, to face Rayleigh backscattering in the drop segment of the access network, and a stabilisation, for the optical modulator, are required. The OLT receiver is simplest. It is based on a commercial XFP 2,5Gbps burst transceiver device.

4.4.1 OLT optical Transmitter

The SARDANA OLT is designed to use intensity modulation (IM) format [147-149] with reduced extinction ratio. The OLT uses fixed wavelength lasers, based on a DFB laser diode, for a cost-effective implementation. It must completely cover the C-band with 50 GHz ITU grid channel spacing in order to be able to pass through any SARDANA RN.

An external modulation, based on a Mach-Zehnder modulator is placed for downstream modulation as the best option for 10Gbps transmission over long distances due to its inherently low chirp.

While the DFB laser diode is fixed to a wavelength channel, it can be tuned by ± 0.5 nm to locate the carrier in the pass-band of the RN. Once the wavelength is settled at its desired channel, it deviates by less than 0.01 nm. In addition, a small triangular modulation of the laser diode current allows for dithering at a frequency of 10 kHz and a frequency deviation of 10 GHz. The residual amplitude modulation that derives from the variation of the laser diode current is reduced at the optical modulator.

The optical Mach-Zehnder modulator is stabilised in its output power with a feedback circuit which receives a small tapped portion of the output signal. The long-term drift was stabilised so that the output power deviates by just 0.02 dB from its nominal value.

The high frequency data interface shows an electro-optical 3dB bandwidth of 10.2 GHz, while reflections are below -13 dB in this frequency range. A functional scheme of the OLT is shown in Fig. 4.16.

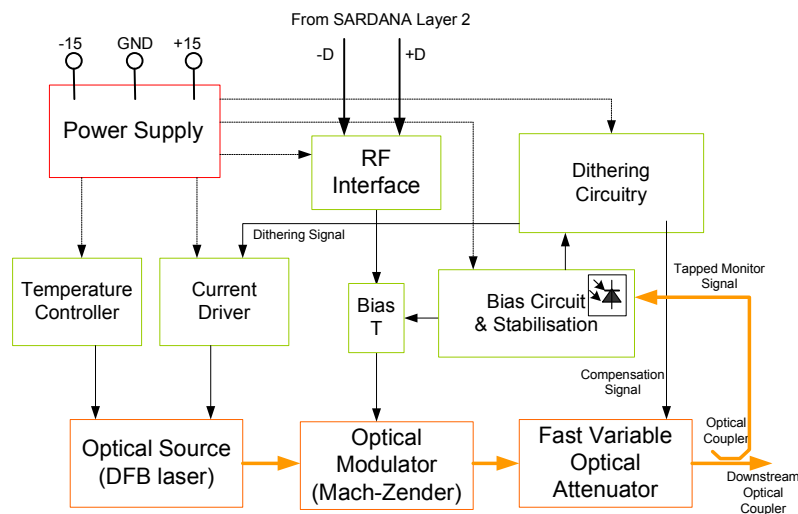


Fig. 4. 16 – Block diagram of the SARDANA OLT transmission

All the different modules (dithering circuit; DFB laser diode board, current driver and temperature controller) have been implemented in a prototype, as shown in Fig. 4.17.

4.4.1.1 Dithering for Rayleigh Backscattering Mitigation

Dithering by frequency modulation of the downstream signal must be used to reduce the spectral overlap and to add incoherence between the upstream and downstream signals to mitigate the penalties generated

by physical effects like Rayleigh Backscattering (RB) as well as from reflections at connectors between the OLT and the ONU due to the bidirectional optical transmission. In IM-IM transmission, error free upstream transmission has only been achieved for OSRR values higher than 17 dB [135]. The reduction of RB requires low modulation frequencies. A significant and stable RB penalty reduction can be obtained with a modulation frequency of above 3 kHz. Improvements in RB compensation gets to saturation for frequency deviations of 10 GHz.

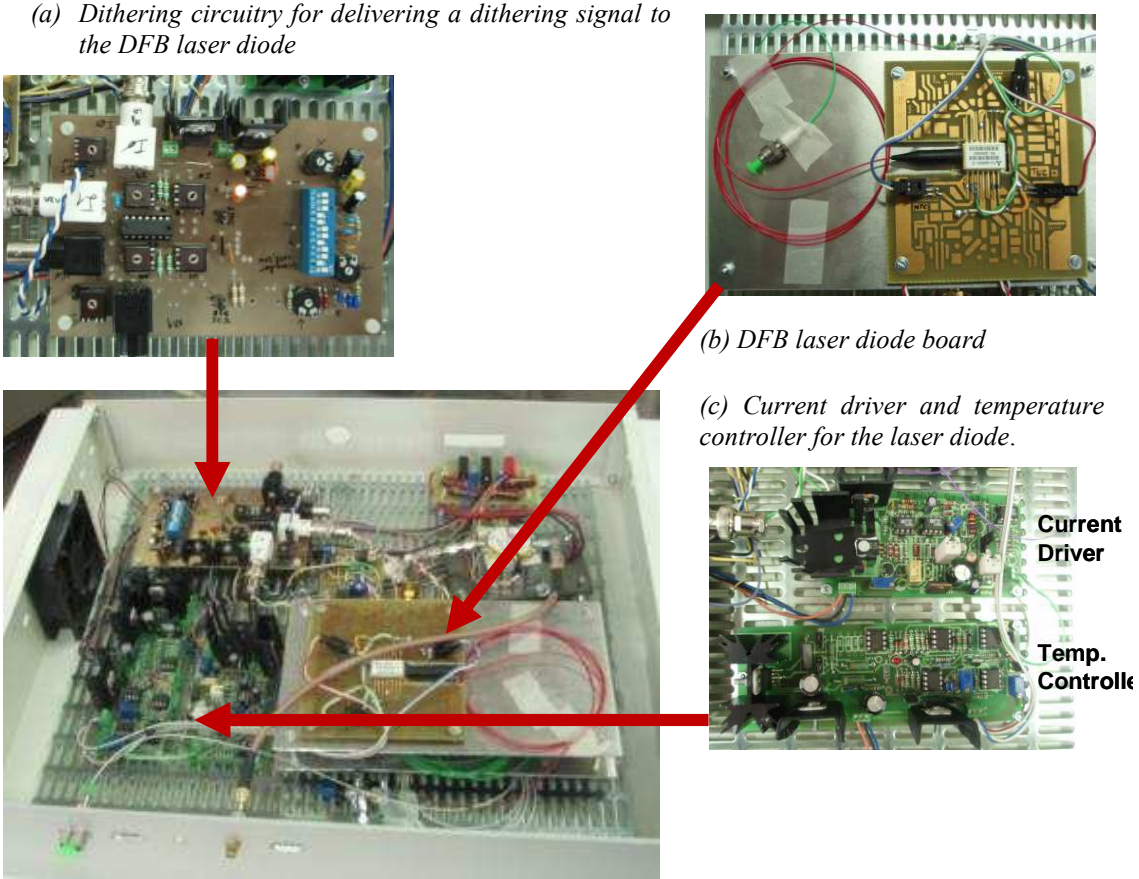


Fig. 4. 17 - Integration of: a) Dithering circuitry for delivering a dithering signal to the DFB laser diode; (b) DFB laser diode board;(c) and Current driver and temperature controller for the laser diode.

4.4.1.2 Optical Source

For the optical source, a DFB laser diode (Mitsubishi FU-68PDF) at a fixed wavelength of 1554.13 nm was taken. The laser diode was packaged in a butterfly module, containing also a thermistor and a Peltier element for temperature control. For this purpose, a temperature control circuit was attached to the DFB laser diode, to stabilize against thermal induced drifts of the wavelength. Besides that, the wavelength can be tuned into the centre wavelength of the drop filters in the RN of the PON. The dependence of the emission wavelength on the temperature can be seen in Fig. 4.18.

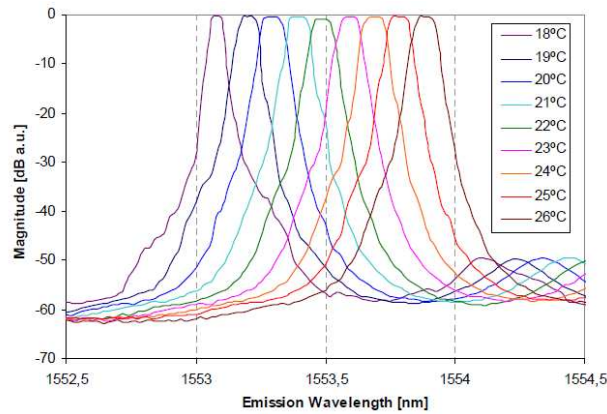


Fig. 4. 18 -Dependence of the emission wavelength on the temperature.

4.4.1.3 Optical Modulator and Stabilization Circuit

An optical intensity modulator based on a Mach-Zehnder modulator (MZM) introduces the downstream onto the optical carrier. Although the achievable ER is less than for an Electro-Absorption Modulator, this adjusts with SARDANA requirements. Typical values are around 3 dB, and the $V\pi$ voltage of the used MZM was 4.1V.

To avoid problems with the polarization sensitivity of the MZM, a DFB laser diode with a polarization maintaining (PM) fibre was connected to the already polarization maintaining fibre pigtail of the MZM.

An integrated attenuator at the MZM was used to counteract the previously induced amplitude modulation in the DFB laser diode during the dithering process. As this variable attenuator was capable of operation at the frequency dithering signal, no signal conditioning for the RF path is necessary, simplifying the complexity and reducing the cost of the OLT transmitter at the same time. In an alternative approach without variable attenuator, the bias of the MZM and the peak-to-peak voltage of the RF signal would have to be adjusted to the dithering signal accordingly, requiring gain control in the RF amplifier at a frequency well above 1 kHz. A stabilization circuit was inserted at the bias circuitry for the MZM to eliminate drifts that are present over longer time-spans. For this reason, a simple PIN photo diode was included in the bias circuit, to monitor the output power after the modulator. The stabilization circuit is provided with the reference bias point, at which the MZM is intended to operate, according to the desired ER that is chosen for the RF signal. By readjusting the bias point slightly – with a magnitude that is low enough not to perturb the ER of the RF signal – the present slow drifts can be significantly suppressed. An optical 5/95 coupler was inserted after the MZM. The overall bias circuitry has to be delivered with a voltage of +15V, and does not take a current bigger than 20 mA. Long-term measurements are shown in Fig. 4.19a for the applying the stabilisation circuit. Here there is no visible drift.

4.4.1.4 RF Data Interface

The RF interface of the OLT transmitter comprises of appropriate driving capabilities for the optical modulator. This includes an RF amplifier and also a bias-T, with which the definition of the operating point is obtained for the optical modulator.

For the input, an AC-coupled CML signal adapted to 50 Ohms is intended to be used, which provides input amplitude higher than 400 mVpp. The lower frequency cut-off was determined by the bias-T and was 200 kHz. GPON payload data should be therefore not penalized, as its low frequency components are not truncated.

The measurement of the upper e/o 3dB bandwidth is shown in Fig. 4.19b. As can be seen, a bandwidth of 10.2 GHz was obtained, which is sufficient high to provide 10 Gb/s downstream modulation.

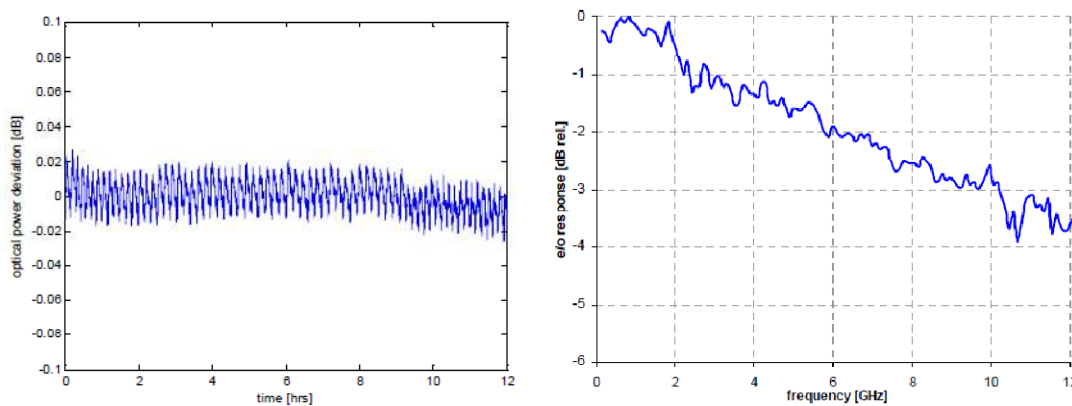


Fig. 4. 19 – a) Long-term measurements of the transmitted optical power over 12 hours for a stabilized modulator. b) Electro-optical response of the optical modulator. The 3dB bandwidth is 10.2 GHz.

4.4.2 OLT receiver

The OLT RX is based on an XFP 2,5Gbps burst transceiver from Zenko. The device LT-05B95B-XFPGX [150] is a 10Gbps continuous mode transmitter at 1577nm and 2,5Gbps burst mode receiver at 1550nm. It is a two fiber transceiver with LC receptacles. It provides LVPECL differential output in burst mode receive direction, which will be DC coupled to the BCM8154 [151] at the OLT Layer 2 assembly. The TX part was not applied in SARDANA as the wavelength falls outside of the defined range.

Table 4.7 shows the receiver optical and electrical specification for the Zenko.

Table 4. 7 - Zenko LT-05B95B-XFPGXreceiver optical and electrical specification

Parameter	Min	Typical	Max	Units
Optical				
Sensitivity			-28	dBm
Saturation Optical Power	-8			dBm

Operation Wavelength	1260		1650	nm
Date Rate	0		2.7	Gbps
Packet-to-packet spacing		25		ns
BM LOS Rise Time		1		ns
Optical Return Loss		40 @ 1550nm		dB
Preamble period	35.2			ns
Electrical				
Power Supply Current		130	160	mA
Data Output Voltage - Low		2.4		V
Data Output Voltage - High		1.6		V
Data Output Rise and Fall Time			150	ps
Tolerance to CID	100			bits

As an alternative to the Zenko receiver, a burst mode 2.5Gbps have been designed to be adapted to the OLT Receiver requirements, as shown in Fig. 4.20. The AC coupled receiver consist of several blocks: the photo-detector PIN+TIA to detect the optical power and convert it into electrical current, a linear amplifier to adequate the signal power, an electrical module which performs the square root mathematical function over the incoming signal [152] and a limiting amplifier with differential CML AC outputs.

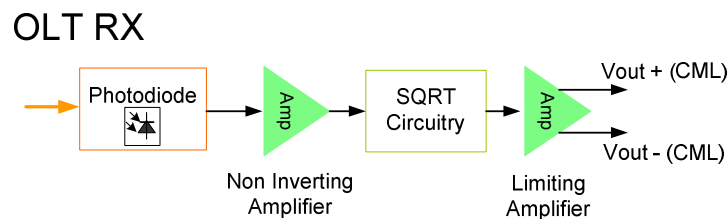


Fig. 4. 20 - OLT AC RX schematic diagram blocks.

4.4.3 Optical Amplification

Despite the functions of TX and RX, the OLT has to provide some extra functionality as optical amplification. Amplification is performed to boost the DS signals and to preamplifier the US signals. The booster's specifications are shown in Table 4.8.

Table 4. 8 - Technical Specification of the high power amplifier

Parameter	Values	Units
Saturated Output Power	1 – 2 Max	W
AC Supply voltage	240	V
Power Consumption	80	W
Mode of Operation	Single Channel	
Optical Bandwidth	1535-1567	nm
Noise Figure	5.5-6	nm
PDL	0.3	dB
PMD	0.7	

Regarding the optical amplifiers, they are facing more challenging burst traffic for the upstream. Several approaches for burst mode optical pre-amplification were analysed and finally, a new approach based in high pumping combined with feed forward stabilization has been implemented in the prototype of optical amplifiers required for the integration of the OLT.

After checking several versions and a comparison of the performances (summarized in table 4.9) the Hybrid (1st stage fully linear plus a second stage stabilized by a feed forward signal) have been implemented, as shown in Fig. 4.21.

Table 4. 9 - Comparison of the performances

	Noise Figure	Pump power requirements	Flexibility	Stability (15 dB dynamic range)
Dual stage fully linear preamplifier	4.6 dB	32dBm	Pump power	Best
Clamped preamplifier	5.1 dB	25 dBm	Pump power + 2 Clamping signals	Good
Hybrid Preamplifier	4.9 dB	29 dBm	Pump power + 1 clamping signal	Good (Best trade Off)

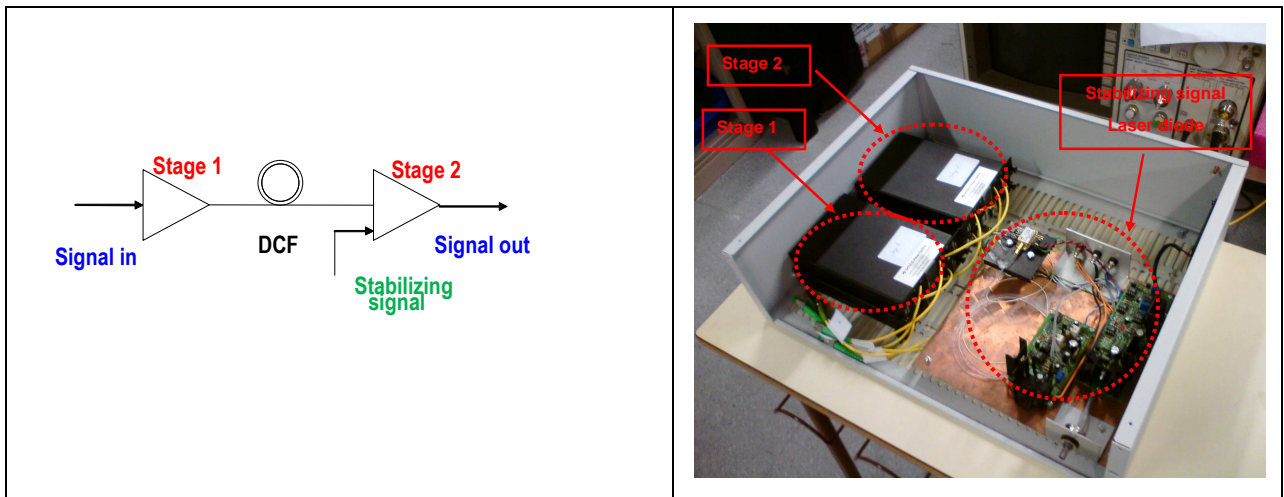


Fig. 4.21 - Hybrid amplifier design and prototype

4.4.3.1 Pump generation

The CO concentrates the pump generation for the remote amplification at the passive fibre plant and the RNs. One prototype has been built (Fig. 4.22) providing up to 8 W of pump at 1480 nm, based in a fibre laser Raman modules fabricated by Keopsys.

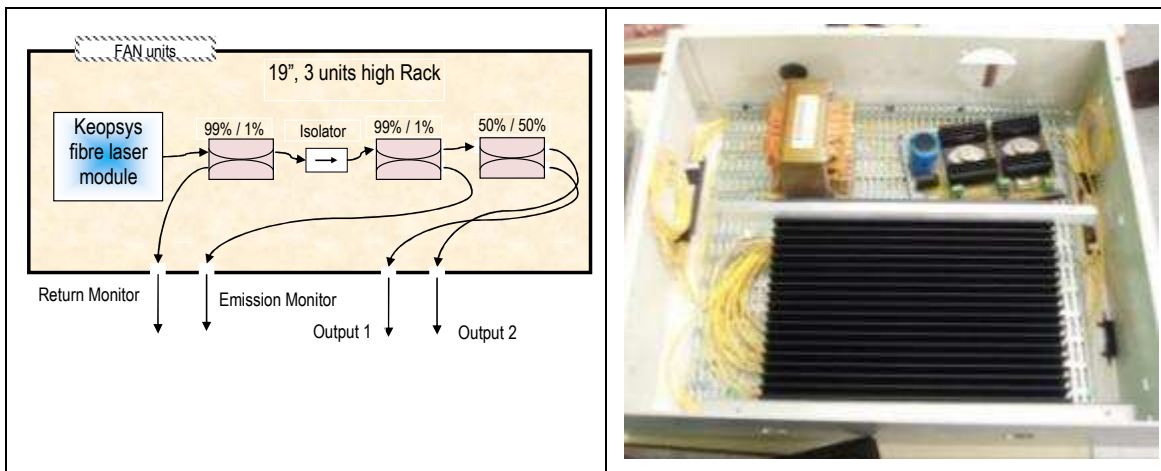


Fig. 4.22 - Internal scheme of the fibre based pump source for remotely pumped amplification and SARDANA prototype fibre laser pump source.

Fig. 4.23 shows the configuration of the Remote Amplification System at the Central Office in the SARDANA network.

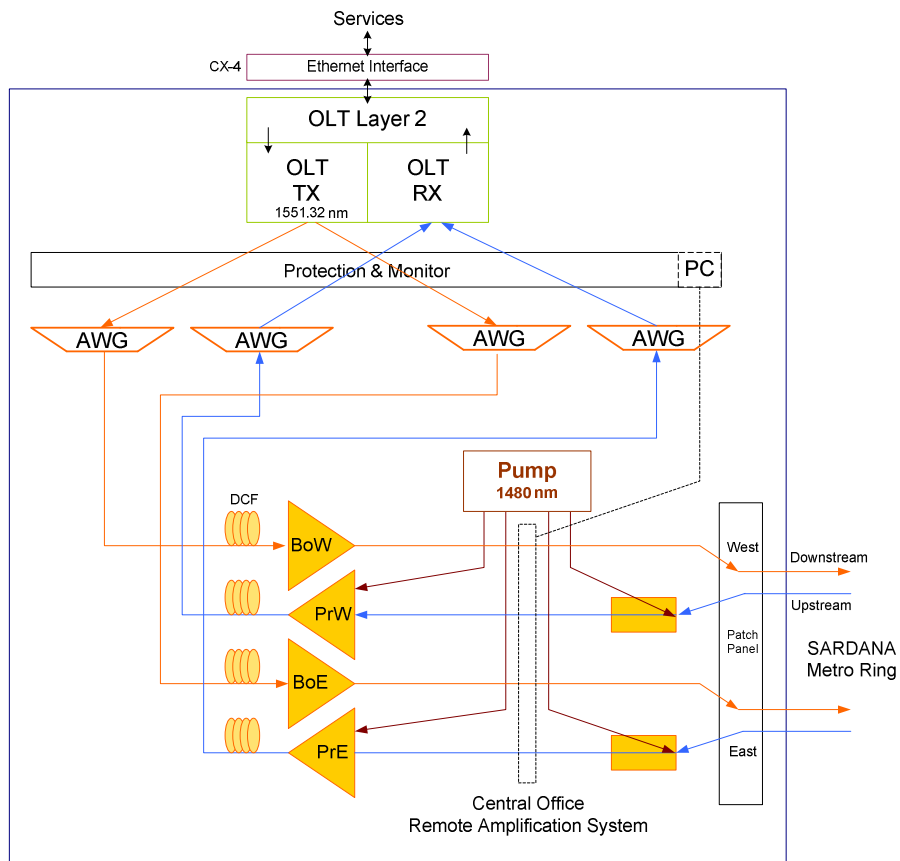


Fig. 4. 23 - Remote Amplification System at the SARDANA Central Office

4.4.4 OLT subsystem racks

Fig. 4.24 shows the fully equipped OLT rack in the SARDANA demo lab environment.

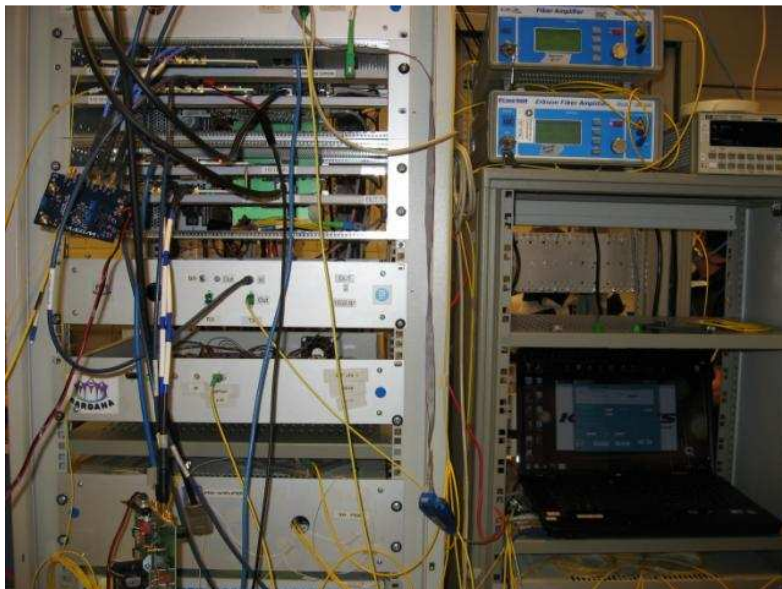


Fig. 4. 24 - OLT racks: The 2100mm rack is equipped with the Service switch, two OLT Layer 2 sub-racks, four OLT transmitter assemblies, two DWDM multiplexer/demultiplexer pairs for East and West ring segments, protection and monitoring assembly, and fibre connect.

4.5 ODN (Optical Distribution Network)

The segment of network approached by SARDANA is the metro-access network. Fig. 4.25 represents the end-to-end segmentation of the architecture with a maximum metro section = 80km and maximum access section = 20km.

The network topology is hybrid with a central WDM ring, to offer instant communication protection in case of fibre cut, plus TDM single-fibre trees, to the homes. The Remote Nodes perform wavelength add&drop routing and optical amplification, although being fully passive. Strict passiveness is preserved in the external fibre plant to minimize infrastructure cost.

The optical connection of the users by ONUs in the network of access is ensured by a point-to-point architecture or point-to-multipoint (PON). At the border of the metro-access, one finds with the central office with a specific optical equipment like the OLT of the PON.

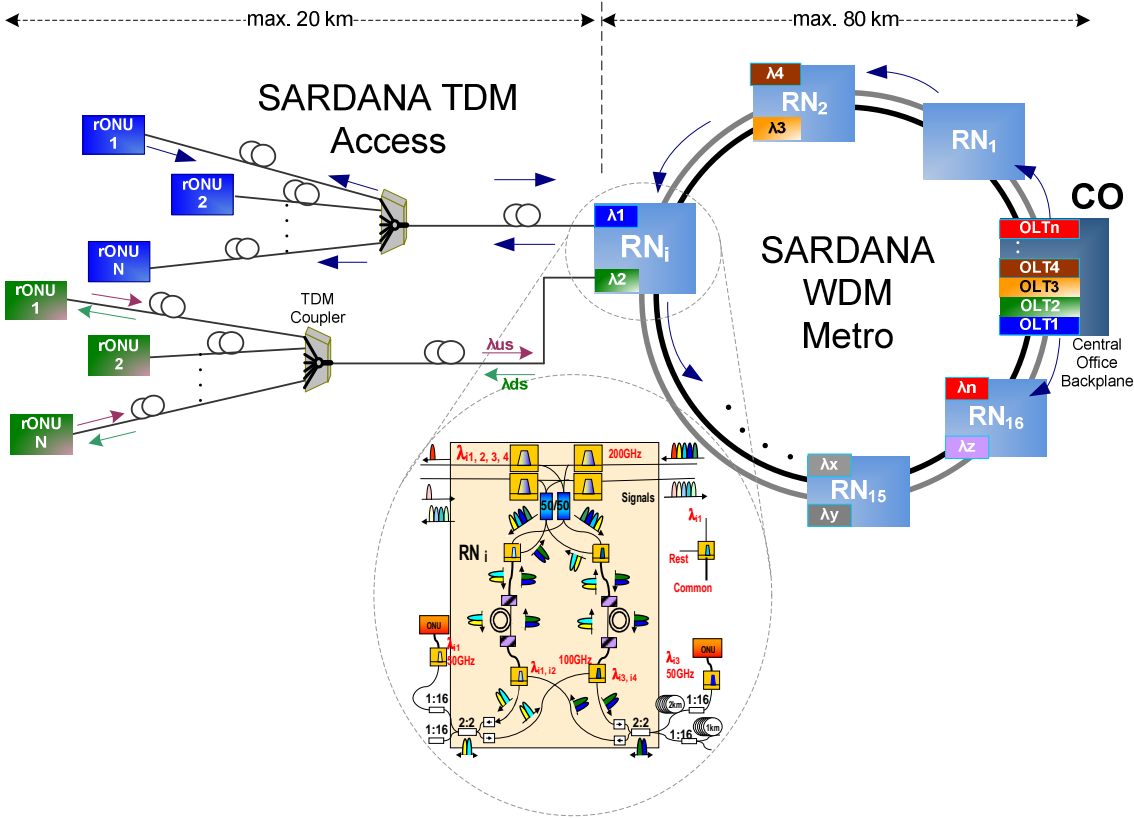


Fig. 4. 25 – SARDANA metro-access Optical Distribution Network

SARDANA can be applied to different geographical and functional scenarios, regarding distances (ring, feeder, drop), user density, user distribution also as integration collector of other access media like xDSL or Cable Modem. Thus, 6 different scenarios have been tested: Urban 1, Urban 2, Metro, Rural, Collector and WDM-PON, as shown in Table 4.10. This last scenario is a particular case of no TDM (1:1 splitting), using for point-to-point connections.

Table 4. 10 - Service Scenarios for SARDANA

SARDANA Scenarios	Max distance Km	Ring Km	Tree Feeder Km (max)	Tree Drop Km	Trees (λ s) (2xRN)	Splitter	ONUs	Guar. BW (10G)	Pump (W) Goal tbd
URBAN 1	20	17	2.9	0.1	32 (2x16)	1:64	2048	>140M	1.2
URBAN 2	20	10	9	1	32 (2x16)	1:32	1024	>280M	1.2
METRO	60	50	9	1	16 (2x8)	1:32	512	>280M	1.2 / 5
RURAL	100	80	19	1	16 (2x8)	1:16	256	>560M	5
COLLECTOR	20-60	80	19	1	16 (2x8)	1:8	128x	300M / 1G	
WDM-PON	80	80	0	0	32 (2x16)	1:1	32	10G	

4.6 Remote Node (RN)

The RN is a key element of the SARDANA network, and many of the performances and functionalities of the network depend on its design, like protection and routing. They implement cascaded 2-to-1 fibre optical add&drop function, by means of athermal fixed filters, splitters that perform spatial diversity for protection and distribute different wavelengths to each of the access trees, and remote amplification, introduced at the RN by means of Erbium Doped Fibers (EDFs) to compensate add&drop losses. Optical pump for the remote amplification is obtained by pump lasers located at the Central Office (CO), also providing extra Raman gain along the ring. The RN is also an interface between the ring and the tree fibre sections, between the metro network and the access network. This new passive network element, incorporated in the new PON, is not present in current standards, but it inherits concepts from the following existing standards:

- ITU-T G.984.6 on PON Extender Box,
- ITU-T G.973 on remotely pumped amplifier (ROPA) for submarine systems,
- ITU-T G.983 PON protection and
- ITU-T G.808 Generic protection switching.

The RN encompasses some key challenges, like passiveness (not using electrical supply), efficient 1480 nm pump use, and burst mode upstream amplification generating gain transients, that are cancelled in this RN thanks to the crossed wavelength direction design and co-amplification of higher power continuous downstream, also avoiding Rayleigh backscattering.

Wavelength extraction is done by means of two athermal thin-film OADMs at alternated 100 GHz or 50 GHz ITU-T grid channels. The implemented RN presents 1 dB insertion loss in by-pass, 6 dB in drop/add, and >30 dB rejection. The losses (dropping, splitting filtering and insertion losses) are largely compensated by about 14 dB gain of the EDF. It allows significant improvement in the scalability of the network, geographical flexibility and average bandwidth per user but decreases the OSNR [153-154]. In [155] this is compared to other types of Extender Boxes for PONs, in terms of reachable trunk & access

power budget. We specify up to 16 RNs, thus 32 wavelength channels, with a splitting ratio between 1 and 32 each. A basic diagram of the RN main blocks and its implementation is shown in Fig. 4.26.

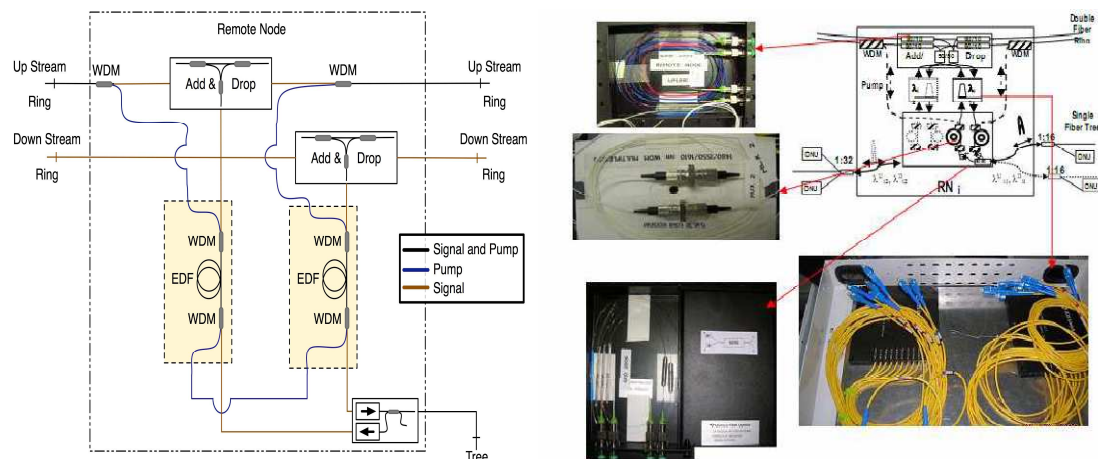


Fig. 4. 26 - Remote Node a) basic structure and b) physical implementation

4.6.1 SARDANA RN operation

A basic operation of a SARDANA RN can be resumed in the next steps:

- The Central Office sends WDM signals to the Remote Nodes (RN)
- Each RN drops its assigned channels as the corresponding wavelength by 2 filters and a splitter 50:50 for resilience that splits the signals to two TDM trees
- Signals are amplified by EDFs
- The Remote Nodes receive the pumping power for the EDFs from the WDM ring
- Once amplified, the signals are transmitted to the ONUs

This operation is presented in Fig. 4.27.

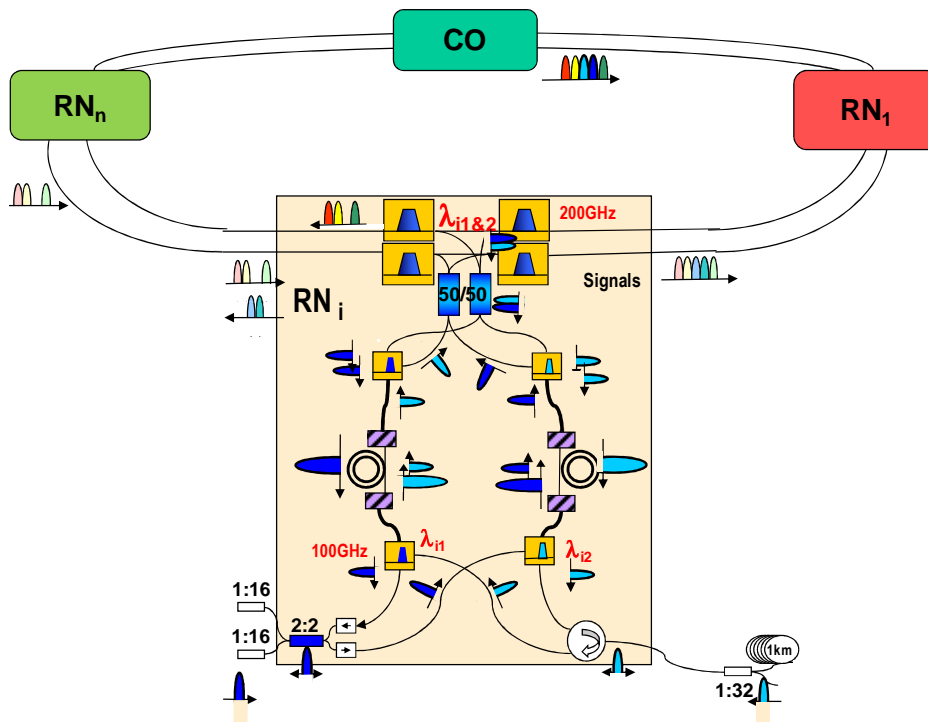


Fig. 4. 27 – Basic operation of a SARDANA Remote Node

The RNs are completely transparent in the ring and compatible with the already deployed fibre structures being no modification required as the network updates. The introduction of a new RN in the ring is a simple task and just implies the transmission of two more wavelengths from the CO (one for each tree served) [156].

4.7 SARDANA Test-bed

The implemented testbed demonstrates the following features: truly-passive extended PON, fundamental resiliency, up to 1024 ONUs per PON, up to 100 km reach, 32 x 10G/2.5 Gbit/s (XGPON1 rates), wavelength-agnostic single-fibre ONUs, neutral multi-operability optical infrastructure and cost efficiency. A set of technological advances has been developed in the project, like remotely pumped optical amplification, colourless reflective ONU, optical downstream cancellation, 10G/2.5G MAC, compatible with the xGPON GTC, etc. To stress the network, advanced new broadband multimedia services are exhibited.

Fig. 4.28 shows the system diagram of the SARDANA test-bed, for the demonstration in Tellabs Oy premises (Helsinki-Finland) [51]. It shows the ring-tree PON optics, the WDM routing and protection modules, the colourless physical transceivers, the MAC section, the Ethernet clients and the service layers. Five ONUs have been assembled for this demo.

The OLT is composed of the optical amplification stages, the pump source, the WDM multiplexing, the Protection & Monitoring system, the coloured burst-mode transceivers, and the electrical circuits of the layer 2 (MAC and the Ethernet interfaces and OMCI control). A 10Gbit/s CX4 electrical Ethernet

interface connects OLT to the service nodes that supplies IP/Ethernet based Internet, IPTV and Videoconferencing services. Different VLANs are used to separate services from each other.

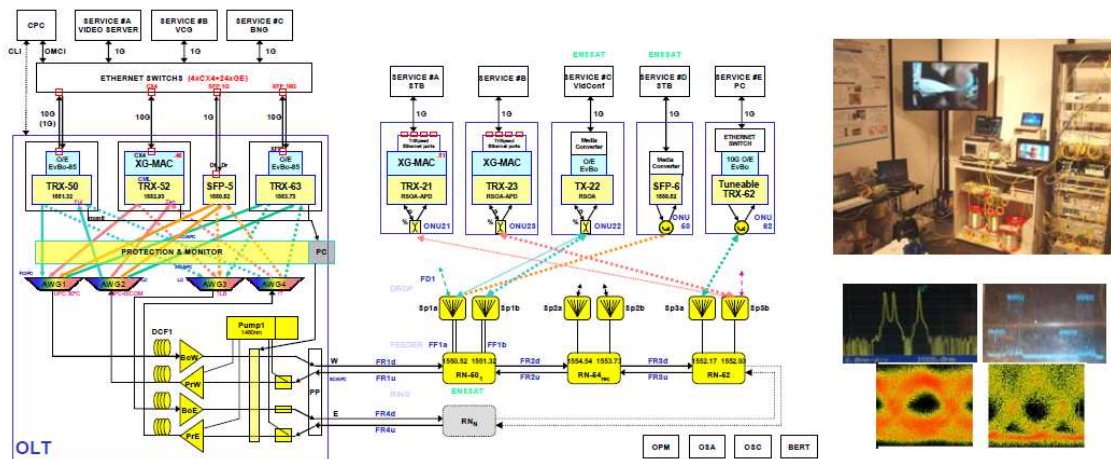


Fig. 4. 28 - SARDANA testbed scheme (left), demo setup, downstream east spectrum, burst mode upstream frame, DS and US eyes (right).

The 10Gbit/s serialized output drives the coloured DFB-MZM transmitters at the C-band in the odd 50 GHz ITU grid; they include frequency dithering for Rayleigh scattering reduction and modulation control, fixing the DS-ER to 3.5 dB. The RX is based on burst-mode PIN TIA with SQRT compressor.

The protection module routes every wavelength channel to the East or West side of the PON ring, depending on the corresponding RN distances and the ring protection conditions. It is based on an array of mechanical switches, with total insertion loss below 2 dB, controlled by the Protection & Monitoring module.

Four AWG multiplexers (East/West, Downstream/Upstream) set the WDM multiplex, passing through DCF modules compensating 40Km of SSMF, optical booster/pre-amplifier and pump couplers. The output power is 7 dBm per channel. The pump module, based on a Keopsys Raman fibre laser (@1480 nm), provides 1 W to the upstream fibres. Fig. 4.29 shows a part of the SARDANA testbed implementation for the demo.

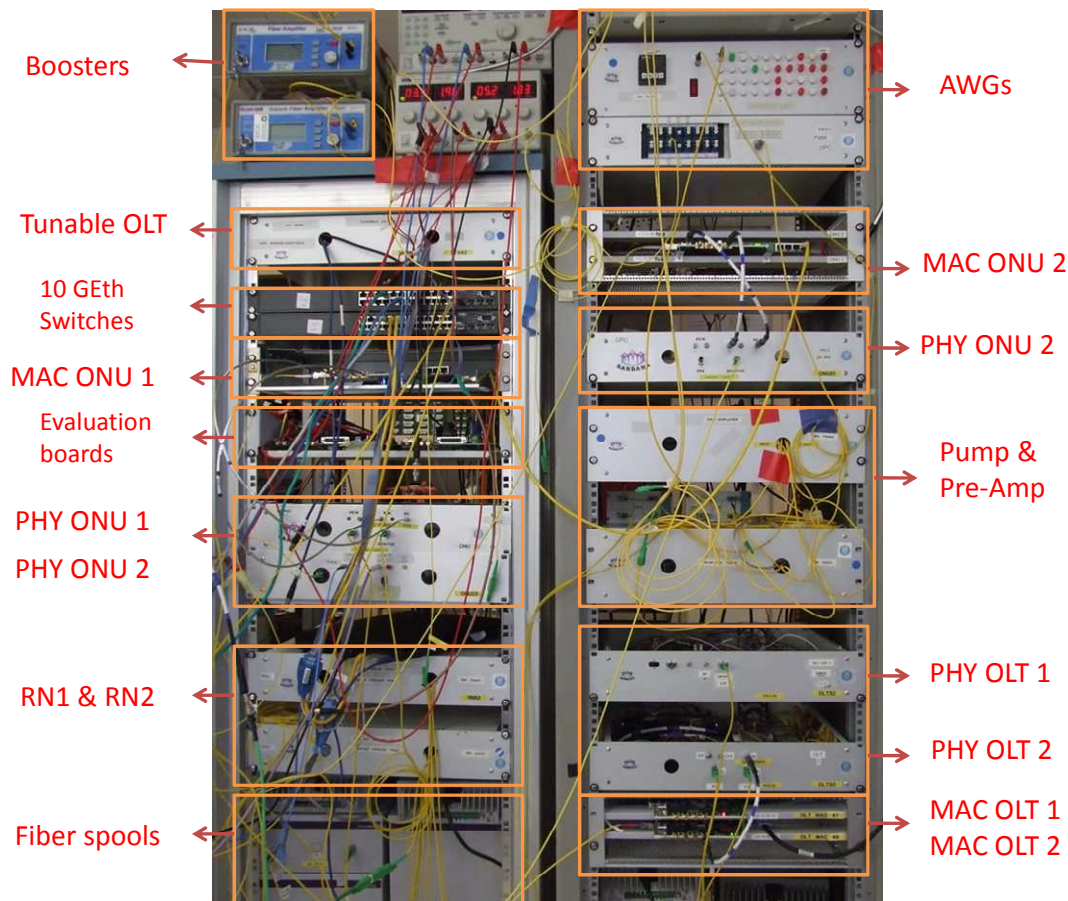


Fig. 4. 29 - SARDANA testbed implementation for the demo.

The central ring, doubled for DS and US, connects the Remote Nodes that add&drop two 100 GHz adjacent wavelength channels to two access trees. This ring fibre length ranged from 20 to 100 Km.

The demo testbed includes three RN (other RNs are emulated with attenuators). The RN provide optical amplification of 10-16 dB, depending on the location, to overcome the extended power budget requirements of the extracted channels, by means of internal EDFs remotely pumped from the OLT. Each RN drops a fraction of the pump power travelling through the upstream ring [157]. The bypass insertion loss of the RNs is only about 1 dB, guaranteeing ring scalability.

Every access TDM tree distributes a wavelength channel to the single-fibre single-wavelength colourless ONUs. Three of them are based on RSOA, in simple TO-CAN package, modulated at 2.5Gbps with pre-emphasis, providing upstream ER of about 7dB, and silent level of -12 dB at burst disable. The APD received 10 Gbps downstream data counteracts the RSOA gain to reduce the DS ER crosstalk from 3.5 dB to 1.5 dB, thus being able to reuse it. The optical ONU gain, including the 30:70 coupler, is about 12.5 dB, launching -4 dBm. Other ONU are based on C-band tuneable laser externally modulated at 10G, on SOA-REAM and on SFP transceiver. A 10/100/1000 Base-T electrical Ethernet interface connects ONU to the user's nodes that receive IP/Ethernet based Internet, IPTV and Videoconferencing services.

The upstream data is replicated to both sides of the ring by the RN, reaching the OLT, where it is pre-amplified, WDM de-multiplexed and direction-selected by the protection module, lead to the RX. To deal

with its bursty nature, specific optical gain clamping techniques have been developed, keeping the transient distortion below 1dB. Extra 2dB of gain were obtained in the last upstream links because of Raman amplification.

4.7.1 SARDANA Network tests

For the first time, the built Scalable Advanced Ring-based passive Dense Access Network Architecture [51] is publicly demonstrated, experimentally showing the key concepts and results. Performances, functionalities, requirements and impact on the deployment will be here discussed.

Three different test-bed public demonstrations with a high positive broad impact were made: the first one in Espoo (Finland) in October 2010, the second in Lannion (France) in January over the metropolitan 18 Km ring cable, and the third one in the FTTH'2011, in Milan, in February [158-162]. In them, the key functionalities and performances were tested and demonstrated using the built SARDANA prototype.

As a part of SARDANA system integration, the following network functionality was tested and demonstrated in the first demo (Stakeholder demo in Helsinki-Finland):

- HD-video downstream/upstream up to eight HD-video channels delivered simultaneously from SARDANA OLT/ONUs to STBs connected to SARDANA ONU/OLT using a commercial IPTV delivery platform.
- Point-to-point Gigabit Ethernet delivery over the SARDANA network wavelength between ONU and OLT sites, showing bidirectional video transmission.
- Ring protection switching between the East and West SARDANA ring for P2P GE transmission based on fault detection by monitoring signals built in the protection and monitoring subsystem (P&M) of the SARDANA system.
- Control IPTV service activation/deactivation from the OLT CPC to the ONU CPC via OMCC over the SARDANA OLT and ONU MAC implementation.

Different services have run in parallel through the SARDANA network over four wavelength channels in operation. Fig. 4.30 shows the network testbed scheme assembled for this demonstrator tests.

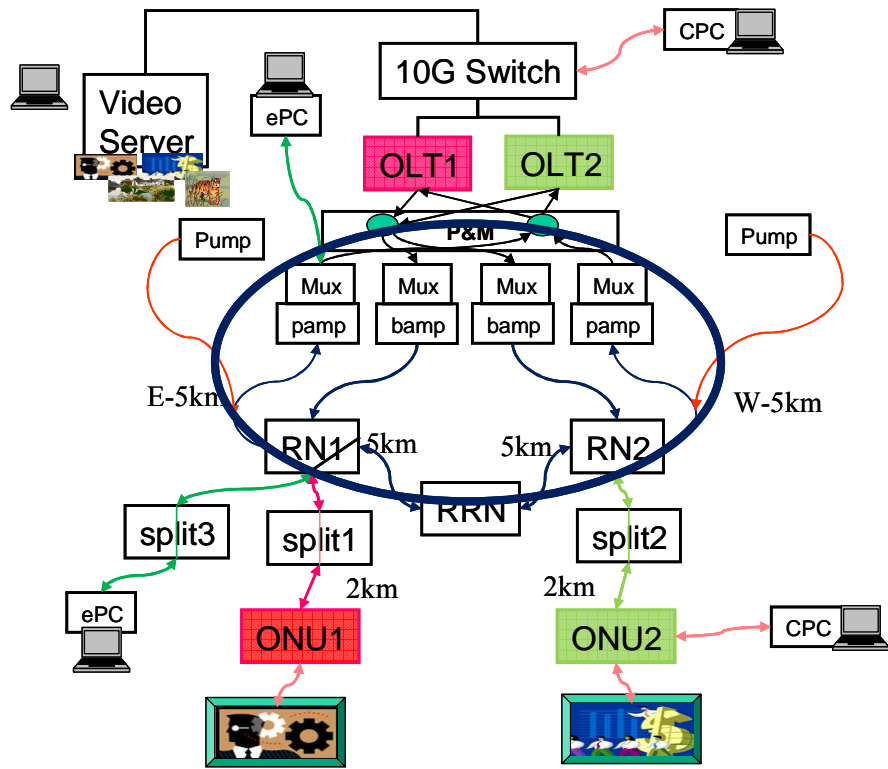


Fig. 4. 30 - Network setup for SARDANA demonstrator tests in Helsinki-Finland.

4.7.2 SARDANA Field Trial

The SARDANA network was installed over open fibre network in the Bretagne Lannion area (France), in January, 2010. An 18 Km 12-fibre ring cable connected the Imagine-Lab (where the OLT and the main equipment were installed), the ENSSAT (with a RN and ONU), and Orange Labs (with another ONU through a distribution tree), drawn in the Fig. 4.31.

The total ring loss was about 9 dB, including the losses of the SC/APC connectors at each location patch panel. Extra 20 Km and 5 Km fibre spools were added between the OLT and the first and last RNs respectively, at Imagine-Lab, composing a 43 Km ring. The single-fibre tree had a length of 5 km, and a splitting of 1:16 (plus variable attenuator). A HD Video-Conferencing was established for live communication with the remote ENSSAT location (at 8.7 East /8.8 km West).

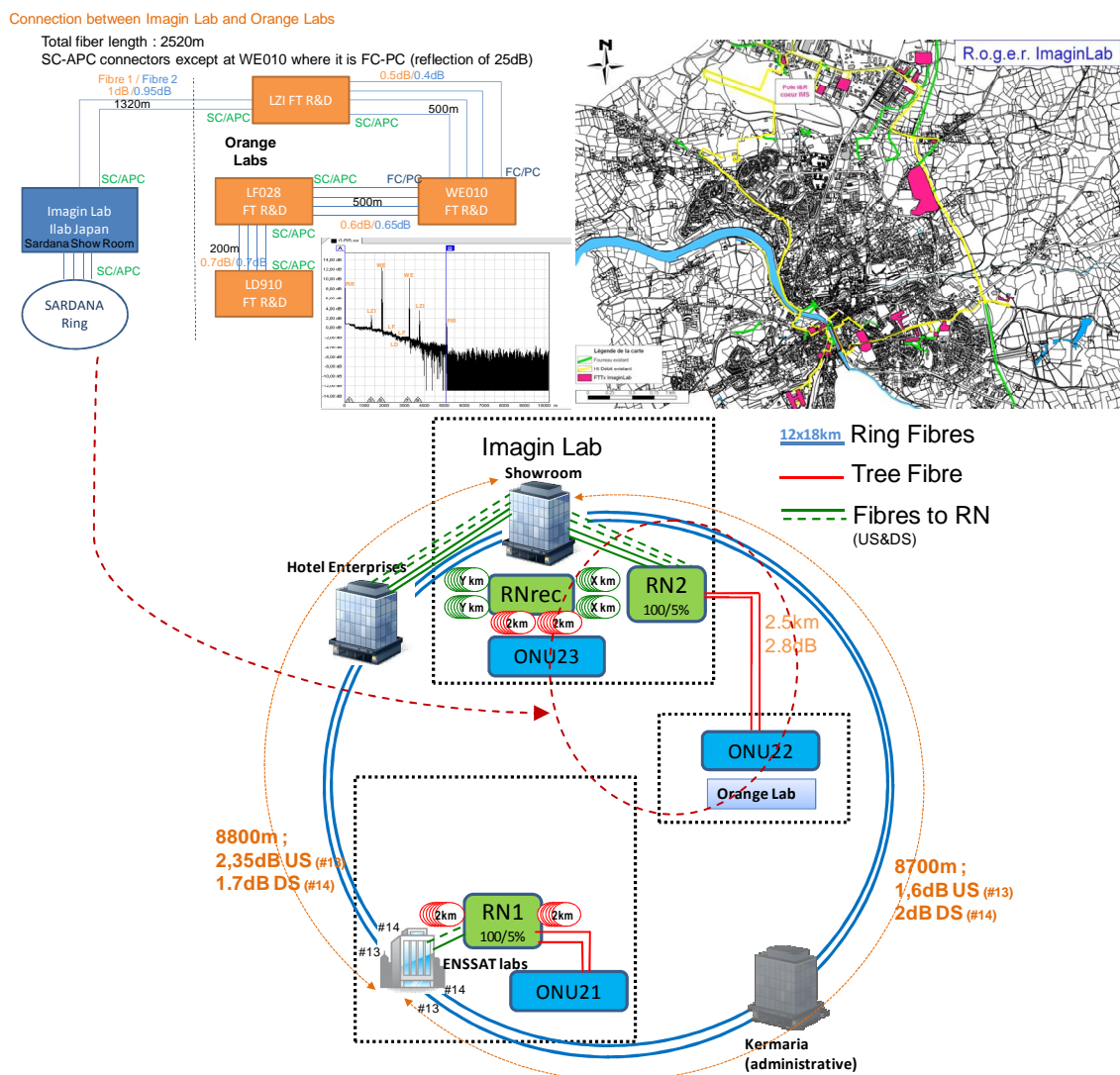


Fig. 4. 31 – a) Field trial network scheme, b) Detail of the Imaging Lab and Orange Lab connection, and c) Lannion ring map (in yellow).

The performed measurements over this test-bed, at the application, Ethernet, MAC and PHY layers, showed the following features:

- Neutral multi-operator/service: different standards, bit rates and protocols were simultaneously transported through the SARDANA network transparently over the wavelength channels. Fig. 4.32 and Table 4.11 summarize the obtained performances in terms of ring length, maximum number of ONUs and down/up bit rates.
 - 10G/2.5G XGPON1 MAC with 2 RSOA ONUs in a tree.
 - Bidirectional 10G Ethernet with tunable lasers at ONU and OLT.
 - Standard 1GEth SFPs with RSOA transceiver and evaluation board.
 - Standard 1GEth SFPs with commercial RSOA SFP transceiver (pure WDM-PON).
 - Standard 1G Eth SFPs, with fixed lasers at 1550.12 nm (up/down with slight drift).
 - 10G/10G $2^{31}-1$ PRBS with SOA-REAM ONU.

Table 4. 11 – SARDANA’s performance in terms of ring length, maximum number of ONUs and down/up bit rates.

Demo	Application	ONU	L ring (km)	Split	ONUs
Espoo	10/2.5 Gbps	RSOA	25	16	256
Lannion	10/2.5 Gbps BM	RSOA	43	16	256
Lannion	10G/10G Eth	Tunable Laser	43	8	128
Lannion	10G/10G PRBS	SOA-REAM	75	4	64
Lannion	10G/2.5G PRBS	RSOA	23	64	1024
Lannion, Milan	1G/1G Eth	RSOA	43	32	512
Lannion	1G/1G Eth	SFP	43	64	1024
Lannion	Commercial 2.5G	RSOA SFP	43	2	32
Barcelona	10G/5G PRBS	RSOA	100	16	256

- High-bandwidth real-time bidirectional HD multimedia services, over the different WDM channels:
 - HD-Video downstream broadcast and HD-Video upstream, from ONU to server.
 - HD-Video Conferencing; a P2P VLAN is configured between two ONUs by creating two 1:1 VLAN from OLT to two ONUs VC service ports that map to VC-GEM port IDs across the SXGPON.
 - Service control over OMCI (CPC-to-CPC).
- MAC ranging over differential 6 Km of two TDM ONU channels in a XGPON frame (70 Km in separate tests).
- ONU colourlessness: a RSOA ONU, first operating at the 1551.32, was exchanged with others RSOA ONUs. The service continued the operation correctly, with sensitivity differences below 2dB.

- The total power budget, considering the metro ring and the access trees, is about 35 dB, for the reference 10/2.5Gbps channel. The DS and US are balanced by means of the DS-ER and the ONU splitter. Sensitivities were measured at 10^{-6} BER, where pixelation starts to be visible.
- 1024-ONUs was practically emulated, adding optical attenuators and dummy channels.
- Rayleigh backscattering and reflection tolerance: with the implemented techniques, like wavelength dithering, the impairment was negligible up to 6 Km of drop fibre, and using angled connectors.

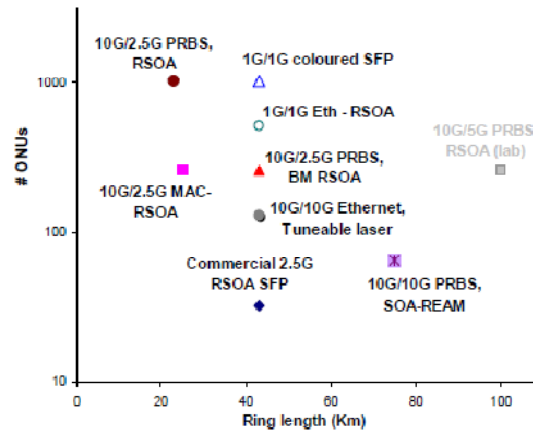


Fig. 4. 32 - Performances of the systems transported in the SARDANA test-bed

- Resiliency; the OLT RX LoS alarms with fibre disconnected between RNs and between OLT and RN, triggering the P&M (Protection and Monitoring) system to reroute the channels. Protection switching proved not to interrupt nor impair the Ethernet connection: video transmission quality remained unchanged to the eye, since switches activation is around 20 to 25 ms. The differential sensitivity between normal mode and protection mode of the different channel transmissions were below 3 dB.

4.8 Energy efficiency

Different long-reach optical access networks are studied with respect to their power efficiency. Special focus is dedicated to the hybrid TDM/WDM PON proposed in the SARDANA project, in which remote amplification is utilized for reach extension. The structures of the remote nodes and subsystems for reach extension are shown and discussed in [163]. In principle two SARDANA situations have been considered: SARDANA with “non-commercial” devices (SARDANA1), and SARDANA with market ready components (SARDANA2).

In Fig. 4.33, the results for unlimited and limited upstream are reported. SARDANA, especially the version 2, expresses the best performances in terms of power efficiency. The influence of uplink capacity limitation on power efficiency is evaluated, i.e., the access networks’ efficiencies are presented for different CO capacities in terms of Watt per user and per Gbit/s of user’s bandwidth as a function of number of users connected to the CO. The results show remarkable power efficiency degradation for high-speed access technologies in case of strong uplink limitation, while or unlimited uplink case, 10G-

EPON and SARDANA networks show the best efficiency. SARDANA2 bears great power efficiency over the largest interval, consuming only about 3 W/Gbps.

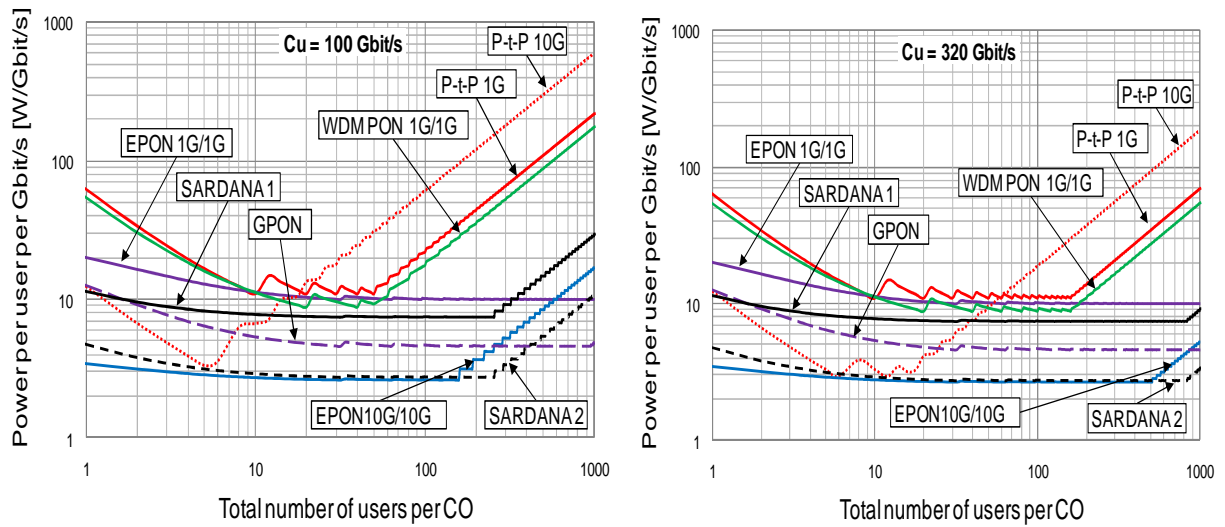


Fig. 4. 33 - Results on the consumption per user and Gbit as a function of the number of ONUs per Central Office, for the uplink limitation of 100 and 320 Gbit/s.

SARDANA offers a PON Green field migration scenario. When NG-PON technology becomes mature, service providers might be interested in using SARDANA to replace copper based infrastructure or to deploy in a brand new development area for the benefit of higher bandwidth and/or higher splitting ratio.

4.9 Conclusion

The new all-optically integrated metro-access network proposed in the SARDANA has demonstrated practical feasibility, extended performances, functionality and efficiency in terms of cost and energy consumption, aiming towards future FTTH. A number of technical innovative advances, summarized in next table, have been developed to achieve the SARDANA goals:

- End Users/PON increased from 64 to 1024 users; 100-kilometer reach, integrating metro & access network; and 2.5 Gbps to 10 Gps, for symmetrical 300 Mbps per user, carry to “One Order of Magnitude” the state-of-art (at that instant).
- WDM Ring + TDM Trees, flexibly allocated, by doing Scalable and Upgradeable the network.
- A competitive cost structure and infrastructure minimized: complexity centralized at the CO, WDM Ring + TDM Trees, passive external plant bi-directional single-fibre / single-wavelength access, colourless reflective ONUs, US for wavelength reuse.
- No Maintenance, No Power Needed with a passive external plant (RN optically powered from Central Office).
- Robustness of network, through the use of a dual-ring protection, for centralized management and light generation, and for a dynamic EE and resource allocation.
- Neutral Network, with support and compatibility with standards XGPON, GPON, BPON, EPON, 10G Ethernet (multi-operator capable).

SARDANA optimize and extends the design, architecture and capabilities of the WDM/TDM PON presented in the chapter 2.

The implemented test-bed demonstrates truly-passive extended PON, fundamental resiliency, XGPON1 rates, wavelength-agnostic single-fibre ONUs, neutral multi-operability optical infrastructure and cost efficiency in practical condition.

The technological advances developed in the project, like distributed add&drop, remotely pumped optical amplification, wavelength dithering, colourless reflective ONU with optical DS cancellation and opto-electronic equalization, and 10G/2.5G XGPON MAC, enable the feasibility of the new network concept for its application in future PON migrations. Enhanced performances can be pursued with improved RSOA or tuneable laser technologies, with burst-mode RX and FEC coding, and with optimization of the MAC and signalling procedures on the Layer 2, as will be seen in the following chapter.

Chapter 5

5. NG-PON Layer 2 Optimization

This chapter provides a comprehensive discussion focused on the architecture, signalling and protocols of the NG-PON layer 2 and its optimization.

From the G.987.3 FSAN-ITU standard recommendation (and backwards compatible), it expands this discussion to propose a design for the SARDANA network architecture, in line with their Metro-Access dimensioning and PHY characteristics.

Special attention is given to the SARDANA Transmission Convergence (STC) layer, each of their sub-layers and the different header formats, as well as the processes of medium access control (MAC) and ONU initialization.

The flexibility of the proposed architecture provided to future Dynamic Bandwidth Assignment algorithms aimed to achieve efficient Quality of Service requirements.

5.1. SARDANA NG-PON (SPON) Layer 2

This section presents a proposal for SARDANA Transmission Convergence (STC) Layer and guidelines of the MAC system as a function of the PHY layer particularities. In general, SARDANA TC protocol could be used or extended to others next generation network architectures.

A number of system functionalities, common to existing networking technologies (metro-WDM, GPON, XG-PON or 10GEth systems), have to be incorporated in the SARDANA's Control and Management planes and others are extended to exploit the SARDANA's PHY layer characteristics.

So, SARDANA 10 Gigabit-capable PON TC Layer proposal is inspired mainly in the ITU/FSAN specifications and preserves relevant features that are straightforward implemented [97,164-168]. Also, SARDANA considers co-existence with GPON [99,125,169-170] and GE-PON [94], compatibility with XG-PON1; and with the SXGPON, the initial proposal for SARDANA from Tellabs [171]. Fig. 5.1 shows a scheme of this genesis.

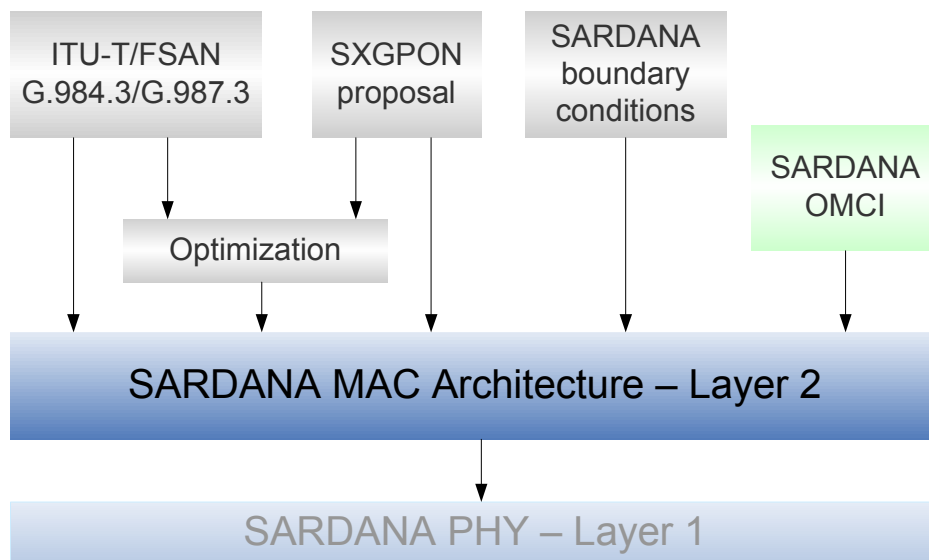


Fig. 5. 1 - SARDANA MAC architecture layer 2 overview

So, this proposal considers boundary conditions related to SARDANA metro/access network, bidirectional transmission on single-fibre/single-wavelength with downstream carrier reuse (by use of rONUs), long reach, physical impairments and cost-effective implementation.

A SARDANA OMCI (ONT Management and Control Interface) was developed as a part of this project. This protocol session allows SARDANA layer-2 architecture to implement control for the ONUs. OMCI discussion is not addressed in this work.

5.1.1.SARDANA NG-PON Layer Architecture

Fig. 5.2 shows a protocol view point of the SARDANA system architecture on the OSI network reference model. SARDANA 10 Gbps Transmission Convergence layer (STC) is positioned between the PHY layer and the SARDANA's services layer (Ethernet and OMCI clients).

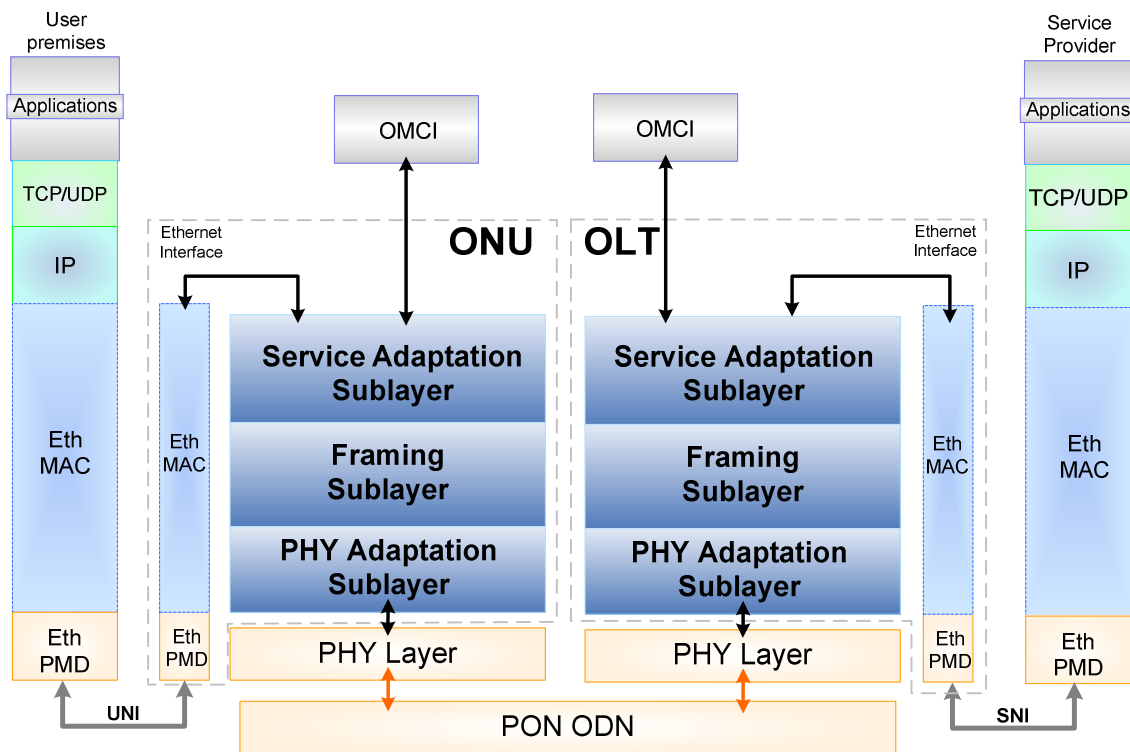


Fig. 5. 2 - SARDANA NG-PON system architecture

Similarly to XGPON-XGTC (in annex A), SARDANA divides the Transmission Convergence (TC) layer in three sub-layers (the STC service adaptation sub-layer, the STC framing sub-layer, and the STC PHY adaptation sub-layer), with basically the same functionality.

The OMCI client is the OMCI message processing entity that communicates with the Service Adaptation sub-layer [164].

An Ethernet interface section at the OLT/ONU allows layer 2 protocol communication between SARDANA and entities (service provider and user premises), and PHY Ethernet frame transport through the SNI/UNI interfaces.

5.1.1.1. SARDANA OLT layer Architecture

Fig. 5.3 shows the layer design for the SARDANA OLT. STC layer consists of a Control and Management (C/M) plane, which manages user traffic flows, OAM features and signalling for reliable data transmission. A User plane (U) carries user data traffic.

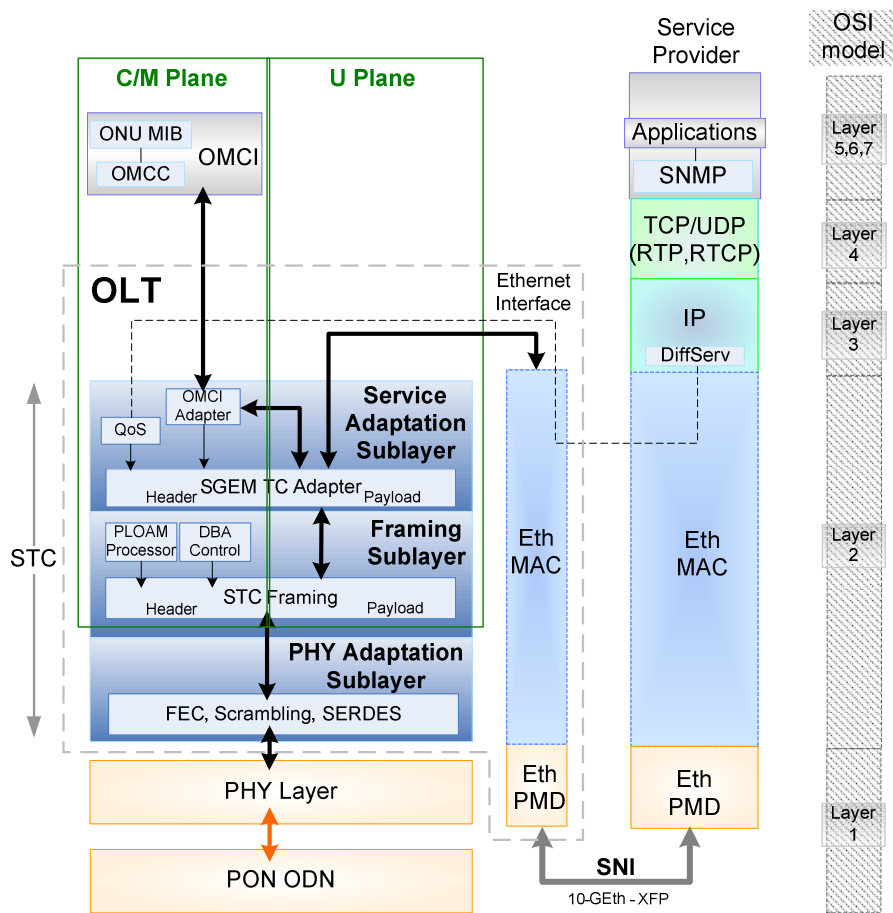


Fig. 5. 3 - SARDANA OLT system architecture on the OSI network reference model

An option to incorporate QoS from the upper layers, in particular from *diffserv* IP layer protocol, is suggested in this work through of the implementation of the SARDANA GPON Encapsulation Method (SGEM) header.

The Physical Layer Operation, administration and management (PLOAM) processor [97] and Dynamic Bandwidth Allocation (DBA) control are implemented on the STC header in the Framing sub-layer.

The STC frame is FEC processed, scrambled and serialized before to be sent to PHY layer.

5.1.1.2. SARDANA ONU layer Architecture

As the OLT, similar functionalities are being developing at the SARDANA ONU layer architecture. However, different to OLT, an upstream bandwidth management implements the functions of sending the T-CONT status information to the OLT DBA control. Fig. 5.4 shows SARDANA ONU system architecture on the OSI network reference model.

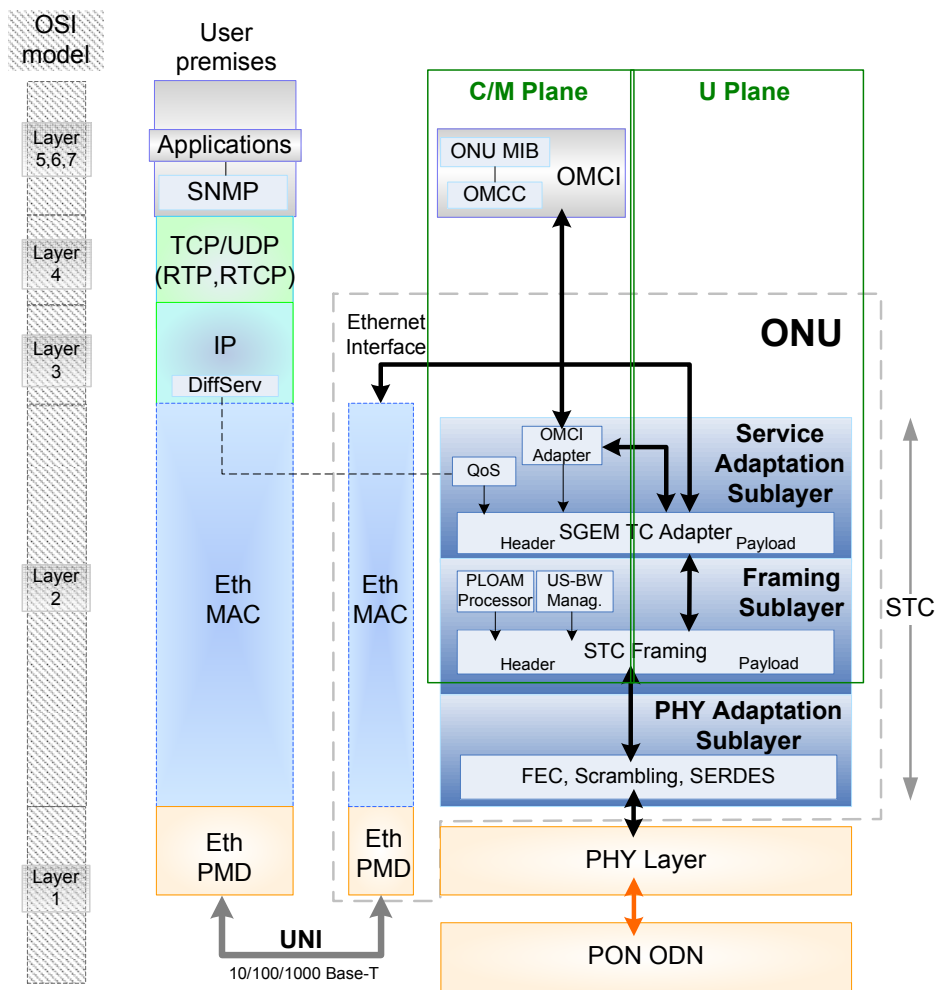


Fig. 5. 4 - SARDANA ONU system architecture on the OSI network reference model

Particular Ethernet SARDANA interface uses an UNI three-port 10/100/1000 Base-T for Ethernet connexion with the user's premises.

5.1.2.SARDANA Transmission Convergence (STC) Design

SARDANA TC layer specifies the formats and procedures of encapsulation from/to upper layer SDUs for its transport via the optical distribution network (ODN) and the ONUs' medium access control (MAC) in the PON.

SARDANA TC system is a mid-term upgrade of the GPON GTC in-line with the XG-PON protocol specification from FSAN participants, specifically XG-PON1 TC (XGTC) for compatibility reasons.

However, necessary modifications, adaptations and extensions are required to the new features of the SARDANA system, attending to:

- The increased service demands in NG-PON: PON long reach, more ONUs and more users per PON;
- Different ODN topologies: WDM ring and TDM tree linked, with aggregation and overlaying from/to GPON/EPON TDM trees by wavelength multiplexation, serving each multiplexed TDM network;
- Passive ODN long-reach (up to 100km), based on the use of passive remote nodes with EDF remote pumping with extra Raman amplification, generating extra power budget for covering extra longer distances;
- Cost-efficient implementation of the PHY Layer with improved performance and complexity reduction: ODN tree section with one fibre/one wavelength and colourless ONUs based on reflective SOAs;
- Network impairments from the downstream channel reuse in the upstream transmission (TDM section) and non-linear transmission impairments from remote pumping (WDM section),requiring new monitoring techniques of impairments;
- FEC techniques. It would provide also strong robustness to access networks;
- Support for multi-operator/multi-service feature. This is an important strategy to implement an open network infrastructure. It provides the capability of a customer to choose between several operators sharing the same external infrastructure. This functionality could be also possible from the Passive Remote Node advanced design, and can be implemented at different layers and with different techniques.

The management & control planes are structured in sub-layers for the processes of service adaptation (from/to higher layers), framing of the information to be transported and physical adaptation to optical transmission/reception. These processes are implemented by means of messages, added on the frame's header. User plane is implemented to data transport into STC payload.

Similar to XGTC, the frame formats are devised so that the frames and their elements are aligned to 4-byte word boundaries. Also, information is transported over the PON network into 125 us frames.

5.1.3.SARDANA TC Service Adaptation Sub-layer

This sub-layer is responsible of the encapsulation, multiplexation and delineation of the SDUs (Ethernet frames or other layer-2 protocols and OMCI information) into GEM frames adapted to SARDANA (SGEM). In the practice, the principal function of this sub-layer is to provide a well-defined service interface for the upper layers in order to send information at the destination on transparent fashion.

5.1.3.1. SARDANA GEM (SGEM) Frame basic functions

A new GEM is proposed for SARDANA, named SGEM. It protocol has two functions: to provide delineation of the user data frames and to provide the port identification for multiplexing. In downstream direction, continuous frames are transmitted from the OLT to the entire ONUs using the SGEM payload partition. In upstream direction, burst frames are transmitted from the ONUs to the OLT using the configured SGEM allocation time.

SGEM Frame structure

The SGEM is a variable-length framing mechanism that provides a transparent SDU encapsulation and connection-oriented transportation over the PON. The SGEM framing is identical in both the DS and the US.

SGEM consists of a header (fixed length) and a payload section (variable length), as shown in Fig. 5.5.

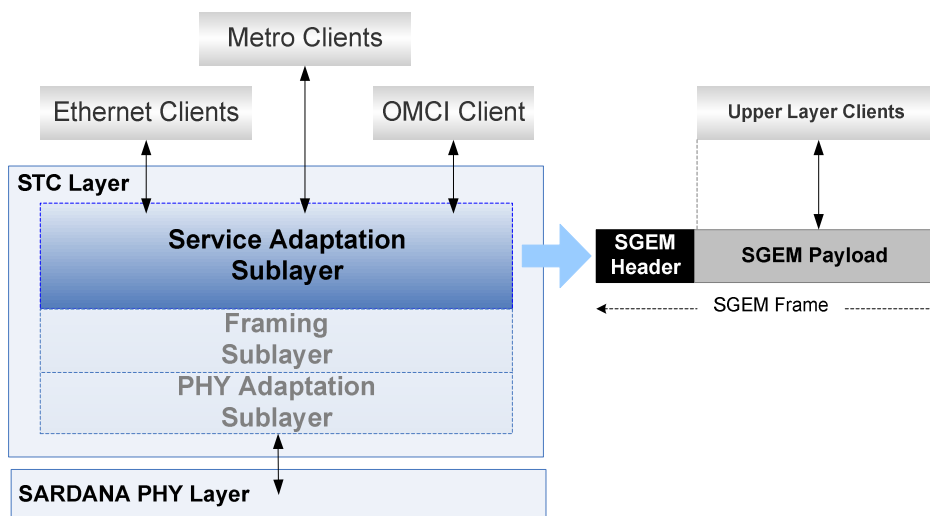


Fig. 5. 5 - Service Adaptation Sub-layer and SGEM framing

a) SGEM Header

SGEM header is extended up to 8 bytes with respect to GEM header (5 bytes), for compatibility with XG-PON, and new fields are incorporated. Fig. 5.6 shows GPON GEM frame [125] and the new formats for the 10 Gbit/s GEM frames from FSAN (XGEM) [97] and SARDANA (SGEM). To maintain co-existence with GPON and XGPON, some fields are similar:

- a) PLI (payload length indicator) field (14-bits).By extending respect to GPON GEM frame (PLI=12-bits, 4095 bytes), this can carry longer data unit from upper layer (up to 2^{14} =16k bytes of payload from the SGEM client).
- b) Key index field (2-bits). The indicator of the data encryption key is used to encrypt the XGEM payload. In SARDANA is also implemented.
- c) Port-ID field (16-bits). Extending the 12-bits in GPON, now can carry up to 64K unique traffic identifiers on the SARDANA PON to provide traffic multiplexing on a T-CONT. In the DS direction, each ONU filters the DS SGEM frames based on their SGEM Port-IDs and processes only the SGEM frames that belong to that ONU. In the US direction, within each bandwidth allocation, the ONU uses the XGEM Port-ID as a multiplexing key to identify the XGEM frames that belong to different US logical connections.
- d) Last Fragment field (1-bit). It is used to identify if the payload transported is a complete SDU (LF=1) or it is the last fragment of a SDU (LF=0).
- e) HEC (header error control) field (13-bit). This operates on the 63 initial bits of the header.

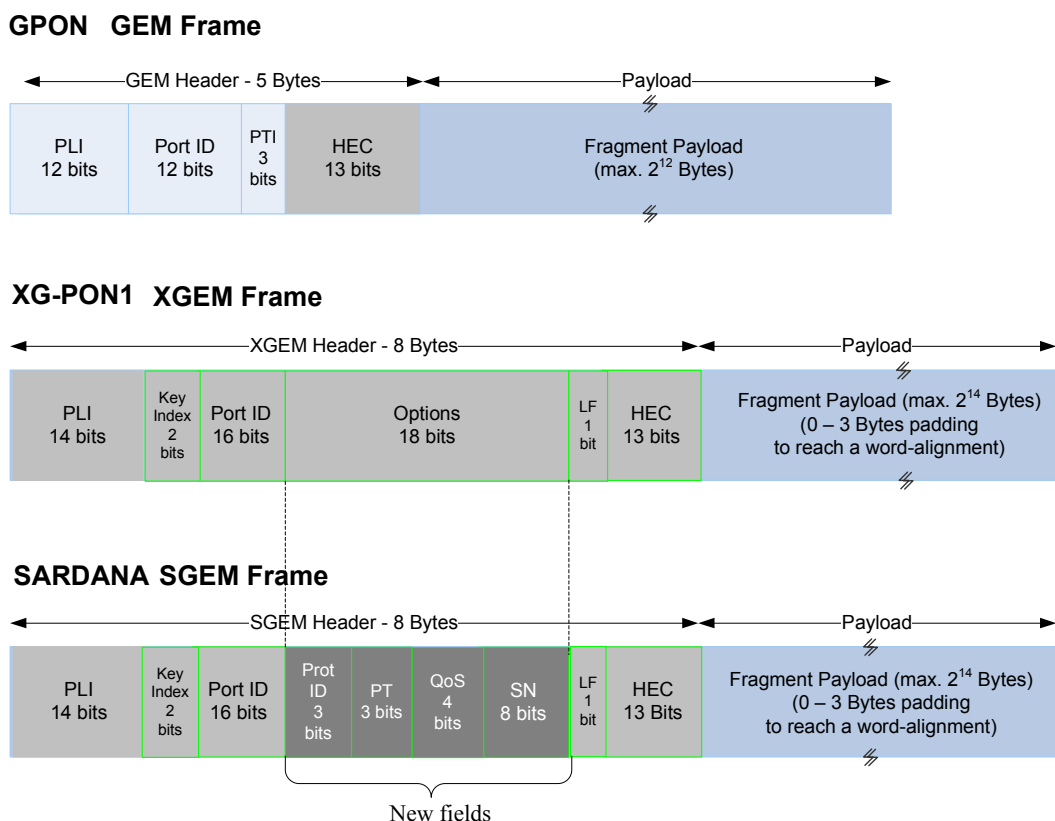


Fig. 5. 6 - GPON GEM frame and the new formats for the 10 Gbit/s GEM frames from FSAN and SARDANA. Different from XGEM, in SARDANA SGEM other fields are included to exploit their metro/access coverage and as a function of the PHY characteristics:

- f) Protocol ID field (3-bits). This field carry information of the protocols used in the upper layers, specially the identification of the protocols used on the metro network (Ethernet, MPLS, SDH/SONET, ATM, others) or transport network connected to SARDANA (GMPLS). Up to 8 protocol IDs could be identified. The field's implementation extends the service capabilities of a PON. It is important in SARDANA for:
- Multi-protocol management, by considering the PHY metro-access characteristics of the SARDANA.
 - Overlay capacity over SARDANA from different service providers working on metro/transport network protocols.
 - Control and management of multiple services (multi-services capability);
 - Control and management of the contents from different operators (multi-operator capability);
- g) PT (payload type) field (3-bits). PT indicates information of the following payload contents (Ethernet, OMCI, others). So, up to 8 different payload types can be differentiated.
- h) QoS (Quality-of Service) field (4-bits). This field would allow optimizing services as real-time transmissions, security, QoS and other higher layer services. Management of quality of services (QoS) for the applications carried between the Ethernet frames or from other link protocols;
- i) Sequence Number (SN) field (8-bits). This field would aid the better order of the packets received, considering the long reach nature of the SARDANA networks and the latency issues. With 8 bits up to 256 information sequences could be maintained.

These new fields give SARDANA TC capacities to deploy internetworking functions. The implementation of these new fields is described in detail in chapter 6.

b) SGEM payload

It transports the SDUs, which include the user data frames (encapsulates in Ethernet frames or other Layer 2 protocols) and high-level PON management frames (OMCI frames). So, the SGEM payload length depends on the length of the encapsulated SDU.

The SGEM payload variable-length field is expected to match the word boundary (to complete the 4-byte word). Adding padding bytes (0~3 bytes) at the end of payload is a possible way to meet the word boundary requirement. The length of actual payload as well as padding is indicated by the PLI field of the SGEM header.

5.1.4.SARDANA TC (STC)Framing Sub-layer

This sub-layer supports the functions of frame/burst encapsulation. The payload is based on one or more SGEM frames from the Service Adaptation sub-layer. The header includes messages of operations, administration and maintenance (OAM) and medium access control, as shown in Fig. 5.7. The SDU resultant is a structure near to 125 μ s (STC) similar by compatibility with XGTC frame.

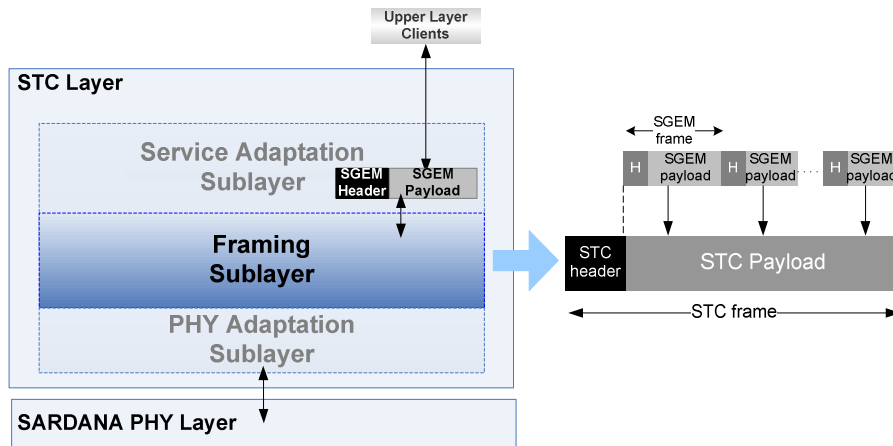


Fig. 5. 7 - Encapsulation process in the SARDANA framing sub-layer

5.1.4.1. SARDANA Downstream Frame

The DS frame length is extended into a word boundary (4-Bytes). It has the fixed size of 135432 bytes and consists of a header and a payload section. Extensions and similarities from the current GTC downstream frame structure (GPON) and the XTC downstream frame (XG-PON) are highlighted, as shown in Fig. 5.8.

a) STC frame header

The STC DS header consists of two variable size partitions: the bandwidth map partition (BWmap) and DS PLOAM (PLOAMd) partition, and four fields of fixed size. The OLT sends the header in a broadcast manner and every ONU receives and then acts upon the relevant information contained therein.

PLOAMd message in SARDANA

In SARDANA the PLOAMd message has a variable length (8, 16, 24 or 32-bytes) instead of a fixed length of 13 bytes (GPON) [125] or 48-bytes (XGPON) [97]. This allows releasing more space in the header to favour the payload section space. Of this way, PLOAM length increased efficiency per transmitted frame of between 1.5 and 6 times with respect to XG-PON can be reached. Also, a little and flexible PLOAMd allows a faster ONU initialization process in the system.

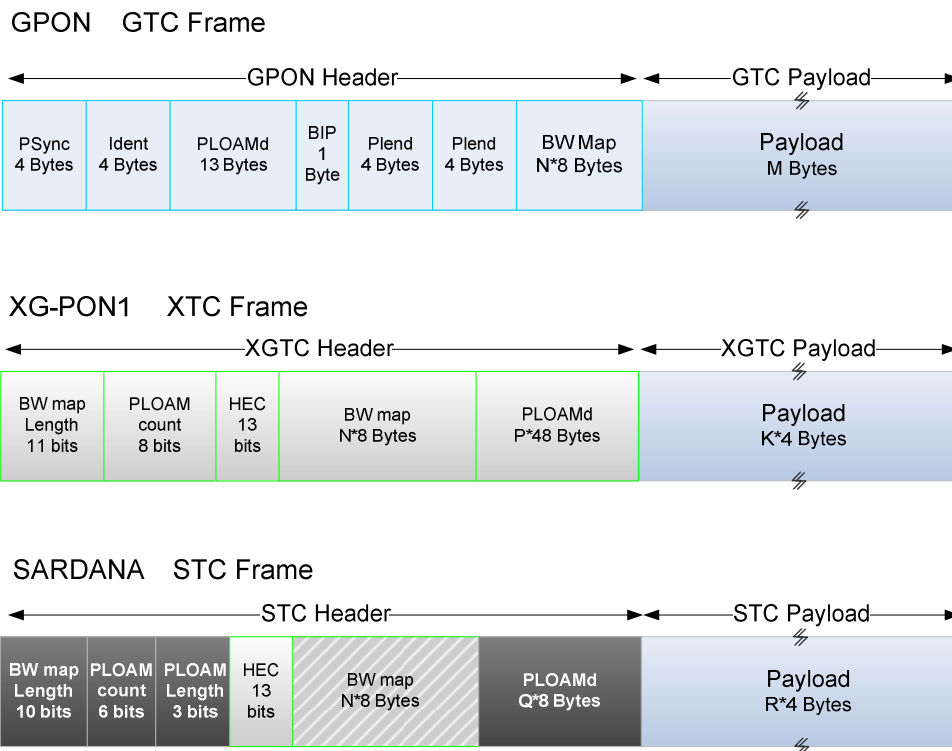


Fig. 5. 8 - Downstream frame header and changes respect to GPON and XGPON

A vector formed by two fields: PLOAM count (6-bits) and PLOAM length (3-bits) will be required to specify the number of PLOAMs and their respective lengths.

HEC field (13-bits) is an error detection and correction field for the BW map Length field and for the PLOAM count and PLOAM length structure. The SARDANA PLOAM message structure is shown in Table 5.1.

Table 5. 1 - PLOAM message structure

Byte	Field	Description
1-2	ONU-ID	It specifies the message recipient in the DS direction or the message sender in the US direction.
3	Message type ID	An 8-bit field that indicates the type of the message and defines the semantics of the message payload.
4	Sequence Number	An 8-bit field containing a sequence number counter that is used to ensure robustness of the PLOAM channel.
5-32	Message Content	In SARDANA is a variable field as a function of the message content. So, a PLOAM messages can reach 8, 16, 24 or 32-bytes

Bandwidth map (BWmap) in SARDANA

The STC BWmap is a series of 8-byte allocation structures, in part similar to XGTC [97]. The number of allocations is given in the BWmap length field. In STC, this field has 10-bits, allowing to 2^{10} Allocs-ID for future expansion. A description of the BWmap structure is shown in Fig. 5.9.

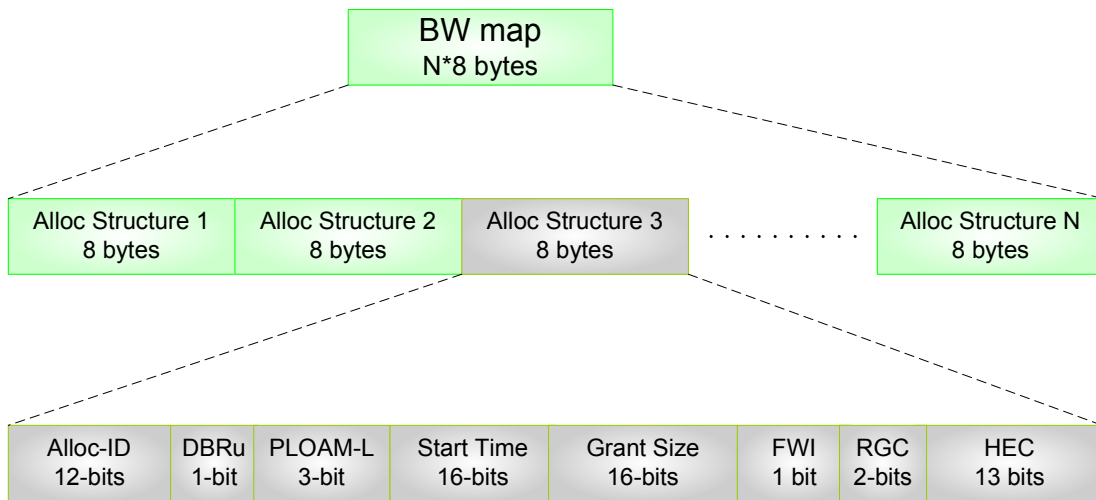


Fig. 5. 9 - BWmap structure in STC

- The *Alloc-ID* field (12-bits). It indicates the recipient of the bandwidth allocation (a T-CONT or an OMCC channel).
- The *DBRu* field (1-bit). If *DBRu*=1, ONU should send the *DBRu* report at the OLT for the given *Alloc-ID*.
- The *PLOAM-L* field (3-bits). The *PLOAM* length indicates at the ONU that should or not send a *PLOAMu* message (of variable length) as a part of the *XGTC* burst header. Table 5.2 shows the *PLOAMu* length options for this field.

Table 5. 2 – *PLOAM-L* field code

<i>PLOAM-L</i> field code	<i>PLOAMu</i> length (bytes)
000	Not <i>PLOAMu</i>
001	8
010	16
011	24
100	32
101	reserved
110	reserved
111	reserved

- The *StartTime* field (16-bits) indicates the location of the first byte of the US *XGTC* burst within the US PHY frame. It has a granularity of 1 word (4-bytes). The value of *StartTime* = 0 corresponds to the first word of the US PHY frame. The maximum *StartTime* value is 9719, and corresponds to the case where the last burst sent from an ONU is a Dynamic Bandwidth Report upstream (*DBRu*).
- The *GrantSize* field (16-bits) indicates the length of the STC payload (plus the *DBRu* overhead, when transmitted), and the STC header (does not include the STC trailer and the FEC overhead). Due to US rate is 2.48832 Gbps (and the US frame can carry 38880 bytes), the maximum allocation size

is 9720 words and the maximum burst size = 9720 words (in the case 1 unique ONU is occupying the entire US frame). Table 6 shows particular *GrantSize* values.

- FWI field (1-bit). This parameter allows OLT to be capable to control the transmission of the rONU. When FWI=1, RSOA switches from off-state to on-state, and is ready to send a burst.
- RGC field (2-bit). The RSOA Gain Control (RGC) field enables capacities to control the gain power in a RSOA, when a rONU implements a gain control circuitry. Up to 4-level of gain could be controlled.
- HEC field (13-bits), used for error detection and correction for the allocation structure.

In SARDANA, each BWmap partition may contain at most 1024 allocation structures (BWmap length=10 bits). In the practice, by design considerations, only a maximum of 512 allocation structures are considered (transmission time = 3.3us). Also, BWmap is sent before any possible PLOAM message and is structured in increasing order of start time. These facts allow ONU the maximum possible time in preparing a response.

The medium access control system of the OLT, based on DBRu and PLOAMu information (and a DBA algorithm), establishes the frequency and size of allocations to each ONU and each *Alloc-ID*.

b) STC Payload

The payload carries data information for all ONUs. Payload length is extended to a word boundary respect to GPON format. This is done by extending the GEM frame format R*4 bytes, as a XGTC payload.

5.1.4.2. SARDANA Upstream Frame

The upstream 125 us frame consists of multiple transmission bursts from different ONUs. The upstream burst from an ONU has a dynamically determined size and consists of a burst header and one or more bandwidth allocation intervals (according to the *BWmap* information), associated with a specific *Alloc-ID*.

a) STC burst header

During each allocation period, according to the OLT control, the ONU can transmit a 4-byte fixed or non-fixed header, by depending of the PLOAMu field presence. Fig. 5.10 shows the upstream burst structures in XGTC and SARDANA TC.

ONU-ID field (12-bit)

The value of this field is assigned to the ONU during the initialization process. The OLT can check this field to confirm that the correct ONU is transmitting.

PLOAMu field

Similar to downstream, PLOAMu message is extended into a word boundary and has variable length (8, 16, 24 or 32-bytes), or 0 bytes. The length is specified by the PLOAMu length sub-field into burst status field.

Burst Status field (7 bits)

SARDANA burst header incorporates *Burst Status field* as an indicator of the messages present into burst. This field will help the OLT to know if the burst carries DBRu structures and PLOAMu message and its respective length, allowing fast decodification of the burst payload.

- **PLOAMu length sub-field (3 bits):** It is an indicator of PLOAM message presence and its length into the burst header. This is shown in Table 5.3.
- **DBRu status sub-field (3 bits):** It is an indicator of allocation overhead for each of the Allocs-ID of the T-CONT buffers (if present). The 4-byte DBRu structure carries a buffer occupancy status report which is associated with a specific Alloc-ID. This is shown in Table 5.3.

Table 5. 3 – PLOAM status and DBRu status information code

	PLOAMuStatus
000	Not PLOAMu
001	8 bytes - PLOAMu
010	16 bytes - PLOAMu
011	24 bytes - PLOAMu
100	32 bytes - PLOAMu
101	reserved
110	reserved
111	reserved

	DBRuStatus
000	Alloc ID default - Not DBRu
001	Alloc ID default with DBRu
010	Alloc ID type 1 - Not DBRu
011	Alloc ID type 1 with DBRu
100	Alloc ID type 2 - Not DBRu
101	Alloc ID type 2 with DBRu
110	Alloc ID type 3 - Not DBRu
111	Alloc ID type 3 with DBRu

- **Dying Gasp (DG) flag (1 bit).** When DG=1, the ONU has detected a problem. This indication may assist the OLT in distinguishing ODN problems from premises issues. This field is similar with XG-PON.

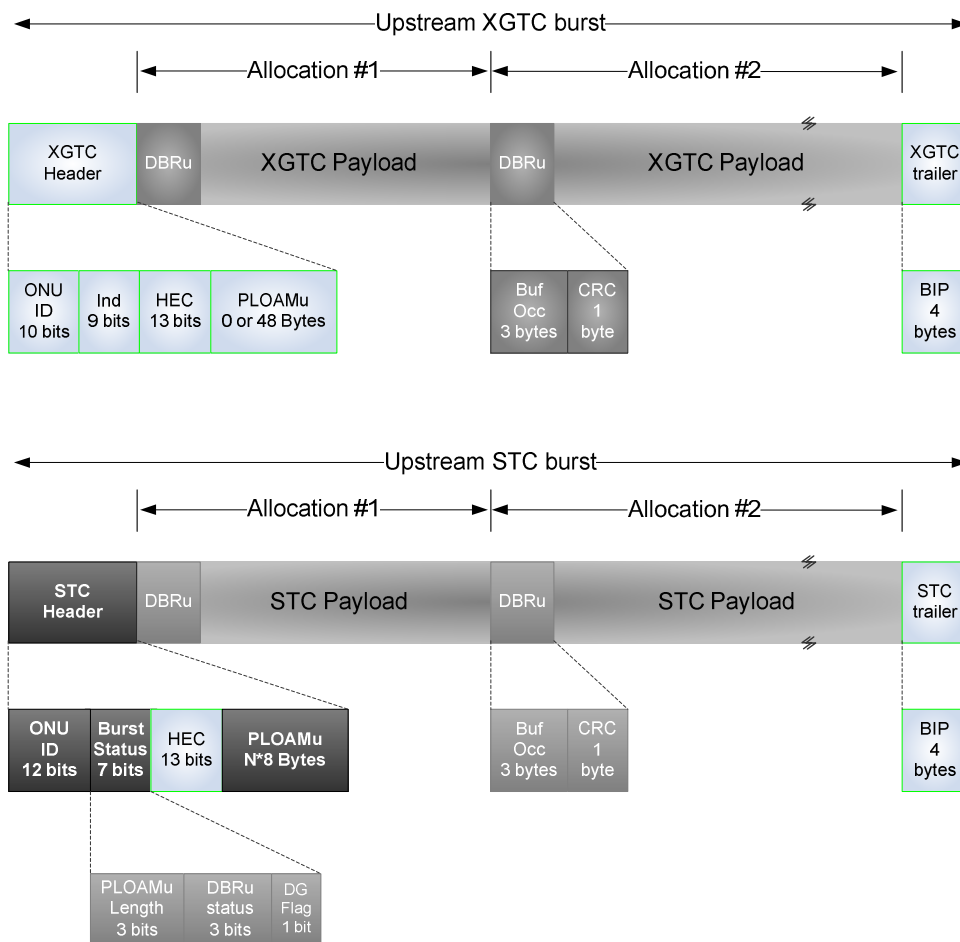


Fig. 5. 10 - Upstream burst structures in XGTC, and changes for SARDANA TC

DBRu field

The Dynamic Bandwidth Report upstream (DBRu) field sends traffic status to OLT in order to enable DBA computation. This structure can or cannot be present in the burst allocation. This is controlled by the OLT. It is formed by the Buffer Occupancy (BufOcc) (3 bytes) that contains the total amount of SDU traffic in the buffers associated with an Alloc-ID at the ONU; and a CRC-8(1 byte) for error detection into the DBRu.

b) Upstream STC burst Payload

The payload length is variable and it is extended to a word boundary, similar to downstream payload.

c) Upstream STC burst trailer

It contains a 4-byte wide bit-interleaved even parity (BIP) field computed over the entire STC burst. If FEC is turned-off, the OLT RX verifies the BIP to estimate the BER on the upstream optical link [97].

5.1.5.SARDANA TC - PHY Adaptation Sub-layer

This sub-layer is responsible for providing physical synchronization, FEC and scrambling for the DS and US transmission. In other words, it is in charge for preparing the STC frame for the PHY layer. Fig. 5.11 shows encapsulation process in the SARDANA PHY adaptation sub-layer.

NRZ (non-return-to-zero) Code and Scrambler

The scrambled NRZ line code is selected for application in both the upstream and downstream directions as XG-PON [97].

FEC

FEC support is mandatory for both OLT and ONU in the upstream/downstream directions. It is used to introduce redundancy in the transmitted data to detect and correct certain transmission errors. It is based on Reed-Solomon (RS) codes. In the downstream direction, the FEC code is RS (248,216). In the upstream direction, the FEC code is RS(248,232). FEC process is similar the XG-PON. An implementation detailed can be obtained in [97].

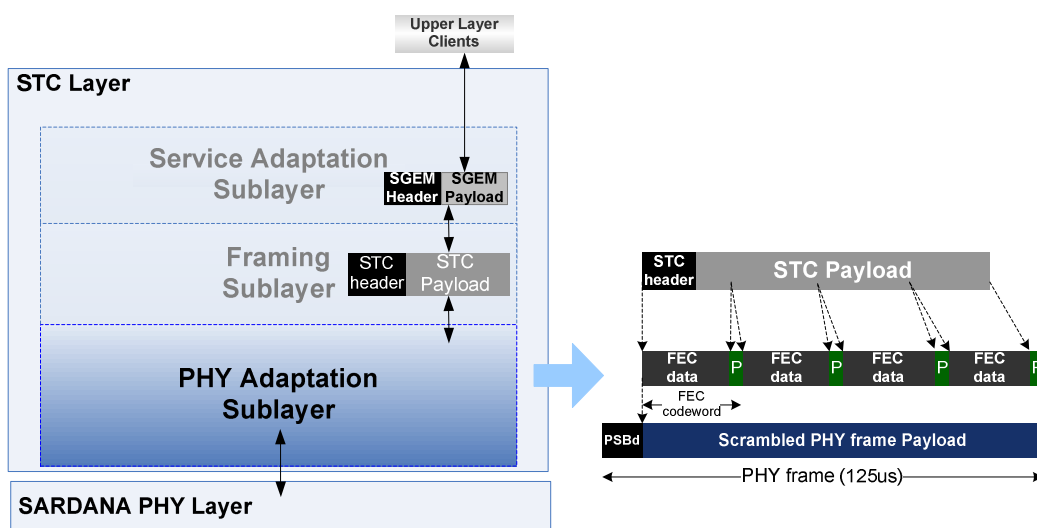


Fig. 5. 11 - Encapsulation process in the SARDANA PHY adaptation sub-layer

5.1.5.1. DS PHY frame

Downstream PHY frame duration is 125 us, which at the rate of 9.95328 Gbit/s corresponds to 155520 bytes. In SARDANA this structure is similar to XG-PON, as shown in Fig. 5.12.

It consists of a 24-byte physical synchronization block (PSBd) and a PHY frame payload protected by FEC and scrambled. Downstream PHY frame is broadcast sent for all ONUs in the PON.

Physical Synchronization Block (PSBd)

As a XG-PON frame, PSBd contains three separate 8-byte structures: PSync, SFC field and PON-ID field, as shown in Fig. 5.13.

PHY synchronization (PSync) contains a fixed 64-bit pattern (0xC5E5 1840 FD59 BB49), used by the ONU to achieve alignment with the OLT.

The Super frame counter (SFC), increments by one in each downstream PHY frame. It has a 51-bit super frame counter and a 13-bit HEC field.

The PON-ID structure is used in SARDANA to identify each PON tree (each PON corresponds with one wavelength), and is an important field for the internetworking functions and to establish different offsets on the systems (as a function of the maximum reach of a PON). It contains a 51-bit PON-ID and a 13-bit HEC field.

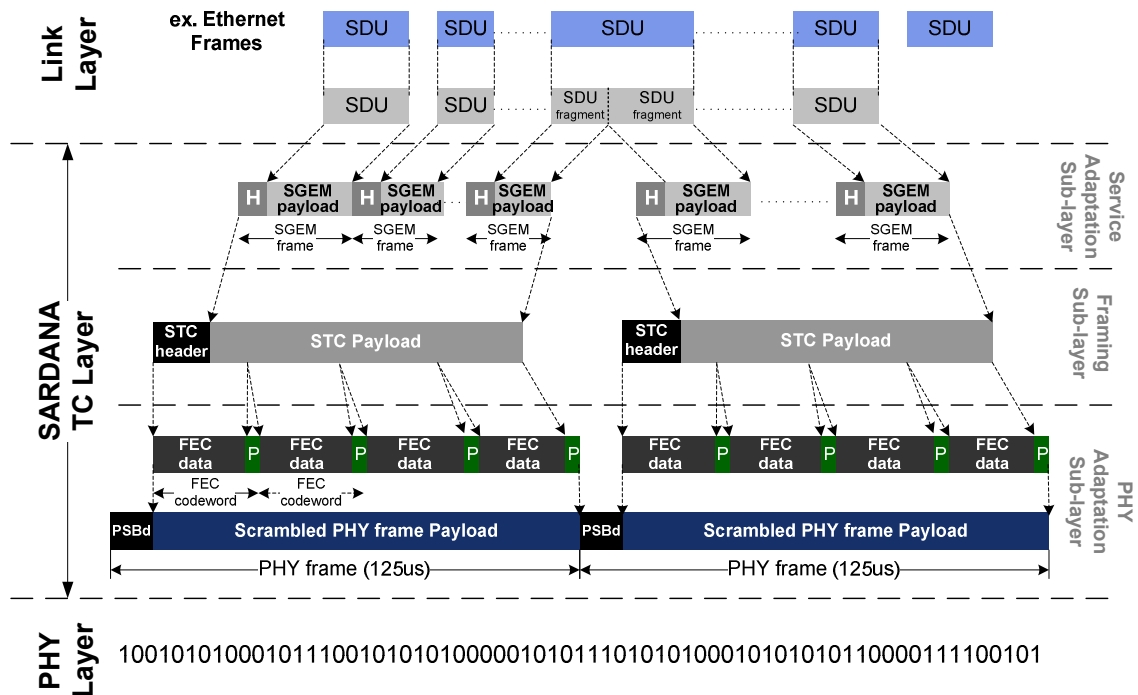


Fig. 5. 12 - Downstream PHY frame structure at the SARDANA TC layer

Downstream PHY frame payload

It is scrambling and has the size of 155496 bytes (135432 bytes of the XGTC frame plus 20064 parity bytes from FEC).

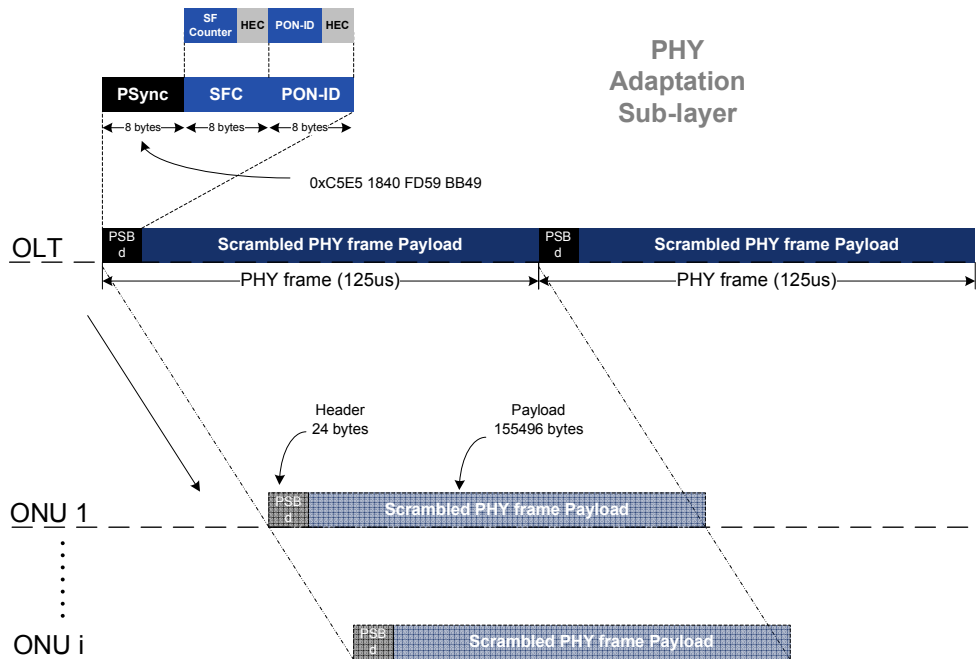


Fig. 5. 13 – Downstream PHY frame with payload and physical synchronization block (PSBd)

5.1.5.2. US PHY burst

Each ONU transmits PHY bursts in the corresponding allocation time and remains idle in-between the bursts. It consists of an upstream physical synchronization block (PSBu) and a PHY burst payload (XGTC burst + FEC + scrambled). Burst timing and duration is controlled by the OLT by means of BWmap. Fig. 5.14 shows US PHY burst from ONUs as contributions into the US PHY frame, and the fields that form the US Physical Synchronization Block (PSBu).

Upstream PHY burst payload

It is achieved from the US XGTC burst, applying FEC and scrambling the result obtained.

Upstream Physical Synchronization Block (PSBu)

It contains Preamble and Delimiter fields that allow the OLT to delineate burst and to adjust to the level and the synchronization of the optical signal. The length and pattern of preamble and delimiter is fixed in SARDANA and is shown in Fig. 5.15.

Preamble and Delimiter bytes mark the start of burst transmission from the ONU. The length of the field increases with higher transmission rate to facilitate clock recovery and frame synchronization in a multi-clock environment.

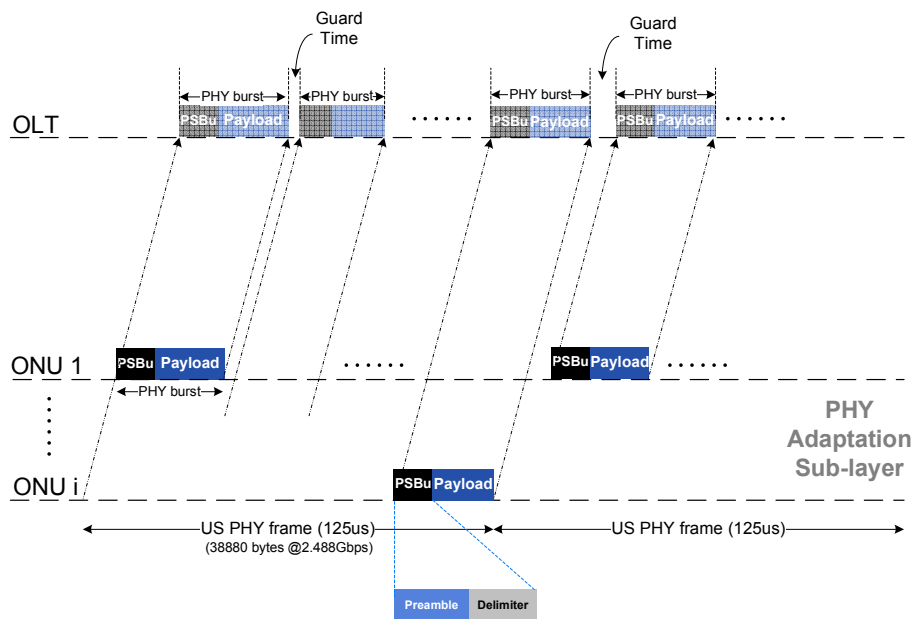


Fig. 5. 14 – Upstream PHY frame and PHY bursts

In SARDANA this overhead time is used to:

- Synchronize RSOA TX on/off time,
- Added timing drift tolerance,
- Signal amplitude recovery,
- Signal phase recovery (clock recovery),
- Start of burst delimitation.

Fig. 5.15 shows the PSBu in SARDANA. The time to each process is determined by experimental considerations, some based on constraint equations.

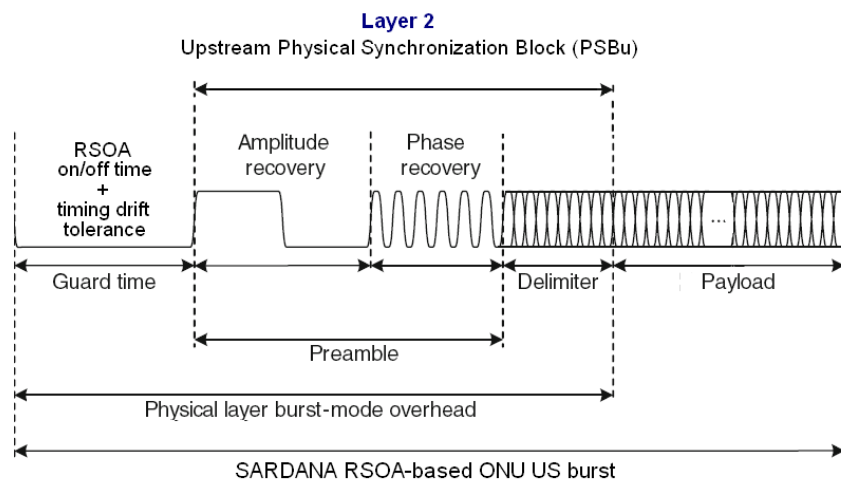


Fig. 5. 15 – Guard Time, Preamble and Delimiter structure in SARDANA networks

Guard Time

Although not part of PSBu, BWmap allows suitable guard time between US bursts from different ONUs to prevent collisions. It fits the RSOA Tx enable/RSOA Tx disable times and includes the margin for the

individual ONU transmission drift. The minimum guard time in XGPON is 64 bits (20 km standard reach) [97]. The constraint equations with which the OLT must comply are [168]:

$$\begin{aligned} t_g > t_{\text{RSOAon}} + t_u, \quad \text{and} \\ t_g > t_{\text{RSOAoff}} + t_u, \quad \dots(5.1) \end{aligned}$$

So, two processes, RSOA TX on/off time and timing drift tolerance (t_u), are considered in the guard time (t_g). In this time the ONU will transmit no more power than the nominal zero level.

The timing drift tolerance is a timing uncertainty. This uncertainty arises from variations of the time caused by fibre and component variations with temperature and other environmental factors. In SARDANA, due to the long distances considered (in the range of 100 km using SSMF), the operation wavelength (third window) and the high speed of 10Gbps, the chromatic dispersion impact on the pulse broadening and consequently, inter-symbolic interference (ISI) can occur.

By considering t_u basically as pulse broadening and the chromatic dispersion for 1550nm $D_{1550}=17\text{ps} / (\text{nm}\cdot\text{km})$ and $\Delta\lambda$ the spectral width of the emitter, hence:

$$t_u = D_{1550} \cdot L_{\text{max}} \cdot \Delta\lambda$$

For $\Delta\lambda=0.2\text{nm}$, the spectral width of a RSOA and a DFB laser, and for a maximum fibre length 100 km then $t_u = 0.34 \text{ ns}$.

RSOA response time

Considering a typical RSOA with commercial parameter values: $L_{\text{cavity}}=600 \mu\text{m}$ (cavity length) and $G=21\text{dB}$ (RSOA gain), as used in SARDANA. Then, phase shifting at the ONU output in $t=t_{\text{RSOAon}}$, as shown in Fig. 5.16, is:

$$\Delta t = \frac{2 \cdot L_{\text{cavity}}}{V_g}$$

with $V_g = \text{group velocity} = c/n$

- Considering the RSOA cavity as a silica SiO_2 optical medium ($n=1.5$), then $\Delta t = 6\text{ps}$.
- Considering the RSOA cavity like a laser cavity $\rightarrow n=3.6$ (refraction index for laser), then $\Delta t = 14.5 \text{ ps}$.

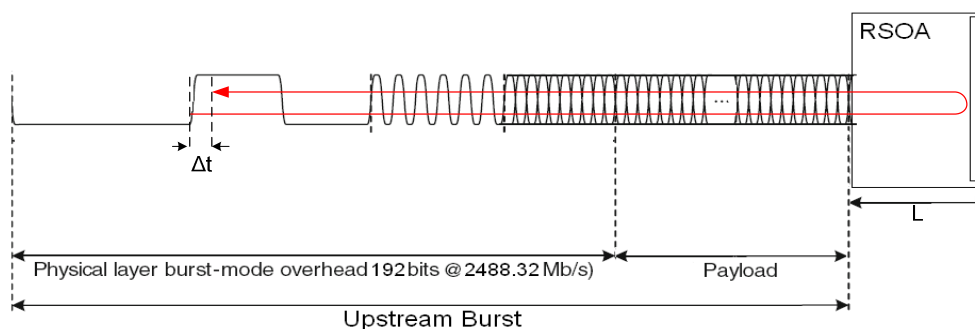


Fig. 5. 16 – Phase shifting between DS Signal and US signal reflected

Then, RSOA device response time can be considered negligible. Now, considering RSOA initialization from the off-state and additional delays due to associated circuitry, $t_{RSOAon} \approx 10$ ns. This value was obtained in practical measures as shown in Fig. 5.17.

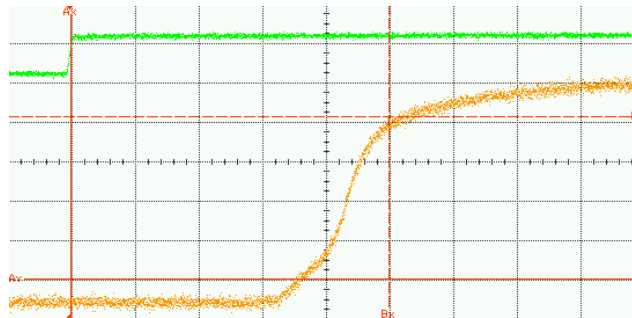


Fig. 5. 17 - RSOA response time: initialization and additional delays due to associated circuitry ($t_{RSOAon} \approx 10$ ns, in 2ns/div).

Then, $t_{RSOAon} = t_{RSOAoff} = 10$ ns. From (1), the minimum guard time is $2 \cdot t_g$

With $t_g > 10$ ns + 0.34 ns = 10.34 ns

For an US bit rate 2.48832 Gbps, this corresponds to $t_g(\text{bits}) > 25.8$ bits.

By incrementing the reliability above 50%, hence $t_g(\text{bits}) = 40$ bits.

Finally, SARDANA Guard Time is fixed in 80 bits

Preamble time

During the preamble time (t_p), the RSOA-based ONU will transmit a preamble pattern that provides maximal transition density for amplitude recovery and clock recovery functions. In SARDANA, the signal level is recovered, in the first 32 bits, using controlled runs of identical digits (16 bits “1” and 16 bits “0”). In this way the decision threshold is fixed. The signal clock phase is recovered using a maximum transition density pattern in the last 128 bits of the preamble.

Finally, the 160-bit SARDANA pattern preamble is 0xFFFF0000AAAA.....AA.

Delimiter time

During the delimiter time (t_d), the ONU will transmit a special data pattern with optimal autocorrelation properties that enable the OLT to find the beginning of the burst. A simple relationship between the number of bits in the delimiter (N) and the number of bit errors tolerated (E) is [125]:

$$E = \text{int}(N/4) - 1 \quad \dots\dots(5.2)$$

Given a BER, the probability of a severely errored burst (P_{seb}) is given by [125]:

$$P_{seb} = \left(\frac{N}{E + 1} \right) \cdot BER^{E+1} \quad \dots\dots(5.3)$$

Substituting (5.2) in (5.3):

$$P_{seb} = \left(\frac{N}{\text{int}\left(\frac{N}{4}\right)} \right) \cdot BER^{\text{int}\left(\frac{N}{4}\right)}$$

Table 5.4 shows some values of delimiter lengths and their Probability of a severely errored burst for a BER=1.0E-4.

Table 5. 4 - Probability of a severely errored burst as a function of delimiter length [125]

Delimiter Length (N)	Probability of a severely errored burst (P_{seb})
16	1.8E-13
32	1.1E-25
64	4.9E-50

With these considerations, the recommended allocations for the SARDANA PSBu are given in Table 5.5.

Table 5. 5 - Burst mode overhead time recommended allocation for OLT functions

Upstream data rate 2.48832(Gbit/s)	RSOA Tx enable ($t_{\text{RSOAon}}+t_u$)	RSOA Tx disable ($t_{\text{RSOAoff}}+t_u$)	Guard time (t_g)	Preamble time (t_p)	Delimiter time (t_d)	Total time (t_T)
bits	40	40	80	160	32	272
Time (ns)			32.15	64.3	12.86	109.3
	Maximum	Maximum	Minimum	Suggested	Suggested	Suggested

So, a PSBu with Preamble and Delimiter fields of 192 bits (77.16 ns) plus a Guard Time of 80 bits (32.15 ns) are consistent with the SARDANA PHY layer. Fig. 5.18 shows the SARDANA PON OLT receiver timing signalling from the Table 5.5 values.

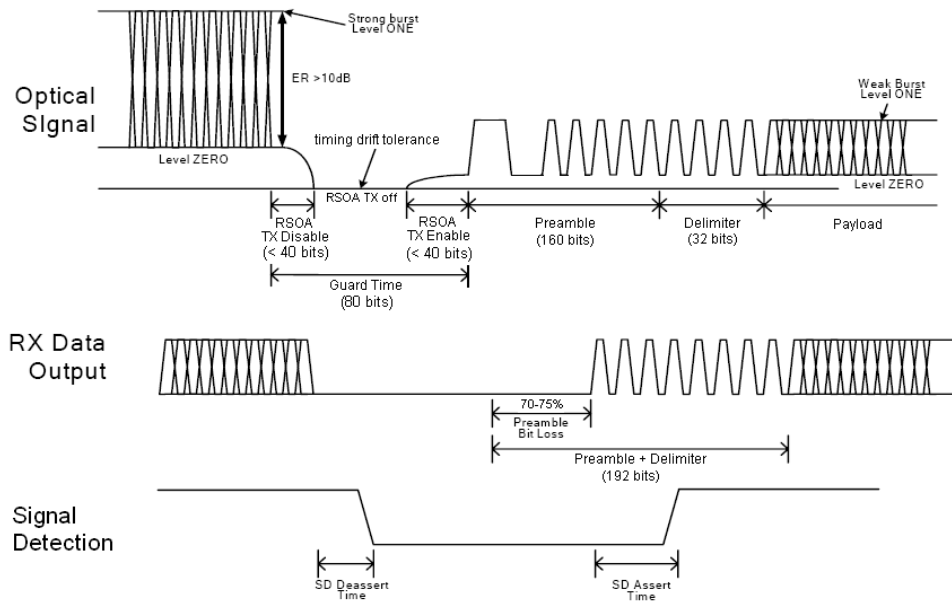


Fig. 5. 18 – SARDANA Upstream Physical Synchronization Block (PSBu) definition values and OLT Receiver Timing setup (adapted from [150])

From Fig. 5.18, it is possible at the OLT receiver a preamble bit loss of 70-75% due to adjust in the RSOA initialization processes. Fig. 5.19 shows an US burst test with a PSBu of 128 ns that we obtained in our lab.

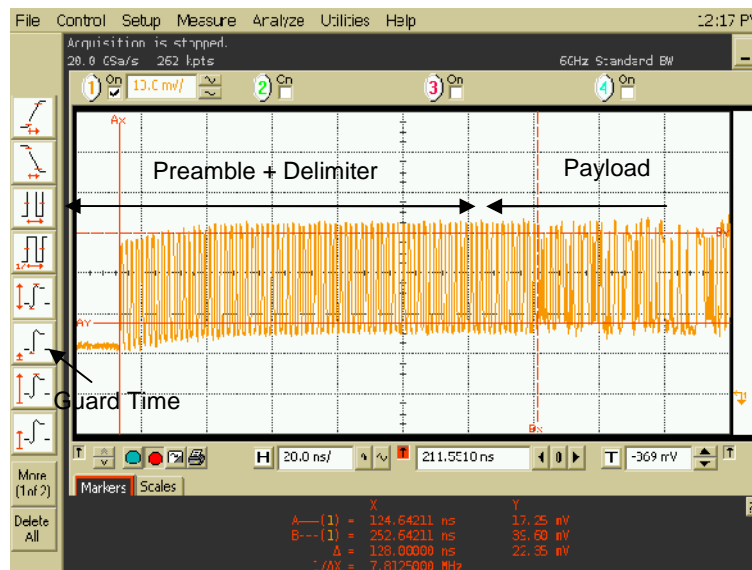


Fig. 5. 19 – US Burst with a PSBu of 128 ns

Upstream Burst Size – Minimum and Maximum values

ONU burst allocation for upstream transmission is defined from the OLT and is indicated on the Grant Size field of the BWmap (in the DS frame header). Minimum and maximum size values for the burst of an US transmission are shown in Table 5.6.

Table 5. 6 - Minimum and Maximum Size values for the burst of an US transmission

BWmap Grant Size	Length	bytes	time
0	Only PLOAM* (not payload)	16	~ 51 ns
1	Only DBRu (not payload)	4	~13ns
4	Payload minimum	16	~ 51ns
9720	Payload maximum	38880	125 us

*It is used in the ONU activation process (in response to SN grants)

5.2.SARDANA Media Access Control Processes

In the downstream direction, the traffic multiplexing functionality is centralized. The OLT multiplexes SGEM frames onto the transmission medium using SGEM Port-ID as a key to identify the ONU target. Each ONU filters the downstream SGEM frames, based on their SGEM Port-IDs, to obtain the information that was addressed towards that ONU.

In the upstream direction, the traffic multiplexing functionality is distributed. The OLT provides media access control for the upstream traffic. Each DS PHY frame (125 us) contains a bandwidth map (BWmap) that specifies a sequence of non-overlapping upstream transmissions by different ONUs in the corresponding US PHY frame.

Each burst contains a start pointer indicating the beginning of the burst within the US PHY frame and a sequence of grant sizes that the ONU is allowed to transmit.

So, the OLT grants allocations to the traffic-bearing entities within the ONUs that are identified by their allocation IDs (Alloc-IDs). Bandwidth allocations to different Alloc-IDs are multiplexed in time. Within each allocation, the ONU uses the SGEM Port-ID to identify the SGEM frames that belong to different upstream logical connections.

The OLT (using the PLOAM channel) assigns an ONU-ID, an identifier to an ONU during its activation. Each ONU is assigned one or more Alloc_IDs. The ONU's default Alloc-ID is implicitly assigned with and is equal to the ONU-ID. Fig. 5.20 shows the bandwidth map allocation for two ONUs and the process of alignment into the US PHY frame.

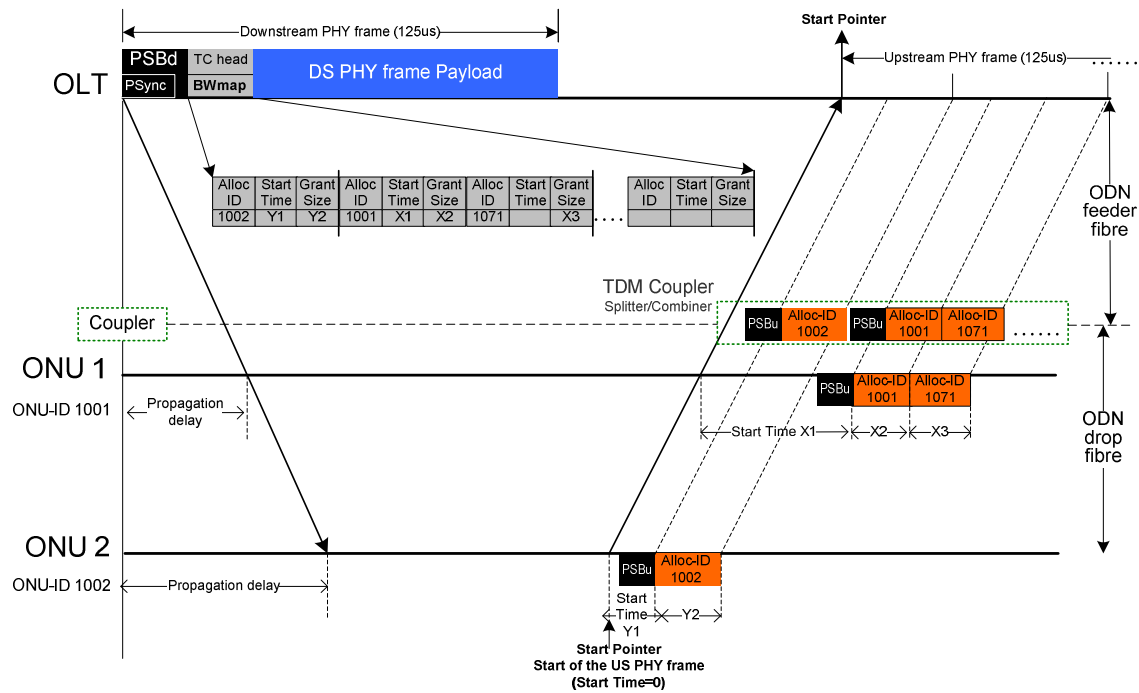


Fig. 5. 20 - Media access control based on bandwidth map allocation for two ONUs

Each DS PHY frame reaches different ONUs at generally different time instants. So, US transmission from different ONUs needs to be equalized. The ranging serve to align the ONU US burst transmissions on such a way that it reaches the OLT at precisely the same instant that other ONUs US transmission.

5.2.1. Timing relationships OLT-ONU in SARDANA network

During the initialization processes from a new ONU, the OLT must temporarily suppress upstream transmission by the in-service ONUs to avoid collisions, because OLT does not yet know the equalization delay for this new ONU. This time interval is referred to as a quiet window.

Quiet window (QW)

Frequently, the OLT opens a QW for ONU discovery (250 – 450us in XGPON). OLT, by means of a serial number grant, invites any ONU onto the PON that has not been activated to connect to the network. The OLT creates a quiet window halting the ONUs using either zero pointers allocation structures, or no allocations at all. The ONUs in “operation state” will stop sending data in the upstream direction as long as the “halt requests” are received. QW must span the time between the earliest ONU response and the latest possible ONU response.

In XG-PON are used two quiet windows (to implement Serial Number (SN) grant and Ranging grant processes). Due to XG-PON normal coverage is 20 km (max. 40 km), this procedure is not very critical. In contrast, the SARDANA network was designed to a coverage \approx 100 km, and then a method more efficient will be necessary.

5.2.2.RSOA-based ONU Starting, Initialization and Registration

In SARDANA network, ONU starting, initialization and registration is conditioned by the particular characteristics of its PHY layer.

The OLT controls the ONU activation process by means of bandwidth grants and exchanging PLOAM messages. To support the activation procedure, the ONU maintains two timers: Ranging timer (T_r) and Loss of Synchronism timer (T_s).

Timer T_r is used to abort an unsuccessful activation attempt by limiting the time in the Ranging process. Initial value of T_r is 10 seconds [97].

Timer T_s is used to assert a failure to recover from an intermittent loss of synchronism condition by limiting the time an ONU in the Failure Process. The initial value is 100 ms [97].

In the ONU activation process, timing relations and messages exchanged between OLT and RSOA-based ONU are defined in only 3 processes, as shown in the activation processes flow (Fig. 5.22).

(1) ONU starting Process

Initially, when an ONU is active, APD RX is active and the RSOA TX is not active. The OLT is transmitting valid downstream frames. The ONU starts operation by listening these DS transmissions and from the Hunt state searches for the PSync pattern and Super Frame Counter (SFC) structure in the PSBd header by using a local state machine, as shown in Fig. 5.21.

In SARDANA, if for 2 consecutive PSBd's either PSync or SFC verification fails; the ONU declares loss of downstream synchronization and returns the Hunt state.

Once two consecutive frames with a valid PSync and SFC are attained, the ONU moves to next process (2).

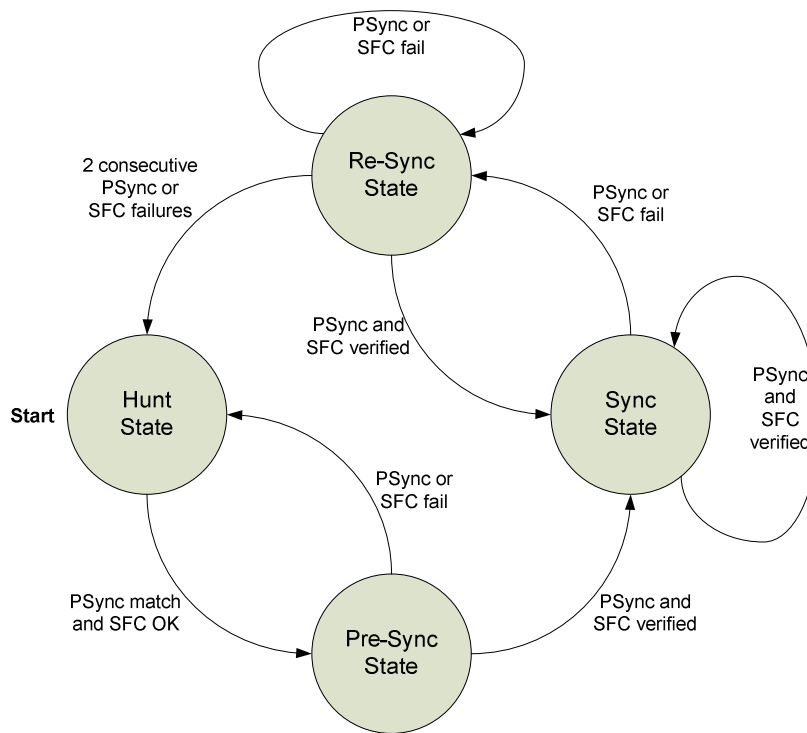


Fig. 5. 21 – ONU synchronization state machine (modified from G.987.3_F10.3).

(2) ONU Parameter Initialization and Ranging Process

Different from XGPON, in SARDANA the Initialization and Ranging Process are done in the same process, in order to optimize the use of the quiet window.

The ONU activates its RSOA TX for burst mode according to the OLT control. The ONU listens to the Profile PLOAM messages (periodically used by the OLT). If the ONU receives a serial number grant (addressed to the broadcast Alloc-ID) with a known burst profile, it responds with a Serial_Number_ONU PLOAM message. So, the OLT discovers the serial number of this new ONU.

During this PLOAMd grant (DS) and PLOAMu acquisition (US), the OLT measures the ONU round trip delay (RTD), computes the equalization delay (EqD) and sends a Ranging_Time message at the ONU. In this process, a quiet window time, established from the OLT, must suspend US TX from the ONUs in-service to avoid collisions between these ONUs and the new ONU in activation process.

SARDANA incorporates the Ranging process together with the Parameter Initialization process by reducing the number of Quiet Window needed to only one, optimizing, thus, network time consumption and operation time of all ONUs in-service of the PON during the activation process of a new ONU.

The OLT sends an *Assign_ONU-ID* PLOAM message to the ONU. The ONU sets the ONU-ID along with the default Alloc-ID and OMCC XGEM Port-ID. Also, the ONU adjusts the start of its upstream PHY frame clock, based on its assigned equalization delay.

Finally, the new ONU transitions to the Operation process (3).

(3) Operation Process

The ONU transmits upstream data and PLOAM messages as directed by the OLT. Once the network is ranged, and all ONUs are working with their correct equalization delays, all upstream bursts will be synchronized in its correct location within the upstream PHY frame. The first burst transmitted from the new ONU must contain the Registration PLOAM message.

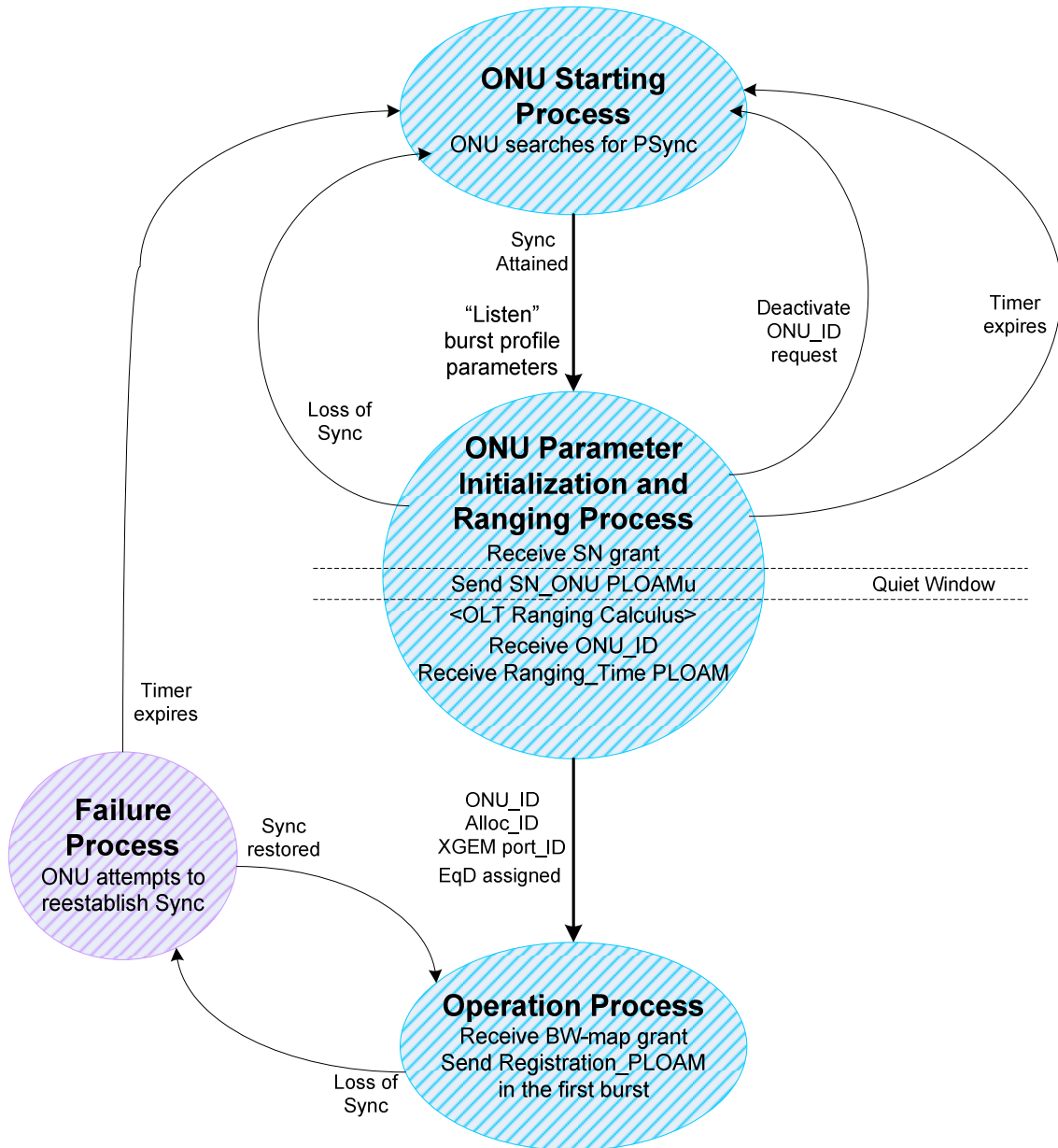


Fig. 5. 22 – ONU Activation processes flow

Failure Process

The ONU enters in this process from the loss of downstream synchronization and the ONU starts loss of synchronization timer (Ts). If the DS signal is re-acquired before Ts expires, the ONU transitions back into the operation process (3), otherwise, the ONU moves to ONU starting process (1).

The OLT monitors the phase and BER of the ONUs in regular operation. Based on the phase information, the OLT may re-compute and update the equalization delay for any ONU.

5.2.3.RSOA-based ONU upstream transmission timing

The round-trip delay (RTD) is the time interval between a DS PHY frame and the reception of the US PHY burst from the ONU earliest. The RTD is composed of the round-trip propagation delay (as a function of the length fibre between OLT-ONU) and the ONU response time. In order to align the burst on the US PHY frame by avoiding collision from other ONUs, an ONU has to delay the transmission beyond its regular response time. This delay is named as ONU equalization delay (EqD).

The start of the DS PHY frame with the BWmap is the reference for all the ONU transmission (and does not the receipt of the corresponding burst allocation itself). The ONU maintains synchronization with the DS PHY frame clock and offset, given by the sum of the ONU response time and the requisite delay. This is shown in Fig. 5.23.

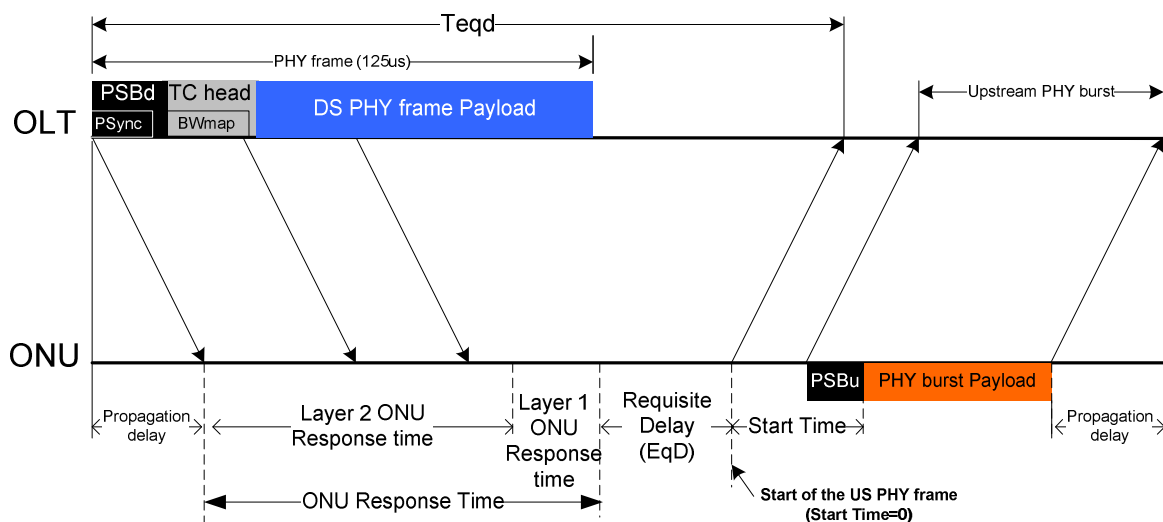


Fig. 5. 23 - ONU transmission timing diagram

a) ONU response time

ONU response time is obtained from the response time of the Layer 2 processes and Layer 1 devices processing.

SARDANA Layer 2 ONU response time

The ONU should be sufficient time to receive the DS frame, perform DS and US FEC and prepare an upstream response. All ONUs are required to have an ONU response time of $35 \pm 1 \mu s$ [97].

SARDANA Layer 1 ONU response time

As demonstrated in section 5.1.5.2, by considering a typical RSOA like a laser cavity ($n=3.6$), then a device response $\Delta t = 14.5$ ps can be expected. With an associated circuitry the response time of the PHY layer can be estimated on $t_{\text{RSOAon}} = t_{\text{RSOAoff}} = 10$ ns. Then, the PHY layer response time is considered negligible compared with the response time due to processing of the Layer 2.

b) ONU's Equalization Delay (EqD)

It is the total extra delays that may be required to apply to the US transmission beyond its response time to compensate for variation of propagation of individual ONUs, in order to avoid the probability of collision with other ONUs.

The upstream data, received at the OLT receiver, is based on the sum of all ONUs transmitted data. To avoid possible collisions, a transmission within the upstream frame is assigned to each ONU, where only this specific ONU is allowed to send data. In addition, all ONUs must appear equidistant from the OLT for upstream framing, i.e., the beginning of all upstream frames from all ONUs should reach the OLT at the same time. In order to achieve this, an Equalization-Delay (EqD) is assigned to each ONU. The ONU delays the upstream phase, in reference to the downstream phase, based on the assigned EqD value.

Once the OLT has supplied each ONU with its EqD value, it is considered synchronized to the beginning of the upstream PHY frame. The US burst is transmitted within the allocation structure specified with respect to the beginning of this upstream PHY frame.

5.1.1. Timing during ONU Serial Number Acquisition and Ranging

Due to the process of the Serial Number (SN) grant and the PLOAM ONU response, it is also possible to compute the ranging. Then, the EqD can be done by using a unique quiet window. So, a less intrusive QW process is implemented. Also, when the ONU is in the Operation state, the OLT may use any grant to this ONU to perform in-service round-trip delay measurement and equalization delay adjustment [97].

a) Serial Number Acquisition process

Although SARDANA ODN maximal distance is $L_{\text{min}} + D_{\text{max}} \approx 100$ km, the calculation to avoid collision between ONUs is basically done over the maximum differential range, due to temporal TDMA process is delimited at the drop section. By following the standard [97], ONUs maximum differential is 20 km. This is shown in Fig. 5.24.

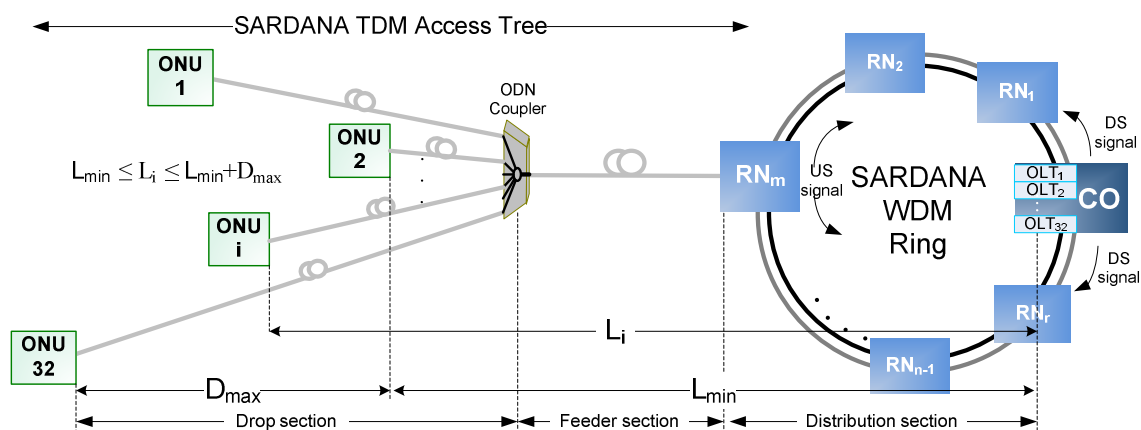


Fig. 5. 24 - SARDANA ODN maximal distance: $L_{min} + D_{max} \approx 100$ km

It is assumed that OLT use discovered Serial_Number method and pre-assigned equalization delay is 0. Since the SN grant is a broadcast BW allocation addressed to all ONUs, other ONUs, also in initialization process, may respond to it, and a collision may occur. So, to reduce the probability of collision between news ONUs the requisite delay in the SN process is a locally-generated random delay.

In SARDANA, the Serial_Number_ONU PLOAMu message is 16 bytes (in XGPON is 48 Bytes), as shown in Table 5.7.

Table 5. 7 - Serial_Number_ONU PLOAMu message

Octet	Content	Description
1-2	0x03FF	Unassigned ONU-ID
3	0x01	Message type ID "Serial_number_ONU"
4	0x00	Sequence number
5-8	Vendor_ID	Code set for the Vendor_ID
9-12	VSSN	Vendor-specific serial number
13-16	Random delay	Random delay used by the ONU when sending this message in bit times.

Considering worst case (64 ONUs trying reconnection at the same time), SN PLOAM burst response from an ONU would need a time slot of ~155ns to avoid collisions with other ONUs, as shown in Table 5.8.

Table 5. 8 - SN PLOAM burst response time from an ONU

Fields	Length (bytes)	Time (ns)
PSBu	32	~ 103
PLOAMu	16	~ 52
total	48	~155

By incrementing this margins to 0.2 us for higher reliability, then in a PON with 32 ONUs, this random delay can be between 0 and 6.4 us. The Timing during ONU Serial Number Acquisition is shown in Fig. 5.25.

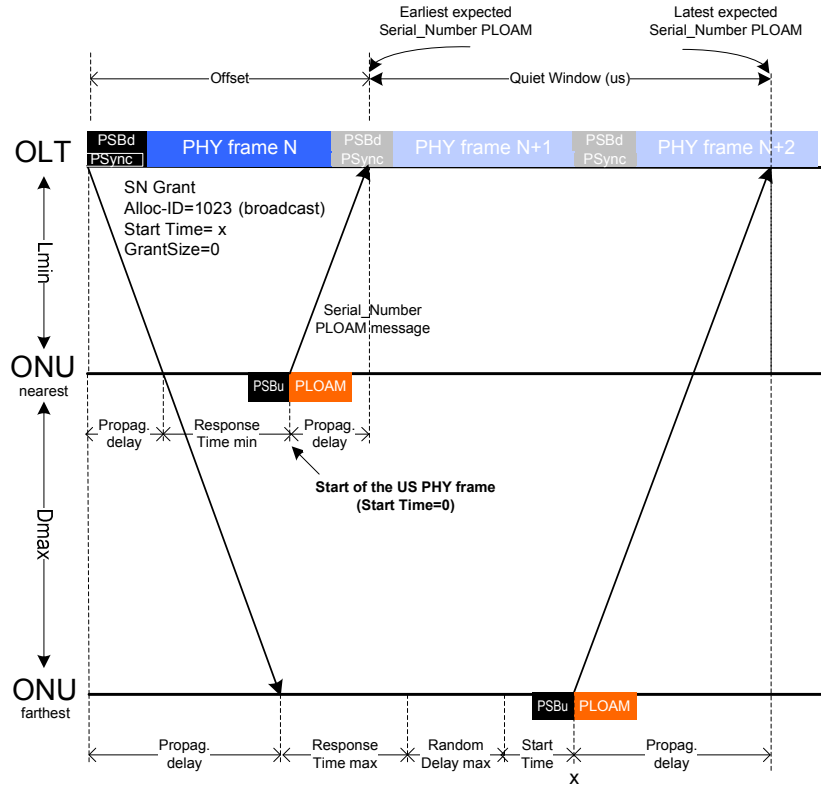


Fig. 5. 25 - Timing during ONU Serial Number Acquisition

In this stage, the OLT starts a Quiet Window process, stopping traffic of the ONUs in service. The offset of the quiet window is determined by the minimum delays in the system: the minimum round-trip propagation delay (RTD_{min}) by considering the nearest ONU expected on the PON (L_{min}), the minimum ONU processing time, and the dynamically generated StartTime value of the serial number grant [97]:

$$QW_{offset} \geq ONURspTime_{min} + RTD_{min} + StartTime \quad \dots\dots(5.4)$$

$$RTD_{min} = 2 \cdot L_{min} \cdot \left(\frac{n_{1552.2}}{c}\right)$$

The Quiet window size during SN acquisition is settled by the maximum variation of the unknown round-trip delay components (round-trip propagation delay, ONU response time, and ONU random delay) and the SN response burst time (preamble, delimiter, PLOAM message):

$$QW_{time} = ONURspTime_{var} + 2 \cdot D_{max} \cdot \left(\frac{n_{1552.2}}{c}\right) + Rand_{max} + T_{burst} \quad \dots\dots(5.5)$$

b) SARDANA quiet window calculation

1) Offset of the quiet window in SN state:

a) Start time considerations:

Response SN burst size: PSBu + PLOAMu = 16 + 32 = 48 bytes

Considering 32 ONUs for each wavelength:

Start Time $_{ONU1} = 0$ (first allocation to ONU nearest) $\rightarrow 0$ us

Start Time $_{ONU32} = 1488$ bytes (372 words) (to ONU farthest) $\rightarrow 9.7$ us

Start Time min = 0 us

Start Time max ≈ 10 us

For this calculation it is considered the *Start Time* minimum (0 us).

b) *Minimum ONU respond Time: 34 us [97]*

c) *Round-trip delay (based on SARDANA ODN - limit case: 100 km):*

OLT – RN_{nearest} = 5 km

OLT – RN_{farthest} = 70 km

RN – TDM Coupler = 10 km

TDM Coupler - ONU_{nearest} = 0 km

ONU_{nearest} - ONU_{farthest} = 20 km (D_{max})

$L_{min} = (OLT - RN_{nearest}) + (RN - TDM\ Coupler) + (TDM\ Coupler - ONU_{nearest}) = 15$ km

$$RTD_{min} = 2 \cdot L_{min} \cdot \left(\frac{n_{1552.2}}{c}\right)$$

RTD_{min} = 150 us

So, the offset quiet window in SARDANA, by using eq. (5.4) is:

$$QW_{offset} = 34 + 150 + 0 = 184\ us$$

For the $L_{max} = 80$ km (Fig. 5.24), the maximum offset quiet window in SARDANA is:

$$QW_{offset} = 34 + 800 + 0 = 834\ us$$

2) Size of the quiet window in SN state (eq. 5.5):

a) Random delay maximum = 6.4 us.

b) ONU Response time variation = 2 us.

c) $RTD_{D_{max}=20km} = 200$ us

d) Burst size = 48 bytes (PSBu + PLOAMu SN response)

Burst time = 0.155 us (this value is negligible).

$$QW_{time} = 2 + 200 + 6.4 = 208.4\ us$$

Finally, Fig. 5.26 shows the ONU initialization values obtained for the SARDANA network.

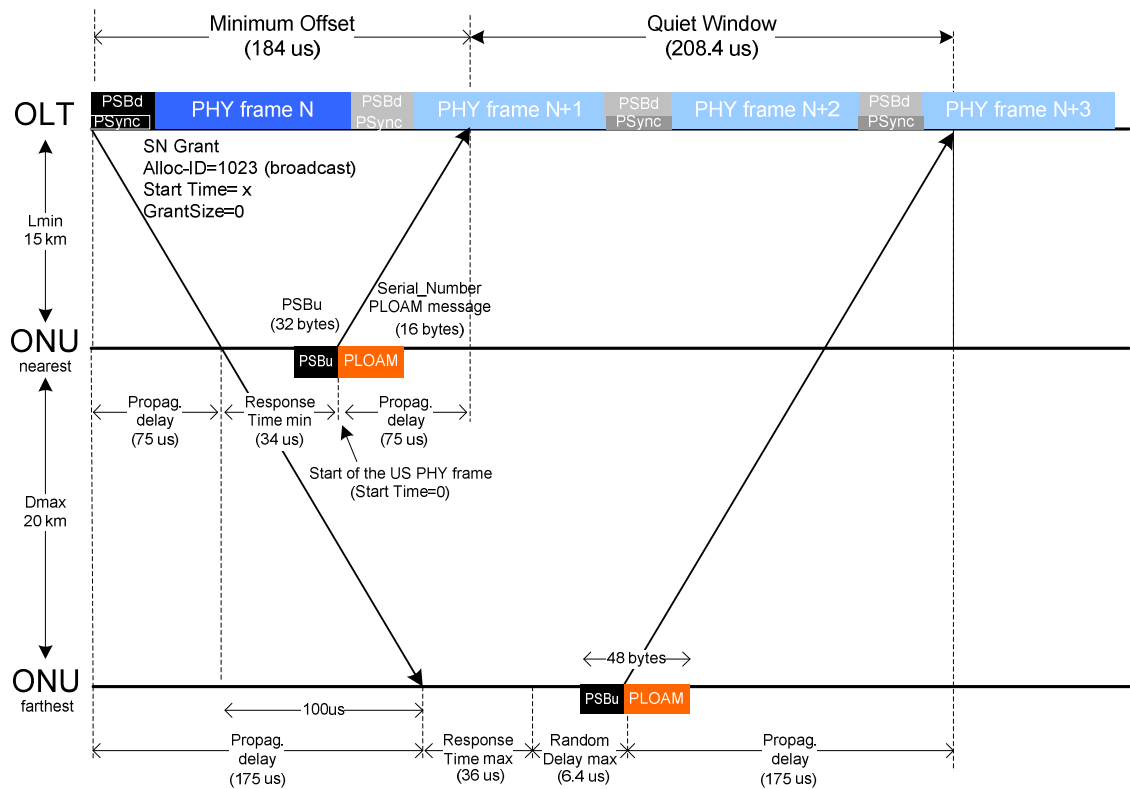


Fig. 5. 26 - ONU initialization values in SARDANA network

In SARDANA the Quiet Window is fixed (since maximum differential length between ONUs remains fixed). Offset QW depends of the OLT – RN – TDM_{coupler} distances. In the best case, when OLT-RN is 5 km, and by considering RN – TDM_{coupler} distances (10 km), this value is 184 us (for a total of 15 km), as shown in Fig. 5.26.

In the worst case (OLT-RN up to 70 km), this value can reach up to 834 us (for a total of 80 km). OLT have capacity to know this OLT – RN distance from the PON-ID field (at the PSBd header), associated with a wavelength and a RN.

c) Ranging Process

In SARDANA, the effective Ranging process is done in two phases:

- The calculus of the EqD: They are done during the QW in the SN PLOAM grant and SN PLOAM response processes.
- The assign of the ONU-ID: the ONU interprets any directed BW allocation with the PLOAMu flag set as a ranging grant and responds to it with a Registration PLOAM message. As seen, in SARDANA it is not necessary to implement a new QW and does not stop transmissions occurring at the ONUs in operation, optimizing the PON processes.

The EqD can be recalculated and adjusted from the US transmission. In-service EqD adjustment allows small corrections without having to re-range the ONU.

5.1.2. Optimization of the ONU activation process

In the initialization process, because the OLT has not yet calculated the EqD for a new ONU, it opens a quiet window to prevent collision between the serial number response of this ONU and the regular transmissions by in-service ONUs. This process affects 4 or 5 consecutive bandwidth maps. An optimization of the OLT relating with the management of this resource should ensure that the impact on the bandwidth and real-time traffic is minimized.

As seen, SARDANA reduces to one the QW in the ONU activation, optimizing this process. However, due to maximum reach of the SARDANA (100 km), the offset with respect to the start of the QW penalizes with extra delay this process. Fig. 5.27 shows the optimization done in SARDANA by using a unique QW and the message exchange OLT-ONU in the initialization process for a new ONU, in this example, located at 80 km from the OLT. Due to ONU maximum differential (D_{max}) is like the standard (20 km), the QW is practically the same than XGPON.

The need to provide a re-arranging of the BWmaps providing extra allocations to the affected Alloc-IDs, immediately before and/or immediately after the quiet window is mentioned in [97]. However, it does not explain the implementation.

By considering that in the activation process of a PON, OLT discovers the OLT-RN and OLT-TDM_{coupler} distances, and knowing that drop section with $D_{max} = 20\text{km}$ ($T_{D_{max}} = 100\mu\text{s}$) is the unique provable scenario of a collision, then:

1. Because OLT knows the OLT-TDM_{coupler} distances and the nearest ONU at the OLT is also at this point (or very close to it), the L_{min} is automatically discovered.
2. A unique 125 μs US frame can provide capacities to transport the SN request from a new ONU ($T_{D_{max}} = 100\mu\text{s} < 125\mu\text{s}$). A quiet window for this time would be sufficient to grant not collision in the drop.
3. So, after the OLT sends a SN_grant PLOAM messages and opening a QW, in the next DS frame (125 μs after), a closing QW should be sent. So, it not would be necessary to await the arrival of the SN_ONU PLOAM response to close the QW, as occurred in (5.4). In this DS frame, also a BWmap with BW allocations, in correspondence with the last reports from the ONUs in service (before the QW) would be attended. A new requirement with $DBRu = 1$ for actualization of the queue status from the ONUs should be also sent.
4. After the arrival of the SN_ONU PLOAMu response, the OLT will send the Assign_ONU-ID message and the Ranging_Time grant with the EqD for a new ONU.
5. In the next US frame, the ONUs in service, as a response at step 3, update the OLT BW allocation table with their Alloc-ID buffer occupation reports. The PON regular operation is then re-established.

6. After receiving Assign_ONU-ID and Ranging Time grant, new ONU know their transmission parameters, and respond with a Registration PLOAM message. The activation process is finished.

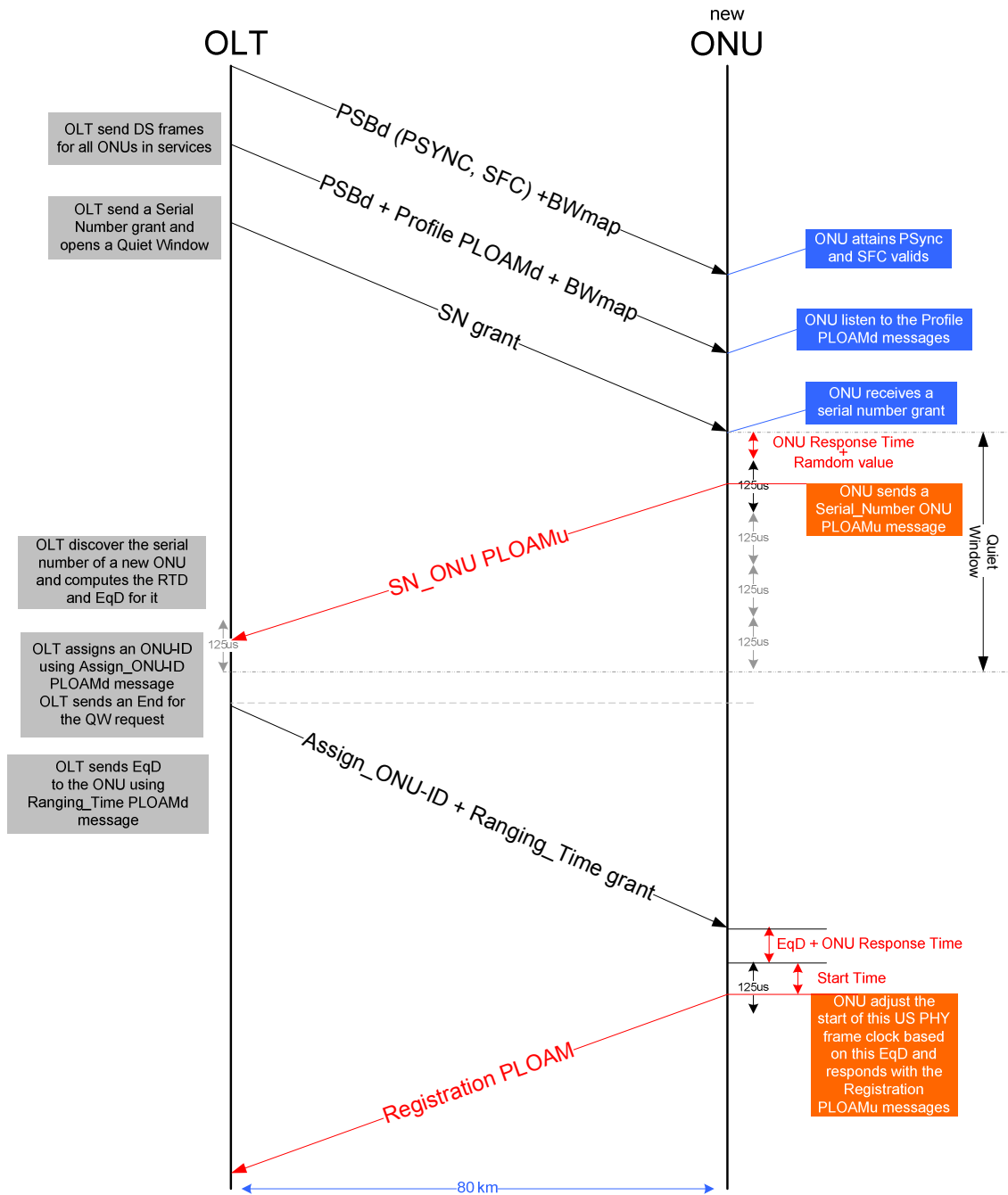


Fig. 5. 27 – Message exchange optimization on the ONU activation process in SARDANA network.

Fig. 5.28 shows the global optimization of the ONU activation in SARDANA network.

By optimizing Quiet Window in SARDANA network new values are obtained for the offset and QW.

Modifying from eq. (5.4):

$$QW_{offset} = ONURspTime_{min} + Delay_{Propagation}_{(80km)} + StartTime \dots\dots\dots(5.6)$$

$$QW_{offset} = 34 us + 400 us + 0 = 434 us$$

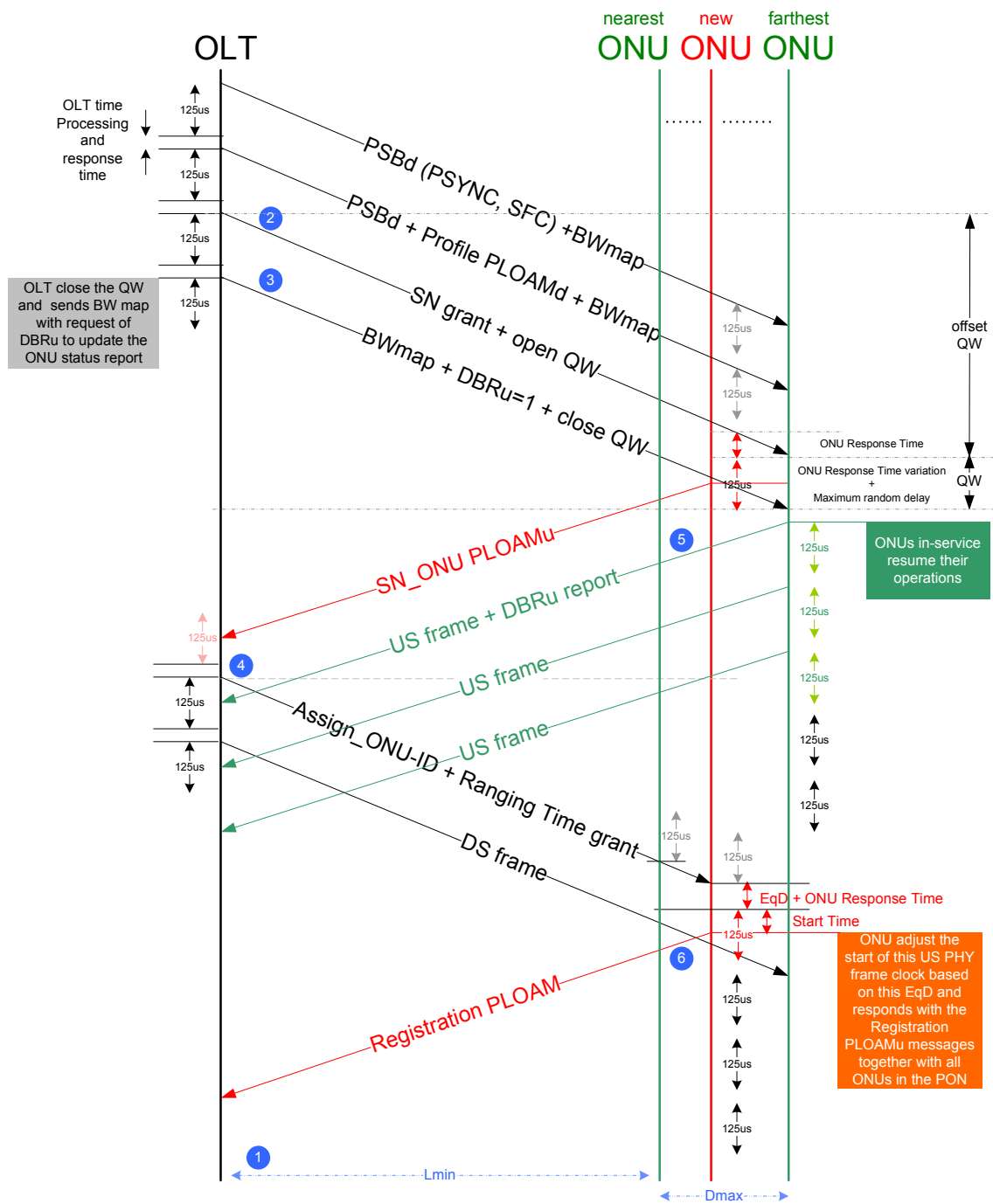


Fig. 5. 28 - Optimization sequence of the ONU activation process in SARDANA network

Modifying from eq. (5.5), with T_{burst} negligible:

$$QW_{time} = ONURspTime_{var} + D_{max} \cdot \left(\frac{n_{1552.2}}{c}\right) + Rand_{max} + T_{burst} \quad \dots\dots(5.7)$$

$$QW_{time} = 2 \text{ us} + 100 \text{ us} + 6.4 \text{ us} = 108.4 \text{ us}$$

These optimization practical results are shown in Fig. 5.29.

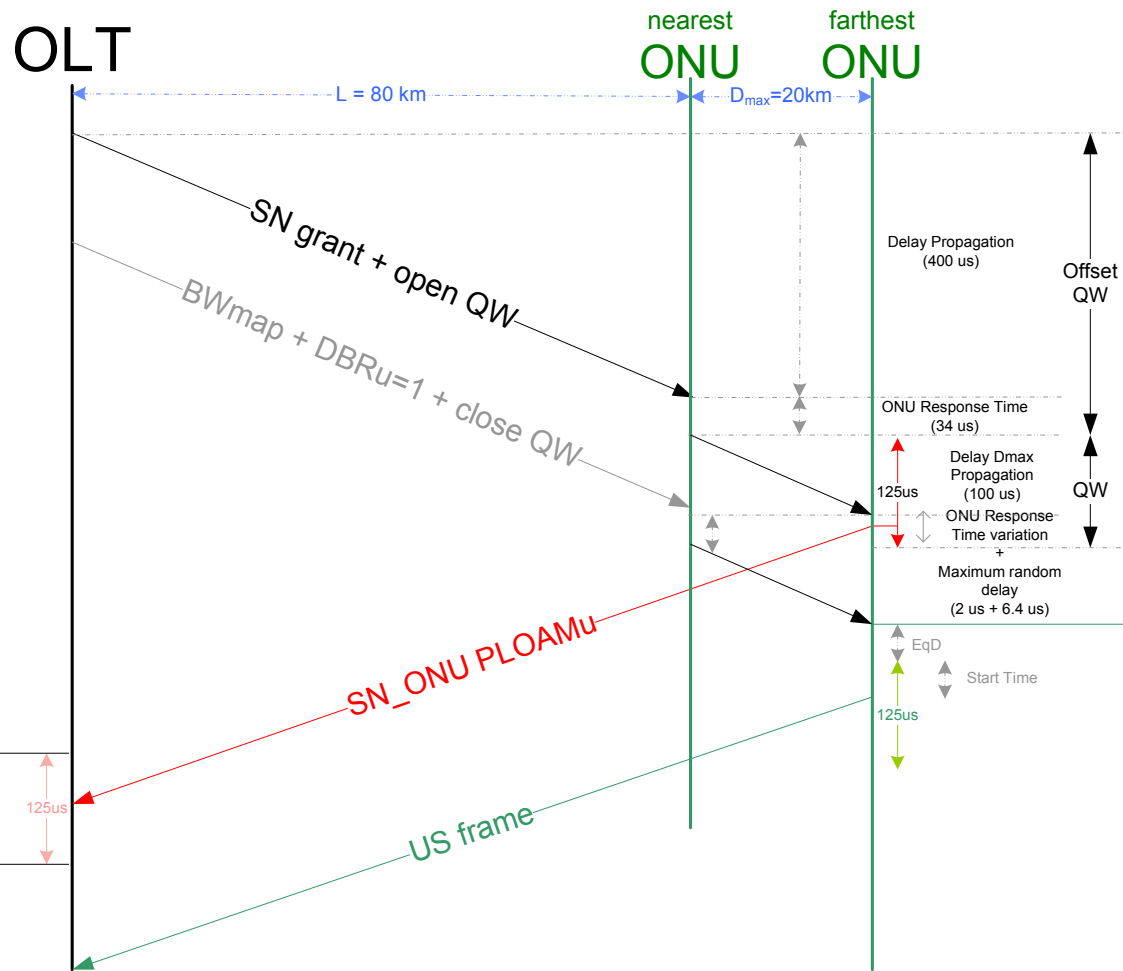


Fig. 5. 29 – Practical values from the optimization on the ONU activation process in SARDANA network

By comparing SARDANA with XG-PON we can see that the implementation of one unique QW by SARDANA practically compensates the differences in ODN coverage (80 km) of both networks.

In the same conditions (both networks with 20 km), SARDANA would need 242.4 us ($QW_{offset} = 134$ us and $QW = 108.4$ us) to implement a QW. So, this ONU activation optimization proposes, by itself, would be 4 times more efficient than the XG-PON recommendation.

By considering that a BWmap is implementable on the STC header of a DS PHY frame and sent, in normal operation state, each 125 us, QW mechanism affects up to eight BWmaps during ONU activation in XGPON. SARDANA optimization reduces the impact of the QW to 5 BWmaps in the most critical ODN scenario (100 km).

By applying optimization on the ONU initialization process it is possible to reduce the penalties due to QW mechanism implementation. This improvement allows flexibility on the frequency control of signalling for the discovering of a new ONU. However, it is a trade-off between better traffic flux and the fast ONU activation.

Fig. 5.30 shows comparative curves between XG-PON (max. 20 km) and SARDANA without/with optimization for the ONU activation process.

In the SARDANA case, are considered the Remote Node nearest (at 5 km from the OLT) and the RN farthest (at 70 km from the OLT). In all the cases is considered a RN to TDM coupler distances of 10 km. The differential distances between ONUs is the same of the XG-PON (20 km).

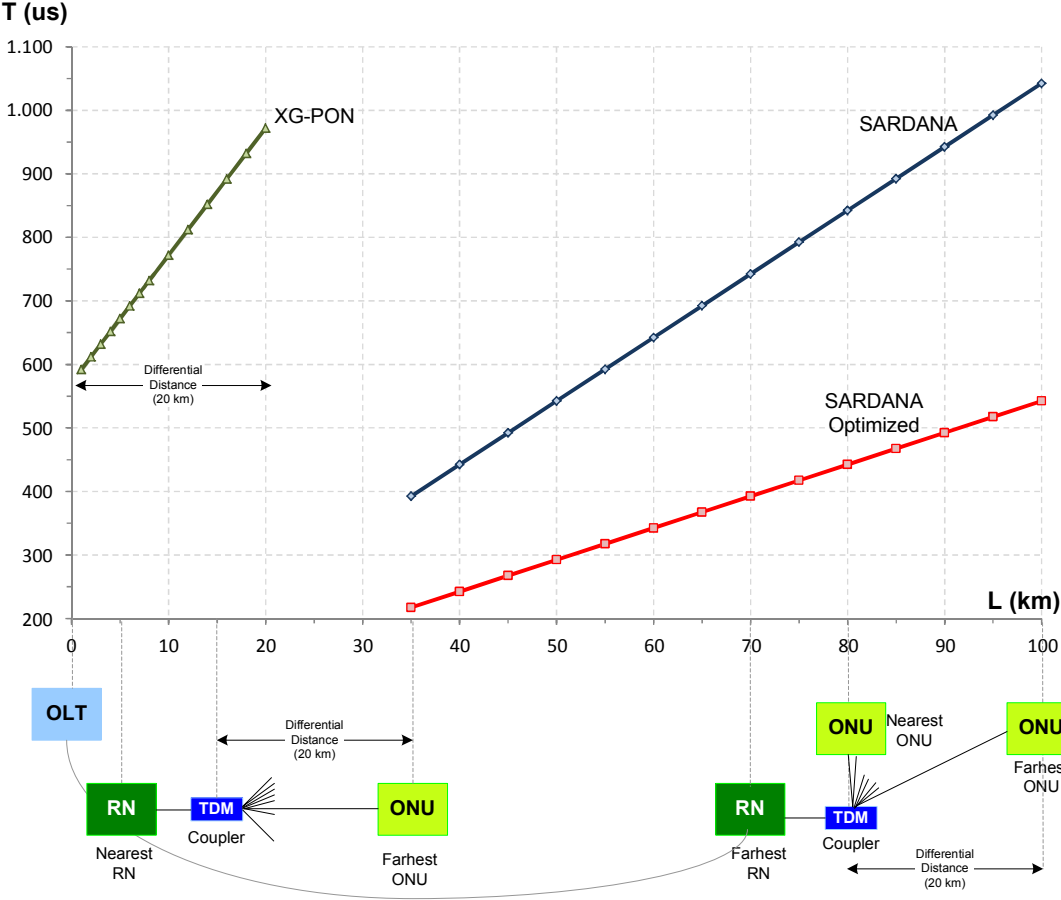


Fig. 5.30 - ONU activation process: XG-PON and SARDANA without/with optimization.

A better performance is shown for using optimization in SARDANA. Initialization process (serial number and ranging acquisition) can be obtained in the worst case on 543 us. This enables SARDANA to implements ranging in critical long-reach distances.

In Fig 5.31, by considering that XG-PON could be extensive up to 100 km and for using this approximation as a reference, and from eqs. 5.4 and 5.5, and [97], we can see a comparative between SARDANA and XG-PON for the ONU initialization process.

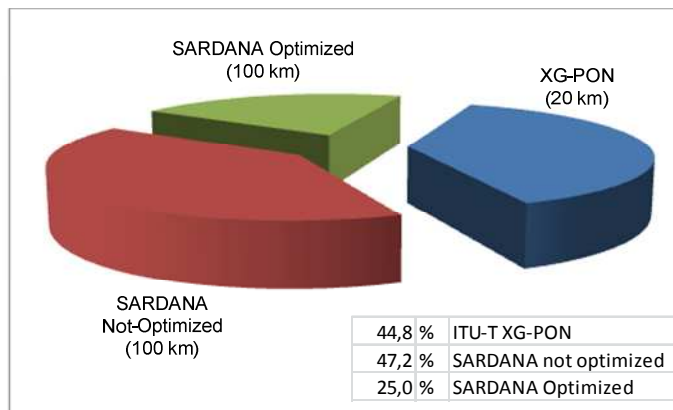


Fig. 5. 31 - A comparative between SARDANA and XG-PON for the ONU initialization process.

An optimization of the SARDANA allows reducing even further, on 22.7%, the total duration of a QW implementation on the same network, by improving on 47.1 % its performance. Also, although SARDANA metro/access network is up to 100 km, this optimization reduces on 19.8 % and improves on 44.2% the performance of a XG-PON (20 km). So, it demonstrates a more agile ONU initialization process than XG-PON.

Table 5.9 shows a comparative between maximal ODN values for XGPON [97], SARDANA and optimized SARDANA, during serial number and ranging acquisition and the total time that is consumed.

Table 5. 9 – Quiet Window and QW offset comparative values between XG-PON and SARDANA

Network	L (km)	Dmax (km)	Offset QW (us)	Quiet Window (us)	Windows used	Total Time (us)
XG-PON	0	20	236	250	2	972
SARDANA	80	20	834	208.4	1	1042.4
SARDANA optimized	80	20	434	108.4	1	542.4

5.1.1. Equalization Delay (EqD) Calculus

The OLT obtains the upstream PHY frame offset (T_{eqd}) using the next expression:

$$T_{eqd} \geq \text{ONU Response Time}_{\max} + 2 (T_{L\min} + T_{D\max}) \quad \dots\dots(5.8)$$

T_{eqd} value remains constant through the lifetime of the PON. The EqD of an ONU is found as:

$$EqD_{ONU_i} = T_{eqd} - \text{RTD} = T_{eqd} - (\Delta^{\text{SN}} - \text{Start_Time}) \quad \dots\dots(5.9)$$

With Δ^{SN} being the elapsed time between the DS PHY frames containing the SN grant and the US PHY burst containing the SN response PLOAM. Fig. 5.32 shows these processes.

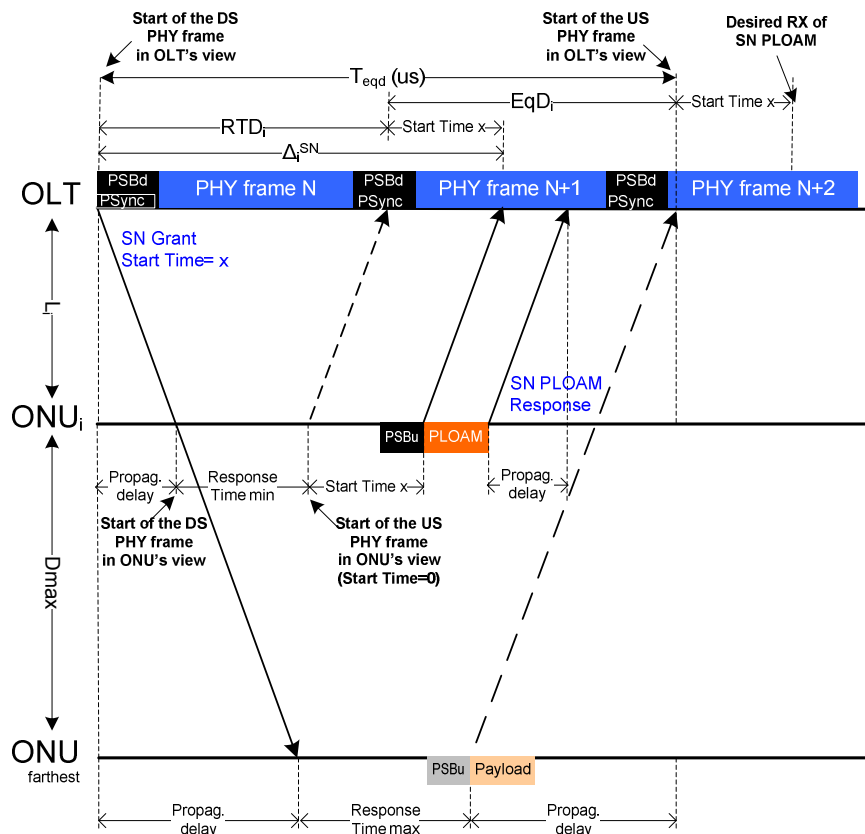


Fig. 5. 32 - Equalization delay calculation during SN process

The ONU is considered synchronized at the beginning of the US PHY frame when it is supplied with its equalization delay value. The US burst is transmitted within the interval specified by the BWmap (start time) with respect to the beginning of the US PHY frame.

In the practice, the EqD value depends of the D_{max} than the ODN length. For SARDANA networks, in the ONU parameter initialization process, will have the following values from (5.8):

$$T_{eqd_max} = 36 \text{ us} + 2 (T_{80\text{km}} + T_{20\text{km}}) = 1036 \text{ us}$$

From (5.9):

$$\text{RTD} = \Delta^{\text{SN}} - \text{Start_Time}$$

For maximum EqD \rightarrow RTD_{min} \rightarrow Start_Time = 0 us

$$RTD_{\min} = \text{ONU Response Time}_{\min} + 2 (T_{80\text{km}}) = 34\mu\text{s} + 2 \cdot (400\mu\text{s}) = 834 \mu\text{s}$$

$$EqD_{\max} = TeqD - RTD = 202 \mu\text{s}$$

Fig. 5.33 shows maximum EqD calculation for the SARDANA network.

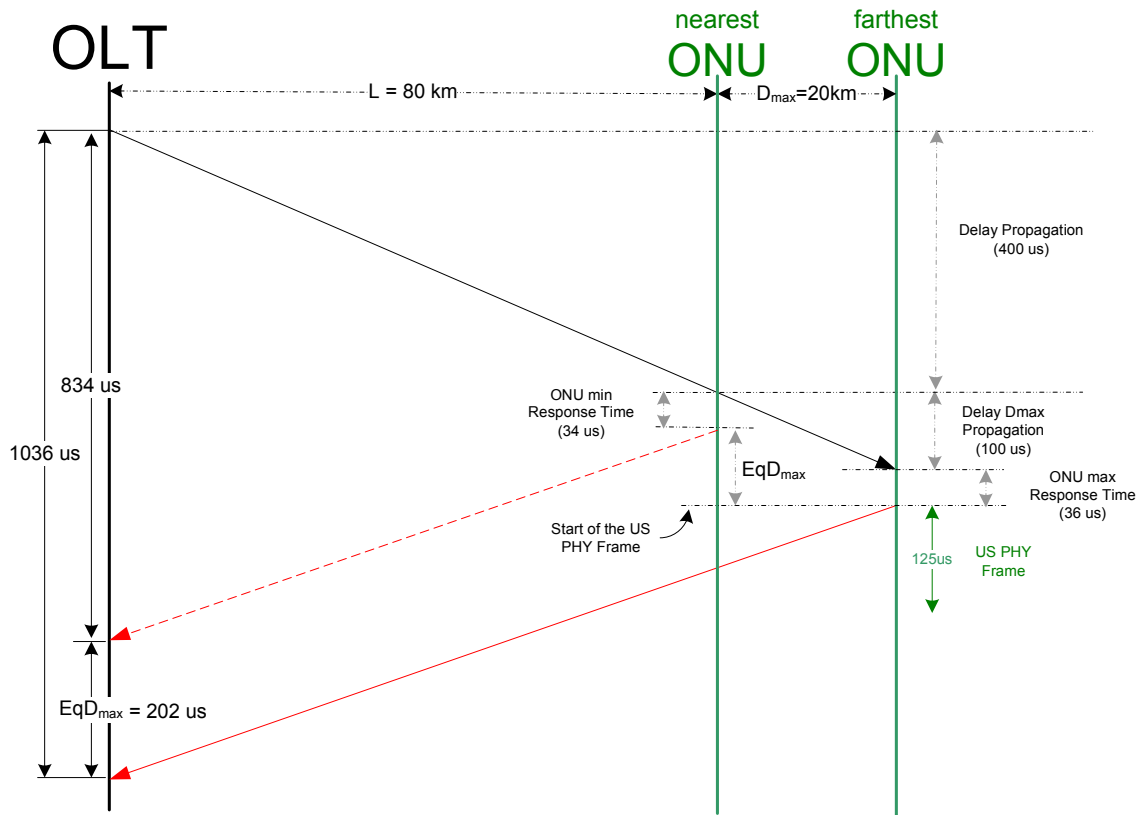


Fig. 5.33 - Maximum EqD value for the $D_{\max} = 20 \text{ km}$ on the SARDANA network.

5.1.2. Timing during the Operation State of the PON

The ONU maintains its US PHY frame clock synchronized with the DS PHY frame clock and offset by the sum of the ONU response time and the assigned EqD, specified by the OLT. The ONU transmits burst data on the US frame according to the content of the BWmap (BW allocation and Start Time) received from the OLT on the DS frame. Fig. 5.34 shows the timing for a burst from an ONU.

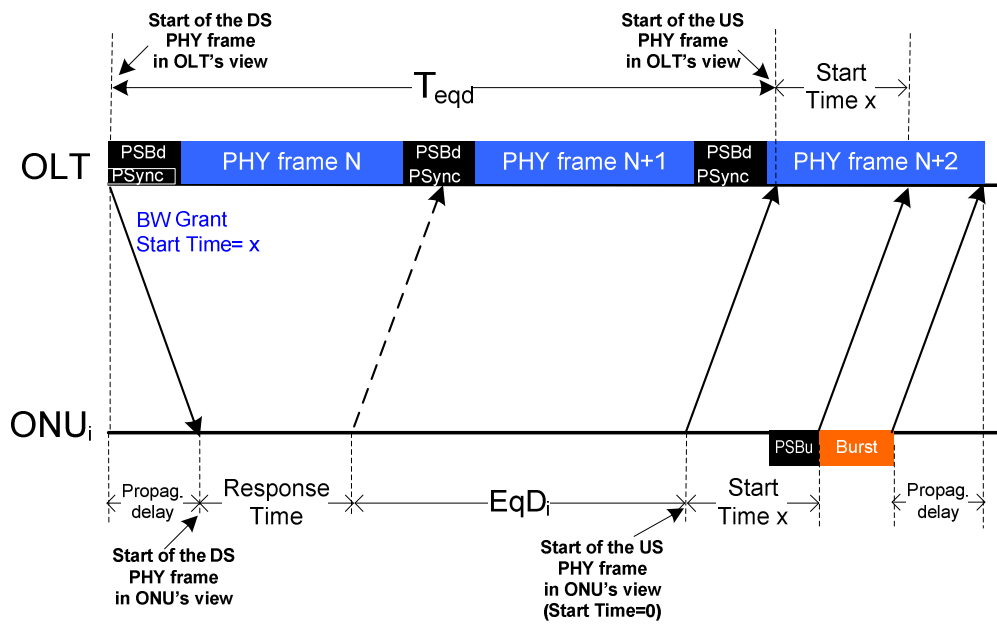


Fig. 5. 34 - Timing during the Operation State

5.2. Conclusions

Different of XGEM from XG-PON, in SARDANA SGEM other fields are included to exploit their metro/access coverage and as a function of the PHY characteristics. So, multi-protocol management, overlay transmission capacity (from different service providers), multi-services and multi-operator capability are deployable. Also, QoS and other higher layer services are possible. These new fields give SARDANA TC capacities to deploy internetworking functions.

In SARDANA, the PLOAM message (downstream and upstream) has a variable length (8, 16, 24 or 32-bytes) instead of a fixed length of 48-bytes (XGPON). In this way, increased efficiency between 1.5x and 6x times can be reached. This allows releasing more space in the header to favour the payload section space.

Also, SARDANA burst header incorporates an indicator of the messages. This field will help the OLT to know if the burst carries DBRu structures and PLOAMu messages, allowing fast decodification of the burst payload.

Calculations to obtain an Upstream Physical Synchronization Block (PSBu) consistent with the SARDANA PHY layer were done. A Preamble and Delimiter fields of 192 bits (77.16 ns) plus a Guard Time of 80 bits (32.15 ns) are specified.

In this work, an agile ONU activation process by simplification of the ranging state is shown. This mechanism reduces to one the use of a QW in the ONU initialization process, by improving the efficiency. Even so, a QW instance penalizes the system. In this work, an optimization to mitigate this issue is presented. Although SARDANA metro/access network 100 km, this optimization improves in 44% the performance with respect to XG-PON (20 km).

In XGPON, QW mechanism affects up to eight BWmaps during ONU activation. SARDANA optimization reduces the impact of the QW to five BWmaps in the most critical ODN scenario (100 km).

Chapter 6

6. SARDANA NG-PON Layer 2 Implementation and Internetworking

In this chapter, an implementation proposal for the STC layer 2 and internetworking processes through SARDANA networks are shown.

A comprehensive detail of the OLT and ONU STC prototype implementation is explained. These sub-systems are deployed using a base board based on a FPGA Stratix IV GX development kit from Altera. Setups for connections between base board and interfaces, and these with clients at the higher layers or OMCI CPC and with the optical PHY SARDANA ODN, through OLT/ONU optical assemblies, are also discussed.

About of SARDANA internetworking, this chapter deals about the relationship of SARDANA with other communications systems in the context of broadband access and aims at describing the connectivity requirements of SARDANA.

Although SARDANA system can sharing the infrastructure with current GPON and GE-PON systems as a NGPON1; however, it cannot make full use of the SARDANA features, so we state that SARDANA is mainly positioned in the NGPON-2 generation. Better than this, SARDANA can transport those different systems in an efficient way.

The requirements of SARDANA from the Service layer viewpoint are detailed. The concept and implementation of multiprotocol management are described. This process enables SARDANA for implementation of internetworking. So, procedures of Interoperability and Overlaying, for cover requirements from higher layers and other providers and networks, are explained.

These internetworking services can be implemented between metro networks (at the metro network level) or as an interconnection add/drop node, into a core transport network.

6.1. SARDANA Layer 2 Implementation

The physical implementation of the SARDANA layer 2 is based on the OLT/ONU SARDANA Transmission Convergence (STC) implementation, in order to obtain the functional characteristics, explained in the previous chapter, operating at 10/2.5 Gbps downstream/upstream data rate.

Similar to the first draft of the SARDANA layer 2 (SXGPON 64-bit data path) [171], a FPGA, such as Altera Stratix IV [173], will be used as a base for the SARDANA layer 2 testbed designs. This FPGA theoretically support clock frequencies up to 600 MHz.

6.1.1. FPGA clock frequency and data path definition

The performance of a FPGA depends of the latency and the throughput. Latency measures how many clock cycles are required to process the data from the input to the output. Throughput defines the maximum amount of data that can be processed in a certain time of frame. The FPGAs speed has a theoretical limit in its maximum clock frequency.

The data rate can be represented to be directly proportional to the data path width and the data processing frequency into the FPGA and is referred to as clock frequency in the FPGA context. This relationship is represented by:

$$\text{Data rate (bps)} = \text{Data path width (bits)} \cdot \text{Clock frequency (Hz)}$$

The clock frequency is inversely proportional to the data processing time referred to as clock cycle in the FPGA context.

For FPGA clock frequency to support downstream 9.95328 Gbps is necessary to parallelize the data to a wide enough data path. By compatibility with XGPON design, where the frame formats are aligned to 4-byte word boundaries [97], a 32-bit data path is considered. Hence, for 10 Gbps, the clock frequency necessary for this data path is:

$$\text{Clock frequency} = 9.95328 \text{ Gbps} / 32 \text{ bits} = 311.04 \text{ MHz}$$

Similarly, in the US path, for 2.48832 Gbps data rate, the clock frequency with 32-bit data path is 77.76 MHz.

Respect to SXGPON (64-bit data path) [171], a 32-bit data path allows to use lower length registers, minor bus resources and to obtain higher granularity, especially in the frame format design. However, although Altera Stratix IV to support clock frequencies up to 600 MHz, optimization process could be necessary for a higher amount of logical operations to be performed during one clock cycle.

For this 32-bit data path, this architecture implements the serialization and de-serialization in two stages: the first stage combines several low-speed data bits to a few LVDS (Low Voltage Differential System) streams, and then the second stage multiplexes the LVDS streams onto one high-speed serial channel. A FPGA easily implements the first stage while an analog-optimized discrete SerDes handles the high-speed serialization. Fig. 6.1 shows a FPGA-SerDes connection [174].

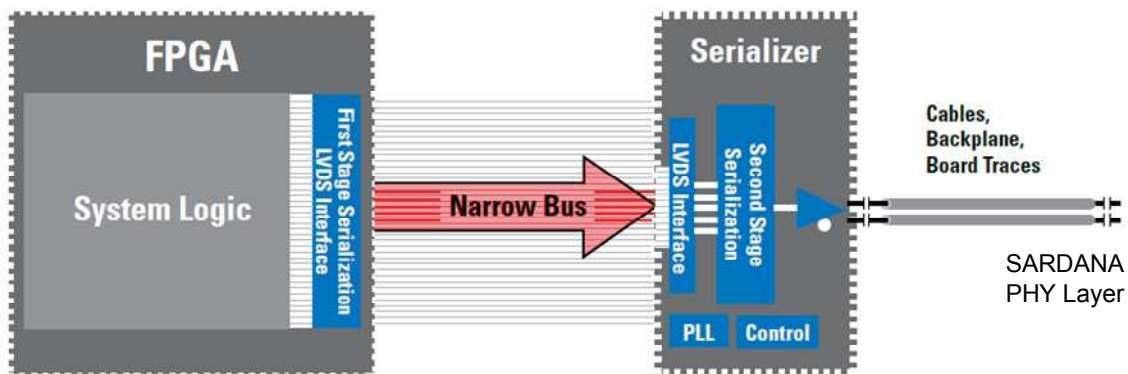


Fig. 6. 1 - Two-stages SerDes implementation for the 32-bit SARDANA data path (modified from [174])

The LVDS parallel interface of the FPGA-Attach SerDes enables higher data rates over fewer board traces while reducing the EMI, power, and noise sensitivity of the system.

SerDes devices in this family typically integrate signal-conditioning schemes like de-emphasis, DC balancing and channel equalization. This optimizes the performance for the highest data rates and longest transmission paths.

6.1.2. SARDANA sub-system prototyping

SARDANA STC Layer 2ONU and OLT prototyping was redesigned and physical implementation suggested for laboratory test and field trial.

OLT and ONU have a common baseboard design which is programmed to support the OLT or the ONU functionality. A single programmable baseboard, based on Altera Stratix IV GX development kit for both, the OLT MAC and the ONU MAC implementation, is used. Fig. 6.2 shows the Altera Stratix IV GX card [173].

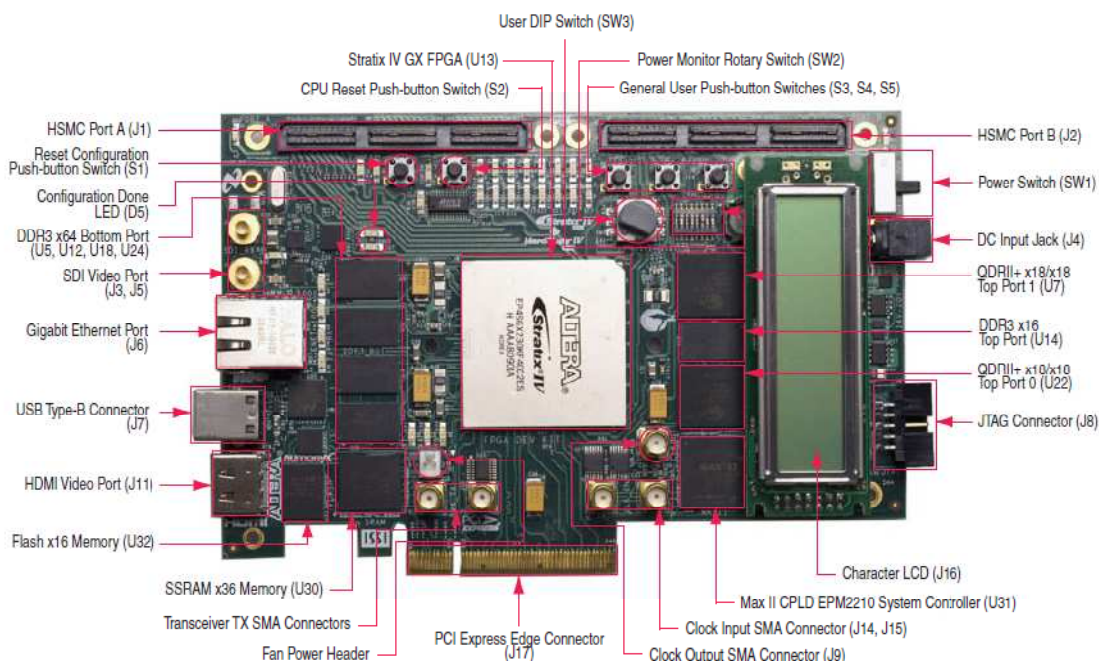


Fig. 6. 2 - OLT/ONU prototype base board based on FPGA Altera Stratix IV GX

Also, two sub-systems are necessary for the interface with the higher layers and the optics assembly. So, the baseboard provides two HSMC (High Speed Mezzanine Connector) for the interconnection of these sub-systems: one is used for SNI/UNI Ethernet interface module in the data link level. The other HSMC is used for optical interface module with the PHY Layer OLT level (OLT Burst Receive/Frame Send) and PHY Layer ONU level (ONU Burst Send/Frame Receive). OLT and ONU PON interface modules are based in the optical module board TST9061 from Tellabs Inc.

6.1.2.1. Ethernet Interface Module

The Ethernet interface module is used according to the application interface (SNI or UNI). SNI and UNI both differ in the transmission rate and the Ethernet protocol(although backward compatible). In the case of SARDANA design, two interfaces are used:

- 10GE interface, for SNI interfaces.
- 10/100/1000Base-T for UNI interface

a) 10GE SNI Interface

The STC FPGA design is using an internal 10G Ethernet MAC IPR (IP reach)-Block that interfaces to an Ethernet HSMC interface module via a XAUI interface. It is used preferably at the OLT like SNI interface by the amount of information exchange. Alternatively, HSMC CX4 Adapter Board can be used with 10G Ethernet applications using CX-4 copper interfaces. Fig. 6.3 shows these interfaces.

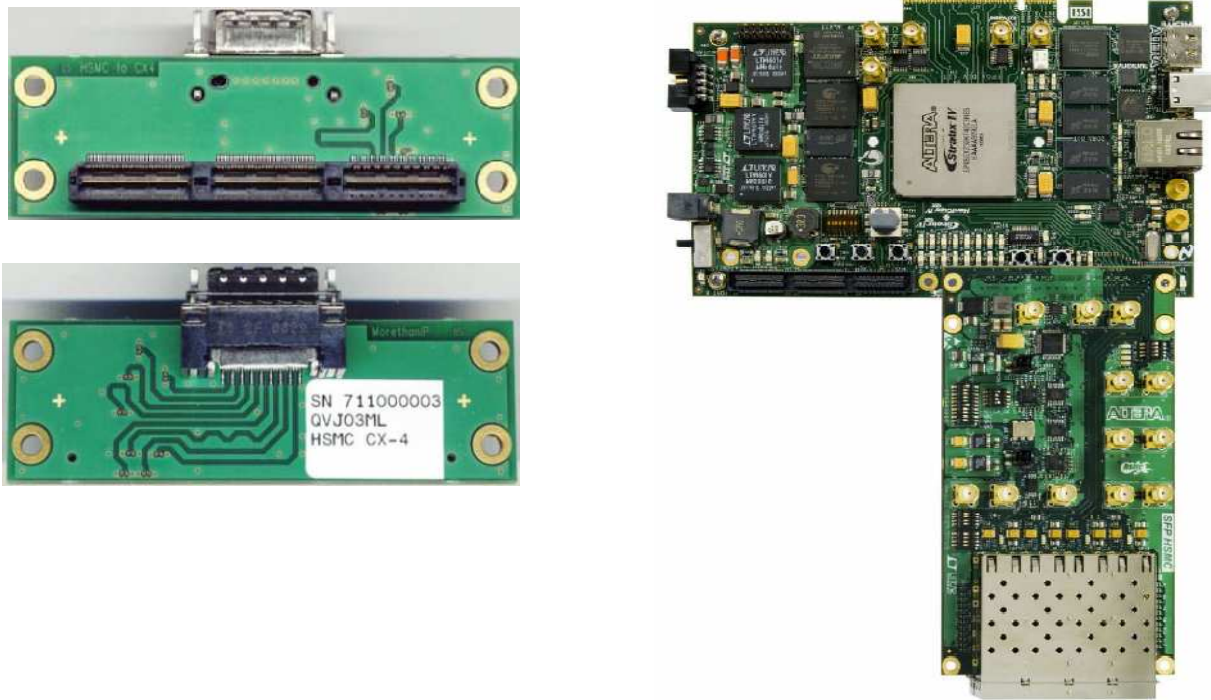


Fig. 6. 3 - Ethernet interface modules for SNI a) HSMC CX4 Adapter Board b) HSMC board based on XAUI interface connects with Altera Stratix IV FPGA Development Kit.

b) 10/100/1000Base-T UNI Interface

The STC FPGA design is using an internal triple speed Ethernet MAC IPR-Block that interfaces to the four port triple speed MAC HSMC interface module via four SGMII interfaces, as shown in Fig. 6.4. Again electrical Ethernet ports 10/100/1000Base-T, using four standard RJ-45 connectors are used to connection to the CPE (Customer Premises Equipment) at the ONU. One of the ports is dedicated for SARDANA OMCI system and the remaining three ports are for Ethernet services (multicast IPTV, Internet access and videoconferencing).



Fig. 6. 4 - Ethernet interface modules for UNI: HSMC 4-Ports 10/100/1000Base-T RJ-45 port Adapter Board

6.1.2.2. Optical interface module (TST 9061)

The Optical interface module (TST9061) provides serial differential SMA connectors for OLT and ONU TX/RX optical PHY layer modules, and a XFP gage for OLT and ONU receiver/transmit signal test, as shown in Fig. 6.5. This module perform electrical interface between framers and serializer/deserializer

parts. A Broadcom BCM8154 [151], a multi-rate low-power 10G NRZ/duobinary transceiver with 10G clock and 16:1 serializer/deserializer clock and data recovery IC is used as both the OLT and ONU transceiver.

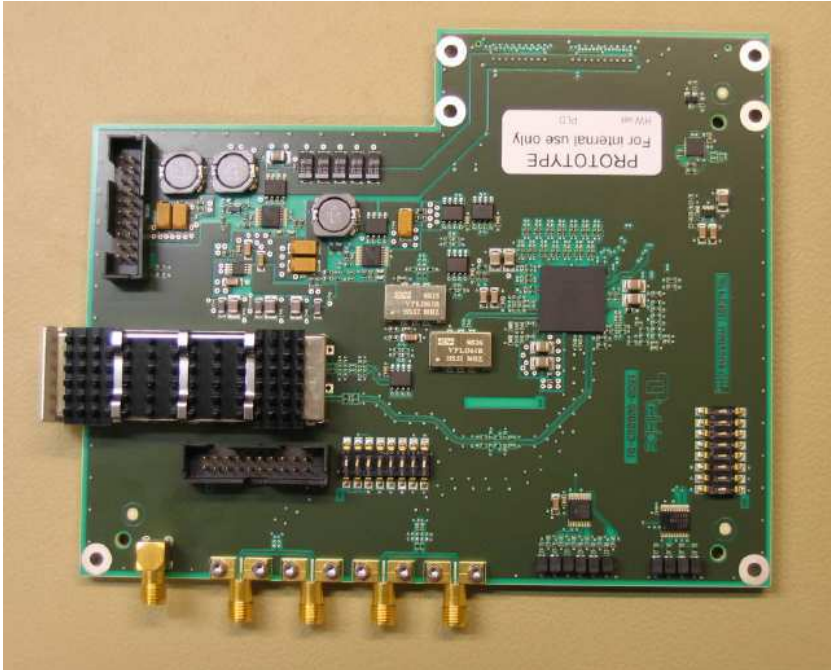


Fig. 6. 5 - Optical HSMC module board (TST9061) for the OLT and ONU assemblies.

The TST9061 connects to the baseboard MAC FPGA Altera Stratix IV via the second HSMC connector, as shown in Fig. 6.6.

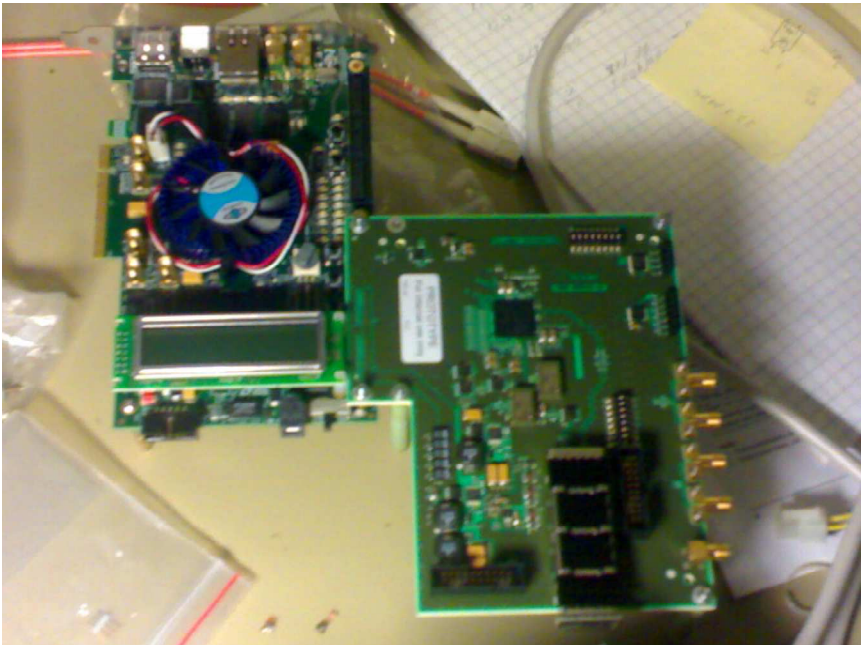


Fig. 6. 6 - Optical interface module (TST9061), connected on the MAC base board Altera Stratix IV GX. There are two variants of optical module TST9061: OLT TX/RX and ONU TX/RX modules. The only difference is the XFP RX components used and the choice of some passive components (coupling resistor and capacitors). The same TST9061 board layout is used for both optical module types.

6.1.3. OLT Layer 2 Prototyping

6.1.3.1. OLT STC TX

The OLT transmits 10Gbps downstream frame to the ONUs. A 32-bit parallel 311 MHz LVDS does interface over the HSMC between the OLT base boards and the OLT optical module interface. On the optical interface module, the BCM8154 serializes this framer interface to an LVDS 10Gbps CML signal. This is transmitted via two differential right angle PCB edged SMA jacks (RPC-2.92) and 50 ohms precision coaxial cables to the transmitter OLT optical assembly at the PHY layer.

Fig. 6.7 shows the block diagram of the layer architecture in the OLT implementation and interfaces. FPGA processor implements all the function and processes of the STC layer. At the Service Adaptation sub-layer, FPGA implements MPM functionality and interfaces with the Ethernet client, at SNI, through the Ethernet CX-410 Gbps interface. At the Framing sub-layer, FPGA deploys framing, PLOAM processing and DBA control. At the PHY adaptation sub-layer, it implements FEC, scrambled and a first stage of SerDes. A second SerDes stage is implemented at the TST-9061 optical interface and delivery/receiving a CML signal to/from OLT optics assembly, at the PHY layer. Finally, OLT optics assembly interfaces with SARDANA ODN at 10 Gbps/2.5Gbps optical signal.

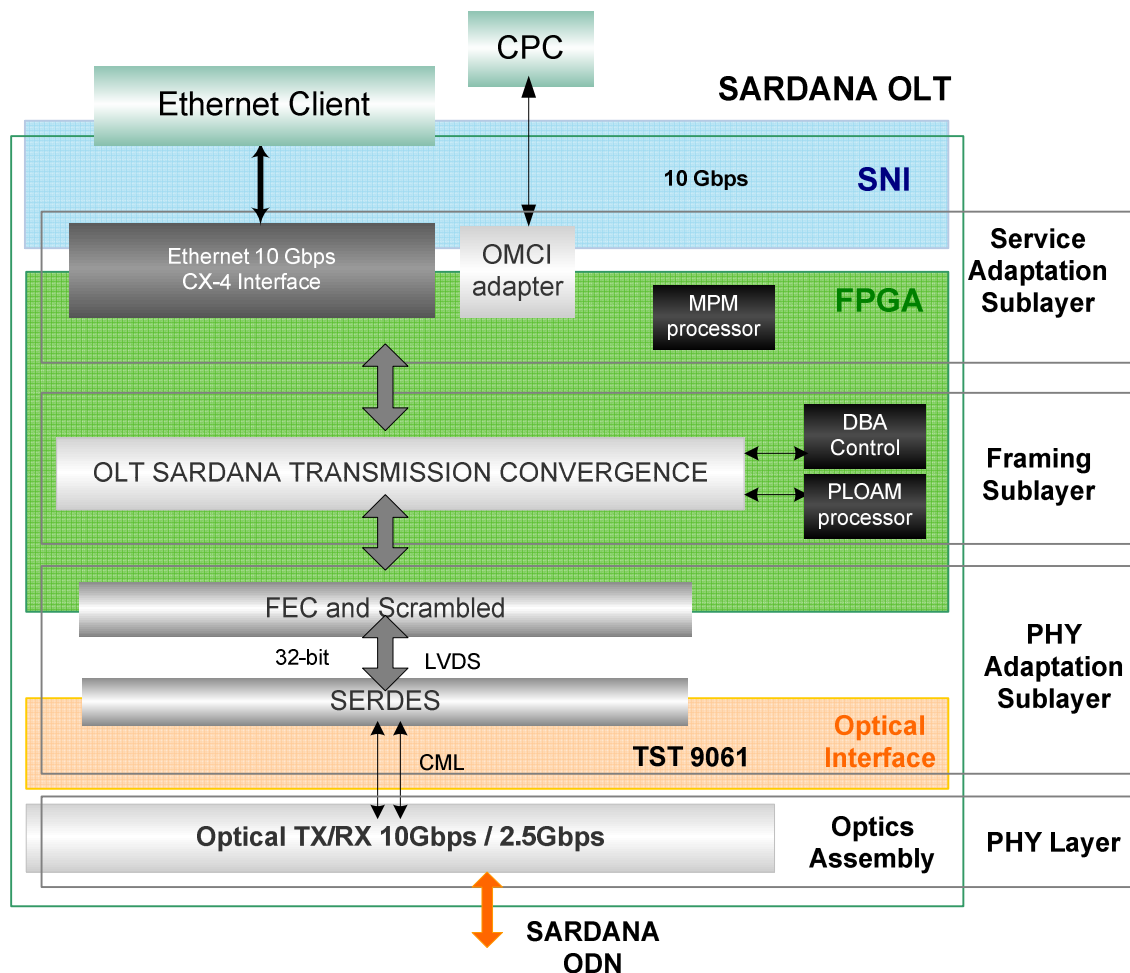


Fig. 6. 7 – Block diagram of the SARDANA OLT Layer1/Layer 2 implementation

6.1.3.2. OLT STC RX

The OLT receives 2.5Gbps upstream frame consisting of bursts sent from the ONUs in the PON. The BCM8154 deserializes the LVDS signal that is received from the OLT RX PHY layer optical module, to 32-bit SPON MAC framer interface. The implementation uses BCM8154 demultiplexer for sampling 2.5 Gbps serial burst received to the parallel 32-bit interface.

Fig. 6.8 presents a pictorial diagram of the OLT Layer 2/Layer 1 setup implementation. It shows the interconnections of the Altera Stratix IV FPGA GX card module with their interface modules: the Ethernet 10 Gbps CX4 adapter (at SNI) and the Optics Interface TST9061, connected at the OLT SARDANA optics assembly. CPC control unit connection and Central Office setup is also shown.

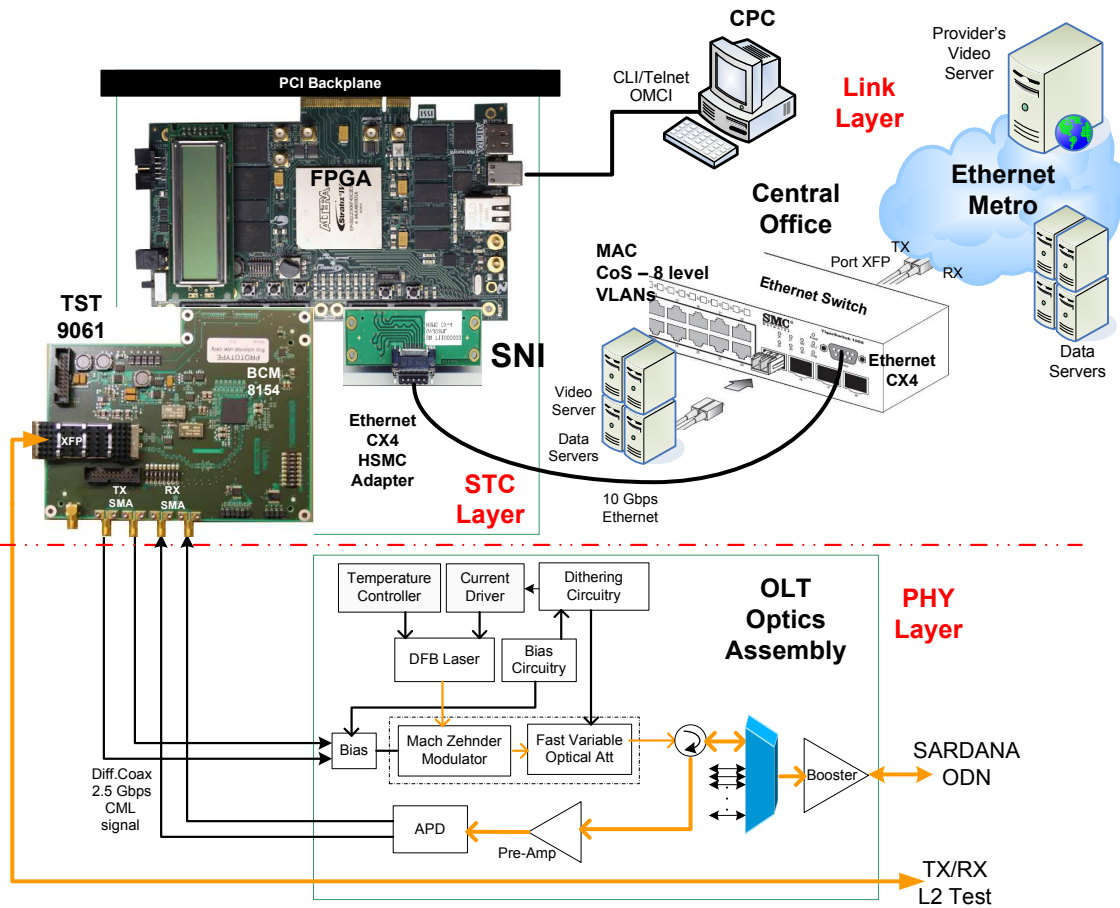


Fig. 6. 8 – OLT Layer 1/Layer 2 implementation based on Altera Stratix IV FPGA GX card module pictorial diagram. The Interfaces through Ethernet CX4 adapter and Optics Interface TST9061, as well as the CPC control unit and the OLT Optics Assembly are shown.

6.1.4. ONU Layer 2 Prototyping

6.1.4.1. ONU STCTX

Upstream burst at 2.5Gbit/s is transmitted from the ONU to the OLT. The ONU base board SPON framer interface is a 32-bit parallel 77.76 MHz LVDS interface to the BCM8154 transceiver on the ONU optical module. This connects to the transmitter ONU optical assembly at the PHY layer, with 50 ohm precision coaxial cables. A control for TX off needs to be provided to suppress the rONU transmitted optical signal between the rONU upstream allocations.

Figure 6.9 shows the block diagram of the layer architecture in the ONU implementation and interfaces. Similar to OLT implementation, FPGA processor implements all the function and processes of the STC layer. It interfaces with the Ethernet client, at UNI, through the 4-port Ethernet 10/100/1000 Base-T interface. At the PHY layer, ONU optics assembly interfaces with SARDANA ODN at 2.5 Gbps /10 Gbps optical signal.

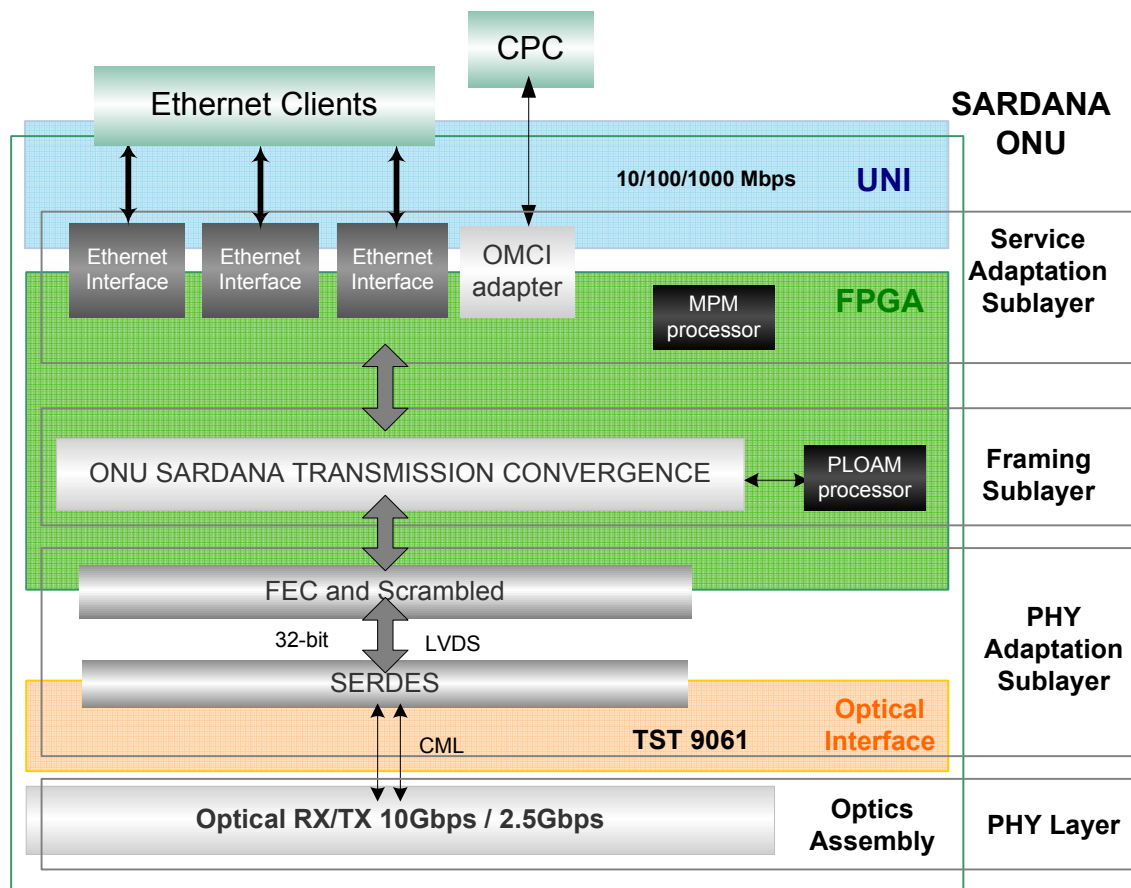


Fig. 6. 9 - SARDANA ONU Layer1/Layer 2 and FPGA implementation

6.1.4.2. ONU STC RX

The ONU optical module receives a 10Gbps downstream frame from the OLT, performs interface from this serial 10Gbps CML signal to 32-bit 311 MHz LVDS, and send it to the ONU base board over HSMC connector.

Fig. 6.10 presents a pictorial diagram of the ONU Layer 2/Layer 1 setup. It shows the interconnections of the Altera Stratix IV FPGA GX card module with their interface modules: the Ethernet 10/100/1000 Base-T adapter (at UNI) and the Optics Interface TST9061, connected at the ONU SARDANA optics assembly. CPC control unit connection and user's premises setup is also shown.

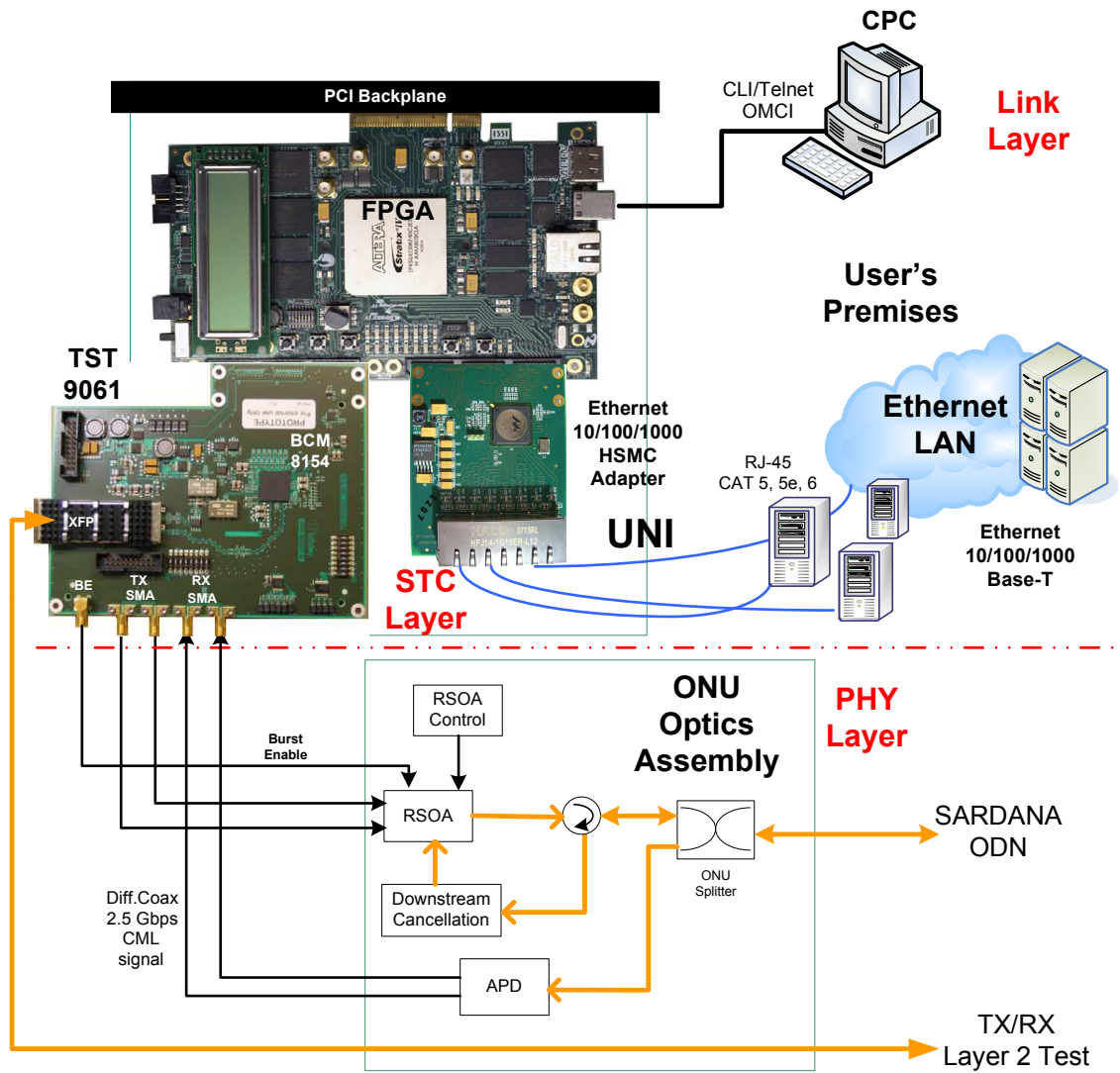


Fig. 6. 10 –The ONU Layer 1/Layer 2 implementation pictorial diagram, based on Altera Stratix IV FPGA GX card module. Interfaces through Ethernet 10/100/1000 Base-T adapter and Optics Interface TST9061, as well as the CPC control unit and the ONU optics assembly

6.1.5. Control of the SARDANA STC processes

A single interface for CLI (Command Line Interface) based on register read/write access is provided by the boards. An external PC is used to configure the boards via this CLI using Telnet connection. The Nios II embedded processor in the FPGA design on the OLT/ONU protoboards and the software running on a PC allows register read/write access for board configuration. An USB Ethernet port on the OLT/ONU protoboards is used for connecting to the Control PC (CPC) configuration Ethernet port.

Fig. 6.11 shows a network test diagram. Control PC connections with the OLT and the ONU are established for network control, through the SARDANA and by means an Ethernet switch for supervision.

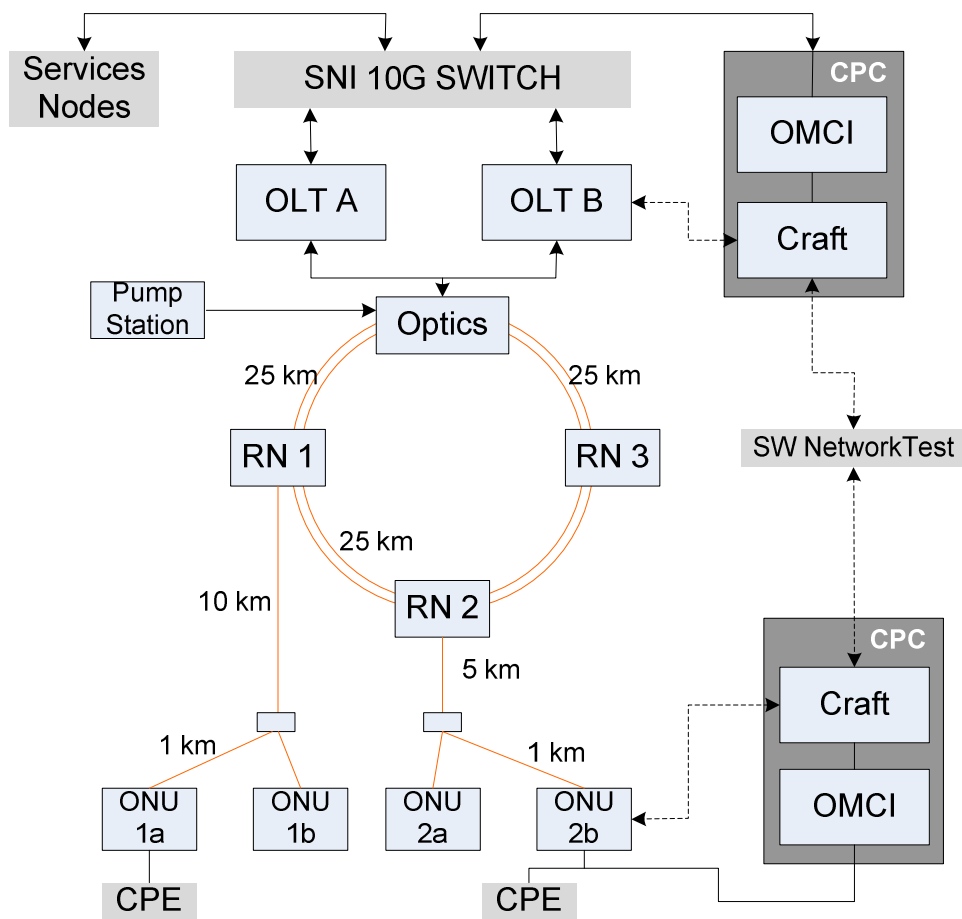


Fig. 6. 11 - SARDANA demonstrator network for Management & Control test

This demonstrator network was implemented to test the functionalities of management and control on the Layer 2 architecture and on the PHY particular topology. Here, SARDANA network allows communications services through the OLT to devices at the customer ONU site. A 10G Ethernet Switch at Central Office site connects Link layer services with the OLT protoboards. Node/Network services and the CPC connect to the services Switch via 1GE interfaces. The protoboards are planned to offer direct 10/100/1000Base-T interfaces (at the UNI/CPC) as well in addition to the electrical 10GBase-CX4 Ethernet interface (at the SNI). The CPE site customer switch interface to the PON uses 1GE ports. The OLT 10GE interface is per SARDANA-PON. So, one 10GE OLT interface is required per each SARDANA wavelength.

Ethernet VLANs are used to separate the different service in the PON level. Each VLAN provided from the Service Switch get mapped to different GEM-ports and each GEM-port from the PON gets mapped to different VLANs in the OLT.

IPTV service is using a dedicated multicast VLAN to Multicast GEM port association. Each ONU and CPE site is provided with all multicast channels to simplify the design. Internet access is provided via 1:1 VLAN access instead of 1:N scheme to avoid MAC switching functionality implementation at the OLT. Videoconference service is also relying on 1:1 VLAN access. CPE video equipment connects to ONU 1G

port at two ONU locations and a VLAN cross-connection is provided at the Service Switch for point-to-point video transmission.

The element management from the Control PC is using a dedicated OMCI-VLAN and OMCC interworking [164-169] to transport management messages over the PON.

Also, some considerations for simplest test implementation are taking into account:

- 1) Just a single PON support for the OLT protoboard is need. This may allow us to fit OLT MAC in a single programmable device.
- 2) Only maximum four ONUs per PON is supported in the prototype. It is anticipated that the number of prototypes we can make is very limited. This low number of ONUs per PON could simplify operation a lot.
- 3) Fixed bandwidth assignment per ONU. This simplifies OLT bandwidth management and grant allocation – OMCI and user data T-CONTs are always allocated
- 4) No downstream encryption, in demos and trial we do not guarantee privacy. This should simplify design.
- 5) FEC is not supported initially. It would be good if it were possible to support it in later releases to get the additional dB or two to the power budget.
- 6) Expect the Access MAC tables to be very small in the SARDANA demo and trial networks – only 1-4 ONUs per PON.
- 7) DBRu is not implemented.
- 8) Upstream BW map SStart and SStop 16-bit field is defined.
- 9) No GEM fragmentation is performed.

6.1.6. SARDANA Layer 2 system operation

Figure 6.12 shows SARDANA system layer 2 implementation via FPGA in-built at the Altera Stratix IV GX board; read/write registers and OMCI control using telnet, via CPC; Ethernet and Optical (TST 9061) interfaces; OLT, ONU and ODN SARDANA.

At a glance, the processes at the SARDANA system (e. g. downstream transmission) are:

- 1) The VLAN tagged Ethernet user frames, received at the baseboard from Ethernet Metro network via SNI, are passed through the 10GE MAC to the 10G OLT transmit block. The user frames are adapted for transport over the PON SGEM port-IDs.
- 2) The OMC/Ethernet frames are passed on to the OMCI interworking function that adapts the OMC/Ethernet to OMC/OMCC-SGEM port-ID transport.
- 3) Both user frames and control frames are multiplexed to the DS SGTC frame payload. A PSBd basic should be implemented by using the Psync code. ASTC frame should be implementing an US BW map, resulting of the DBA algorithm. In first instance, a static bandwidth assignment will be used.
- 4) The downstream frame is sent to OLT optical module interface over the HSMC in 16 bits parallel 622MHz LVDS logic.
- 5) The BCM8154, on the optical module, serializes this framer interface to an LVDS 10Gps CML signal that is connected via two right angle PCB edged SMA jacks (RPC-2.92) and 50 Ohm precision coaxial cables to the transmitter OLT optics assembly.
- 6) In this OLT optics assembly, electrical 10 Gbps CML signal modulates a 1550nm optical carrier via an MZM. Resultant optical signal is multiplexed on a fibre and sent to SARDANA optical distribution network (ODN).
- 7) At the user's premises, the ONU optics assembly receiver gets it 10GbpsDS frame. It implements optical-to-electrical conversion via PD.
- 8) The electrical 10Gbit/s CML signal is converted to 16-bits parallel 622MHz LVDS signal by the BCM81541:16 SERDES transceiver. This signal is transport to the baseboard via HSMC connector.
- 9) This DS-frame is fed into the ONU MAC RX block which finds frame delineation and drops the user data SGEM port-ID and OMCC SGEM port-ID fragments from STC payload for either frame reassembly or OMCI IWF for adaptation to Ethernet/OMC.

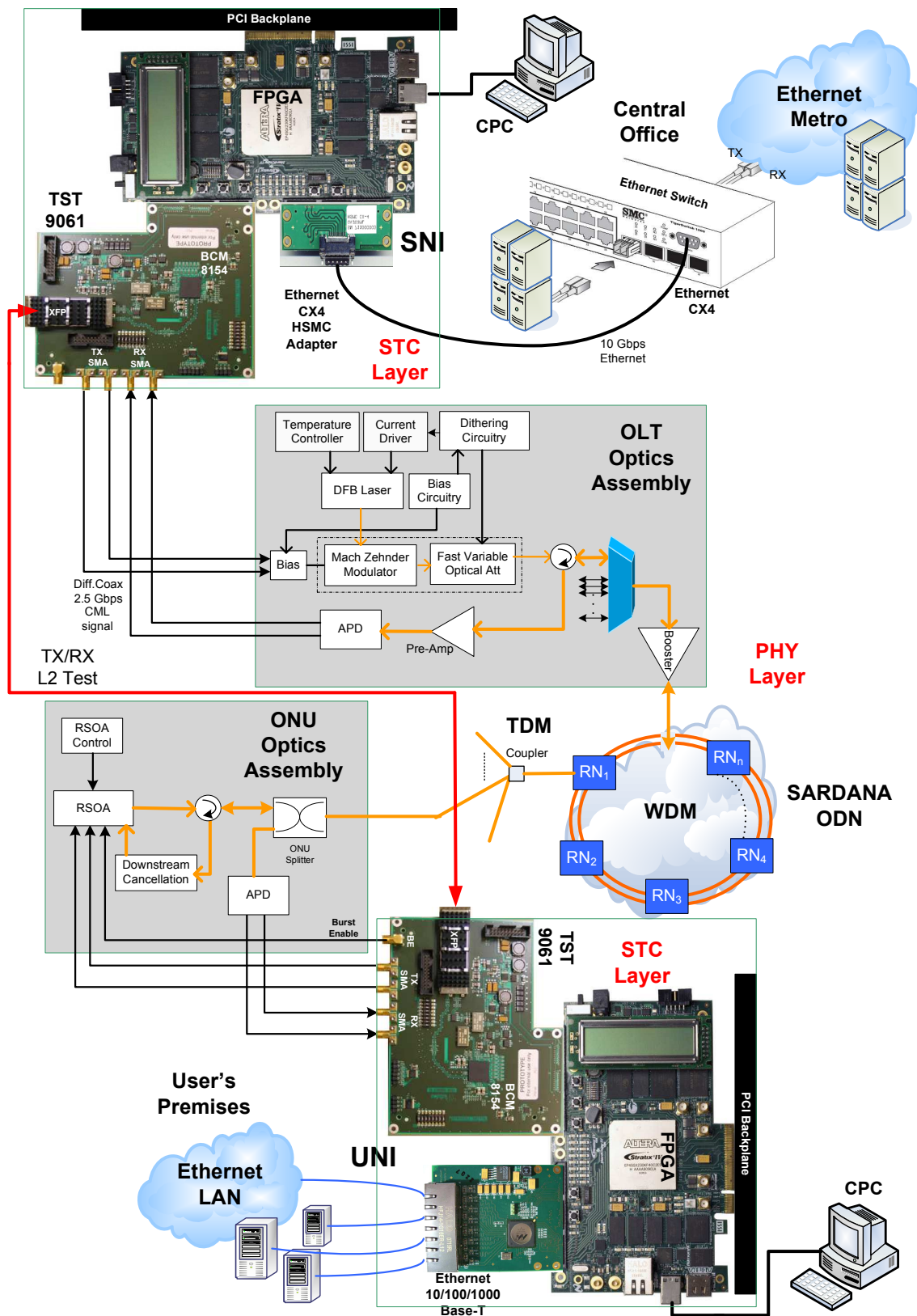


Fig. 6. 12 - SARDANA network system: MAC and PHY implementation

10) Ethernet frames are delivered to user equipment, via UNI interface.

11) Also, ONU STC RX read the US BW map from STC frame header and organizes the upstream burst signal to send.

A direct connection between OLT and ONU protoboards for using XFP transceiver [150] at 10 Gbps is implemented for layer 2 test for compliance.

It is interesting to note that OMCI management operation has a processing slower than PLOAM or OAM embedded, for this reason it is a GEM client (OMCI information is into GEM payload).

A SARDANA Layer2 back-to-back for OMC/Ethernet and CLI/Telnet tests was done in Tellabs-Oy, in Finland. It is shown in Fig. 6.13.

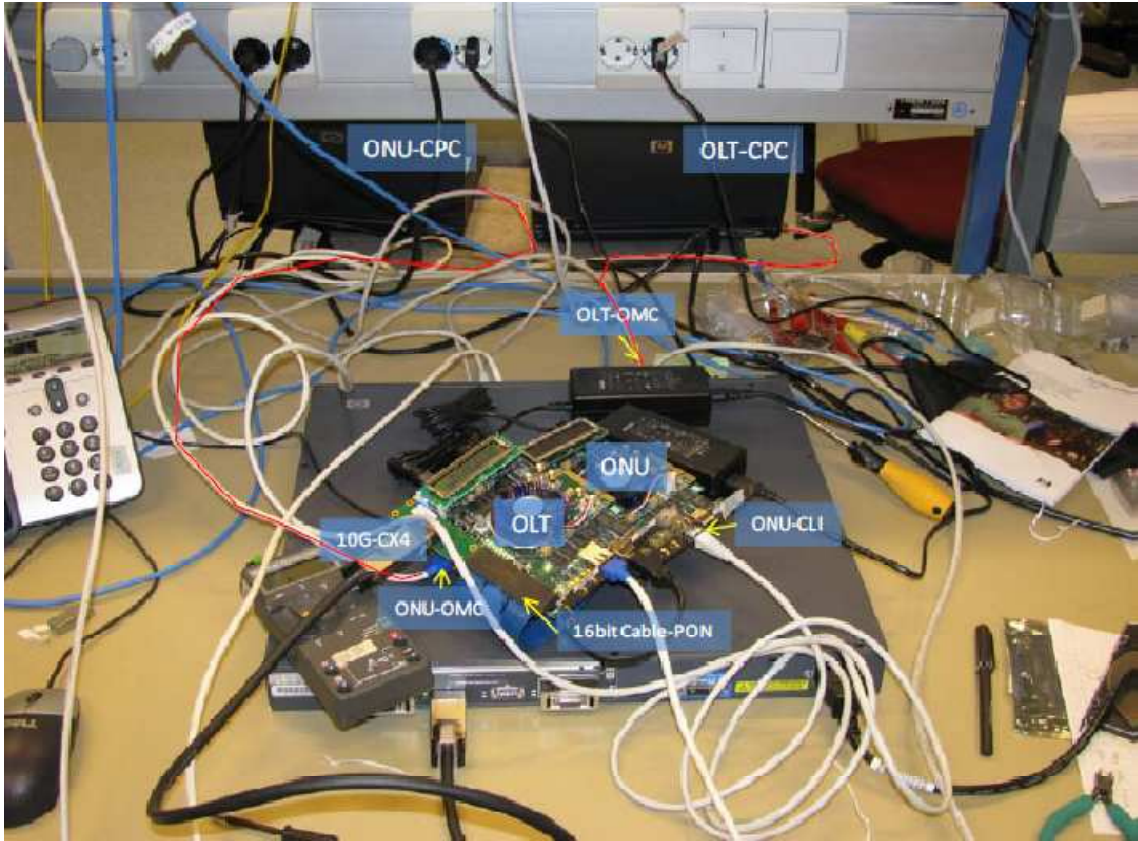


Fig. 6. 13 – SARDANA Layer 2 B2B setup used at the Tellabs OY (Espoo-Finland) for OMC/Ethernet and CLI/Telnet tests.

6.1.7. Interlayer encapsulation process in SARDANA

Figure 6.14 presents the sequence of operations between layers in the encapsulation process in downstream transmission on SARDANA network. To facilitate the presentation of this sequence, it is considered that an entire Ethernet frame is allocated in the SGEM frame and, therefore, full Ethernet frame is transmitted.

User's Data and OMCI information are transferred to the SARDANA TC layer from application software in the Application layer. In SARDANA, OMCI commands use a CLI (Command Line Interface) to interact with TC layer by means Ethernet protocol.

In the Transport layer, the information is fragmented. Here, two protocols are used depending on the nature of the information or services to transmit, as data can be time-sensitive or not:

- Internet data information or e-mail, they are not latency sensitive. They use TCP (Transmission Control Protocol).
- Videoconferencing, VoIP, IPTV, etc, are real time data services. They use UDP (User Datagram Protocol), often together with RTP (Real-time Transport Protocol) or Real-Time Control Protocol (RTCP), for the reliable transmission.

A transport header is added it to associate this fragment to a socket. The PDU (protocol data unit) in this layer is named "segment". Here it is necessary to make a distinction. In layered systems, the PDU is a unit of data that is specified in a protocol of a given layer and that consists of protocol-control information of the given layer and possibly user data of that layer; whilst a service data unit (SDU) is a unit of data that has been passed down from a higher layer (n) to a lower layer (n-1) and that has not yet been encapsulated into a protocol data unit (PDU) by this lower layer [172,175]. All the data contained in the SDU becomes encapsulated within the PDU.

By continuing, at the Network Layer, a header with IP address and other network parameters are added at this segment. The information is sent as a "packet" (PDU of layer 3) to the Link layer.

At the Link layer, the Ethernet protocol takes this SDU as its payload and adding a Destine/Source MAC address as header. This frame is the frame client (SDU) of the SARDANA TC layer.

So, considering real-time data transmission (e.g. Videoconferencing), where SIP or H.323 protocols are used at the OSI model Session Layer (considered here as a part of the Application Layer), and RTP/UDP/IP is the popular protocol stack, the application-layer packets go through RTP, UDP, IP and Ethernet.

Therefore, $12 \text{ (UDP)} + 8 \text{ (RTP)} + 20 \text{ (IP)} + 18 \text{ (Ethernet)} = 58$ bytes is added into each packet before SGEM encapsulation.

So, the data frame flows in the U-Plane, it is fragmented and encapsulated into a SGEM payload and is identified by its traffic type (implicitly indicated by an Alloc-ID) and its Port-ID (used to identify flows) allocated in a SGEM header.

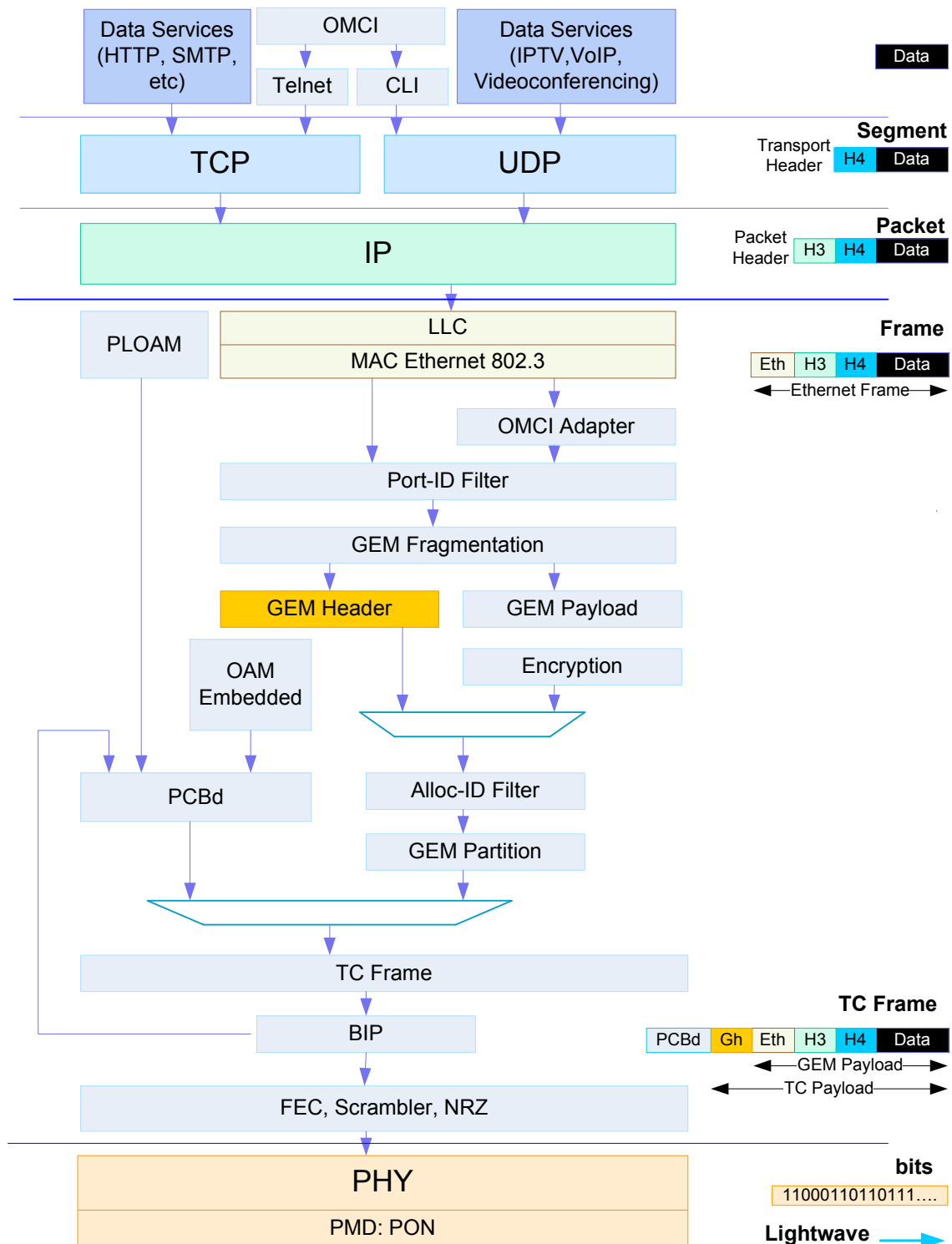


Fig. 6. 14 - Interlayer encapsulation in the SARDANA Network Downstream process

This SGEM frame is multiplexed into a STC frame together other SGEM frames. Now, a new header, named STC header, is added to this data frame. This header is formed by parameters and messages from Embedded OAM block and PLOAM block. Embedded OAM provides time sensitive OAM

functionalities consisting of Granting, Key switching for security and DBA related functionalities. Bandwidth assignment and QoS control are performed in every T-CONT. PLOAM block provides PON management functionalities, such as ranging, activation of ONU, establishment of OMCC, etc.

This downstream STC frame is finally adapted at the physical layer with a PSBd (PSync) and FEC, Scrambler and NRZ processes, into a 125 us DS PHY frame, before it to be sent.

6.2. SARDANA Internetworking

Traditionally, the optical layer of the network has been viewed as a simple transport medium. Its primary function has been to provide a connection between electrical layer devices in the form of static, high-capacity pipes [176]. The introduction of intelligent optical networking changes this paradigm. SARDANA optical network introduces increased functionality that electrical layer devices (e. g. IP routers, Ethernet switches) can now use to enhance and optimize end-user network services.

SARDANA Internetworking capabilities are shown in this section. This contribution deals about the relationship of SARDANA with other communications systems in the context of broadband access, and aims at describing the connectivity requirements of SARDANA. Because their Metro-Access coverage and Transmission Convergence (TC) layer capabilities, SARDANA network can provide transport services to other providers networks.

Although SARDANA system can sharing the infrastructure with current GPON [125] and GE-PON systems [177] as a NG-PON1; however, these systems cannot make full use of the SARDANA features, so we state that SARDANA is mainly positioned in the NG-PON2 generation. Better than this, SARDANA can transport those different systems in an efficient way.

These internetworking services can be implemented between metro networks (at the metro network level), or as an interconnection add/drop node, into a backhaul transport network, or as an overlay gateway between different networks.

For each of these services, SARDANA network can offer end-to-end transport by encapsulating information (into SGEM/STC frames) at L2/L3 management levels or by using transparent transport services, at L1 level.

In order for different protocols from different layers can be transported by SARDANA network, a multi-protocol management mechanism is proposed for implementation at STC SARDANA. This enables SGEM header incorporates new fields (different of XGEM, from ITU-T G.987.3, as shown in 5.2.3.1 section) to offer new features as advanced networking functionalities and QoS.

So, *Protocol ID* field carry information from protocols used in the upper layers of a metro network (Ethernet, MPLS, SDH/SONET, ATM, IP, others) or protocols used in transport networks (e.g. GMPLS). This implementation extends the service capabilities of a PON. Also, *PT (payload type)* field, transport information of the payload contents, and *QoS (Quality-of Service)* field can be used to ensure privileged services at real-time transmissions, security-sensitive data and QoS itself.

6.2.1. Ethernet frame over SGEM

Ethernet frame over a GEM frame is the typical and regular transmission mode in a G-PON FTTH network [97]. Ethernet frame (except preamble and SFD fields) is carried directly in the SGEM payload, equal to XGEM. Each Ethernet frame is mapped into a single SGEM or, as maximum, two SGEM

frames. An SGEM frame may not encapsulate more than one Ethernet frame. Fig. 6.15 shows a part of the Link Layer (OSI model) from a viewpoint of framing.

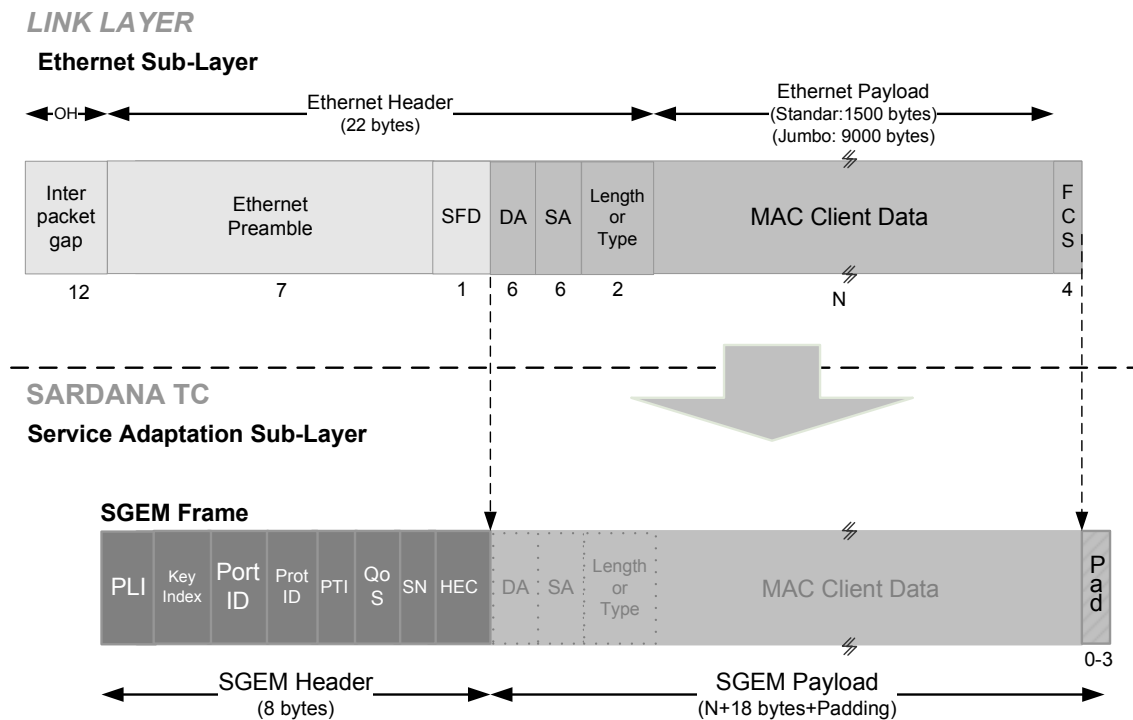


Fig. 6. 15 - Ethernet frame mapping into SGEM payload (modified from G.987.3_F9-5)

After, the SGEM frame (header + Payload) will be encapsulated as a payload of next SARDANA sub-layer (the Framing sub-layer) and will be a new SDU of the STC frame.

6.2.2. Multi-Protocol Management (MPM)

In SARDANA Transmission Convergence (STC) architecture, a mechanism based on a fast analysis of the L2/L3 (link layer/network layer) headers allows to obtain relevant information of protocols, formats and services operating in the upper layers. This information is very important to implement internetworking and interoperability services. This mechanism is deployable via a multi-protocol management (MPM) processor, as an additional processing function of the FPGA at the STC Service Adaptation Sub-layer, previous to SGEM encapsulation process.

6.2.2.1. MPM processing

In normal operation, the delineation process in MPM relies upon the presence of a Link protocol header at the beginning of every SDU frame. By considering that a SGEM frame may not encapsulate more than one Link protocol frame, the SGEM payload section will contain the Link protocol header (or a part of it, e.g. in Ethernet are relevant 14 bytes of its header, as shown in Fig. 6.15), as well as all the Link protocol payload content. This last payload, in turn, contains, in their first bytes, the header from the Network protocol (L3) (e.g. an IP header), at which gives the link services.

So, MPM detects the start of the SDU, establish the boundaries of both two headers using a bit counter and making a mapped of this information. Subsequently, read the content of the fields detected and process this information. Relevant essence is transmitted to the SGEM header, into the Protocol-ID, PT and QoS fields. This SGEM frame is sent to framing sub-layer where is encapsulated into a STC 125us frame to be transmitted afterwards to all network. Fig. 6.16 shows the encapsulation process between layers, based on the OSI model, and the MPM processing.

Also, MPM processor provides this information to QoS process and DBA control. By considering that traffic classification may be carried out at various levels of the OSI model: at the application layer (by means of the user’s identity, the URL, etc.), at the transport layer (by means of TCP or UDP ports), at network layer (by means of IP packet addresses, the ToS fields, diffServ), and at the link layer (e.g. VLAN identifier), a system as SARDANA MPM, capable to detect traffic type of the higher layers, gives at the network client capabilities to management transparently its services for each of their network users.

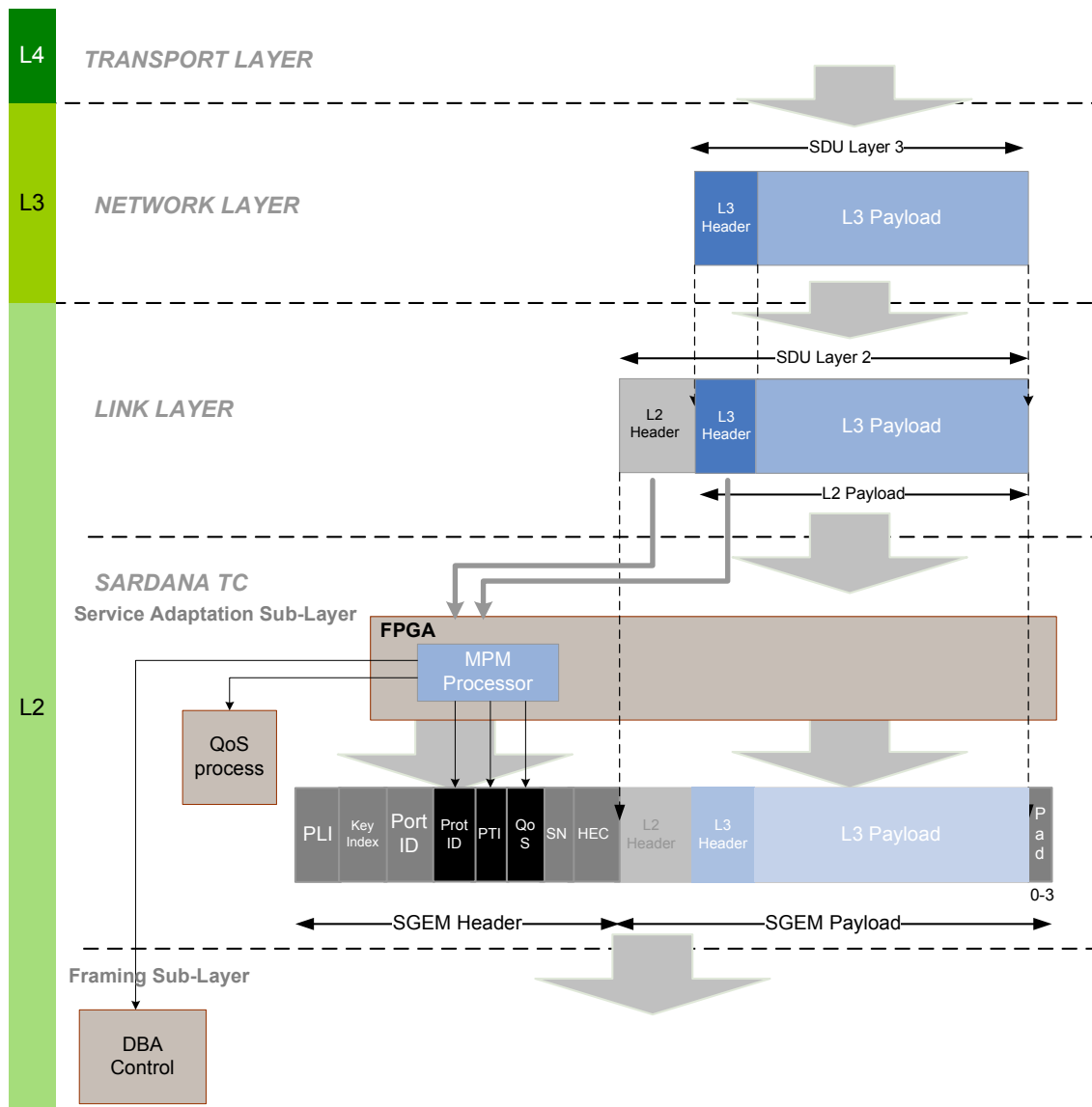


Fig. 6. 16 - Encapsulation between layers based on the OSI model and MPM processes.

6.2.2.2. MPM processing for IP over Ethernet services

By considering Ethernet protocol [177] and IP protocol [178] the most used link layer/network layer protocols, these will be used to explain the process done by MPM.

IP Packet Header

The IPv4 packet header consists of 14 fields, of which 13 are required and one is optional. So, without considering the *optional* field, its length is 20 bytes. IP header is shown in Fig. 6.17.

The most significant fields of this header for MPM STC SARDANA are:

Version: Identify the IP version field. In this example, we consider the IPv4. IP version 6 header can be found in [179]. Also, because not all networks support dual-stack (IPv4/IPv6), tunneling is used for IPv4 networks to talk to IPv6 networks (and vice-versa).

Internet Header Length (IHL): This field specifies the size of the header. The minimum value for this field is 5, which is a length of 20 bytes. The maximum length is 60 bytes [178].

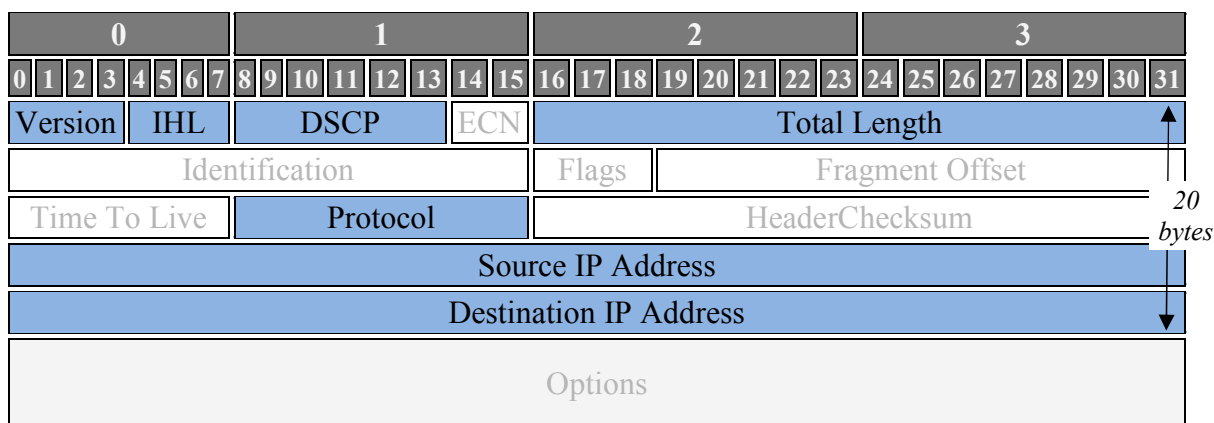


Fig. 6. 17 - IP header format

Protocol: This field defines the protocol used in the data portion of the IP datagram. The Internet Assigned Numbers Authority (IANA) maintains a list of IP protocol numbers which was originally defined in the RFC 790 and actualized in the RFC 1700 [180]. Also, a list of IP protocol numbers used in this field can be found in the RFC 5237 [181] and IANA list [182]. A part of these protocol numbers (in Hexadecimal) and references are shown in Table 6.1.

Table 6. 1 – Partial list of IP protocol numbers used in the Protocol field.

Hex	Keyword	Protocol	References
0x01	ICMP	Internet Control Message Protocol	RFC 792
0x02	IGMP	Internet Group Management Protocol	RFC 1112
0x04	IPv4	IPv4 (encapsulation)	RFC 791
0x05	ST	Internet Stream Protocol	RFC 1190, RFC 1819
0x06	TCP	Transmission Control Protocol	RFC 793
0x08	EGP	Exterior Gateway Protocol	RFC 888
0x09	IGP	Interior Gateway Protocol	

0x11	UDP	User Datagram Protocol	RFC 768
0x29	IPv6	IPv6 (encapsulation)	RFC 2473, RFC 3056
0x2E	RSVP	Resource Reservation Protocol	RFC 2205
0x84	SCTP	Stream Control Transmission Protocol	
0x85	FC	Fibre Channel	

Differentiated Services Code Point (DSCP): Or “Type of Service” field. This field is now defined by RFC 2474[183] for Differentiated services (*DiffServ*).

Total Length: Defines the entire packet (fragment) size, including header and data, in bytes. The minimum-length packet is 20 bytes (20-byte header + 0 bytes data) and the maximum is 65,535 bytes (the maximum value of a 16-bit word). The largest datagram that any host is required to be able to reassemble is 576 bytes.

Source address and Destination address: This field is the IPv4 address of the sender/receiver of the packet.

Fig. 6.18 shows an IP packet being encapsulated into an Ethernet frame. Important parameters from the IP header [178] for networking procedures are processed by the multi-protocol management processor and transmitted via new fields into SGEM header.

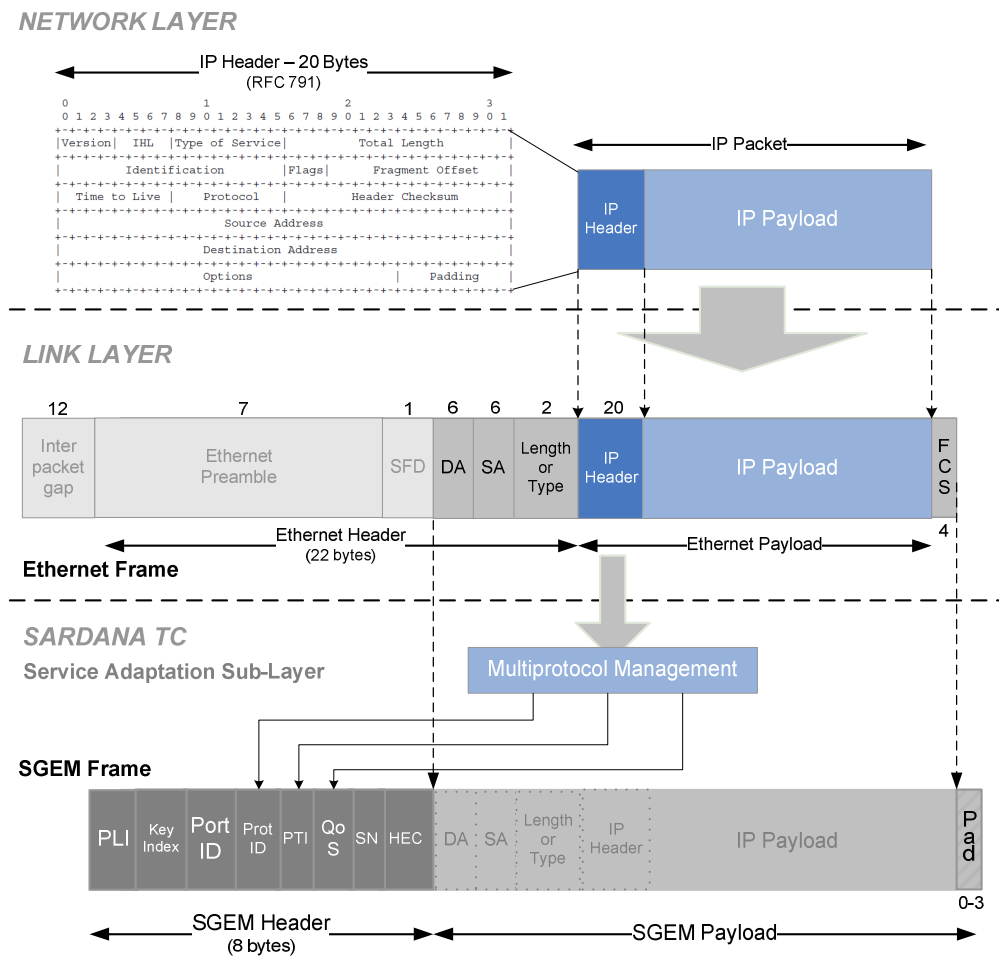


Fig. 6. 18 – IP header mapping from Ethernet frame for multi-protocol management in SARDANA metro/access network

A more explicit mapping scheme how MPM STC SARDANA processes the information obtained from the L3/L2 headers is shown in Fig. 6.19.

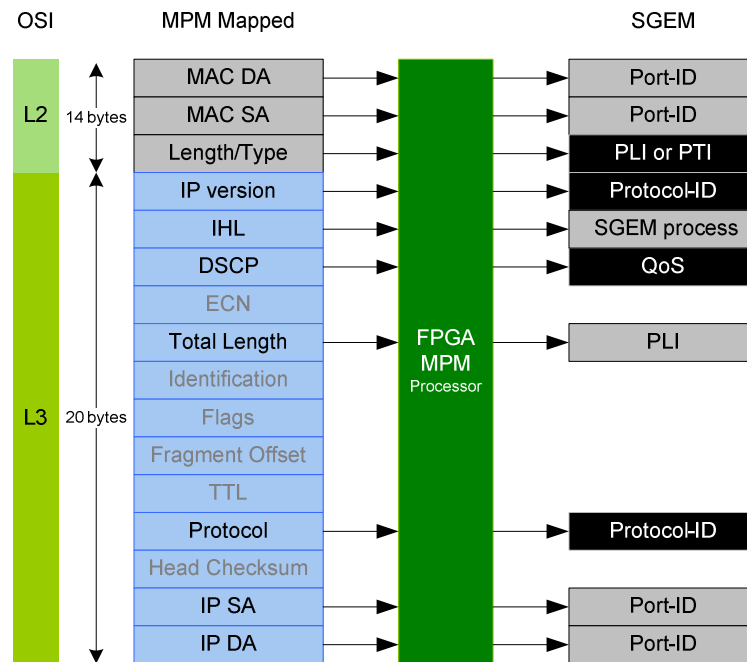


Fig. 6. 19 – MPM mapped of the IP/Ethernet headers (from Ethernet frame), on the SGEM frame.

Information from field Address *MAC DA* and *MAC SA* (Ethernet header), and *IP SA* and *IP DA* (IP header), are processed to establish users/networks target, and are carried in the *Port-ID* field on the SGEM header.

From the *Length/Type* field (Ethernet) is possible obtain up to two information: if this value is higher than or equal 1536 (decimal, maximum value of an Ethernet frame) [177], it indicates the protocol type into the payload, and this information is presented in the *PTI* field of the SGEM. Otherwise, this will shows Ethernet frame length information, which will be used in the *PLI* SGEM field. Also, IP *Total Length* field can be used to estimate the value in *PLI*.

From the *IP version* and *Protocol* fields are possible to determine the transport protocol type beyond the layer 3 (e. g. an UDP with RTCP Transport layer protocols for real-time audio/video transmission). This information is presented in the *PTISGEM* field.

From the IP DSCP field, differentiated service type (based on *diffServ* mechanism) can be obtained to establish the quality of services levels for this particular IP payload. This information is shown in the *QoS* SGEM field.

6.2.3. Network interoperability across SARDANA

SARDANA can be considered as a neutral/open network layer that can be shared by different PON operators in equal terms, with a high level of transparency, to guarantee their independency. Interoperability at different levels is possible. It ensures the interconnection of the network elements of SARDANA at the physical layer and management levels (layer2 or layer3).

6.2.3.1. SARDANA interoperability at Layer 1 level

Where SARDANA can provide a more advantageous solution is in the physical layer, specifically in the wavelength domain. The ring-tree topology of SARDANA provides an extra degree of freedom to allocate Remote Nodes or wavelengths to groups of users in a flexible way, as shown in Fig. 6.20.

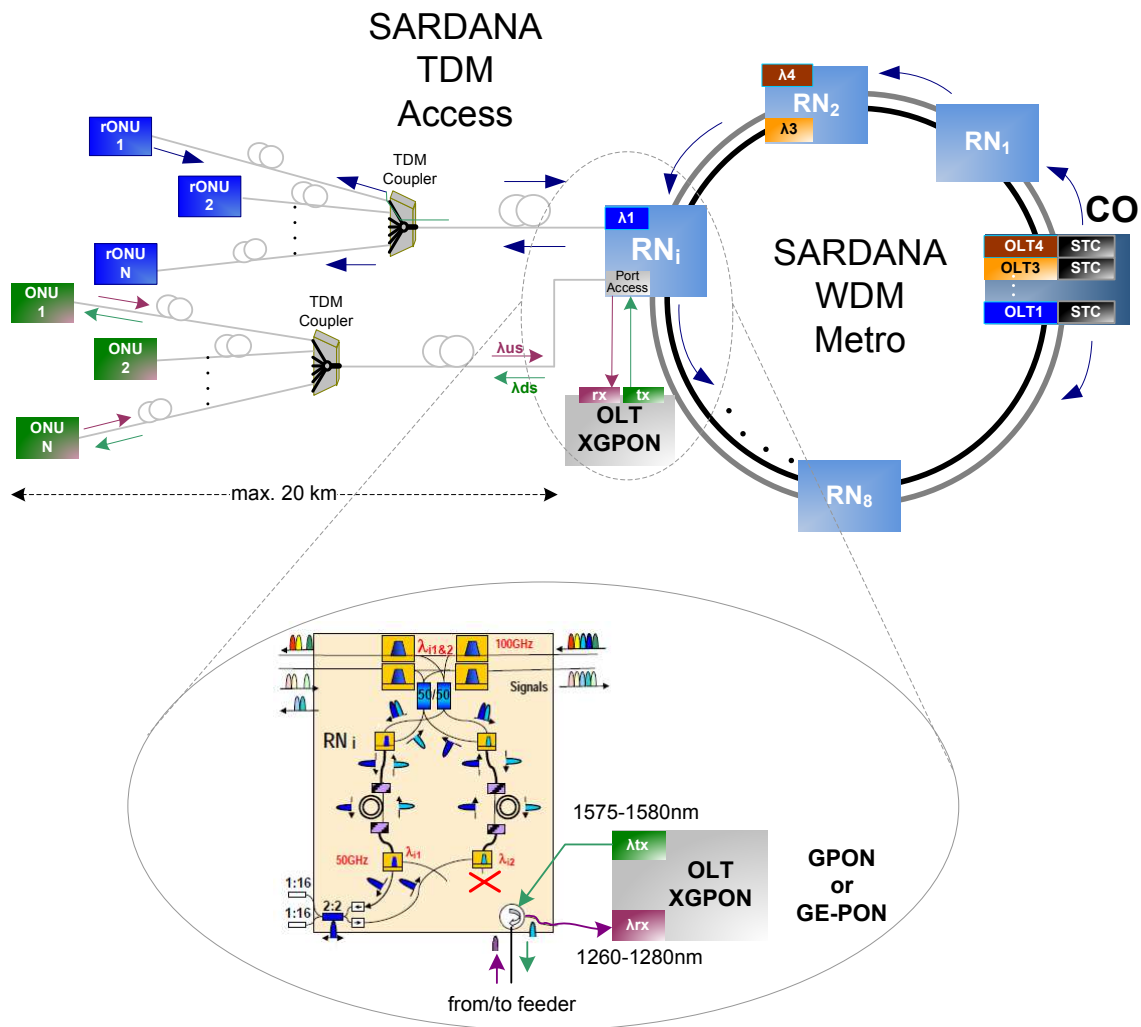


Fig. 6. 20 – SARDANA – XGPON (or GPON/GE-PON) interoperability PHY layer processes, for interconnection through a SARDANA remote node (RN).

Fig. 6.20 shows interoperability PHY layer between SARDANA and PON networks from operators using XGPON/GPON or 10GE-PON/GE-PON standards. In order to reach this purpose, a SARDANA remote node (RN) is adapted by disconnecting one of the branches of its regular wavelength filter and leasing this

port for TX/RX from the PON client. Here, different of SARDANA, XGPON/GPON or 10GE-PON/GE-PON networks use at least two wavelengths (DS/US) to implement their transmissions.

6.2.3.2. SARDANA interoperability at higher Layer level

Interoperability end-to-end between networks must consider management at the higher level (internetworking). SARDANA offer capabilities for transmission end-to-end in its Metro/Access network for encapsulating the PDU higher layers from Service's networks.

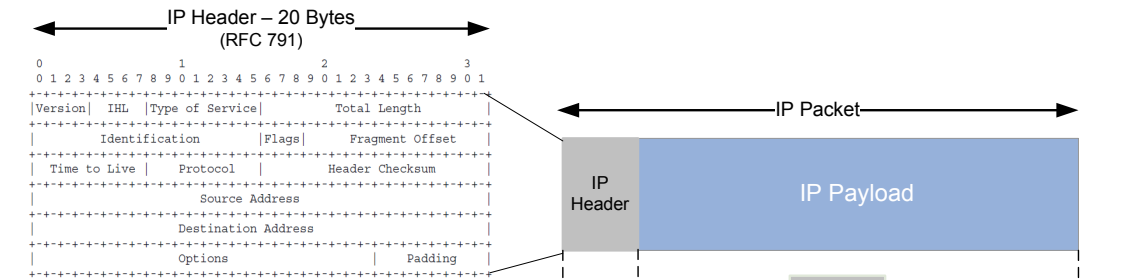
MPLS over SGEM

Multi-protocol label switching (MPLS) is a hybrid technology aimed at enabling very fast forwarding. IP packets are switched through the MPLS domain through simple label lookups. In the practice, labels are used to differentiate the type of service to each packet within the MPLS domain [176,184-185].

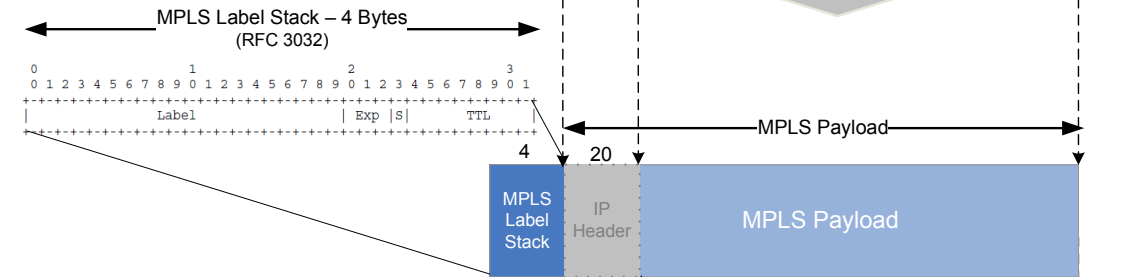
In MPLS, the assignment of a particular packet to a particular Forwarding Equivalence Class (FEC) is done just once, as the packet enters the network. The FEC (a set of packets with similar characteristics which may be forwarded the same way) to which the packet is assigned is encoded as a short fixed length value known as a "label". When a packet is forwarded to its next hop, the label is sent along with it; that is, the packets are "labeled" before they are forwarded [185-186].

In SARDANA, MPLS packets are carried directly in the SGEM frame payload. In this case, SARDANA network transmit edge-to-edge this information. From the MPLS viewpoint, SARDANA network provides a tunnelling point-to-point for a MPLS Label Edge Router (LER) in order to transport their SDUs. As shown in Fig. 6.21, a MPLS packet from the Link Layer is encapsulated into a single SGEM frame at the Service Adaptation sub-layer. Also, it is possible mapping into multiple SGEM frames. An SGEM frame may not encapsulate more than one MPLS packet.

NETWORK LAYER



LINK LAYER



SARDANA TC

Service Adaptation Sub-Layer

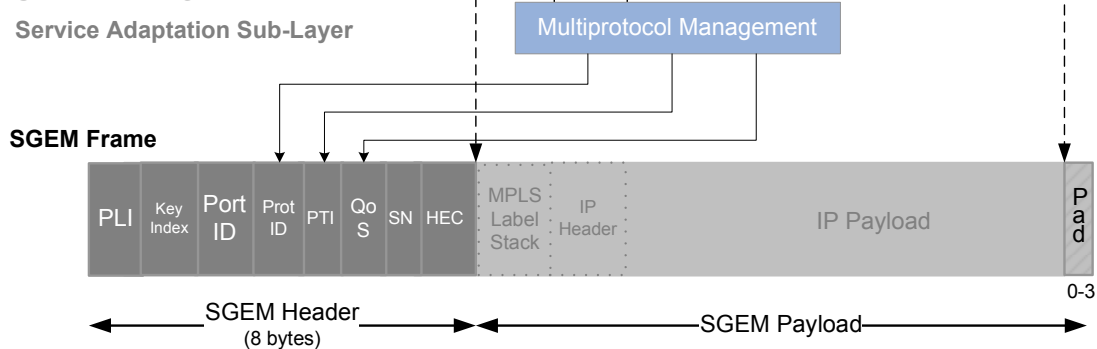


Fig. 6. 21 – MPLS packet mapping into XGEM frame

Also, significant information can be obtained for the MPLS payload (from the encapsulated IP header), for using multi-protocol management utility to the transport of the upper layer data with QoS.

6.2.3.3. SARDANA capabilities for Core Network Services

A SARDANA OLT can be used as an edge node of a transport (core) network and offer overlay capacities. The overlay model is commonly referred to as the user-network interface model. The electrical (or optical) layer devices (user/client) operate more or less independently of the optical devices (network). In this client-server network architecture provisioning of bandwidth is made possible. The client device (e.g. a router, a switch or an OXC) request the connection and the server (the SARDANA network) grants the request for bandwidth.

Fig. 6.22 shows this scenario. In this case, SARDANA is doing tunnelling, between the OLT and a Remote Node (RN), for the client data transport. A requirement for this particular implementation is that the network client, to whom the service is given, is working at the same wavelength of any OLT - RN

pair of the SARDANA network and this is available. These constraints are due to the WDM filters at the RN (as seen in Chapter 5), and the traffic conditions of the network in that moment.

GMPLS transport over SARDANA

Generalized MPLS (GMPLS) [172,187-189] is a common control and signalling transport protocol for switching and routing at the backbone. This extends MPLS to encompass time-division (e.g., SONET/SDH, PDH, G.709), wavelength (lambdas), and spatial switching (e.g., incoming port or fibre to outgoing port or fibre). So, Different of MPLS, in GMPLS transport protocol a label can be a wavelength. Thus, GMPLS network switched lambdas between their entities.

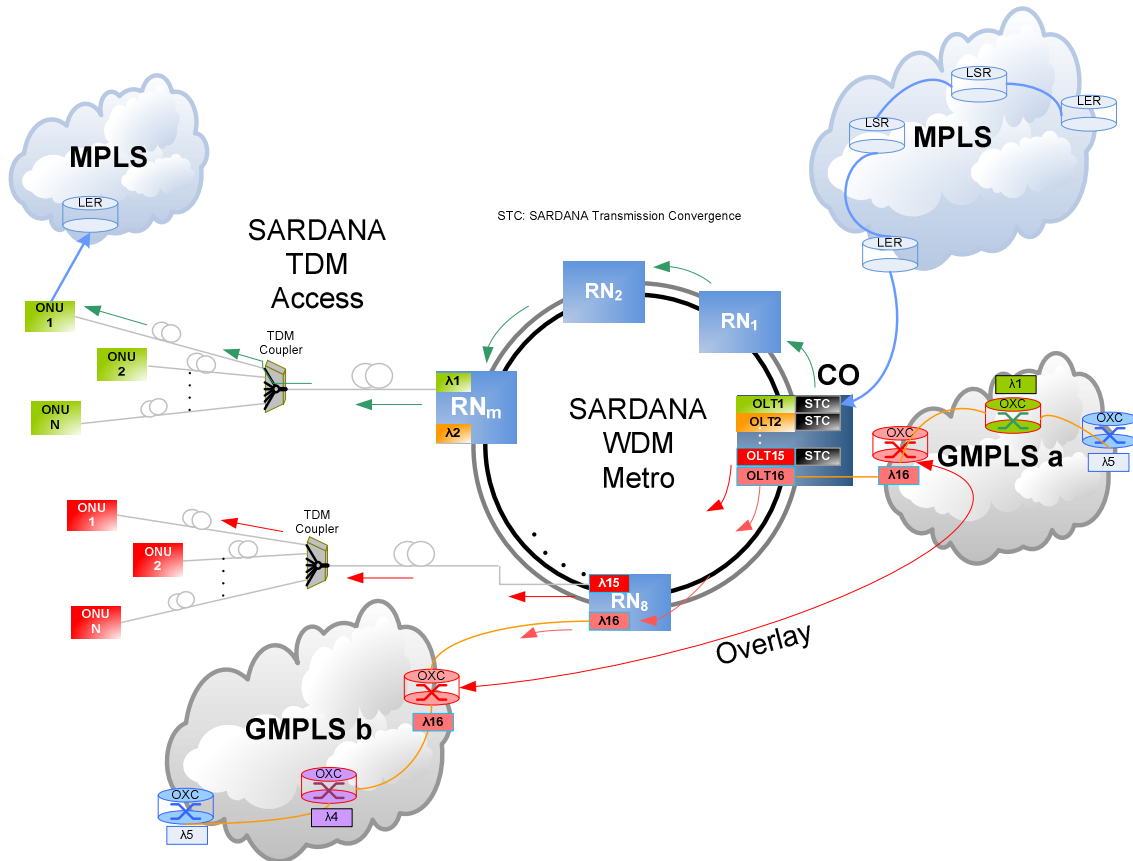


Fig. 6. 22 - SARDANA metro MPLS point-to-point transmission and overlay capacities for the GMPLS Transport Network

For conveying SDUs from the GMPLS transport network, SARDANA OLT should behave like a Lambda Switch Capable (LSC) interfaces and switch SDUs based on the wavelength on which these data are received. A LSC, such as an Optical Cross-Connect (OXC), can operate at the level of an individual wavelength.

a) Internetworking at the SARDANA PHY level

An edge OXC should transport information in the same lambda of an OLT of the SARDANA central office (associated with a RN of the ring), if this OXC want to use the SARDANA overlay capabilities.

In Fig. 6.22, two GMPLS networks (GMPLS_a and GMPLS_b) are linked through SARDANA network. OXCs switching lambdas into GMPLS network as a function of the lighthpath to be used. In this example, the edge OXC uses the λ_{16} (a wavelength capable of being filtered by a SARDANA RN) to connect straightforward with the OLT output port. Here, it is not necessary any STC layer 2 processing. Interoperability occurs at the SARDANA PHY level. SARDANA metro makes tunnelling functions between OLT output and RN and vice versa, offering add/drop bidirectional remote passive amplification for the GMPLS data transmitted, working as a transparent lighthpath between these transport networks.

Also, Fig. 6.22 shows MPLS packets carried edge-to-edge directly for SARDANA. Here, layer 2 interoperability is implemented through STC capabilities. MPLS packets are loaded into SGEM frame payloads and transport across the entire infrastructure.

b) Internetworking at the SARDANA L2/L3 Layer

Although STC layer corresponds to the Layer 2 of the OSI model, SARDANA STC is able to perform transport capabilities between different networks, by using tunnelling, and with QoS for using multi-protocol management utility.

As seen in section 6.2.1.1., SARDANA STC implementation uses Ethernet protocol as natural interface with other client networks. Then, to implement support for Layer 3 connectivity, some transmission devices should be added at the Central Office (CO). An edge-to-edge connection through SARDANA to provide support at the Layer 3 communications between a GMPLS network (at the backhaul) and an IP network (at the access) is shown in Fig. 6.23. In this GMPLS network, the Interface Switching Capability (ISC) is a LSC (lambda switch capable) [188]. This LSC is deployable via a GMPLS OXC. This OXC, associated at an IP Switch/Router, allows the CO operates as a GMPLS edge, offering transport services to an IP network at other edge of the network. For this configuration, due to electric connection between routers, lambda requirement for traffic through SARDANA network is irrelevant.

IP packets, encapsulated into Ethernet frames by this IP Switch/Router, are sent via a 10G Ethernet port to the 10 Gbps Ethernet CX-4 HSMC adapters at the SARDANA OLT. The first 34 bytes of each Ethernet frame are examined into the STC layer for the multi-protocol management utility to obtain relevant information, before to be capsulated into SGEM frames and tunnelled over SARDANA ODN.

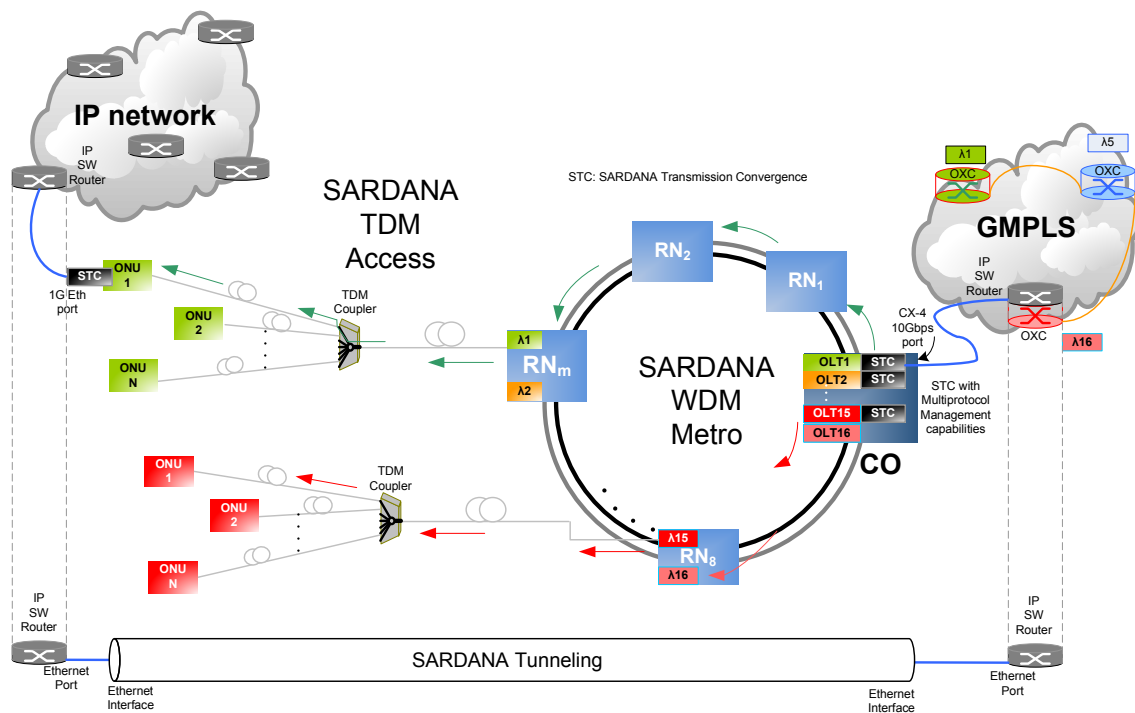


Fig. 6. 23 – Internetworking between a GMPLS network and an IP network by SARDANA tunnelling capabilities. At the other edge, according to the Port-ID, DS frame is filtered, SGEM frames are demultiplexed and decapsulated, and then sent to the 10/100/1000 Base-T Ethernet port corresponding. This port is connected to an edge IP Switch/Router into the IP network target.

6.3. Conclusions

An implementation proposal for the STC SARDANA architecture over the SXGPON original draft is shown in this chapter. OLT and ONU prototypes are deployable based on an FPGA that implements a 32-bit architecture, and suitable interfaces for interconnection with higher layer clients and OLT/ONU optical assemblies at the PHY layer.

Connectivity requirements and possible configurations for SARDANA internetworking with other communications systems in the context of broadband access are proposed. A Multi-Protocol Management processor, deployable at FPGA, is defined and its function necessary to do feasible advanced characteristics of connectivity and interoperability, enhancing Metro-Access capabilities of the SARDANA network and empowering Transmission Convergence (TC) layer functionalities.

These internetworking services can be implemented at the metro network level or at core transport network level.

Chapter 7

7. Conclusions and future work

7.1. General Conclusions

Because the increasing demands on broadband access for interactive applications, clients and operators expect more from standard and commercial PON networks. Solutions have been presented for FSAN and IEEE standardization groups to improve bandwidth. Nevertheless, other requirement that includes long reach and service support capabilities, as well as cost-effective architectures, enhanced performance and real passiveness of access nodes, improved bandwidth assignments and metro/access networks capacity need to be satisfied. A powerful alternative is the optimization over existing PON networks in direction to NG-PON networks.

In such sense, this Thesis proposes a redesign and optimization of three PON architectures: WDM-PON, TDM-PON and the hybrid WDM/TDM PON, in terms of minimum deployment cost and enhanced performance oriented to greenfield NG-PON.

At PHY level, a cost-effective long reach truly-passive WDM/TDM rONU-based PON network for 1000 users, and at MAC level, with an efficient access control and latency requirements, are the target.

In WDM-PON different parameters are susceptible to be optimized to obtain a better performance of the system. So, by analysing the RB behaviour in a WDM-PON, the better performance can be achieved if the distribution element (a Demux) is placed either in the ONU or OLT vicinity, by demonstrating that the Rayleigh substantially varies depending on the position of the distribution element since they are determined by the fibre length and by the ONU gain applied, where the ONU gain takes a new optimum

depending on that exact position of the Demux. These results can be used efficiently to minimize the RB effect in the next generation WDM access networks.

Also, a SCM WDM/TDM PON with ONU rSOA based, cost-effective, simple design and full service coverage, was designed, simulated, optimized and implemented. Several parameters (OLT output power, ONU splitting ratio, ERs, feeder fibre length, RSOA gain, modulation formats, etc.), become important optimization elements in order to find the best upstream/downstream trade-off. This prototype was successfully tested showing high performance, robustness, versatility and reliability. So, the system is able to give coverage up to 1280 users at 2.5 Gb/s / 1.25 Gb/s downstream/upstream, over 20 Km, and being compatible with the GPON ITU-T recommendation.

Rayleigh backscattering in burst mode TDM-PON transmission was for the first time deeply analyzed and their effects and behavior deterministically formulated. Critical cases are present in downstream transmission for configurations with lower ONU numbers (ex. rural scenarios) due to a higher energy concentration in the upstream burst and lower tree losses, and the resulting Rayleigh effect. In these cases, a network design with suitable bandwidth assignment (at layer 2 - MAC) and ONU gain control /power output control (at layer 1 - PHY) can mitigate these issues.

In the upstream direction, the difficulties are for scenarios with 32/64 ONUs, due to higher tree losses. Single-fibre/wavelength reflective PON has been optimized focusing on the best tradeoff between ODN power budget and US-oSRR. RSOA gain is the key parameter. By using FEC to BER $5E-4$, an optimal DS cancellation, a RSOA gain=21dB, an OLT output power between 0 to 3 dBm and a 90/10 TX/RX ONU splitting ratio, up to 32 users can be reached with a power budget margin tolerance to >0.5 dB. By redistributing the ODN (by feeder fibre reduction and drop increases), it is possible to improve the power budget tolerance to > 1.5 dB.

These optimization precedents have enabled the SARDANA to extend the design, architecture and capabilities of a WDM/TDM PON for a long reach metro-access network. The implemented test-bed demonstrates truly-passive extended PON, fundamental resiliency, XGPON1 rates, wavelength-agnostic single-fibre ONUs, neutral multi-operability optical infrastructure and cost efficiency in practical condition.

The technological advances developed in this project, like distributed add&drop, remotely pumped optical amplification, wavelength dithering, colourless reflective ONU with optical DS cancellation and opto-electronic equalization, and 10G/2.5G Gb/s rates, enable the feasibility of the new network concept for its application in future PON migrations. Enhanced performances can be pursued with improved RSOA or tuneable laser technologies, with burst-mode OLT RX and FEC coding.

To optimize the MAC and signalling procedures of the SARDANA, a proposal of Transmission Convergence sub-layer, (OSI model layer 2) is presented as a relevant contribution of this work. It is

based on the optimization of the standards GPON and XG-PON (for compatibility), but applied to a long reach metro-access TDM/WDM PON rSOA-based network.

New fields in the GEM (now SGEM) are included to encompass long reach metro/access coverage and as a function of their PHY characteristics. So, multi-protocol management, overlay transmission capacity (from different service providers), multi-services and multi-operator capability are deployable. Also, QoS and other higher layer services are possible. These new fields give SARDANA TC capacities to deploy internetworking functions.

The PLOAM message has a variable length. In this way, increased efficiency between 1.5x and 6x times can be reached, with respect to XG-PON. This allows releasing more space in the header to favour the payload section space.

An optimal Preamble and Delimiter fields of 192 bits (77.16 ns) plus a Guard Time of 80 bits (32.15 ns) as a function of the SARDANA PHY layer are defined.

In this work, an agile ONU activation process, by simplification of the ranging state, is presented. This mechanism reduces to one the use of a QW, by improving the efficiency. Although SARDANA metro/access network is up to 100 km, this optimization improves up to a 44% the performance with respect to XG-PON (20 km).

In XGPON, QW mechanism affects up to eight BWmaps during ONU activation. SARDANA optimization reduces the impact of the QW to five BWmaps in the most critical ODN scenario (100 km).

A physical implementation proposal for this STC SARDANA is also presented. OLT and ONU prototypes are deployable based on an FPGA that implements a 32-bit architecture, and suitable interfaces for interconnection with higher layer clients and PHY optical layer.

Connectivity requirements and possible configurations for SARDANA internetworking with other communications systems in the context of broadband access at the PHY level, at the metro network level or at core transport network level are proposed. A Multiprotocol Management processor, deployable at FPGA, is defined to do feasible advanced characteristics of connectivity and interoperability, enhancing Metro-Access capabilities of the SARDANA network and empowering Transmission Convergence (TC) layer functionalities.

7.2. Future research

Three themes are proposed to meet the requirements of a WDM/TDM long reach PON network at the layer 2 management:

1. A deep study on PON traffic for a metro-access network on different scenarios, in order to obtain relevant information for the optimization of the bandwidth management.
2. By considering that Quality of Service (QoS) capabilities are an integral part of the end-to-end QoS provisioning mechanisms, we propose a study and implementation of QoS levels. They are necessary, but not sufficient, to ensure that the QoS objectives of end-to-end traffic flows are met. It is associated with the ways and means to allocate available resources (including processing capacity, buffer space, and bandwidth), to individual traffic flows and traffic flow aggregates.
3. With these two inputs we propose the design of a most fair Dynamic Bandwidth allocation (DBA) for a more optimum bandwidth management. Thus, the network operator can add more subscribers to the metro-access network due to more efficient bandwidth use, and subscribers can enjoy enhanced services, such as those requiring variable rate with peaks extending beyond the levels that can reasonably be allocated statically.

Annex A

A. ITU-T XG-PON Layer 2 Architecture

XG-PON Layer 2 architecture is based on the transmission convergence layer (XGTC layer) for 10-gigabit capable passive optical network systems and is specified in the recommendation ITU-T G.987.3 from FSAN [97]. This provides a wide range of broadband and narrow-band services to end-users.

A.1. XGTC layer structure

The XGTC layer specifies the formats and procedures for mapping between upper layer SDUs (Service Data Users) and suitable bit streams for modulating the optical carrier, and it is present at both the OLT and ONU sides of an XG-PON system. It is composed of three sub-layers: the XGTC service adaptation sub-layer, the XGTC framing sub-layer, and the XGTC PHY adaptation sub-layer. The frame formats are devised so that the frames and their fields are aligned to 4-byte word boundaries [97] whenever possible.

A.2. XGTC layer procedures

a) In the downstream direction

The interface between the XGTC layer and the PMD (Physical Medium Dependent) layer [97], is represented by a continuous bit stream at the nominal interface rate, which is partitioned into 125 μ s frames. Fig. A1 shows the stages involved in the mapping between the upper layer SDUs and the PHY bit stream, where “H” is the frame header of the XGEM (XG-PON Encapsulation Method), “P” is the FEC Parity field, and “PSBd” is the physical synchronization block for downstream.

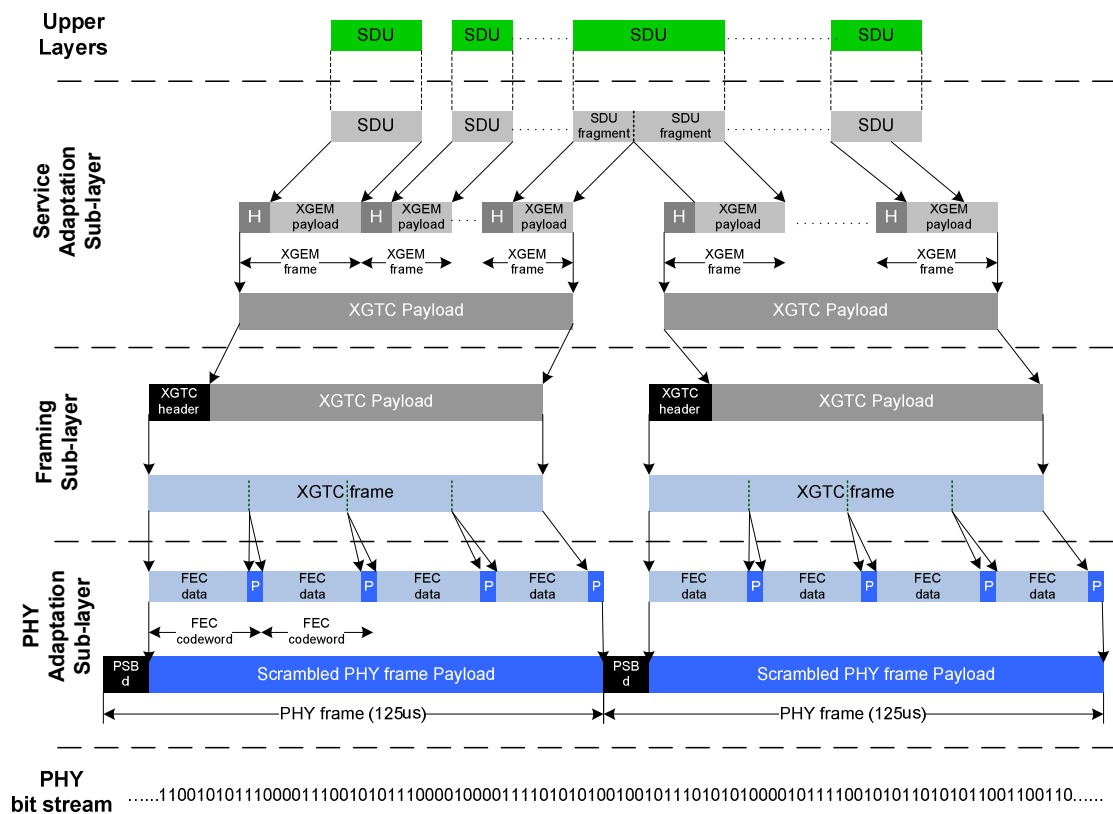


Fig. A. 1 - Downstream SDU mapping at the XGTC layer (Modified from G.987.3_F6-1)

The SDUs can be from different layer 2 protocols (MPLS, ATM, Ethernet). The most popular is the Ethernet protocol. In this work, the SDUs are Ethernet frames.

b) In the upstream direction

In this direction, the interface between the XGTC layer and the PMD layer is represented by a sequence of bursts. Fig. A2 shows these processes. A remaining fragment of the SDU is sent in the next allocation with the same Allocation ID (Alloc-ID). This may occur because an ONU can have more than one Alloc-ID as a function of the T-CONT (Transmission container) type or the QoS contracted by the user.

Here, “PSBu” is the physical synchronization block for upstream and “AO” is the allocation overhead.

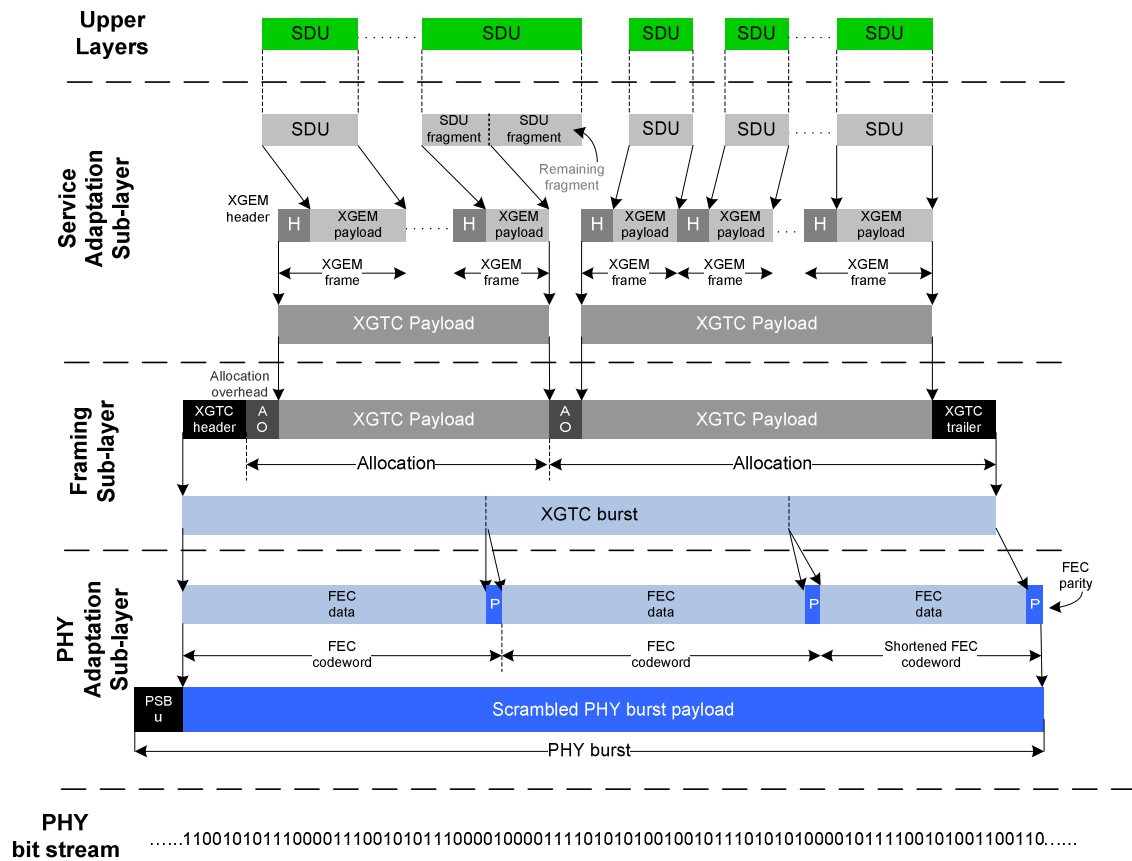


Fig. A. 2 -Upstream SDU mapping at the XGTC layer (Modified from G.987.3_F6-2)

A.3. Sub-Layers of the XGTC Layer

The XGTC layer is composed of three sub-layers, as shown in the Figs. A2 and A3:

- Transmission Convergence (TC) Service adaptation sub-layer:** implements the concepts of frame encapsulation based on XGEM (XG-PON encapsulation method) and port identification (XGEM Port-ID).

In TX, it performs the functions of SDU fragmentation (user data frame and OMCI (ONU management and control interface) traffic), XGEM port-ID assignment and frame encapsulation to obtain a XGEM frame.

In RX, it performs XGEM frame delineation, filtered of XGEM (based on the XGEM port-IDs) and reassembles the fragmented SDUs, delivering them to their respective clients.

- TC framing sub-layer:** is concerned with the structure of the 125 μ s XGTC frame. It supports the functions of frame/burst encapsulation based on XGTC and delineation frame/burst, embedded operations, administration and maintenance (OAM) processing, physical layer OAM (PLOAM) transport (an operation and management channel between the OLT and the ONUs that is close to real time and is based on a fixed set of messages), and Alloc-ID filtering.

It has three functionalities:

1) Multiplexing and demultiplexing

DS: PLOAM and XGEM portions are multiplexed into a 125us XGTC frame.

US: Each portion is abstracted according to header indicator.

2) Header creation and decode

DS: XGTC frame header is created and is formatted in a DS frame.

US: XGTC header is decoded. Embedded OAM is performed.

3) Routing function based on Alloc-ID

It is performed for data from/to XGEM TC Adapters.

- c) **PHY adaptation sub-layer:** Responsible for the reception and delineation of the signal transmitted over the ODN. This sub-layer executes forward error correction (FEC) over the XGTC frame/burst and performs scrambling (it manipulates the FEC data stream before transmitting, and the process is reversed by a descrambler at the receiving side, to improve the consecutive identical digit (CID) immunity). After, sets the PSBd (in downstream), or burst mode overhead (PSBu, in upstream), and provides timing alignment and line coding.

A.4. XGPON Management System

This part describes practical issues between the service node interface (SNI: at the OLT side), and the user-network interface (UNI: at the ONU side). The control, operation and management information in the system is carried over three channels: embedded OAM and PLOAM channels (these manage the functions of the PMD and XGTC layers) and OMCI channel (managing higher (service-defining) layers).

- a) **Embedded OAM.** This channel is implemented on several fields, defined in the DS/US frame/burst header and in the embedded structures for time-sensitive OAM functionalities (US PHY burst timing, profile control and dynamic bandwidth assignment (DBA) signalling).
- b) **PLOAM channel.** The physical layer OAM (PLOAM) messaging channel is an operations and management facility between OLT and ONUs that is based on a set of fixed messages (48 bytes), transported within a XGTC header. It supports the following functions: burst profile communication, ONU activation, ONU registration, protection switching signalling and power management [97]. The ONU processing time and the response generation from a downstream PLOAM message is 750 us.
- c) **ONU management and control interface (OMCI).** The OMCI uses the OMCI channel (OMCC) to manage the service-defining layers (above the XGTC) [164]. The XGTC layer must provide an XGEM-based transport interface for this management traffic.

Fig. A3 shows the XGTC information flow from/to clients at the upper layers passing through the XGTC layer and the functionalities of the three sub-layers.

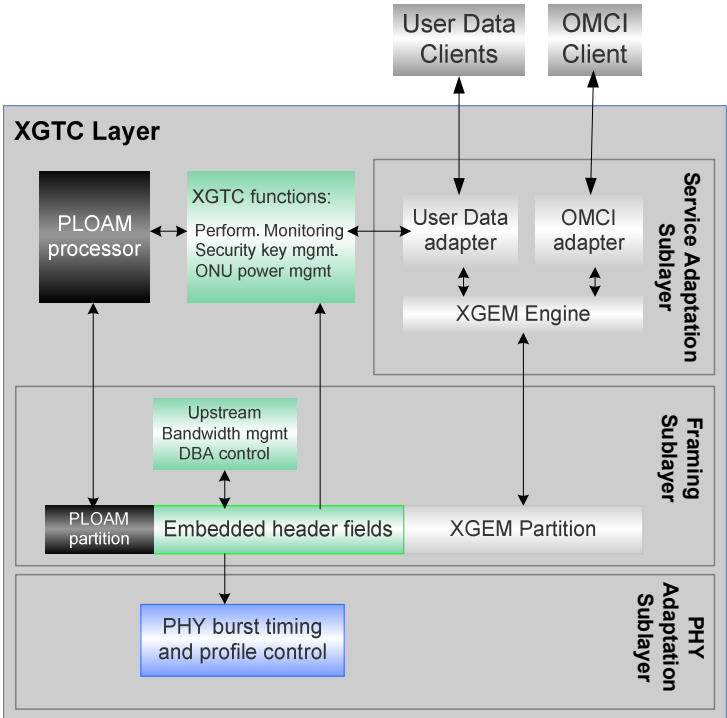


Fig. A. 3 - The XGTC information flow (Modified from G.987.3_F6-3)

References

- [1] ITU-T; “G.987.1 - 10 Gigabit-capable Passive Optical Network (XG-PON): General Requirements”; Geneva, January 2010.
- [2] IEEE; “802.3av – Part 3: Carrier Sense Multiple Access with Collision Detection (CSMA/CD) Access Method and Physical Layer Specifications – Amendment 1: Physical Layer Specification and Management Parameters for 10 Gb/s Passive Optical Networks”; 30 October 2009.
- [3] Dissanayake, S.D. ; Armstrong, J. ; “Comparison of ACO-OFDM, DCO-OFDM and ADO-OFDM in IM/DD Systems”; *Journal of Lightwave Technology*, Volume: 31, Issue: 7; Publication Year: 2013 , Page(s): 1063 - 1072
- [4] Linglong Dai ; Z.Wang ; Zhixing Yang; “Time-Frequency Training OFDM with High Spectral Efficiency and Reliable Performance in High Speed Environments”; *IEEE Journal on Selected Areas in Communications*, Volume: 30 , Issue: 4; Publication Year: 2012 , Page(s): 695 – 707.
- [5] Hussin, S. ; Punturi, K. ; Noe, R.; “Performance analysis of optical OFDM systems”; 3rd International Congress ICUMT 2011; Publication Year: 2011 , Page(s): 1 – 5.
- [6] Guoying Zhang ; De Leenheer, M. ; Morea, A. ; Mukherjee, B.; “A Survey on OFDM-Based Elastic Core Optical Networking”; *Communications Surveys & Tutorials*, IEEE; Volume: 15 , Issue: 1 ; Publication Year: 2013 , Page(s): 65 – 87.
- [7] Guoying Zhang ; De Leenheer, M. ; Mukherjee, B.; “Optical traffic grooming in OFDM-based elastic optical networks”; *IEEE/OSA Journal of Optical Communications and Networking*, Vol. 4 , Issue: 11, Publication Year: 2012 , Page(s): B17 - B25.
- [8] Xingwen Yi ; Fontaine, N.K. ; Scott, R.P. ; Yoo, S.; “Tb/s Coherent Optical OFDM Systems Enabled by Optical Frequency Combs”; *Journal of Lightwave Technology*, Volume: 28 , Issue: 14, Publication Year: 2010 , Page(s): 2054 – 2061.
- [9] Qi Yang ; Yan Tang ; Ma, Y. ; Shieh, William; “Experimental Demonstration and Numerical Simulation of 107-Gb/s High Spectral Efficiency Coherent Optical OFDM”; *Journal of Lightwave Technology*, Volume: 27 , Issue: 3, Publication Year: 2009 , Page(s): 168 – 176.
- [10] Charrua, P.M.A.; Cartaxo, A.V.T.; “Optimized filtering for AMI-RZ and DCS-RZ SSB signals in 40-Gb/s/ch-based UDWDM systems”; *Photonics Technology Letters*, IEEE, Volume: 17 , Issue: 1; Publication Year: 2005 , Page(s): 223 – 225.
- [11] Smolorz, S. ; Gottwald, E. ; Rohde, H. ; Smith, D. ; Poustie, A.; “Demonstration of a coherent UDWDM-PON with real-time processing”; *OFC/NFOEC*, 2011, Publication Year: 2011 , Page(s): 1 – 3.
- [12] Pavlovic, N.B. ; Cartaxo, A.V.T.; “Optimization of Single-Sideband DCS-RZ Format for Long-Haul 43-Gb/s/channel Ultradense WDM Systems”; *Journal of Lightwave Technology*, Volume: 25 , Issue: 2, Publication Year: 2007 , Page(s): 481 – 489.
- [13] Kasai, K. ; Otuya, D.O. ; Yoshida, M. ; Hirooka, T.; “Single-Carrier 800-Gb/s 32 RZ/QAM Coherent Transmission Over 225 km Employing a Novel RZ-CW Conversion Technique”; *Photonics Technology Letters*, IEEE, Vol. 24 , Issue: 5, Publication Year: 2012 , Page(s): 416 – 418.
- [14] Nakazawa, M., Okamoto, S., Omiya, T., Kasai, K., Yoshida, M.; “256-QAM (64 Gb/s) Coherent Optical Transmission Over 160 km with an Optical Bandwidth of 5.4 GHz”; *Photonics Technology Letters*, IEEE, Volume: 22, Issue: 3, Publication Year: 2010, Page(s): 185 - 187.
- [15] Creaner, M.J.; et.al.; “Field demonstration of coherent transmission system with diode-pumped erbium doped fibre amplifiers”; *Electronics Letters*, Vol. 26 , Issue: 7, Publication Year: 1990 , Page(s): 442- 444.
- [16] Karlsson, M. ; Agrell, E.; “Four-dimensional optimized constellations for coherent optical transmission systems”; 36th European Conference and Exhibition on Optical Communication (ECOC), 2010, Publication Year: 2010 , Page(s): 1- 6.
- [17] R. P. Davey, et al., “DWDM Reach Extension of a GPON to 135 km”, *IEEE/OSA J.Lightwave Technol.*, vol. 24, pp. 29-31, Jan. 2006.
- [18] M. Maier and M. Herzog, “STARGATE: The Next Evolutionary Step toward Unleashing the Potential of WDM EPONs”, *IEEE Comm. Mag.*, vol. 45, pp. 50-56, May 2007.
- [19] B. Zakowski, “Passive vs. Active Optical Networking: Real Estate Developers Wonder”; *BROADBAND PROPERTIES* journal; www.broadbandproperties.com, May 2004
- [20] F.T. An et al., “SUCCESS: A Next-Generation Hybrid WDM/TDM Optical Access Network Architecture,” *IEEE/OSA J. Lightwave Technol.*, vol. 22, pp. 2557-2569, Nov. 2004.
- [21] J.M. Oh, S.G. Koo, D. Lee, and S.J. Park, “Enhancement of the Performance of a Reflective SOA-Based Hybrid WDM/TDM PON System With a Remotely Pumped Erbium-Doped Fiber Amplifier”, *IEEE/OSA J. Lightwave Technol.*, vol. 26, pp. 144-149, Jan. 2008.
- [22] J.A. Lazaro, C. Bock, V. Polo, R.I. Martinez, and J. Prat, “Remotely amplified combined ring-tree dense access network architecture using reflective RSOA-based ONU”, *OSA J. of Optical Netw.*, vol. 6, pp. 801-807, Jun. 2007.

- [23] C.-H. Lee, W. V. Sorin, and B. Y. Kim, "Fiber to the Home Using a PON Infrastructure," *Lightwave Technology, Journal of*, vol. 24, pp. 4568-4583, 2006.
- [24] C. Martin, "Realization of a Super PON Demonstrator", in Proc. NOC'97, Antwerp, Belgium, pp. 188-193, Jun. 1997.
- [25] M. O. van Deventer et al., "Architecture for 100 km 2048 split bidirectional Super PONs from ACTS-PLANET", *Proc. SPIE*, vol. 2919, pp. 245-251, Nov. 1996.
- [26] D.P. Shea and J.E. Mitchell, "A 10 Gb/s 1024-Way Split 100-km Long Reach Optical Access Network", *IEEE/OSA J. Lightwave Technol.*, vol. 25, pp. 685-693, Mar. 2007.
- [27] K.-I. Suzuki, Y. Fukada, D. Nesses, and R. Davey, "Amplified gigabit PON systems", *OSA J. Optical Netw.*, vol. 6, pp. 422-433, May 2007.
- [28] A. Lovric, and S. Aleksic, "Power Efficiency of Extended Reach 10G-EPON and TDM/WDM PON", in Proc. OFC'10, NMC4, San Diego (CA), United States, Mar. 2010.
- [29] B. Schrenk, "Characterization and Design of Multifunction Photonic Devices for Next Generation Fiber-to-the-Home Optical Network Units", Doctoral Thesis, March 2011.
- [30] C. Arellano, "Investigation of Reflective Optical Network Units for Bidirectional Passive Optical Access Networks"; Doctoral Thesis, Universitat Politecnica de Catalunya, June 2007.
- [31] Christopher Ferenc Marki; "Design and optimization of bidirectional and optical logic systems in the presence of noise"; Doctoral Thesis, UNIVERSITY OF CALIFORNIA, SAN DIEGO, 2007.
- [32] J.R. Stern, J.W. Balance, D.W. Faulkner, S. Hornung, D. Payne and K. Oakley, "Passive optical local networks for telephony applications and beyond", *IEE Electron. Lett.*, vol. 23, pp. 1255-1256, 1987.
- [33] L.G. Kazovsky, W. Shaw, D. Gutierrez, N. Cheng, and S. Wong, "Next-Generation Optical Access Networks", *IEEE/OSA J. Lightwave Technol.*, vol. 25, pp. 3428-3442, Nov. 2007.
- [34] R.D. Feldman, E.E. Harstead, S. Jiang, T.H. Wood, and M. Zirngibl, "An Evaluation of Architectures Incorporating Wavelength Division Multiplexing for Broad-Band Fiber Access", *IEEE/OSA J. Lightwave Technol.*, vol. 16, pp. 1546-1559, Sept. 1998.
- [35] Bernhard Schrenk; "Characterization and Design of Multifunction Photonic Devices for Next-Generation Fiber-to-the-Home Optical Networks Units"; Doctoral Thesis, Universitat Politecnica de Catalunya, March 2011.
- [36] O. Gerstel, "Optical Networking: A Practical Perspective", *IEEE Hot Interconnects*, Aug. 2000.
- [37] P. P. Iannone and K. C. Reichmann, "Strategic and Tactical Uses for Extended PON", in Proc. OFC'08, Workshop Presentation, Feb. 2008.
- [38] R. P. Davey et al., "DWDM Reach Extension of a GPON to 135 km", *IEEE/OSA J. Lightwave Technol.*, vol. 24, pp. 29-31, Jan. 2006.
- [39] I. Van de Voorde, C.M. Martin, J. Vandewege, and X.Z. Qiu, "The super PON demonstrator: an exploration of possible evolution paths for optical access networks", *IEEE Comm. Mag.*, vol. 38, pp. 74-82, Feb. 2000.
- [40] J. Bauwelinck et al., "Full-Duplex 10 Gb/s Transmission in Ultra-Dense PONs With Tree Splits >1:1k and Noise-Powered Extender Box", in Proc. ECOC'10, Tu.5.B.4, Torino, Italy, Sept. 2010.
- [41] C. Antony et al., "Demonstration of a Carrier Distributed, 8192-Split Hybrid DWDM/TDMA PON over 124km Field-Installed Fibers", in Proc. OFC'10, PDPD8, San Diego (CA), United States, Mar. 2010.
- [42] R. Kjaer, I. T. Monroy, L. K. Oxenløwe, P. Jeppesen, and B. Palsdottir, "Bi-directional 120 km Long-reach PON Link Based on Distributed Raman Amplification", in Proc. LEOS'06, WEE3, Montreal, Canada, Oct. 2006.
- [43] A. Banerjee et al., "Wavelength-division-multiplexed passive optical network (WDM PON) technologies for broadband access: a review", *OSA J. Optical Netw.*, vol. 4, pp. 737-758, 2005.
- [44] K. Takada, M. Abe, T. Shibata, and K. Okamoto, "1-GHz-Spaced 16-Channel Arrayed-Waveguide Grating for a Wavelength Reference Standard in DWDM Network Systems", *IEEE/OSA J. Lightwave Technol.*, vol. 20, pp. 822-825, May 2002.
- [45] W. Jiang, K. Okamoto, F.M. Soares, F. Olsson, S. Lourduoss, and S.J.B. Yoo, "5 GHz Channel Spacing InP-Based 32-Channel Arrayed-Waveguide Grating", in Proc. OFC'09, OWO2, San Diego (CA), United States, Mar. 2009.
- [46] Bond, Rob (Telcordia); "ITU PON – Past, Present, and Future"; FTTH Council Webinar, July 30, 2008
- [47] J.A. Lázaro, C. Bock, V. Polo, R.I. Martinez, and J. Prat, "Remotely amplified combined ring-tree dense access network architecture using reflective RSOA-based ONU", *OSA J. of Optical Netw.*, vol. 6, pp. 801-807, Jun. 2007.
- [48] M. O. van Deventer et al., "Architecture for 100 km 2048 split bidirectional Super PONs from ACTS-PLANET", *Proc. SPIE*, vol. 2919, pp. 245-251, Nov. 1996.
- [49] D.P. Shea and J.E. Mitchell, "A 10 Gb/s 1024-Way Split 100-km Long Reach Optical Access Network", *IEEE/OSA J. Lightwave Technol.*, vol. 25, pp. 685-693, Mar. 2007.
- [50] C. Antony, et al., "Demonstration of a Carrier Distributed, 8192-Split Hybrid DWDM/TDMA PON over 124km Field-Installed Fibers", in Proc. OFC'10, PDPD8, San Diego (CA), United States, Mar. 2010.
- [51] J. Prat, et. al. "Results from EU Project SARDANA on 10G extended reach WDM PONs", *OSA, OFC/ NFOEC 2010*, paper OThG5.

- [52] G. Das et al., Proc. ECOC'09, P6.28 (2009).
- [53] T. Koonen, et al., Photonic Network Comm., vol. 3 (3), July 2001.
- [54] B. Lannoo et al., Proc. ICTON'10, Mo.C4.3, Invited (2010).
- [55] G. Das, B. Lannoo, D. Colle, M. Pickavet, P. Demeester, "A Hybrid WDM/TDM PON Architecture Using Wavelength Selective Switches", IEEE 4th International Symposium on Advanced Networks and Telecommunication Systems, 2010.
- [56] J. Prat, J. Lazaro, P. Chancelou, R. Soila, P. Velanas, A. Teixeira, et. al., "Hybrid Ring-Tree WDM/TDM-PON Optical Distribution Network", Th.B3.1, ICTON 2009.
- [57] J.J. Lepley, M.P. Thakur, I. Tsalamanis, C. Bock, C. Arellano, J. Prat, S.D. Walker, "VDSL Transmission over a Fibre Extended Access Network", OSA J. Optical Netw., vol. 4, pp.517-523, 2005.
- [58] J.H. Lee et al., "First Commercial Deployment of a Colorless Gigabit WDM/TDM Hybrid PON System Using Remote Protocol Terminator", IEEE/OSA J. Lightwave Technol., vol. 28, pp. 344-351, Feb. 2010.
- [59] H. Rohde, S. Smolorz, E. Gottwald, and K. Kloppe "Next Generation Optical Access: 1Gbit/s for Everyone", in Proc. ECOC'09, Th.10.5.5, Vienna, Austria, Sept. 2009.
- [60] S. Yamashita et al, Electron. Lett., 32 (1996), 1298-1299
- [61] J. Hubner et al, Electron. Lett., 33 (1997), 139-140
- [62] A. Bellemare et al, J. Lightwave Technol., 18 (2000), 825-831
- [63] S. Kim, et al, Optics Comm., 190 (2001), 291-302.
- [64] J. Buus, and E.J. Murphy, "Tunable lasers in optical networks", IEEE/OSA J. Lightwave Technol., vol. 24, pp. 5-11, Jan. 2006.
- [65] M. Mestre et al., "Tuning Characteristics and Switching Speed of a Modulated Grating Y Structure Laser for Wavelength Routed PONs", in Proc. ANIC'10, AthC2, Karlsruhe, Germany, Jun. 2010.
- [66] G. Talli and P. D. Townsend, "Hybrid DWDM-TDM Long-Reach PON for Next-Generation Optical Access", IEEE/OSA J. Lightwave Technol., vol. 24, pp. 2827-2834, July 2006.
- [67] G. de Valicourt et al., "High Gain (30 dB) and High Saturation Power (11 dBm) RSOA Devices as Colorless ONU Sources in Long-Reach Hybrid WDM/TDM-PON Architecture", IEEE Photonics Technol. Lett., vol. 22, pp. 191-193, Feb. 2010.
- [68] A. Garreau et al., "10Gbit/s Amplified Reflective Electroabsorption Modulator for Colorless Access Networks", in Proc. IPRM'06, Tu.A2.3, pp. 168-170, Princeton, United States, May 2006.
- [69] J. Prat, P. E. Balaguer, J.M. Gené, O. Díaz and S. Figuerola, "Fiber-to-the-Home Technologies," Kluwer Academic Publishers, ISBN1-4020-7136-1, 2002.
- [70] Lopez, E.T. ; Lazaro, J.A. ; Arellano, C. ; Polo, V. ; Prat, J.; "Optimization of Rayleigh-Limited WDM-PONs With Reflective ONU by MUX Positioning and Optimal ONU Gain"; Photonics Technology Letters, IEEE, Volume: 22 , Issue: 2, January 2010 , Page(s): 97 – 99.
- [71] Lopez, E.T. ; Lazaro, J.A. ; Arellano, C. ; Polo, V. ; Prat, J.; "ONU optimal gain and position of the distribution element in rayleigh-limited WDM and TDM PONs with reflective ONU"; 35th European Conference on Optical Communication, 2009. ECOC '09. Publication Year: 2009 , Page(s): 1 – 2.
- [72] Segarra, J. ; Sales, V. ; Prat, J.; "Traffic Performance of an Access Hybrid WDM/TDM PON with Colorless Reflective-ONUs under Different Distances OLT-ONUs"; 9th International Conference on Transparent Optical Networks, 2007. ICTON '07. Volume: 1, 2007, Page(s): 287 – 292.
- [73] El-Sahn, Z.A. ; Buset, J.M. ; Plant, D.V.; "Bidirectional WDM PON enabled by reflective ONUs and a novel overlapped-subcarrier multiplexing technique"; Optical Fiber Communication Conference and Exposition (OFC/NFOEC), 2011, Page(s): 1 – 3.
- [74] Arellano, C. ; Langer, K.-D. ; Prat, J.; "Reflections and Multiple Rayleigh Backscattering in WDM Single-Fiber Loopback Access Networks"; Journal of Lightwave Technology, Volume: 27 , Issue: 1 Publication Year: 2009 , Page(s): 12 – 18.
- [75] Kwon, Hyuk-Choon ; Yong-Yuk Won ; Sang-Kook Han; "A self-seeded reflective SOA-based optical network unit for optical beat interference robust WDM/SCM-PON link"; Photonics Technology Letters, IEEE Volume: 18 , Issue: 17, 2006 , Page(s): 1852 – 1854.
- [76] Fresi, F. ; Berrettini, G. ; Das Barman, A. ; Debnath, S. ; Poti, L. ; Bogoni, A.; "Single RSOA based ONU for RZ symmetrical WDM PONs at 2.5 Gb/s"; International Conference on Photonics in Switching, 2008. PS 2008. Page(s): 1 – 2.
- [77] Jin, X.Q. ; Groenewald, J. ; Hugues-Salas, E. ; Giddings, R.P. ; Tang, J.M.; "Upstream Power Budgets of IMDD Optical OFDMA PONs Incorporating RSOA Intensity Modulator-Based Colorless ONUs"; Journal of Lightwave Technology, Volume: 31 , Issue: 12, 2013 , Page(s): 1914 – 1920.
- [78] M. D. Feuer, et. al., "Single-port laser-amplifier modulators for local access," P. Technology Letters, Vol. 8, No. 9, pp. 1175-1177, September 1996.
- [79] N. Buldawoo, S. Mottet, F. Le Gall, D. Sigonge, D. Meichenin and S. Chelles, "A Semiconductor Laser Amplifier-Reflector for the future FTTH Applications," Proc. ECOC97 Edinburgh, pp. 196-199, 1997.
- [80] N. Buldawoo, S. Mottet, H. Dupont, D. Sigogne and D. Meichenin, "Transmission Experiment using a laser amplifier-reflector for DWDM access network," Proc. ECOC98 Madrid, pp.273-274, 1998.

- [81] J.J. Koponen and M. J. Söderlund, "A duplex WDM passive optical network with 1:16 power split using reflective SOA remodulator at ONU," Proc. OFC 2004 Los Angeles, MF 99.
- [82] J. Prat, C. Arellano, V. Polo and C. Bock, "Optical Network Unit Based on a Bidirectional Reflective Semiconductor Optical Amplifier for Fiber-to-the-Home Networks," IEEE Photonics Technology Letters, vol. 17, no. 1, pp. 250-252, January 2005.
- [83] ITU-T G.984.2-Amendment; "Gigabit-capable PON (G-PON): Physical Media Dependent (PMD) layer Specifications". Nov. 10, 2005.
- [84] I. Tafur et al., "Monolithically integrated reflective SOA-EA carrier re-modulator for broadband access nodes." OSA Optics Expr., vol. 14, pp. 8060-8064, Sept. 2006.
- [85] E.K. MacHale et al., "Extended-Reach PON Employing 10 Gb/s Integrated Reflective EAM-SOA", in Proc. ECOC'08, Th.2.F.1, Brussels, Belgium, Sept. 2008.
- [86] M. Omella, V. Polo, J. Lazaro, B. Schrenk, and J. Prat, "RSOA Transmission by Direct Duobinary Modulation", in Proc. ECOC'08, Tu.3.E.4, Brussels, Belgium, Sept. 2008.
- [87] K.Y. Cho, Y. Takushima, and Y.C. Chung, "Demonstration of 11-Gb/s, 20-km Reach WDM PON using Directly-Modulated RSOA with 4-ary PAM Signal", in Proc. OFC'10, OWG1, San Diego (CA), United States, Mar. 2010.
- [88] K. Petermann, "Laser Diode Modulation and Noise," Dordrecht, Kluwer, 1988.
- [89] J.E. Bowers, "High speed semiconductor laser design and performance", Solid-State Electronics, vol. 30, pp. 1-11, Jan. 1987.
- [90] P.J. Corvini and T.L. Koch, "Computer Simulation of High-Bit-Rate Optical Fiber Transmission Using Single-Frequency Lasers", IEEE/OSA J. Lightwave Technol., vol. 5, pp.1591-1595, Nov. 1987.
- [91] K. Kanayama, Y. Ando, R. Nagase, S. Iwano, and K. Matsunaga, "Advanced physical contact technology for optical connectors," Photonics Technology Letters, IEEE, vol. 4, pp. 1284-1287, 1992.
- [92] Van Deventer, M. Oskar; "Fundamentals of Bidirectional Transmission over a Single Optical Fibre", Kluwer Academic Publishers, 1996.
- [93] D. Derickson, "Fibre optics test and measurement" Hewlett-Packard Professional Books, Ed. Prentice Hall, 1997.
- [94] IEEE 802.3ah (E-PON); "Part 3: Carrier Sense Multiple Access with Collision Detection (CSMA/CD) Access Method and Physical Layer Specifications"; 7 September 2004.
- [95] Telcordia; "ITU PON – Past, Present, and Future - A Review of ITU-T PON Activities", FTTH Council Webinar, July 30, 2008.
- [96] ITU-T G.987.2; "10-Gigabit-capable Passive Optical Networks (XG-PON): Physical Media Dependent (PMD) layer Specific.". Jan, 2010.
- [97] ITU-T G.987.3; "10-Gigabit-capable passive optical networks (XG-PON): Transmission convergence (TC) specifications", October, 2010.
- [98] ITU-T G.987.4; "10-Gigabit-capable passive optical networks (XG-PON): ONU management and control interface specification (OMCI)", Nov, 2010.
- [99] ITU-T G.984.2; "Gigabit-capable PON (G-PON): Physical Media Dependent (PMD) layer Specifications". March, 2003.
- [100] Junichi Kani, Ken-Ichi Suzuki "Standardization Trends of Next-generation 10 Gigabit-class Passive Optical Network Systems", NTT Technical Review, Vol. 7, No. 11, Nov. 2009.
- [101] E. MacHale, G. Talli, P.D. Townsend, et.al, "Signal-Induced Rayleigh Noise Reduction using Gain Saturation in an Integrated R-EAM-SOA" OFC 2009 – OThA6. Conference on 22-26 March 2009 Page(s):1-3.
- [102] G.Talli, C.Chow, P.D. Townsend, "Modeling of Modulation Formats for Interferometric Noise Mitigation", IEEE JLT vol. 26 no. 17, Sep. 2008.
- [103] J. A. Lazaro, C. Arellano, J. Prat, "Rayleigh Scattering Reduction by Means of Optical Frequency Dithering in Passive Optical Networks With Remotely Seeded ONUs", IEEE PTL, Vol. 19, No. 2, 2007
- [104] ITU-T GPON 984.2 Amendment 1 to G.984.2, Gigabit-capable Passive Optical Networks (G-PON): Physical Media Dependent (PMD) layer Specifications (2006).
- [105] Y. Shibata, *et al.*, "2.5-Gbit/s wavelength channel data rewriter using semiconductor optical saturator/modulator for drop-and-rewrite WDM networks", in Proc. ECOC 2003, paper Th2.3.3, 2003.
- [106] C. W. Chow, "Wavelength remodulation using DPSK down-and-upstream with extinction ratio for 10-Gb/s DWDM-passive optical networks," IEEE. Photon. Technol. Lett., vol. 20, no. 1, Jan., pp. 12-14, 2008.
- [107] L. Y. Chan, *et al.*, "Demonstration of data re-modulation for upstream traffic in WDM access networks using injection-locked FP laser as modulator", in Proc. OFC 2001, paper WU5, 2001.
- [108] W. R. Lee, *et al.*, "Bidirectional WDM-PON based on gain-saturated reflective semiconductor optical amplifier," IEEE. Photon. Technol. Lett., vol. 17, no. 11, Nov., pp. 2460-2462, 2005.
- [109] Miyazaki, T.; "Superposition of QPSK over inverse-RZ for 3-bit/symbol transmission", in Proc. ECOC 2004, paper We3.4.7, 2004

- [110] Y. Tian, Y. Su, L. Yi, L. Leng, X. Tian, H. He, and X. Xu, "Optical VPN in PON based on DPSK erasing/rewriting and DPSK/IM formatting using a single Mach-Zehnder modulator," in *Proc. ECOC*, Cannes, France, Sep. 24–28, 2006, Paper Tu4.5.6.
- [111] J. Fabrega, A. El Mardini, V. Polo, E. T. López, R. Soila, J. Prat, "Deployment analysis of TDM/WDM Single Fiber PON with Colourless ONU Operating at 2.5 Gbps Subcarrier Multiplexed Downstream and 1.25 Gbps Upstream", In *Proc. OFC/NFOEC 2010*, paper NWB5.
- [112] J. Fabrega, E. T. López, J. A. Lázaro, M. Zuhdi, J. Prat, "Demonstration of a full duplex PON featuring 2.5 Gbps Sub Carrier Multiplexing downstream and 1.25 Gbps upstream with colourless ONU and simple optics", in *Proc. ECOC'08*, paper We.1.F.6.
- [113] J. Fabrega, V. Polo, E. T. López, J. A. Lázaro, J. Prat, "Optical Network Based on Reflective Semiconductor Optical Amplifier Using Electrical Subcarrier Multiplex for Enhancing Bidirectional Transmission", 6a Reunión española de Optoelectrónica OPTOEL'09, paper COM-8
- [114] W. Hung, et al., "An Optical Network Unit for WDM Access Networks with Downstream DPSK and Upstream Re-modulated OOK Data Using Injection-Locked FP Laser", *IEEE PTL*, Oct. 2003.
- [115] M. Schneider et al, "Monolithically integrated optoelectronic circuits using HBT, EAM, and TEAT", in *Proc MWPO3*, pp.349-352.
- [116] H. Takesue, T. Sugie, "Data rewrite of wavelength channel using saturated SOA modulator for WDM Metro/Access networks with centralized light sources", *Proc. ECOC'02*, 8.5.6, Copenhagen (DE), September 2002
- [117] Arellano, C.; Polo, V.; Bock, C.; Prat, J. "Bidirectional single fibre transmission based on a RSOA ONU for FTTH using FSK-IM modulation formats", *Optical Fiber Communication Conference*, 2005. Technical Digest. OFC/NFOEC, On page(s): 3 pp. Vol. 3 Volume: 3, 6-11 March 2005
- [118] K. Y. Cho and et al. "Demonstration of RSOA-based WDM-PON operating at symmetric rate of 1.25 Gb/s with high rejection tolerance". In *Proceedings of the Conference on Optical Fiber Communication and the National Fiber Optic Engineers Conference*, 2008 (OFC/NFOEC 2008), San Diego (CA), March 2008.
- [119] C. J. Clark, A. A. Moulthrop, M. S. Muha, and C. P. Silva. "Transmission response measurements of frequency-translating devices using a vector network analyzer". *IEEE Transactions on Microwave Theory and Techniques*, 44(12):2724-2737, December 1996.
- [120] J. G. Proakis, "Digital Communications," Chapter 5, pp. 233-320
- [121] B. Schrenk, et al. "Employing feed-forward downstream cancellation in optical network units for 2.5G/1.25G RSOA-based and 10G/10G REAM-based PON for efficient wavelength reuse", *ICTON '09* (2009).
- [122] F. Payoux, P. Chanclou, T. Soret, N. Genay, "Demonstration of a RSOA-based Wavelength Remodulation Scheme in 1.25 Gbit/s Bidirectional Hybrid WDM-TDM PON", *OFC 2006*, 5-10 March 2006.
- [123] E. T. Lopez, et al, "Network dimensioning for a TDM-PON deployment single-fibre single-wavelength-reuse based on reflective ONUs" D3.5, 14th *ICTON 2012*, 4 Sep 2012.
- [124] ITU-T G.987.3; "10-Gigabit-capable passive optical networks (XG-PON): Transmission convergence (TC) specifications", October, 2010.
- [125] ITU-T G.984.3; "Gigabit-capable passive optical networks (G-PON): Transmission convergence (TC) specifications", February, 2004.
- [126] Eduardo Tommy López, J.A. Lázaro, V. Polo, and J. Prat; "Bandwidth assignment criteria against Rayleigh Backscattering effect in TDM-PON single-fibre wavelength-reuse networks", 13th *International Conference on Transparent Optical Networks (ICTON)*, 26-30 June 2011, Stockholm, Sweden.
- [127] Eduardo Tommy López, Victor Polo, J.A. Lázaro, and Josep Prat; "Optimal Trade-off for a Bidirectional Single-Fibre Single-Wavelength TDM-PON rSOA-based ONU", 15th *International Conference on Transparent Optical Networks (ICTON)*, 24-27 June 2013, Cartagena, Spain.
- [128] J.H. Yu, N. Kim, B.W. Kim, "Remodulation schemes with reflective SOA for colorless DWDM PON", *JON*, vol. 6, pp. 1041, Aug. 2007.
- [129] E. Conforti, et. al. "Carrier reuse with gain compression and feed-forward semiconductor optical amplifiers", *Transactions on Microwave Theory and Techniques*, vol. 50, pp. 77-81, Jan. 2002.
- [130] E. Kehayas, et al, "All-Optical Carrier Recovery with Periodic Optical Filtering for Wavelength Reuse in RSOA-based Colorless ONUs in Full-Duplex 10Gbps WDM-PONs", *Proc. OFC'10, OWG4* (2010).
- [131] European 7th Framework Programme project SARDANA (www.ict-sardana.eu).
- [132] ITU-T G984.1, "Gigabit-capable Passive Optical Networks (G-PON): General characteristics", March, 2003.
- [133] ITU-T G987.1, "10-Gigabit-capable passive optical networks (XG-PON): General requirements", January, 2010.

- [134] B. Schrenk, F. Bonada, M. Omella, J.A. Lazaro, J. Prat, "Enhanced Transmission in Long Reach WDM/TDM Passive Optical Networks by Means of Multiple Downstream Cancellation Techniques", ECOC 2009, paper We.8.5.4, Vienna.
- [135] V. Polo, B. Schrenk, F. Bonada, J. Lazaro and J. Prat, "Reduction of Rayleigh Backscattering and Reflection Effects in WDM-PONs by Optical Frequency Dithering", ECOC 2008, Brussels, Sept. 2008, paper P421.
- [136] M. Omella, I. Papagiannakis, B. Schrenk, D. Klionidis, A. N. Birbas, J. Kikidis, J. Prat and I. Tomkos, "Full-Duplex Bidirectional Transmission at 10 Gbps in WDM PONs with RSOA-based ONU using Offset Optical Filtering and Electronic Equalization" OFC 2009, San Diego, Paper OThA7.
- [137] D. Torrientes, P. Chanclou, F. Laurent, S. Tsyier, Y. Chang, B. Charbonnier and C. Kazmierski, "10Gbit/s for Next Generation PON with Electronic Equalization using Un-cooled 1.55 μ m Directly Modulated Laser", ECOC 2009", Vienna, PDP Th.3.5.
- [138] B. Schrenk, J.A. Lazaro, C. Kazmierski, J. Prat, "Colourless FSK/ASK Optical Network Unit Based on a Fabry P rot Type SOA/REAM for Symmetrical 10 Gb/s WDM-PONs", ECOC 2009, Vienna, paper We.7.5.6.
- [139] M. Omella, J.A. L zaro, J. Prat, "Driving Requirements for Wavelength Shifting in Colorless ONU with Dual-Arm Modulator", IEEE/OSA J. Lightwave Technol., vol. 27, no. 17, Sept. 2009.
- [140] J. Fabrega, "Homodyne OLT-ONU design for access optical networks", Doctoral Thesis, February, 2010.
- [141] P. Gysel, R. K. Staubli, "Statistical Properties of Rayleigh Backscattering in Single-Mode Fibres", IEEE J. Lightwave Technol., vol.8, no.4, pp.561-567, April 1990
- [142] P. Gysel, R. K. Staubli, "Spectral properties of Rayleigh backscattered light from single mode fibres caused by a modulated probe signal, IEEE J. Lightwave Technol., vol.8, no.12, December 1990.
- [143] R. K. Staubli, P. Gysel, "Crosstalk penalties due to coherent Rayleigh noise in bidirectional optical communication systems" IEEE J. Lightwave Technol. vol.9, no.3, March 1991.
- [144] P. P. Bohn, S. K. Dass, "Return Loss Requirements for Optical Duplex Transmission", IEEE J. Lightwave Technol., vol.5, no.2, February 1987.
- [145] T. H. Wood, R. A. Linke, "Observation of Coherent Rayleigh Noise in Single-Source Bidirectional Optical Fiber Systems", IEEE J. Lightwave Technol., vol.6, no.2, February 1988.
- [146] S. Radic, N. Vukovic, S. Chandrasekhar, A. Velingker and A. Srivastava, "Forward Error Correction Performance in the Presence of Rayleigh-Dominated Transmission noise", Photonic. Technol. Lett., vol.15, no.2, February 2003.
- [147] Nataša B. Pavlovic, Liliana N. Costa, and Antonio L. J. Teixeira, "SSB NRZ and SSB Manchester Downstream Signals for Remodulated Extended Reach WDM-TDM PONs," Proc. ECOC'09, 20-24 September, 2009, Vienna, Austria, paper P6.26, 2009.
- [148] Nataša B. Pavlovic, Liliana N. Costa, and Antonio Teixeira, "Intensity Modulated Remodulation Scheme Based on Single-Sideband Manchester Downstream Signal for Usage in Ring Tree Networks," Proc. CONFTELE 2009, S^a M^a Feira, Portugal, paper 90, May 2009.
- [149] P. J. Winzer, et. al., "Advanced optical modulation formats," Proceedings of the IEEE, vol. 94, no. 5, pp. 952-985, May 2006.
- [150] Zenko, "1577 nm TX / 1550 nm RX, 3.3V, 10 Gbps Continuous TX/2.5Gbps Burst-Mode RX, XFP NG-PON OLT Transceiver with RSSI; DDM Capability, RoHS Compliant LT-05B95B-XFPGX", Zenko Technologies Inc., Preliminary Data Sheet, ver.1, April 2009.
- [151] Broadcom, "BCM8154 Multirate 10Gbps NRZ/DuobinaryTranceiver", BroadcomPreliminary Data Sheet, 8154-DS202-R, 2008.
- [152] J. Prat et al., "Electronic Equalization of Photo-detection by Means of an SQRT Module", Proc. ICTON'07, Rome, Italy, paper We.C3.6 (2007).
- [153] C. Bock, J. A. Lazaro, J. Prat, "Extensions of TDM-PON standards to a single-fibre ring access network featuring resilience and service overlay", IEEE/OSA Journal of Lightwave Technology, June 2007, pp. 1416-1421.
- [154] J. A. Lazaro, J. Prat, P. Chanclou, G. M. Tosi, A. Teixeira, I. Tomkos, R. Soila, V. Koratzinos, "Scalable Extended Reach PON", Proceedings OFC'08,OThL2 (invited), 24-28 Feb. 2008.
- [155] F. Saliou, P. Chanclou, F. Laurent, N. Genay, J.A. Lazaro, F. Bonada and J. Prat. "Reach Extension Strategies for Passive Optical Networks", J. Opt. Com. Networks, vol.1, no.4, Sept. 2009.
- [156] J. A. Lazaro, C. Bock, V. Polo, R. I. Martinez, J. Prat, "Remotely amplified combined ring-tree dense access network architecture using reflective RSOA-based ONU", Journal of Optical Networking, May 2007 vol. 6, Issue 6, pp. 801-807.
- [157] B. Schrenk et al., "Remotely Pumped Long-Reach Hybrid PON", IEEE/OSA JLT, vol. 29, no.5, March 1, 2011.

- [158] IEEE Communications Surveys, “Long-Reach Optical Access Networks”, <http://networks.cs.ucdavis.edu/~mukherje/links/huan-cst-lrpsonsurvey-1Q2010.pdf>, 1-mar-2009.
- [159] Fibresystems.org, “France Telecom: bring it PON”, fibresystems.org/cws/article/tech/39443, 10-jun-2009.
- [160] Imagine LAB; “SARDANA Field-Trial in Lannion, on January 20th”, <http://imaginlab.fr/blogen/?p=299>, Jan-2011.
- [161] ABC newspaper, “El proyecto Sardana de fibra óptica liderado por UPC super aprueba en Francia”, <http://www.abc.es/agencias/noticia.asp?noticia=681962>, 7-Feb-2011.
- [162] La Vanguardia newspaper “El proyecto Sardana se presenta en Milán”, 8-Feb-2011.
- [163] A. Lovrić, S. Aleksić, J.A. Lazaro, G.M. TosiBeleffi, J. Prat, V. Polo, "Power Efficiency of SARDANA and Other Long-Reach Optical Access Networks", accepted in ONDM'11.
- [164] ITU-T Rec. G.988, “ONU management and control interface (OMCI) specification”; October, 2010.
- [165] Effenberger, F; Mukai, H; Kani, J; Rasztoivits-Wiech, M; “Next-Generation PON—Part III: System Specifications for XG-PON”, IEEE Communications Magazine, Nov. 2009.
- [166] Luo, Y; Effenberger, F; Gao, B; “Transmission Convergence Layer Framing in XG-PON1”, Sarnoff Symposium, 2009. SARNOFF '09. IEEE, March 30 2009-April 1 2009 Page(s):1 – 5.
- [167] Kani, J; Bourgart, F; et.al; “Next-Generation PON—Part I: System Specifications for XG-PON”, IEEE Communications Magazine, Nov. 2009.
- [168] Effenberger, F; Mukai, H; Pfeiffer, T; “Next-Generation PON—Part II: System Specifications for XG-PON”, IEEE Communications Magazine, Nov. 2009.
- [169] ITU-T Rec. G.984.4, “Gigabit- Capable Passive Optical Networks (G PON): ONT Management and Control Interface Specification,” 2008.
- [170] ITU-T G.984.3 Implementers’ Guide for ITU-T Rec. G.984.3 Gigabit-capable Passive Optical Networks (G-PON): Transmission convergence layer specification 2004.
- [171] Leino, Dmitri, “10 Gigabit-capable Passive Optical Network Transmission Convergence layer design”; Master Thesis - Aalto University School of Science and Technology; Espoo, 23 April 2010.
- [172] Tanenbaum, Andrew S. “Computer Networks”, Fourth Edition, Ed. Prentice Hall, August 2002
- [173] Altera Stratix IV Device Handbook, Altera Inc. November, 2009. Available on-line in: http://www.altera.com/literature/hb/stratix-iv/stratix4_handbook.pdf.
- [174] National Semiconductors; “LVDS Owner’s Manual: Including High-Speed CML and Signal Conditioning”; Fourth Edition, 2008.
- [175] Federal Standards 1037C; “Telecommunications: Glossary of Telecommunication Terms”, August, 1996
- [176] Dixit, Sudhir S.; “IP over WDM: Building the Next Generation Optical Internet”; Ed. Wiley-Interscience, 1st edition, 2003.
- [177] IEEE Std 802.3; “Part 3: Carrier sense multiple access with collision detection (CSMA/CD) access method and physical layer specifications”; March, 2002.
- [178] RFC 791 -“INTERNET PROTOCOL - DARPA INTERNET PROGRAM PROTOCOL SPECIFICATION”, IETF, September,1981.
- [179] RFC 2460 - Internet Protocol, Version 6 (IPv6) Specification, Network Working Group, IETF, December 1998
- [180] RFC 1700 -“ASSIGNED NUMBERS”; Network Working Group, IETF, October 1994
- [181] RFC 5237 - “IANA Allocation Guidelines for the Protocol Field”; Network Working Group, IETF; February, 2008
- [182] IANA Protocol Numbers <http://www.iana.org/assignments/protocol-numbers/protocol-numbers.xml>
- [183] RFC 2474 – “Definition of the Differentiated Services Field (DS Field) in the IPv4 and IPv6 Headers”; Network Working Group, IETF, December 1998
- [184] López Pastor, E.T.; Martins Soares, A.J.; Abdalla Junior, H.; et. al. “Redes de Comunicação Convergentes: Tecnologias e Protocolos” – Ed. Universidade de Brasilia, 2008, 272 p.
- [185] RFC 3031 – “Multiprotocol Label Switching Architecture”; Network Working Group, IETF, January, 2001
- [186] RFC 3032 – “MPLS Label Stack Encoding”; Network Working Group, IETF, January, 2001.
- [187] RFC 3945 – “Generalized Multi-Protocol Label Switching (GMPLS) Architecture”, Network Working Group, IETF, October, 2004.
- [188] RFC 5212 – “Requirements for GMPLS-Based Multi-Region and Multi-Layer Networks (MRN/MLN)”; Network Working Group, IETF; July,2008
- [189]Maier, Martin; “Optical Switching Networks”; Cambridge University Press, 2008.